UNIVERSITEIT VAN PRETORIA
UNIVERSITY OF PRETORIA
YUNIBESITHI YA PRETORIA
Denkleiers • Leading Minds • Dikgopolo tša Dihlalefi

The Libor market model and its calibration to the South African market

by

Kepler Vincent Klynsmith

Submitted in partial fulfilment of the requirements for the degree

Magister Scientiae

in the Department of Mathematics and Applied Mathematics
in the Faculty of Natural and Agricultural Sciences

University of Pretoria
Pretoria

April 2011

Declaration

I, Kepler Vincent Klynsmith declare that the thesis/dissertation, which I hereby submit for the degree Magister Scientiae at the University of Pretoria, is my own work and has not previously been submitted by me for a degree at this or any other tertiary institution.

Signature: .....

Date: .....

Abstract

The Libor market model and its calibration to the South African market

Kepler Vincent Klynsmith

Magister Scientiae
Department of Mathematics and Applied Mathematics
University of Pretoria
April 2011
Supervisor: Prof. Eben Maré

The South African interest rate market has mainly been focused on vanilla interest rate products and hence can be seen as underdeveloped in this regard when compared, for instance, to the associated equity market. Market participants subscribe this aspect to a lack of demand and sophistication of investors within the market. This is, however, expected to change given the influx of international banks into the South African market over the past couple of years.

The current market methodology, for the pricing of vanilla interest rate options in the South African market, is the standard Black model with some mechanism to incorporate interest rate smiles. This mechanism is typically in the form of the SABR model. The most significant drawback of this approach is the fact that it models each forward rate in isolation. Hence, there is no way to incorporate the joint dynamics between different forward rates and consequently cannot be used for the pricing of exotic interest rate options.

In anticipation of these new market developments, we explore the possibility of calibrating the LIBOR market model to the South African market. This dissertation follows a bottom up approach and hence considers all aspects associated with such an implementation. The work mainly focuses on the calibration to at-the-money interest rate options. A possible extension to the SABR model, while remaining within the LMM framework, is considered in the final chapter.

Acknowledgements

I would like to thank the following people and who have contributed to making this work possible:

- To all my work colleagues, for endless discussions regarding derivative models and the assistance provided in understanding new concepts,
- Yvonne McDermot of the University of Pretoria for all the administrative assistance provided throughout my course of study,
- Prof. E. Maré of the University of Pretoria as my supervisor.

Dedications

This thesis is dedicated to my friends and family, for all your words of encouragement and patience during the course of study.

Contents

List of Figures

List of Tables

Abbreviations and Notation

ARCH Autoregressive Conditional Heteroscedasticity

ATM At the Money

CCA Cascade Calibration Algorithm

CIR Cox, Ingersoll and Ross

FRA Forward Rate Agreement

GARCH Generalized Autoregressive Conditional Heteroscedasticity

HJM Heath, Jarrow and Morton

HW Hull and White

IRS Interest Rate Swap

JIBAR Johannesburg Interbank Agreed Rate

LIBOR London Interbank Offer Rate

LMM LIBOR Market Model

PCA Principal Component Analysis

RCCA Rectangular Cascade Calibration Algorithm

RCCAEI Rectangular Cascade Calibration Algorithm with Endogenous Interpolation

SABR Stochastic Alpha Beta Rho

SDE Stochastic Differential Equation

SSE Sum of Squared Errors

T_i Forward date used in the calculation of a particular rate

$\alpha_{T_iT_{i+1}}$ Year fraction between T_i and T_{i+1}

$L_{T_i,T_{i+1}}(t)$, $L_{i+1}(t)$ Simple compounded forward rate, at time t, for time period T_i to T_{i+1}

$B(t,T_{i+1})$ Stochastic discount factor, at time t, for maturity T_{i+1}

$N(\cdot)$ Standard normal distribution function

$\sigma_{T_iT_{i+1}.\text{caplet}}$ Black caplet volatility associated with the forward $L_{T_i,T_{i+1}}(t)$

$\sigma_{T_0T_i.\text{cap}}$ Market observable flat volatility, for a cap with maturity date T_i

$SR_{n,N}(t)$ Forward swap rate, at time t, starting at time T_n and maturing at time T_N

$V_{n,N}$ Black swaption volatility of the forward swap rate $SR_{n,N}(t)$.

F_B Forward bond price

$\sigma_{T_{.\text{bondopt}}}$ Black bond price volatility associated with the forward F_B

$r(t)$ Instantaneous short rate at time t

$B(t)$ Risk-free money account at time t

$\lambda(t)$ Market price of risk at time t

$f(t,T)$ Instantaneous forward rate at time t for maturity T

W_t Brownian motion under the Risk Neutral measure

W_t^U Brownian motion under the measure associated with the numeraire U

W_t^T Brownian motion under the T forward measure

Q Risk neutral or equivalent martingale measure

Q^U Measure associated with the numeraire U

Q^T T forward measure

E Expectation under the risk neutral measure

E^Q Expectation under the probability measure Q

E^U Expectation under the probability measure Q^U associated with the numeraire U

E^T Expectation under the T forward measure

$M(t)$ Strictly positive martingale with respect to the filtration generated by W^Q

ρ Correlation matrix of a set of forward rates

$\mathbf{C}$ Matrix used to define correlations between different forward rates, i.e. $\rho = \mathbf{CC}'$

$\rho_{L(i,i+1);L(j,j+1)}$, $\rho_{i+1,j+1}$ Instantaneous correlation between forward rates $L_{T_i,T_{i+1}}(t)$ and $L_{T_j,T_{j+1}}(t)$

$A_{s,N}$ Numeraire used in the forward swap rate model

$\sigma_{T_iT_{i+1}}(t)$ Instantaneous volatility, at time t, of the forward rate $L_{T_i,T_{i+1}}(t)$

$\sigma_{T_iT_{i+1},q}(t)$ The sensitivity of the forward rate $L_{T_iT_{i+1}}(t)$ towards the q'th orthogonal Wiener process

$\sigma_{s,N}(t)$ Instantaneous volatility, at time t, of the swap rate $SR_{n,N}(t)$

$\mathbf{\Sigma}$ Covariance matrix of a set of forward rates

$z(t,T)$ Zero rate at time t for maturity T

Cpl^{Black} Caplet price, as implied by the Black model, for a given set of input parameters

Cap^{MKT} Cap price, for a given set of input parameters, using the market quoted flat volatility

$\sigma_{i,j}$ Piecewise constant volatility of forward rate $L_{T_{i-1},T_i}(t)$, for the time period j

Chapter 1

Introduction

The South African interest rate options market can be argued to be underdeveloped when compared, on a liquidity basis, to some of the international markets (or even the local equity market). Market participants consequently focused on the pricing and risk management of vanilla interest rate derivatives, as opposed to extending the range of available exotic products. The significant amount of time spent on these basic derivatives is a direct result of some of the complexities associated with this market.

Yield curve construction, for example, focused on the selection of benchmark instruments and interpolation techniques for different parts of the curve (all while accounting for front office system limitations). Another point within this area was the recent widening of spreads between rates with different cash flow frequencies. This was driven by the credit crunch which resulted in more demand for payments with shorter time intervals (see papers by Piterbarg [45] and Whittall [59]-[58] for discussions around some of the impacts of the credit crisis on the pricing of derivatives). Unfortunately, as encountered frequently within our market, there are no actively quoted instruments that can be used to derive these basis spreads. Hence we are forced to try and obtain this information from similar international markets. Alternatively, we can try to obtain these from our local market through either regular price requests, or deducing these relationships from the current spreads between some of the JIBAR instruments. All of which will be an estimation at best and consequently will complicate processes such as price testing and value-at-risk calculations within an investment bank.

Volatility surface construction was in turn focused on the incorporation of the (mostly) unobservable interest rate smile. This is where models such as the Stochastic Alpha Beta Rho (SABR) volatility model became popular, which allowed the trader to incorporate the smile into the surface through the manipulation of only a few parameters. Such an approach would typically consist of finding parameters that most accurately reflect the trader's view, as well as, the limited amount of prices obtained from the market. The effective con-

struction of bond option volatility surfaces was another heavily debated point within this area. Points considered here relates to duration matching between bonds and swaps and the conversion of yield volatility to the equivalent price volatility.

The above mentioned points are already starting to emphasize some of the aspects underlying our local interest rate options market, i.e. the possible lack of data and its underdeveloped nature when compared with some of the international markets (or even the local equity market). This should be kept in mind when attempting to implement any interest rate model.

From the points made above, the question might arise as to why we then even need to consider a different interest rate model. At the moment, the implemented option pricing methodologies (i.e. standard Black model with some sort of smile adjustment) seem to be sufficient for the current demand.

I believe the answer to this question lies in a possible increase in the complexity of interest rate products in the near future. Some market participants subscribe the vanilla nature of our market to a lack of demand and sophistication of the available investors (and consequently the liquidity in the market). This is, however, expected to change given the influx of international banks into the South African market over the past couple of years. Familiar examples of these are the 2005 Barclays Bank purchase in Absa of 53.96% and the 2008 ICB purchase in Standard Bank of 20%. Furthermore, we also witnessed a possible 70% purchase in Nedbank by HSBC (although the purchase did not go through in the end, it is evident that there is some significant international interest). As a result, we need to consider different possible pricing techniques that can cater for more complex interest rate derivatives.

The most significant drawback of the current SABR approach (or the Black model for ATM vanilla options) is the fact that it models each forward rate in isolation. Hence, there is no mechanism to incorporate the joint dynamics between different forward rates and consequently cannot be used for the pricing of exotic interest rate options (Rebonato [49]). Even simple interest rate derivatives, such as Bermudan swaptions, will fall outside this framework.

An alternative to the current approach, would be to turn to different possible short rate models. These, however, result in a number of different limitations. The first obvious limitation is that short rate models are based on the assumption that the dynamics of the entire yield curve is only driven by the instantaneous short rate. In the case of single-factor models we only have one source of uncertainty implying perfectly correlated rates. In order to improve correlation modeling we need to add additional factors to the model which adds more complexity to the model. Furthermore, the instantaneous short rate is not a directly observable market variable. This then complicates the calibration and implementation of these models and hence reduces some of its financial appeal (Hunt and Kennedy [33]).

In reply to the above mentioned arguments, we will mainly focus in this thesis on the LIBOR market model with deterministic volatilities (will com-

ment later in this section on the extension to the SABR volatility model). The specific choice of model relates to its ability to price exotic options in such a way that is internally consistent with the Black framework (Rebonato [47]), i.e. it will allow the pricing of exotic options in such a way that is internally consistent with the current market methodology for ATM vanilla options. This is an extremely important point, given the fact that exotic options traders will typically look at hedging their positions with vanilla interest rate options (Rebonato [47]). As a result, we will regularly refer to this property during the implementation of the different calibration algorithms.

Another favourable aspect of this model relates to its financial appeal. Instead of having a model that is based on unobservable rates, we have that the state variables in the LIBOR market model are discretely compounded forward rates (Rebonato [47]). These are market observable rates and are assumed to be lognormally distributed (in the deterministic volatility setting and under their associated T-forward measures (Björk [4])). Furthermore, we have that the no-arbitrage evolution of the discrete forward rates can be expressed purely as a function of the instantaneous covariance elements. These conditions will be derived and presented in a later chapter.

Björk [4] mentions that these covariance elements should be determined by the market, which then allows the pricing of derivatives under the market implied measure. The question remains whether these covariance functions could be uniquely determined. This will then imply a unique measure and hence unique exotic prices. Rebonato [47] argues that this is in fact not possible and hence the market for instantaneous covariances is incomplete.

The above mentioned property will have a significant impact on the implementation of the LIBOR market model. It will require that the user of the model make some financially justifiable assumptions regarding the covariance structure of the model (Rebonato [47]). Within this setup, we will consider a number of different types of instantaneous volatility specifications while assuming an exogenously given correlation matrix.

The volatility specifications will range from piecewise constant to parametric forms, each of which can be defined in a number of different ways. In particular, we will highlight the importance of time-homogeneous specifications (such as future implied hedging costs) and how they can be implemented to ensure the exact pricing of market observable caplets.

The decision regarding the use of an exogenous correlation matrix is motivated by the difficulty of obtaining reliable correlation information from market traded instruments. We will, for instance, discuss why it is not possible to obtain correlation estimates from vanilla swaption quotations. The exogenous correlation matrix, will in turn be estimated from historical market data.

Irrespective of these complexities, it will be argued that it is more favourable to express views in terms of these market traded quantities, as opposed to some of the factors embedded in short rate models (Rebonato [47]).

Given the simplistic setting considered in this thesis (i.e. mainly based on

the calibration to ATM vanilla options, with a possible stochastic volatility extension in the final chapter), we will be able to consider in detail the procedures associated with the calibration of such a model. We will, for instance, provide detailed market inputs as obtained from one of the South African investment banks. Furthermore, we will consider how to obtain similar rates, given inputs from data sources such as Bloomberg or Reuters. From this data, we will then illustrate key concepts such as caplet stripping and curve bootstrapping (taking into account different interpolation techniques as well as the impact of these techniques on the associated forward rates) procedures. This analysis will allow us to highlight some important aspects specific to the South African market, such as illiquidity, compounding frequencies etc. The historical estimation of volatilities and correlations, from the above mentioned bootstrapped forward rates, will also be explained and presented.

Given the above mentioned market inputs, we will then consider the calibration of the model. We will start with the volatility portions of the instantaneous covariance functions. This will result in different calibration routines for the different instantaneous volatility specifications. In particular, we will analyze cases in which volatilities are not well defined, as well as consider implied term structure evolutions for each of the different specifications. We will also use this opportunity to comment on a very simplistic stochastic volatility scenario, as well as comment on the calibration to input swaption volatilities.

We will also consider the joint calibration of different forward rates. These applications will be based on the fact that we can separate the market observable volatility component from the component used for correlation modeling (Rebonato [47]). As a result, we will use the historically estimated correlation matrix for the South African market (following relevant sanity checks, as well as an appropriate correlation smoothing technique).

Calibration routines considered here, range from two rank reduction techniques, to a set of different cascade calibration techniques (based on the exact calibration to a swaption volatility matrix, assuming piecewise constant instantaneous volatilities). Following the implementation of the latter calibration algorithm, we also compare the model implied caplet volatilities with those obtained from market inputs (the importance of such an comparison is also highlighted).

In theory there should be no additional calibration required in a purely forward rate based implementation once the instantaneous volatility functions, as well as, the exogenous correlation matrix are determined. However, such an approach would then assume a dimensionality equal to the number of forward rates under consideration (Rebonato [47]). This is not practical from an implementation perspective and hence the introduction of different rank reduction calibration techniques.

In the final chapter we will briefly consider extending our approach to incorporate observable interest rate smiles (stochastic volatility setting). The focus in this chapter will be on the SABR model (although there are a number

of alternative approaches). This choice was mainly motivated by the fact that it is already implemented in the South African market for vanilla interest rate options. Such an approach will then allow for the joint modeling of forward rates, while at the same time producing vanilla option prices that are consistent with the observed market prices (as opposed to modeling each forward rate in isolation in the standard SABR model). This extension will be based on the recent work by Rebonato [49] and Rebonato and White [52].

The above mentioned chapter, will mainly focus on some of the obtained results as well as what these results imply. An in depth analysis of this model as well as other possible extensions, require significantly more work and can be regarded as a research project on its own. Hence, this project will not attempt to provide a complete description of these types of models, or even provide proofs or implementations. Instead, this chapter is intended to serve as a brief introduction into this field of research, and will be pursued outside this thesis as an ongoing project.

Throughout the thesis, we will provide results for both the South African and European markets. The latter set of inputs were mainly obtained from textbook examples and were included to confirm the correctness of our implementations.

The outline of the thesis is as follows. Chapter 2 will provide a brief overview of some of the interest rate models currently available within the literature. We will then move on to consider the required mathematical concepts and techniques in Chapter 3. These tools will then be used in Chapter 4 to derive the necessary forward rate dynamics implied by the LIBOR Market Model. Given these rates are fully specified in terms of volatilities and correlations, we will then move on to consider different possible specifications for these quantities in Chapters 5 and 6 respectively. Chapters 7 and 8 will then be focused at obtaining the different market inputs for the European and South African markets. Following this, we will consider in Chapter 9 the calibration of the volatility parameters to the data obtained in the previous chapters. Chapter 10 will introduce algorithms that can be used to obtain the joint dynamics of forward rates, while exactly recovering the prices of input cap or swaption volatilities. One of the more recent LMM developments are considered in Chapter 11, i.e. the extension of the LMM to the SABR volatility model. Conclusions are presented in Chapter 12.

Chapter 2

Interest Rate Models Overview

The introduction of this thesis was mainly focused on practical aspects relating to the South African market, with only a brief mention made to the different available interest rate models. This chapter will be used to expand on this discussion through providing an overview of some of the interest rate models typically encountered within the literature. The arguments presented will be along the lines of the work by Rebonato [47] and hence will try and reflect the order as well as reasons for development.

2.1 Standard Market Models

The market methodology used for the pricing of vanilla ATM interest rate caps/floors, swaptions and bond options is based on the Black [5] framework. Given the fact that these instruments (will only consider caps/floors and swaptions in the thesis) form such an integral part of the LIBOR and swap market models, we will take the time to discuss the pricing of these instruments as well as state some useful properties and results relating to them. The pricing of these instruments, as we move away from ATM, will be discussed at a later stage.

2.1.1 The Black Framework

The methodology proposed by Fischer Black [5] presented the market with a model to value options on commodity futures. This model assumed a lognormally distributed futures contract as underlying to the option under consideration. The interest rate market shortly followed and started pricing vanilla ATM options through assuming lognormally distributed forward rates as underlying variables.

We will present in the following sections the resulting formulas when applied to some of the different vanilla ATM options. For now, it was only

presented for completeness and the reader is referred to Appendix A.6 for more details.

2.1.2 Caps and Floors

An interest rate caplet can be defined as a call option on a single interest rate while the equivalent floorlet is defined as a put option on the same interest rate (Götsch [22]). Hence, interest rate caplets can provide protection against rising rates while interest rate floorlets provides protection against falling rates (Hull [32]). The interest rate under consideration resets at a predefined date T_i against the prevailing floating rate, or reference rate, on the day of reset. Payments are however only made at T_{i+1}. We can present the payoff of a caplet as given below

$$\text{payoff} = \alpha_{T_iT_{i+1}} \max(L_{T_iT_{i+1}}(T_i) - X, 0), \tag{2.1.1}$$

where X is the strike price of the caplet under consideration, $L_{T_iT_{i+1}}(T_i)$ is the value of the lognormally distributed forward rate at the time of reset (Götsch [22]) and $\alpha_{T_iT_{i+1}}$ is the year fraction between time T_i and T_{i+1}.

A cap is a portfolio of N such options and hence the value of the cap is simply given by the sum of the values of the underlying caplets. This is due to the important fact that the payoff of each caplet is only dependent on one forward rate at a time and hence independent of the correlation between different forward rates (Brigo and Mercurio [11]). Given the nature of a cap, it can have a number of different resets. The period between different resets can differ according to the attached reference rate.

The market standard for pricing vanilla ATM caps/floors is through using the Black [5] model. The underlying variable used for caps/floors is the lognormally distributed forward reference rates. Using the results given in Appendix A.6 we can obtain

$$c_i = B(0, T_{i+1})\alpha_{T_iT_{i+1}}[L_{T_iT_{i+1}}(0)N(d_1) - XN(d_2)], \tag{2.1.2}$$

where

$$d_1 = \frac{\ln\left(\frac{L_{T_iT_{i+1}}(0)}{X}\right) + \frac{1}{2}T_i\sigma^2_{T_iT_{i+1}.\text{caplet}}}{\sqrt{T_i\sigma^2_{T_iT_{i+1}.\text{caplet}}}}, \tag{2.1.3}$$

$$d_2 = \frac{\ln\left(\frac{L_{T_iT_{i+1}}(0)}{X}\right) - \frac{1}{2}T_i\sigma^2_{T_iT_{i+1}.\text{caplet}}}{\sqrt{T_i\sigma^2_{T_iT_{i+1}.\text{caplet}}}}, \tag{2.1.4}$$

and $N(\cdot)$ denotes the cumulative distribution function of the standard normal distribution and $\sigma_{T_iT_{i+1}.\text{caplet}}$ is the Black caplet volatility associated with the

forward $L_{T_i,T_{i+1}}(t)$. Hence, we can write the value of the associated cap as

$$c = \sum_{i=0}^{N-1} B(0,T_{i+1})\alpha_{T_iT_{i+1}}[L_{T_iT_{i+1}}(0)N(d_1) - XN(d_2)]. \tag{2.1.5}$$

Given the similarity in instruments we will only consider caplets and consequently only caps.

2.1.3 Swaptions

An European Swaption gives the holder the right to enter into a swap at a pre-determined date called the expiry date of the swaption (Hull [32]). The underlying swap will start at the time of option expiry and end at a time called the maturity of the underlying swap. A swaption is another form of protection against raising or falling interest rates (depending if pay fixed or receive fixed when enter into the underlying swap). Another point worth mentioning is that swap rates can give more information regarding future rate expectations. The fixed rate of a par swap is simply the average rate that is needed in order for the value of the floating side to equal the value of the fixed sided (see Hull [32] for more details). Similarly, swaptions can give an indication of expected forward average rates. Swaptions may be seen more attractive than swaps given market circumstances and risk profile of the holder (factors such as costs play a pivotal role) as you can still capitalize for instance on falling rates if the underlying swap to the option is to pay fixed. Swaps, in general, are popular instruments as they can, for example, fix costs relating to a set of future cash flows, facilitating better cash management practices.

Given the above information we can now define the payoff functions of a swaption. The swap rate of the underlying swap is fixed at the time of option expiry. Following this fixing (and given it is favorable to exercise), we will have a series of cash flows that are effectively the differences between the prevailing fixed rate and the rate that was agreed upon the issue of the option. Hence, following Hull [32], we have a series of payoffs equal to (assuming we are considering a payer swaption)

$$\text{payoff} = \alpha_{T_iT_{i+1}}\max(SR_{n,N}(T_n) - X, 0), \tag{2.1.6}$$

where X is the strike price of the swaption and $SR_{n,N}(T_n)$ is the swap rate at the option expiry T_n. The second subscript in the swap rate indicates the maturity of the underlying swap, i.e. T_N.

The market standard for pricing vanilla ATM swaptions is through using the Black [5] model. The underlying variable in this case is the lognormally distributed forward swap rate. Using the results given in Appendix A.6 we can obtain

$$c_i = \alpha_{T_iT_{i+1}}B(0,T_{i+1})[SR_{n,N}(0)N(d_1) - XN(d_2)], \tag{2.1.7}$$

where

$$d_1 = \frac{\ln\left(\frac{SR_{n,N}(0)}{X}\right) + \frac{1}{2}T_n V_{n,N}^2}{\sqrt{T_n V_{n,N}^2}}, \tag{2.1.8}$$

$$d_2 = \frac{\ln\left(\frac{SR_{n,N}(0)}{X}\right) - \frac{1}{2}T_n V_{n,N}^2}{\sqrt{T_n V_{n,N}^2}}. \tag{2.1.9}$$

and $V_{n,N}$ is the Black swaption volatility of the forward swap rate $SR_{n,N}(t)$. Therefore, we can write the value of the swaption as

$$c = \sum_{i=n}^{N-1} \alpha_{T_i T_{i+1}} B(0, T_{i+1})[SR_{n,N}(0)N(d_1) - XN(d_2)]. \tag{2.1.10}$$

2.1.4 Bond Options

Although we will not be considering bond options in the rest of the thesis, we will briefly discuss the modeling of these products. A European bond option gives the holder the right to purchase a bond for a certain price, also called the strike price, at a pre-determined time (Hull [32]). The central assumption in this modeling framework is that the forward bond prices follow a lognormal distribution. Hence, given the previous sections and the results in Appendix A.6, one can easily extend the methodology to cover the instrument type under consideration. The pricing results for a vanilla ATM European call option expiring at time T, as given by Hull [32], is presented below

$$c = B(0,T)[F_B N(d_1) - XN(d_2)], \tag{2.1.11}$$

where

$$d_1 = \frac{\ln\left(\frac{F_B}{X}\right) + \frac{1}{2}T_n \sigma_{T_{.\text{bondopt}}}^2}{\sqrt{T_n \sigma_{T_{.\text{bondopt}}}^2}}, \tag{2.1.12}$$

$$d_2 = \frac{\ln\left(\frac{F_B}{X}\right) - \frac{1}{2}T_n \sigma_{T_{.\text{bondopt}}}^2}{\sqrt{T_n \sigma_{T_{.\text{bondopt}}}^2}}. \tag{2.1.13}$$

and $\sigma_{T_{.\text{bondopt}}}$ is the Black bond price volatility associated with the forward bond price F_B.

2.1.5 Limitations

There are numerous well documented constraints regarding this type of modeling. This section will only provide a brief description of some of the constraints applicable to the concepts presented throughout this thesis.

Rebonato [47], for instance, pointed out that there is no inherent mechanism that can be used to incorporate views about the joint dynamics between different variables. Hull [32] on the other hand mentioned that this model does not describe how interest rates evolve through time and hence cannot be used for all instrument types (for example American options). Another significant constraint is the assumption of constant volatilities.

2.2 Short Rate Models

Short rate models assume that the dynamics of the entire yield curve is driven by the instantaneous short rate (Rebonato [47]). The short rate is in turn defined as the rate r at time t that applies to an infinitesimally short period of time (Hull [32]). In order to model the short rate we assume that its dynamics is given by some SDE. There is a vast amount of papers on the different possible specifications, resulting in a relatively large and sometimes complex (as the complexity of the SDE increases) research area.

This section intends to briefly examine some of the properties of short rate models and to present a few examples. Typical properties considered in practice are for example (later sections will only consider a few of these) implied distributions, positivity of rates, implied volatility structures (i.e. does the model produce term structures compatible with the observed humped or inverted ATM term structures), existence of analytical solutions (affine term structure models important in this regard, see Duffie and Kan [20]), application of different numerical pricing techniques (for example tree construction, monte carlo simulation or finite differences), mean reversion of rates, required change in parameters due to re-calibration, fitting to an exogenous yield curve and/or a set of caplet volatilities, modeling of dependence between different rates etc. (see Brigo and Mercurio [11] for a more detailed discussion).

The discussion is however far from comprehensive and is only intended to give the reader a better understanding of the evolution of interest rate models from the Black [5] framework to the stochastic short rate models. This will also help with understanding some of the links between these and the models presented in the following sections and why new models such as the HJM [28] and LMM were developed. We will start the discussion with single-factor short rate models and will indicate at a later stage how these results can be extended to multi-factor models.

The different types of specifications can effectively be divided into two sub categories, i.e. endogenous (or time-homogeneous) term structure models and exogenous term structure models (number of different sources stating this, see for example Brigo and Mercurio [11], Björk [4], Rebonato [47] and Cairns [15]). These two types will be discussed independently for the single-factor short rate models.

2.2.1 Modeling Framework

The economy under consideration, as given by Björk [4], can be expressed in the following equations

$$dr = \mu(t, r(t))dt + \sigma(t, r(t))dW^P(t), \tag{2.2.1}$$

where W^P is the Brownian motion under the objective probability measure. The only exogenously given asset is the risk-free money account B with its process given by

$$dB(t) = r(t)B(t)dt. \tag{2.2.2}$$

Given the short rate dynamics we will, for example, be able to derive bond price dynamics since we are assuming that the yield curve is driven by the instantaneous short rate.

Market completeness plays a very important role in the modeling of interest rate products. The arguments in this section will briefly outline the work by Björk [4].

As can be seen from Equations (2.2.1) and (2.2.2) we have only one exogenously given asset, i.e. the risk-free money account. However, interest rate derivatives will be driven by the dynamics of the instantaneous short rate. Hence, we will not be able to create a self-financing portfolio to replicate the payoff of simple derivatives (excluding the risk-free asset).

Theorem A.4.1 then implies that the market is incomplete and that the prices of derivatives, for example bonds, are not uniquely determined. Despite the fact that bond prices are not uniquely determined, we are able to derive conditions that should ensure arbitrage-free pricing. This is in fact given by the market price of risk which is defined below (results taken from Björk [4])

$$\lambda(t) = \frac{\alpha_T(t, r(t)) - r(t)}{\sigma_T(t, r(t))}, \tag{2.2.3}$$

where $\alpha_T(t)$ is the rate of return on the T-bond, r is the rate of return on the risk-free asset and $\sigma_T(t)$ is the volatility of the T-bond. Firstly note that this condition, if satisfied by all T-bonds (can be extended to other derivatives), will result in arbitrage-free pricing for all of the bonds. Secondly, and probably more importantly, is that these prices will be unique for a given market price of risk. We can now re-write the short rate dynamics under the martingale measure as

$$dr = (\mu(t, r(t)) - \lambda(t)\sigma(t, r(t)))dt + \sigma(t, r(t))dW(t). \tag{2.2.4}$$

Note from above that choosing a market price of risk is equivalent to choosing a measure (Brigo and Mercurio [11]). Furthermore, only the drift of the short rate dynamics changed when we switched between measures. This is in line with Girsanov's theorem that will be discussed in Section 3.2.1.

There are a number of papers proposing and examining different short-rate specifications. The market price of risk is implicitly stated in each of the different models (Brigo and Mercurio [11], Björk [4] and Rebonato [47]). The market price of risk is then determined when we calibrate the model to market data (Heath, Jarrow and Morton [28]). This will then provide us with the martingale measure necessary for derivative pricing.

The results presented in this section focused on single-factor specifications. These can easily be extended to multi-factor specifications. In this case we will, for example, work with a market price of risk vector instead of the scalar value used above. See for instance Björk [4] in this regard.

2.2.2 Endogenous Single-Factor Short Rate Models

Endogenous short rate specifications has the disadvantage that it cannot be calibrated exactly to market yield curves (with the obvious exception of simple yield curve shapes). This is due to the fact that the models only have a small number of parameters that can be used in the fitting process whereas an exact match will require a much larger number of parameters. Rebonato [47], however, mentions that this was originally welcomed by, for example, the bond traders. The argument was that if the assumptions underlying the model were accurate and financially justifiable, then the model could possibly indicate future trading opportunities. However, this type of specification proved to be problematic for vanilla options traders as the model could not accurately recover the prices of the underlying instruments and hence the associated hedging costs. A few of the endogenous models are presented in Table 2.1. For each of these models we can derive a number of different properties

Model	Short Rate Dynamics
Merton [38]	$dr = \mu dt + \sigma dW$
Dothan [19]	$dr = \mu r dt + \sigma r dW$
Vasiček [56]	$dr = \alpha(\mu - r)dt + \sigma dW$
CIR [17]	$dr = \alpha(\mu - r)dt + \sigma\sqrt{r}dW$

Table 2.1: Endogenous short rate specifications.

indicating the quality of the model. In order to illustrate this, let us consider these models in isolation.

The Merton [38] model is the simplest of the four and hence will be discussed in detail below. Brief mention will be made regarding the rest of the models in order to keep the discussion as concise as possible.

The SDE associated with the Merton [38] model has a very simple form, which allows one to obtain a solution for the short rate through virtual inspection. From above it is evident that the short rate will grow at a constant rate

with some added noise (hence the model assumes a normally distributed short rate). The fact that the drift term is constant and not mean reverting implies that the short rate can explode. Furthermore, the dynamics allow for the short rate to turn negative which is financially undesirable. The specification can be classified as an affine term structure model. Affine term structure models are defined as interest rate models where the continuously compounded spot rate is an affine function in the short rate (Brigo and Mercurio [11]). In this case bond prices can be expressed in a simple exponential form. From the resultant spot rate process it is clear that the spot rate yield curve is driven by the instantaneous short rate. Given this property, we have that the level of the yield curve can explode as well as turn negative. Another interesting property is that the spot rate will approach $-\infty$ as we increase the maturity under consideration. This then directly implies that bond prices will explode as the maturities of bonds increase. It can also be shown that instantaneous forward rates tend to $-\infty$ as we increase the maturity of these rates.

Dothan [19], on the other hand, proposed a model in which the short rate is lognormally distributed. This property ensures that rates remain positive at all times. This model does not provide an explicit mean reversion mechanism. Brigo and Mercurio [11] however pointed out that a 0 mean reversion level can be enforced through setting the drift parameter $\mu < 0$ (due to fact that rates are always positive under this specification). The process is not affine. Although analytical bond pricing solutions exist, these can be shown to be complicated and difficult to implement. There are no analytical formulas for options on zero coupon bonds (Brigo and Mercurio [11]). Given lognormal distribution, we have that rates can explode.

The Vasiček [56] model is similar to the Merton [38] model in the sense that the short rate is assumed to be normally distributed. Hence properties relating to simple analytical solutions, as well as the possibility of negative rates, are also applicable to this model. One significant difference appears in the drift of the process. This model explicitly specifies a mean reversion component which then prevents rates from exploding. It can be seen from the SDE of this model that the short rate will revert to the level μ at a reversion speed of α. This is an affine term structure model and hence we have that the level of the spot rate yield curve is driven by the instantaneous short rate.

CIR [17] proposed a model similar to the Vasiček [56] model. This model however ensures positive interest rates while preserving the mean reversion behaviour (for certain choices of the parameters α, μ and σ). This specification also allows for analytical bond and option prices (although more complex). Furthermore, this is an affine term structure model and hence similar properties to the Merton [38] and Vasiček [56] models hold in this regard.

2.2.3 Exogenous Single-Factor Short Rate Models

Exogenous short rate specifications allow the model to be fitted exactly to either the initial yield curve, initial volatility term structure or both. An exact fit to the initial yield curve can be achieved through making the drift parameters of the short rate dependent on time. Similarly, an exact fit to the initial volatility term structure can be achieved through making the volatility parameters dependent on time (Brigo and Mercurio [11]). These models can consequently be termed as arbitrage free.

Rebonato [47] mentions that this is favorable for the vanilla options traders since their hedges are correctly priced. A few of the exogenous models are presented in Table 2.2.

Model	Short Rate Dynamics
Ho-Lee [29]	$dr = \theta(t)dt + \sigma dW$
Hull-White [30]	$dr = (\theta(t) - ar)dt + \sigma dW$
Black, Derman and Toy [6]	$d\ln r = \left[\theta(t) + (\sigma'(t)/\sigma(t))\right] dt + \sigma(t)dW$
Black-Karasinski [7]	$d\ln r = (\theta(t) - a(t)\ln r)dt + \sigma(t)dW$

Table 2.2: Exogenous short rate specifications.

For each of these models we can once again derive a number of different properties indicating the quality of the model. Let us proceed as before and consider these models in isolation.

Ho-Lee [29] were the first to propose an exogenous term structure model. This is similar to the Merton [38] model, with the drift parameter adjusted to be time dependent. This then allows for an exact fit to the current term structure of rates. Most of the properties of the Merton [38] model are also applicable here. For instance, rates can explode and turn negative. This is an affine term structure model with simple analytical solutions. There is no mean reverting mechanism. The model is arbitrage free. The short rate in the model is normally distributed.

Hull-White [30] proposed an extension of the Vasiček [56] model. This then allowed for an exact fit to the initial term structure of interest rates while ensuring mean reversion. The short rate is also normally distributed. This implies simple analytical solutions, however rates can turn negative. This is an affine term structure model. The model is arbitrage free.

The continuous time equivalent of the Black Derman and Toy [6] model, as presented in Table 2.2, was obtained from the article by Hull and White [30]. Positive rates are ensured through assuming that the short rate is lognormally distributed. This model allows for an exact fit to both the initial yield curve as well as an exogenous set of volatilities. Rebonato [48] pointed out that mean

reversion can only be obtained if the volatility of the short rate decays with time. The model is arbitrage free.

Black-Karasinski [7], similar to the Black Derman and Toy [6] model, ensures positive rates through assuming that the short rate is lognormally distributed. This model allows for an exact fit to both the initial yield curve as well as an exogenous set of volatilities (Rebonato [48]). Importantly, Rebonato [48] pointed out that the evolution of the term structure of volatilities under this specification is much more time stationary than the evolution implied by the Black Derman and Toy [6] model. The log of the short rate in this model is mean reverting. The short rate itself is lognormally distributed. No analytical formulas are available for zero coupon bonds or options on these instruments. The model is more difficult to calibrate than the rest of the models presented in this section. The model is arbitrage free.

2.2.4 Multi-Factor Short-Rate Models

The models considered in the previous section only had a single source of uncertainty. This, however, is somewhat limited since we have that the entire yield curve is only driven by a single factor. Brigo and Mercurio [11] and Rebonato [47] points out that this implies a correlation of 1 between different interest rates which is far from desirable if the payoff of a derivative is dependent on the joint dynamics of a number of interest rates. Hence, in order to obtain better correlation modeling we need to introduce more factors. This requirement has lead to a number of papers examining the inclusion of extra factors, some of which are complex and difficult to implement. We will briefly examine some of these models in the rest of the section. Note that the mathematical results, for example the market price of risk, can easily be expanded to the multi-factor case. This is fully illustrated in the text by Björk [4].

An important driver and explanation for the success of one-factor and multi-factor models relates to the decomposing of interest rate movements into a few key driving factors (Rebonato [47]). These factors can be determined using a technique called principal component analysis (PCA).

Principal component analysis can be used to get a better idea of the factors driving a multi-variate set of data. The process consists of finding a set of orthogonal (and hence independent) vectors that can be used to describe the multi-dimensional space containing the original input data subject to certain specific conditions.

Various research projects in the interest rate literature have shown that the bulk of historical yield curve movements can be explained by the first two or three components (Brigo and Mercurio [11]) and that these can, for example, represent level, curvature and steepness (Litterman and Scheinkman [36]). The Matlab functions for principal component analysis will be used in this thesis (functions such as *princomp* and *pcacov*) and hence the exact process of obtaining the principal components will not be presented here.

Balduzzi, Das, Foresi and Sundaram [3] provides a nice summary of the different developed two-factor models. Below are some of the models mentioned in the study. This is only a small subset of the available two-factor short rate models and is intended to give the reader a feel of some of the possible extensions.

In the model by Brennan and Schwartz [9] they introduce the long-term interest rate as an additional factor. Schaefer and Schwartz [54], on the other hand, introduced the spread between the long-term rate and the instantaneous short-term rate. Several models were introduced in the literature to include an inflation linked component (see for example CIR [17]) while others included as addition factors the mean level of the short-term rate Balduzzi, Bertola, and Foresi [2] or the volatility of the short-term rate (Longstaff and Schwartz [37]).

Given the discussion regarding PCA we know that it might be useful to increase the number of factors even further. Rebonato [48] also mentions that it may require more factors to produce historically implied instantaneous correlation structures.

An example of increasing the number of factors even further can be found in the paper by Balduzzi, Das, Foresi and Sundaram [3]. The authors proposed a three-factor affine term structure model. The three proposed factors are the short-term rate of interest, the long-run mean of the short-rate and the volatility of the short-term rate. They also show that the affine nature of the model lead to relatively simple bond price solutions as well as a relatively simple calibration of the model.

The addition of factors does in general lead to an increase in the complexity of the model. Stability of the model should also be considered as we increase the number of factors.

2.2.5 Limitations

The first obvious limitation is that short rate models are based on the assumption that the dynamics of the entire yield curve is only driven by the instantaneous short rate. In the case of single-factor models we only have one source of uncertainty implying perfectly correlated rates. In order to improve correlation modeling we need to add additional factors to the model which adds more complexity to the model. Furthermore, the instantaneous short rate is not a directly observable market variable and short rate modeling is not consistent with the Black framework (in order for short rate modeling to be consistent with the Black framework, we need short rate dynamics that will imply lognormally distributed forward rates).

2.3 The Heath-Jarrow-Morton Framework

The paper by Heath, Jarrow and Morton [28] presented a framework for valuing contingent claims under a stochastic term structure of interest rates. The

processes modeled in the approach is the instantaneous forward rates. The key result of the HJM framework is that the no-arbitrage evolution of the state variables can be expressed purely as a function of the instantaneous volatilities (Rebonato [47] and Heath, Jarrow and Morton [28]). This model does not require an inversion of the yield term structure to eliminate the market prices of risk and take as given an initial forward curve (Heath, Jarrow and Morton [28]). Another important point mentioned in the paper by Heath, Jarrow and Morton [28] is that all the existing arbitrage models can be obtained through certain volatility specifications.

2.3.1 Modeling Framework

To get a better idea of the processes involved we will consider the work by Björk [4]. Let us assume for every fixed $T > 0$, that the stochastic differential equations of the instantaneous forward rates under the objective probability measure P are given by

$$df(t,T) = \alpha(t,T)dt + \sigma(t,T)dW^P, \tag{2.3.1}$$
$$f(0,T) = f^*(0,T), \tag{2.3.2}$$

where $f^*(0,T)$ is the observed forward rate curve.

The required condition for arbitrage-free pricing is given by the following

$$\alpha(t,T) = \sigma(t,T)\int_t^T \sigma(t,s)'\,ds - \sigma(t,T)\lambda(t), \tag{2.3.3}$$

where

$$\lambda(t) = [\lambda_1(t), \ldots, \lambda_d(t)]'$$

is the market price of risk vector. Setting the local rate of return of bonds equal the risk-free rate, we obtain the important HJM drift specification under the martingale measure

$$\alpha(t,T) = \sigma(t,T)\int_t^T \sigma(t,s)'\,ds. \tag{2.3.4}$$

This is a very important and useful result since it states that the drift parameters are uniquely determined once the volatility structure is specified (Björk [4]). The other way of looking at it is that we can freely specify the volatility structure, and will then be able to use Equation (2.3.4) to uniquely specify the drift parameters. This flexibility can however create some issues in the calibration of the model and will be discussed in the section on the LIBOR and swap market models. Also note that Equation (2.3.4) is independent of the market price of risk. This is in line with the comment at the start of the section.

2.3.2 Limitations

The short-rate process implied by the model is in general non-Markovian (see discussions by Brigo and Mercurio [11], Hullhull and Rebonato [47]). This has serious implications for tree-building procedures as it will result in non-recombining latices. There are, however, studies showing conditions that will allow for the trees to be re-combining (Brigo and Mercurio [11] and Carverhill [16]). Hence, the preferred choice of implementation will be through making use of Monte Carlo simulations. Another issue is that there are no observable instantaneous forward rates in the market which in turn complicates the calibration procedure (Rebonato [47]). Furthermore, a number of authors (see for example Brace, Gatarek and Musiela [8]) mention that the instantaneous forward rate processes explodes with positive probability in a lognormal setting. Rebonato [47], however, mentions that this is highly unlikely in any practical implementation.

2.4 LIBOR and Swap Market Models

One of the biggest disadvantages of short rate models and the framework proposed by Heath, Jarrow and Morton [28] is that these models are expressed in terms of rates which are not observable in the market. This then complicates the calibration and implementation of the models and hence reduces some of its financial appeal (Hunt and Kennedy [33]). The HJM framework however showed significant promise due to the fact that the model provided the capability to model a large number of factors and the flexibility of the covariance structure (Götsch [22]). This flexibility in the choice of the covariance structure can however lead to difficulties relating to calibration. This will be discussed in more detail in the section on market completeness.

2.4.1 Modeling Framework

Various papers were written on these two models, however the literature often refer to research articles by Brace, Gatarek and Musiela [8] and Miltersen, Sandmann and Sondermann [39] as the basis papers relating to the LIBOR market model whereas the article by Jamshidian [35] is seen as the basis paper relating to the swap market model. The popularity of the models are mainly due to its consistency with the Black [5] framework (Pelsser [44]). Before the introduction of the market models the Black [5] pricing formulas for interest rate derivatives were only justifiable through some inconsistent assumptions (James and Webber [34]). The LIBOR market model is a discrete time equivalent of the HJM framework.

The state variables in the LIBOR market model are discretely compounded forward rates (Rebonato [47]). These are market observable rates and are assumed to be lognormally distributed. Each of the forward rates can be

modeled as a martingale under its associated $T-$ forward measure (Björk [4]). This allows the pricing of caplets and hence caps (can be generalized to floorlets and hence floors) that is consistent with the Black [5] framework. Note however that more than one forward rate cannot be martingales under the same martingale measure (Brigo and Mercurio [11] and Björk [4]).

The state variables in the swap market model are in turn defined as discretely compounded forward swap rates (Rebonato [47]). Similar to the LIBOR market model these are market observable rates and are assumed to be lognormally distributed. Each of these rates can be modeled as a martingale under the forward swap martingale measure (Björk [4]). This allows the pricing of swaptions in a manner that is consistent with the Black [5] framework.

LIBOR and swap market models are however not compatible (mentioned by a number of authors; see for example Brigo and Mercurio [11], Björk [4] and Rebonato [47]). This can be seen through noting that a swap rate can be expressed as a linear combination of forward rates with stochastic weights (Rebonato [47]). Hence, the pricing of swaptions in the LIBOR market model will not be consistent with the Black [5] framework (similar result can be derived for the pricing of caps/floors in the swap market model). This then implies that one has to decide, based on the problem at hand, which one of the models to work with. We will focus our attention on the LIBOR market model. From above it is evident that this will imply simple calibration to cap/floor prices and we will have to use approximations for the calibration to swaption prices (Brigo and Mercurio [11], Björk [4]).

2.4.2 Market Completeness

Rebonato [47] repeatedly points out the importance of market completeness in the LIBOR market model framework and provides a very nice description of the problem at hand. This is by far one of the better accounts available in the literature and hence the arguments presented in this section will be based along the same lines.

To start off the discussion, note that it was previously mentioned that the LIBOR market model is a discrete time equivalent of the HJM framework. From Section 2.3.1 we know that the no-arbitrage conditions in the HJM framework amounts to expressing the drift of the instantaneous forward purely as a function of the instantaneous covariance elements. It will be shown later in the text that the same can be done for the LIBOR market model. Björk [4] mentions that these quantities should be determined by the market, which then allows the pricing of derivatives under the market implied measure. The question however remains if these volatility functions (will for now only focus on volatilities) can be uniquely determined. This will then imply an unique measure and hence unique exotic prices.

Rebonato [47] argues that this is in fact not possible and hence the market for instantaneous volatilities is incomplete. Furthermore, he mentions that the

market will only be complete if serial options are liquidly traded out to 30 years. The reason for this will be discussed below, however before we can proceed we need to define the payoff of a serial option. This is given by Rebonato [47] as

$$\text{Payoff}_{T_{\text{pay}}} = [L_{T_{\text{reset}},T_{\text{reset}}+\tau}(T_{\text{opt}}) - K]^{+}\tau, \tag{2.4.1}$$

where $T_{\text{opt}} \leq T_{\text{pay}} \leq T_{\text{reset}}$, but $T_{\text{opt}} < T_{\text{reset}}$. This instrument then has the important property that the expiry of the option, T_{opt}, occurs before the reset date T_{reset}. The importance of these options are that different volatility functions of the forward rates will result in different root-mean-square volatilities up to time T_{opt}. This is not the case with caplets. Hence, caplet prices cannot be used to uniquely determine the actual shape of the instantaneous volatility functions and hence the pricing of exotic options are not unique. Rebonato [47] further mentions that swaptions might provide more information regarding the volatility functions (ignoring that these two markets does not have to be in line in the first place). Swaptions however depend on both volatilities and correlations, which subsequently complicates the estimation of the required forward rate volatility functions.

Above mentioned property will have a significant impact on the implementation of the LIBOR market model. It will require that the user of the model make some financially justifiable assumptions regarding the covariance structure of the model. The covariance structure will then ultimately reflect the market views of the user.

2.4.3 Limitations

Given the dimensionality of the model, as well as non re-combining lattices, the user is typically forced to use Monte Carlo techniques for the pricing of interest rate derivatives (with the exception of some of the vanilla interest rate derivatives). Also, this model requires careful consideration regarding the choice of the covariance functions (given the fact that the market in instantaneous volatilities is not complete). Extension of results to volatility smiles can be complex (depending on the methodology).

Chapter 3

Mathematical Setup

This chapter will present some of the required mathematical results and definitions. These are intended to provide the reader with a broad overview of the mathematical requirements associated with the setup of market models. For more mathematical rigour the reader is referred to the source material mentioned in the chapter.

It was stated in Chapter 2 that there are a number of papers written on the LIBOR and swap market models (see for example Brace, Gatarek and Musiela [8], Miltersen, Sandmann and Sondermann [39], Jamshidian [35] and Musiela and Rutkowski [42]).

We will mainly consider the version as presented by Rebonato [47]. This approach introduce bond prices in order to define forward rates and assume volatilities of forward LIBOR rates to be deterministic of nature. Hence, before we can proceed, we need to introduce a set of bonds and the relationship between bonds and market rates. This is given in the following section.

3.1 Financial Framework

As mentioned above, we will consider an economy consisting of $N+1$ zero coupon bonds (Rebonato [47]). The value at time t, of a bond expiring at time T_i, will be given by $B(t,T_i)$. We will assume the usual properties of bonds within this economy (such as unit payoff at maturity and the fact that the bond processes have to be strictly positive). The bond price dynamics will not be explicitly defined in this thesis, we will focus more on the dynamics of forward rates.

These bonds will then be used to define a set of N spanning forward rates (Brigo and Mercurio [11]). Spanning forward rates are in turn defined as forward rates such that the expiry time of a forward rate corresponds with the payment time of the forward rate preceding the one under consideration (Rebonato [47]). In order to define the forward LIBOR rates, we will consider a set of dates $\Omega = \{T_0, \ldots, T_N\}$ from which (T_i, T_{i+1}) indicates the expiry-

maturity pair associated with the forward rate $L_{T_i,T_{i+1}}(t)$ at time t (Brigo and Mercurio [11]). Furthermore, the year fraction between dates T_i and T_{i+1} will be indicated by $\alpha_{T_iT_{i+1}}$. We are now in a position to define the underlying instruments to the market models, i.e. forward LIBOR and forward swap rates.

The LIBOR forward rate can be defined as the rate, at time t, for the time period between T_i and T_{i+1}. This is formally presented in the definition below

Definition 3.1.1 (Forward LIBOR/JIBAR Rate - Björk [4]) *The simple forward rate at time t, for the time period between T_i and T_{i+1}, is defined as*

$$L_{T_iT_{i+1}}(t) = -\frac{B(t,T_{i+1}) - B(t,T_i)}{\alpha_{T_iT_{i+1}} B(t,T_{i+1})}.$$

The forward LIBOR rate however gets fixed at the time of reset at the prevailing rate for the period under consideration (Hull [32]). This rate is called the spot LIBOR rate and is presented in the definition below

Definition 3.1.2 (Spot LIBOR/JIBAR Rate - Björk [4]) *The simple spot rate rate at time t, for the time period between T_i and T_{i+1} , is defined as*

$$L_{T_iT_{i+1}}(T_i) = -\frac{B(T_i,T_{i+1}) - 1}{\alpha_{T_iT_{i+1}} B(T_i,T_{i+1})}.$$

The next financial quantity to define is the forward swap rate. We will consider par forward swaps (Pelsser [44]), i.e. swaps where the floating side of the swap equals the fixed side. The formula for the swap rate is presented in the definition below (see Appendix B.1 and work by Gatarek, Bachert and Maksymiuk [21]).

Definition 3.1.3 (Forward Swap Rate - Gatarek, Bachert and Maksymiuk [21]) *The par swap rate at time t, for the swap starting at time T_s and maturing at time T_N, is defined as the fixed rate that will result in the value of the fixed leg of the swap to equal the value of the floating leg. The rate is given as*

$$SR_{s,N}(t) = \frac{B(t,T_s) - B(t,T_N)}{\sum_{i=s+1}^{N} B(t,T_i)\alpha_{T_{i-1}T_i}}.$$

It will be shown at a later stage that the forward swap rate can be expressed as a linear combination of forward LIBOR rates (with stochastic weights, see Rebonato [47] and Brigo and Mercurio [11]). This will be used to derive an approximation for swaption volatility within the LIBOR market model (number of sources using this approximation, see for example Rebonato [47], Brigo and Mercurio [11] and Gatarek, Bachert and Maksymiuk [21]).

3.2 Arbitrage-Free Pricing

The pricing of financial instruments can be described as the process of finding unique (if possible, otherwise prices under the martingale measure implied by the market, see Björk [4]) and arbitrage-free prices for the derivative securities under consideration. We will, however, only focus on arbitrage-free pricing; uniqueness of prices will only be discussed in later chapters and will follow arguments by Rebonato [47].

In order to obtain arbitrage-free prices, we will consider a technique known as the martingale approach (see Björk [4], Rebonato [47], Brigo and Mercurio [11] and Pelsser [44]). The technique is essentially based on measure transformations to martingale measures and is described by Björk [4] as the most general approach existing for arbitrage pricing.

3.2.1 Definitions and Theorems

This section will provide a set of definitions and theorems necessary for the martingale approach to arbitrage pricing. Please note that all of the results presented in this section were taken almost directly from Björk [4] and Rebonato [47]. Hence, below is intended to act as a short summary rather than an original presentation.

Let us start this discussion by presenting a theorem that is at the center of arbitrage pricing. Björk [4] describes it as the first fundamental theorem of mathematical finance. This will be used to define certain conditions that will prevent arbitrage opportunities and is presented in the theorem below.

Theorem 3.2.1 (First Fundamental Theorem - Björk [4]) *Consider a market model consisting of the asset price processes $S_0, S_1, \ldots, S_N$ on the time interval $[0, T]$. The market model is free of arbitrage if and only if there exists a martingale measure, i.e. a measure $Q \sim P$ such that the processes*

$$\frac{S_0(t)}{S_0(t)}, \frac{S_1(t)}{S_0(t)}, \ldots, \frac{S_N(t)}{S_0(t)}$$

are (local) martingales under Q. The numeraire process S_0 is assumed to be strictly positive.

From above it is clear that there is a strong connection between absence of arbitrage and martingales. Hence, the remainder of the section will be dedicated to introducing and defining various aspects relating to these concepts.

Rebonato [47] mentions that the forward rate processes, depending on the choice of numeraire and assuming absence of arbitrage, will be either martingales or semi-martingales (see Theorem 3.2.1 and the next chapter). However, given the financial requirement that these rates should be positive, we will focus our attention on strictly positive martingales as well as strictly positive

semi-martingales. Furthermore, the semi-martingale property allows us to decompose a forward rate process into previsible and surprise components. This is formally stated in the theorem below.

Theorem 3.2.2 (Doob-Meyer Decomposition - Rebonato [47]) *Each element in the set of strictly positive semi-martingales can be uniquely decomposed into the sum of a pure martingale component, referred to as the innovation part, and a previsible process, called the predictable part.*

Next, Rebonato [47] imposes the following condition on the innovation part of the Doob-Meyer decomposition. This is presented below.

Condition 3.2.1 (Innovation Restriction - Rebonato [47]) *As far as the martingale component of the Doob-Meyer decomposition is concerned, we will restrict our attention to innovations that are Wiener processes.*

The derivation of forward rate processes will be shown in the next chapter to be dependent on movements between different measures. Rebonato [47] mentions that these should be restricted to special sets of measures in order to preserve the properties presented in this section. These are presented below.

Definition 3.2.1 (Equivalent Measures - Rebonato [47]) *Two measures Q and P are said to be be equivalent (indicated by $Q \sim P$) if they share the same null set.*

Definition 3.2.2 (Equivalent Martingale Measures - Rebonato [47]) *A measure Q, equivalent to P, is said to be an equivalent martingale measure if the process X is a martingale with respect to both Q and P.*

The definitions and condition presented thus far constitutes the fundamental modeling choices as given by Rebonato [47]. Both Björk [4] and Rebonato [47] then go on to introduce useful tools that will be used in the derivation of the arbitrage-free forward rate processes.

The first theorem will provide us with an expression for the SDE of an martingale. This is presented in the theorem below.

Theorem 3.2.3 (Martingale Representation - Rebonato [47]) *Let M be a strictly positive martingale with respect to the filtration generated by a $Q-$Wiener process, W^Q be a standard Wiener process under Q and $\gamma(t)$ (not necessarily deterministic) be a real valued previsible process integrable with respect to W^Q. Then, given some technical conditions, it is aways possible to represent M in the form*

$$dM(t) = M(t)\gamma(t)dW^Q(t). \tag{3.2.1}$$

Using the results presented in this section, we are now in a position to present a very useful pricing formula. Let us consider a $T-$claim X, under the chosen martingale measure Q (note that this measure will only be unique if the market is complete). The price of this claim is given in the theorem below.

Theorem 3.2.4 (Martingale Pricing Formula- Björk [4]) *If absence of arbitrage is assumed, then the value of X is given by the formula*

$$\Pi(t;X) = S_0(t)E^Q\left[\frac{X}{S_0(T)}\middle|\mathcal{F}_t\right], \tag{3.2.2}$$

where Q is a martingale measure for $[S_0, S_1, \ldots, S_N]$, with S_0 as the numeraire.

The results presented thus far have illustrated that there is a clear link between arbitrage pricing and different measures. In particular, we know that if we assume or enforce the no-arbitrage condition, then there exists an equivalent martingale measure (Björk [4]). This measure can then in turn be used to price derivatives according to Equation (3.2.2). There is however no indication as to what impact this transformation will have on the processes of the underlying assets. This is presented in the theorem below (taken directly from Björk [4]).

Theorem 3.2.5 (Girsanov's Theorem - Björk [4]) *Let W^P be a d-dimensional standard $P-$Wiener process on $(\Omega, \mathcal{F}, P, \underline{\mathcal{F}})$ and let φ be any d-dimensional adapted column vector process. Choose a fixed T and define the process L on $[0,T]$ by*

$$\begin{aligned} dL_t &= \varphi_t' L_t dW_t^p, \\ L_0 &= 1, \end{aligned}$$

i.e.

$$L_t = e^{\int_0^t \varphi_s' \, dW_s^P - \frac{1}{2}\int_0^t \|\varphi_s\|^2 \, ds}.$$

Assume that

$$E^P[L_T] = 1,$$

and define the new probability measure Q on $\mathcal{F}_T$ by

$$L_T = \frac{dQ}{dP}, \text{ on } \mathcal{F}_T.$$

Then

$$dW_t^P = \varphi_t dt + dW_t^Q,$$

where W^Q is a $Q-$Wiener process.

This theorem provides us with the tool necessary to move between measures. A well known property of above result (can be seen through looking at the specification of dW_t^P) is that the change in measure will only affect the drift part of a stochastic processes. The following sections will derive useful techniques stemming from the results in this section.

3.3 Basic Change of Numeraire Concepts

The arguments presented below are extremely important to illustrate how the results derived up till now can be applied in a pricing framework. Due to its importance, and the part that it will play in following sections and chapters, the theory will once again closely follow the work of Björk [4] in an attempt to keep the discussion as accurate as possible. Therefore, please note that the aim of this section is to highlight an already derived result, and not to present a new framework. Björk [4] illustrates the use of the change of numeraire technique in the following setting.

Assume that we are interested in changing a martingale measure from a measure with numeraire S_0 to a measure with numeraire S_1. The associated martingale measures are indicated by Q^0 and Q^1 respectively. We know from Girsanov's Theorem 3.2.5 that this is possible through a suitable specification of the Girsanov kernel φ_t. However, the obvious question remains, i.e. how do we go about determining the value of this variable? Björk [4] suggests, that since we assume arbitrage free pricing, we know from Theorem 3.2.4 that the price processes (under the two different martingale measures) of an arbitrary $T-$claim X will be given by

$$\Pi(0;X) = S_0(0)E^0\left[\frac{X}{S_0(T)}\right], \tag{3.3.1}$$

and

$$\Pi(0;X) = S_1(0)E^1\left[\frac{X}{S_1(T)}\right]. \tag{3.3.2}$$

Note that the two price processes given above are expressed in expected values. This is promising considering the fact that it can be shown (outside the scope of this thesis) that expected values under two different probability measures are linked via a function called the Radon-Nikodym derivative (Björk [4]). Taking this into account and assuming some technicalities, Björk [4] then obtains the following result

$$S_0(0)E^0\left[\frac{X}{S_0(T)}\right] = S_1(0)E^0\left[\frac{X}{S_1(T)}\cdot L_0^1(T)\right], \tag{3.3.3}$$

where $L_0^1(T)$ represents the Radon-Nikodym derivative. From Equation (3.3.3) we then have that the likelihood process is given by

$$L_0^1(t) = \frac{S_0(0)}{S_1(0)}\cdot\frac{S_1(t)}{S_0(t)},\ 0 \le t \le T. \tag{3.3.4}$$

Girsanov's Theorem 3.2.5 indicate that we will be able to derive the Girsanov kernel φ_t once we have the dynamics of the likelihood process. Björk [4] mentions that the likelihood process is a nonnegative martingale under the measure

Q^0 with an initial value of 1.0 (see also Appendix A.3). Hence, through the use of Itô it is easy to determine that

$$dL_0^1(t) = \{\sigma_1(t) - \sigma_0(t)\}L_0^1(t)dW^0(t).$$

Thus, the Girsanov kernel $\varphi_0^1(t)$ for the transition from Q^0 to Q^1 is given by the volatility difference

$$\varphi_0^1(t) = \sigma_1(t) - \sigma_0(t). \tag{3.3.5}$$

3.4 Change of Numeraire Technique

The previous section illustrated some of the change of numeraire concepts and showed how the value of the Girsanov kernel $\varphi_0^1(t)$ can be obtained. The work presented so far on this subject mainly followed arguments by Björk [4]. We still need to extend this technique to show exactly what impact a change of numeraire will have on a process in the economy under consideration. This impact and a useful change of numeraire technique will be derived below. The technique will show what the new drift of a $T-$ claim X should be following a change in measure. From this we will for example be able to calculate no-arbitrage drifts of forward LIBOR rates in the following chapter. The derivation of this result will be based on the work Brigo and Mercurio [11]. Brigo and Mercurio [11] refer to this result as the change of numeraire toolkit in their book.

Let us assume as in the previous section that we have two numeraires S_0 and S_1. We will present the same dynamics for these assets as those given by Brigo and Mercurio [11]. Hence, these assets are assumed to evolve under Q^0 according to

$$dS_0(t) = (\ldots)dt + \sigma_0 C dW^0(t),$$
$$dS_1(t) = (\ldots)dt + \sigma_1 C dW^0(t),$$

where both σ_0 and σ_1 are $1 \times n-$vectors (can be dependent on S_0 and S_1 respectively), $W^0(t)$ is an $n-$dimensional driftless (under Q^0) standard Brownian Motion and the $n \times n$ matrix C is introduced to model correlation among the vector Wiener processes (CdW is equivalent to an $n-$dimensional Brownian motion with instantaneous correlation matrix $\rho = CC'$ - see Brigo and Mercurio [11] and Appendix A.5).

The reason for this type of correlation modeling, i.e. explicitly showing the matrix C, was chosen to illustrate the importance of the final result of this section. It will be shown that the formula representing the change in drift, when move from one measure to another, will not contain the matrix C. This will then enable us to easily apply the same formula to uncorrelated processes.

Next, Brigo and Mercurio [11] introduce a $T-$claim X into the model which will allow us to examine the dynamics of a derivative under different possible measures. In order to do this, let us firstly consider the dynamics of

the derivative under the measure associated with the numeraire asset S_0 (note that this measure will be indicated by Q^0). This is presented below.

The dynamics of the $T-$claim X under Q^0 is given by

$$dX(t) = \mu_X^0 dt + \sigma_X C dW^0(t), \tag{3.4.1}$$

where W^0 is a $n-$dimensional standard Brownian motion under Q^0. Assume that we are interested in expressing the dynamics of X under the measure associated with a new numeraire S_1. The dynamics will then be

$$dX(t) = \mu_X^1 dt + \sigma_X C dW^1(t), \tag{3.4.2}$$

where W^1 is a $n-$dimensional standard Brownian motion under Q^1.

Given the inclusion of the matrix C, it is easy to see that the Girsanov kernel, given by Equation (3.3.5), needs to be adjusted to

$$\varphi_0^1(t) = \frac{S_0(t)}{S_1(t)} \left[\sigma_t^{S_1/S_0} C\right]'. \tag{3.4.3}$$

The Girsanov kernel presented above was calculated through directly determining the dynamics of the likelihood process. Alternatively, we can calculate this variable through applying the main result Girsanov's Theorem 3.2.5. This is briefly explained below.

Changing the measure from Q^0 to Q^1 will, according to Girsanov's Theorem 3.2.5, imply a change in drift of the process of $X(t)$. Furthermore, from Equations (3.4.1)-(3.4.2), we have that the drift of the process will change from μ_X^0 to μ_X^1. This change in drift can be determined through applying Girsanov's Theorem 3.2.5 as follows.

$$\begin{aligned} dX(t) &= \mu_X^0 dt + \sigma_X C dW^0(t), \\ &= \mu_X^0 dt + \sigma_X C\{dW^1(t) + (\sigma_X C)^{-1}\left[\mu_X^1 - \mu_X^0\right] dt\}, \\ &= \mu_X^1 dt + \sigma_X C dW^1(t). \end{aligned}$$

From above, we have that the Girsanov kernel is also given by

$$\varphi_0^1(t) = (\sigma_X C)^{-1}\left[\mu_X^1 - \mu_X^0\right]. \tag{3.4.4}$$

Setting Equation (3.4.3) equal to Equation (3.4.4) and solving for μ_X^1, we obtain the following result

$$\mu_X^1 = \mu_X^0 + \frac{S_0(t)}{S_1(t)} \sigma_X \rho \left(\sigma_t^{S_1/S_0}\right)'.$$

The result presented above was derived for the general case in which no assumptions were made regarding the volatilities and drifts of the various processes.

We will now consider a specific case that will be used repeatedly in the next chapter. Let us assume that the volatilities of the numeraires and the process $X(t)$ are level proportional, i.e.

$$\begin{aligned}\sigma_0 &= v_0(t)S_0(t),\\ \sigma_1 &= v_1(t)S_1(t),\\ \sigma_X &= v_X(t)X(t),\end{aligned}$$

where the v's are deterministic $1 \times n$ vectors of time. Next, let us assume that the drift of $X(t)$ under Q^0 is given by

$$\mu_X^0 = m_X^0 X(t),$$

where m_X^0 is not necessarily a deterministic function of time. Then, using the results derived in this section, we have that m_X^1 is given by

$$m_X^1 dt = m_X^0 dt - (dlnX(t))(dln(S_0(t)/S_1(t))).$$

Note the importance of the last equation, i.e. not only does it provide us with the change in drift but is also independent of the terms ρ and C. This in turn implies that we can use this formula for both correlated as well as uncorrelated Wiener processes. Furthermore, it is worth mentioning that we did not restrict ourselves to the case in which the derivative is denominated in a specific numeraire, i.e. we did not restrict ourselves to drift-less processes. This is a necessary property for the next chapter and will be used frequently in the derivation of all forward LIBOR processes under a single measure. This technique is formally presented in the theorem below.

Theorem 3.4.1 (Change of Numeraire Technique - Brigo and Mercurio [11]) *Assume that the two numeraires S_0 and S_1 evolve under Q^0 according to*

$$\begin{aligned}dS_0(t) &= (\ldots)dt + \sigma_0 C dW^0(t),\\ dS_1(t) &= (\ldots)dt + \sigma_1 C dW^0(t),\end{aligned}$$

where both σ_0 and σ_1 are $1 \times n-$vectors (can be dependent on S_0 and S_1 respectively), $W^0(t)$ is an $n-$dimensional driftless (under Q^0) standard Brownian Motion and the $n \times n$ matrix C is introduced to model correlation among the vector Wiener processes (CdW is equivalent to an $n-$dimensional Brownian motion with instantaneous correlation matrix $\rho = CC'$). Similarly, the dynamics of the $T-$claim X under Q^0 is given by

$$dX(t) = \mu_X^0 dt + \sigma_X C dW^0(t).$$

Now suppose that we are interested in expressing the dynamics of X under the measure associated with a new numeraire S_1. The dynamics will then be

$$dX(t) = \mu_X^1 dt + \sigma_X C dW^1(t),$$

where W^1 is a $n-$dimensional standard Brownian motion under Q^1. We then have the following change-in-drift result

$$\mu_X^1 = \mu_X^0 + \frac{S_0(t)}{S_1(t)}\sigma_X \rho \left(\sigma_t^{S_1/S_0}\right)'. \tag{3.4.5}$$

Assume that the volatilities of the numeraires and the process $X(t)$ are level proportional, i.e.

$$\begin{aligned} \sigma_0 &= v_0(t)S_0(t), \\ \sigma_1 &= v_1(t)S_1(t), \\ \sigma_X &= v_X(t)X(t), \end{aligned}$$

where the v's are deterministic $1 \times n$ vectors of time. Next, assume that the drift of $X(t)$ under Q^0 is given by

$$\mu_X^0 = m_X^0 X(t),$$

where m_X^0 is not necessarily a deterministic function of time. Then we have that m_X^1 is given by

$$m_X^1\, dt = m_X^0\, dt - (dlnX(t))(dln(S_0(t)/S_1(t))). \tag{3.4.6}$$

Chapter 4

Forward Rate Dynamics

In order to price derivatives in the LIBOR and swap market models we need to know the dynamics of the underlying instruments. It was mentioned in Chapter 2 that we will use forward LIBOR rates as underlying instruments for the LIBOR market model and forward swap rates as underlying instruments for the swap market model. This chapter will mainly focus on the derivation of arbitrage-free processes for the LIBOR market model, however we will present a short section on the swap market model. The derivation of the different forward rate dynamics will be based on the change of numeraire technique presented in the previous chapter.

The sections in this chapter will be labeled and hence discussed according to the work by Götsch [22]. This provides a nice transition of ideas from the models that are linked to the Black [5] framework to the more general cases where we have to model several forward rates under the same measure.

4.1 Forward LIBOR Rate Process as a Martingale

Let us start the section by deriving some useful formulas with respect to forward LIBOR rates. According to Definition 3.1.1 the simple forward LIBOR rate at time t, for the time period between T_i and T_{i+1} , is defined as

$$L_{T_iT_{i+1}}(t) = -\frac{B(t,T_{i+1}) - B(t,T_i)}{\alpha_{T_iT_{i+1}} B(t,T_{i+1})}. \tag{4.1.1}$$

From Equation (4.1.1) we can derive the following two results (Götsch [22])

$$B(t,T_i) = (1 + \alpha_{T_iT_{i+1}} L_{T_iT_{i+1}}(t))B(t,T_{i+1}), \tag{4.1.2}$$

$$\alpha_{T_iT_{i+1}} L_{T_iT_{i+1}}(t) = \frac{B(t,T_i) - B(t,T_{i+1})}{B(t,T_{i+1})}. \tag{4.1.3}$$

Notice from Equation (4.1.3) that $\alpha_{T_iT_{i+1}} L_{T_iT_{i+1}}(t)$ expresses the market observable asset $B(t,T_i) - B(t,T_{i+1})$ in terms of the market observable asset $B(t,T_{i+1})$. If we assume that the market is arbitrage free and that the bond

$B(t, T_{i+1})$ is a valid numeraire (framework proposed by Rebonato [47] assumes that bond prices are strictly positive semi-martingales), then we have from Theorem 3.2.1 that $\alpha_{T_iT_{i+1}} L_{T_iT_{i+1}}(t)$ is a martingale under the martingale measure associated with the numeraire $B(t, T_{i+1})$ (Götsch [22] and Pelsser [44]). This measure is called the $T-$forward measure (Björk [4] and Hull[32]) and will be indicated with Q^{i+1}.

Since, $\alpha_{T_iT_{i+1}}$ is a constant, we have that $L_{T_iT_{i+1}}(t)$ is a martingale under Q^{i+1} (Götsch [22] and Pelsser [44]). Hence, we can model $L_{T_iT_{i+1}}(t)$ according to a driftless and strictly positive process under the measure Q^{i+1} (Pelsser [44]). This is presented below

$$dL_{T_iT_{i+1}}(t) = \sigma_{T_iT_{i+1}}(t) L_{T_iT_{i+1}}(t)\, dW^{i+1}(t), \tag{4.1.4}$$

where $W^{i+1}(t)$ (assumed to be scalar for now) represents the Wiener process under the probability measure Q^{i+1}. The volatility $\sigma_{T_iT_{i+1}}(t)$ of $L_{T_iT_{i+1}}(t)$ is assumed to be a deterministic function of time (Rebonato [47]).

From above it is evident that $L_{T_iT_{i+1}}(t)$ is a lognormal variable. This will consequently allow us to model each forward LIBOR rate as a lognormal variable under the associated forward measures. Hence, each caplet/floorlet can be priced in a manner which is consistent with the Black [5] framework (Brigo and Mercurio [11] and Rebonato [47]). Furthermore, the results can easily be extended to caps/floors since the underlying caplets/floorlets are independent variables. Rebonato [47] points out that this is a very favourable property for exotic traders. The model they use to value their exotic trades can now correctly recover the prices of some of the underlying instruments. This type of setting will then also imply simpler calibration strategies.

To conclude the section we present the relationship between the LMM and Black caplet volatilities

$$T_i \sigma^2_{T_iT_{i+1}.\text{caplet}} = \int_0^{T_i} \sigma^2_{T_iT_{i+1}}(t) dt, \tag{4.1.5}$$

where $\sigma_{T_iT_{i+1}.\text{caplet}}$ represents the Black caplet volatility. The proof of this result can be found in Appendix B.2.

The setting presented thus far is rather simplistic. In later sections we will consider the modeling of different forward LIBOR rates under the same measure. This will allow us to price derivatives that are dependent on more than one LIBOR rate at any given time (Götsch [22]). The framework will also be extended to the case where we have several driving factors which might be correlated.

4.2 Forward Swap Rate Process as a Martingale

We will now consider the market model that uses as underlying the forward swap rate. Similar to the previous section we will start the discussion through

presenting the formula used to calculate the forward swap rate.

According to Definition 3.1.3 we have that the swap rate at time t, for the swap starting at time T_s and maturing at time T_N, can be expressed as

$$SR_{s,N}(t) = \frac{B(t,T_s) - B(t,T_N)}{\sum_{i=s+1}^{N} B(t,T_i)\alpha_{T_{i-1}T_i}}. \tag{4.2.1}$$

Note from above that the numeraire in this case is a combination of market observable assets and will be indicated by

$$A_{s,N}(t) = \sum_{i=s+1}^{N} B(t,T_i)\alpha_{T_{i-1}T_i}. \tag{4.2.2}$$

Similar to the previous section we have from Equation (4.2.1) that $SR_{s,N}(t)$ expresses the market observable asset $B(t,T_s)-B(t,T_N)$ in terms of the market observable asset $A_{s,N}(t)$. If we assume that the market is arbitrage free and that the variable $A_{s,N}(t)$ is a valid numeraire, then we have from Theorem 3.2.1 that $SR_{s,N}(t)$ is a martingale under the martingale measure associated with the numeraire $A_{s,N}(t)$ (Hull [32]). This measure is called the forward swap measure (Brigo and Mercurio [11] and Hull[32]) and will be indicated with $Q^{s,N}$. Hence we can model $SR_{s,N}(t)$ according to a driftless and strictly positive process under the measure $Q^{s,N}$ (Brigo and Mercurio [11]). This is presented below

$$dSR_{s,N}(t) = \sigma_{s,N}(t)SR_{s,N}(t)\,dW^{s,N}(t), \tag{4.2.3}$$

where $W^{s,N}(t)$ (assumed to be scalar for now) represents the Wiener process under the probability measure $Q^{s,N}$. The volatility $\sigma_{s,N}(t)$ of $SR_{s,N}(t)$ is assumed to be a deterministic function of time (Rebonato [47]). We can now present the same findings as in the previous section.

From above it is evident that variable $SR_{s,N}(t)$ has a lognormal distribution. This will consequently allow us to model each forward swap rate as a lognormal variable under the associated forward swap measure. Hence, each swaption can be priced in a manner which is consistent with the Black [5] framework (Brigo and Mercurio [11] and Rebonato [47]).

The relationship between the LMM and Black swaption volatilities is presented below

$$T_n V_{n,N}^2 = \int_0^{T_n} \sigma_{n,N}^2(t)dt, \tag{4.2.4}$$

where $V_{n,N}$ represents the Black swaption volatility. The proof of this result can be found in Appendix B.3.

It is important to point out that the two models introduced thus far are not compatible (Brigo and Mercurio [11] and Rebonato [47]). This can for example be seen trough noting that forward LIBOR rates and forward swap rates cannot be martingales under the same measure. The rest of the thesis will

however only focus on the LIBOR market model and hence the swap market model was only included for completeness.

If we only want to model interest rate derivatives within the LIBOR market model framework, then we need to introduce a mechanism for modeling the joint dynamics of several forward rates. This is due to the fact that the payoff of some derivatives, like interest rate swaptions, are dependent on more than one forward rate at the same time. This extension of the LIBOR market model will be discussed in the following sections.

4.3 Forward LIBOR Rates under the Forward Measure

In this section we will derive the drifts of forward LIBOR rates under different forward measures. We will still assume that the process of the LIBOR rate under consideration is driven by a scalar Wiener process. We will extend this in a later section to several Wiener processes that may be correlated. Note that the spot measure, i.e. the measure associated the zero coupon bond with maturity equal to the reset date, will not be considered here (Götsch [22]).

Recall from the previous section that the the dynamics of the forward rate $L_{T_iT_{i+1}}(t)$ under the measure Q^{i+1} is given by

$$dL_{T_iT_{i+1}}(t) = \sigma_{T_iT_{i+1}}(t)L_{T_iT_{i+1}}(t)\,dW^{i+1}(t),$$

where the Wiener process $W^{i+1}(t)$ is assumed to be a scalar function. Suppose now that we are interested in changing the numeraire to the zero coupon bond with maturity T_i (Götsch [22]). We know from Girsanov's Theorem 3.2.5 that this will result in a change in drift of the process given above. In order to determine the exact change, we will use the change in numeraire technique derived in the previous chapter (Brigo and Mercurio [11]). The argument presented below will follow the work by Götsch [22].

From Equation (3.4.6) we have that

$$\begin{aligned} m_L^i\,dt &= -d\ln L_{T_iT_{i+1}}(t)\,d\ln\left(\frac{B(t,T_{i+1})}{B(t,T_i)}\right), \\ &= d\ln L_{T_iT_{i+1}}(t)\,d\ln(1+\alpha_{T_iT_{i+1}}L_{T_iT_{i+1}}(t)), \end{aligned}$$

since, from Equation (4.1.2), we have that

$$\ln\left(\frac{B(t,T_{i+1})}{B(t,T_i)}\right) = -\ln(1+\alpha_{T_iT_{i+1}}L_{T_iT_{i+1}}(t)).$$

Furthermore, through the use of Itô we get that

$$d\ln L_{T_iT_{i+1}}(t) = (\cdots)dt + \sigma_{T_iT_{i+1}}(t)\,dW^i(t),$$

and

$$d\ln(1+\alpha_{T_iT_{i+1}}L_{T_iT_{i+1}}(t)) = (\cdots)dt + \frac{\alpha_{T_iT_{i+1}}\sigma_{T_iT_{i+1}}(t)L_{T_iT_{i+1}}(t)}{1+\alpha_{T_iT_{i+1}}L_{T_iT_{i+1}}(t)}\,dW^i(t).$$

Hence, according to Equation (3.4.6), we have that

$$m_L^i = \frac{\alpha_{T_iT_{i+1}}\sigma_{T_iT_{i+1}}(t)L_{T_iT_{i+1}}(t)}{1+\alpha_{T_iT_{i+1}}L_{T_iT_{i+1}}(t)}\sigma_{T_iT_{i+1}}(t).$$

Given above, and the assumption that forward LIBOR rates are lognormally distributed under the associated forward measure, we have that

$$\begin{aligned} dL_{T_iT_{i+1}}(t) &= \frac{\alpha_{T_iT_{i+1}}\sigma_{T_iT_{i+1}}(t)L_{T_iT_{i+1}}(t)}{1+\alpha_{T_iT_{i+1}}L_{T_iT_{i+1}}(t)}\sigma_{T_iT_{i+1}}(t)L_{T_iT_{i+1}}dt \\ &+ \sigma_{T_iT_{i+1}}(t)L_{T_iT_{i+1}}(t)\,dW^i(t). \end{aligned}$$

Using above technique repeatedly, the process for $L_{T_iT_{i+1}}(t)$ under Q^{m+1}, where $m+1 < i+1$, will be given by

$$\begin{aligned} dL_{T_iT_{i+1}}(t) &= \sum_{j=m+1}^{i}\frac{\alpha_{T_jT_{j+1}}\sigma_{T_jT_{j+1}}(t)L_{T_jT_{j+1}}(t)}{1+\alpha_{T_jT_{j+1}}L_{T_jT_{j+1}}(t)}\sigma_{T_iT_{i+1}}(t)L_{T_iT_{i+1}}dt \\ &+ \sigma_{T_iT_{i+1}}(t)L_{T_iT_{i+1}}(t)\,dW^{m+1}(t). \end{aligned}$$

To show the application of above methodology for the case where we change the numeraire to zero coupon bonds with longer maturities than $i+1$, the process for $L_{T_iT_{i+1}}(t)$ under Q^{i+2} is taken (Götsch [22]).

From Equation (3.4.6) we have that

$$m_L^{i+2}\,dt = -d\ln L_{T_iT_{i+1}}(t)\,d\ln(1+\alpha_{T_{i+1}T_{i+2}}L_{T_{i+1}T_{i+2}}(t)),$$

since, from Equation (4.1.2), we have that

$$\ln\left(\frac{B(t,T_{i+1})}{B(t,T_{i+2})}\right) = \ln(1+\alpha_{T_{i+1}T_{i+2}}L_{T_{i+1}T_{i+2}}(t)).$$

If we now follow the same procedure as previously, then we obtain the dynamics for $L_{T_iT_{i+1}}(t)$ under Q^{N+1}, where $N+1 > i+1$, as

$$\begin{aligned} dL_{T_iT_{i+1}}(t) &= -\sum_{j=i+1}^{N}\frac{\alpha_{T_jT_{j+1}}\sigma_{T_jT_{j+1}}(t)L_{T_jT_{j+1}}(t)}{1+\alpha_{T_jT_{j+1}}L_{T_jT_{j+1}}(t)}\sigma_{T_iT_{i+1}}(t)L_{T_iT_{i+1}}dt \\ &+ \sigma_{T_iT_{i+1}}(t)L_{T_iT_{i+1}}(t)\,dW^{N+1}(t). \end{aligned}$$

Above results are summarized in the following theorem. The format of the theorem is the same as that of Brigo and Mercurio [11].

Theorem 4.3.1 (Forward LIBOR Dynamics Assuming A Scalar Wiener Process - Brigo and Mercurio [11]) *Given above assumptions, we obtain that the dynamics of $L_{T_iT_{i+1}}(t)$ under the forward measure T_{k+1} in the three cases $k+1 < i+1$, $k+1 = i+1$ and $k+1 > i+1$ are, respectively,*

$k+1 < i+1, t \leq T_{k+1}$:

$$dL_{T_iT_{i+1}}(t) = \sum_{j=k+1}^{i} \frac{\alpha_{T_jT_{j+1}}\sigma_{T_jT_{j+1}}(t)L_{T_jT_{j+1}}(t)}{1+\alpha_{T_jT_{j+1}}L_{T_jT_{j+1}}(t)}\sigma_{T_iT_{i+1}}(t)L_{T_iT_{i+1}}dt + \sigma_{T_iT_{i+1}}(t)L_{T_iT_{i+1}}(t)\,dW^{k+1}(t),$$

$k+1 = i+1, t \leq T_i$:

$$dL_{T_iT_{i+1}}(t) = \sigma_{T_iT_{i+1}}(t)L_{T_iT_{i+1}}(t)\,dW^{k+1}(t),$$

$k+1 > i+1, t \leq T_i$:

$$dL_{T_iT_{i+1}}(t) = -\sum_{j=i+1}^{k} \frac{\alpha_{T_jT_{j+1}}\sigma_{T_jT_{j+1}}(t)L_{T_jT_{j+1}}(t)}{1+\alpha_{T_jT_{j+1}}L_{T_jT_{j+1}}(t)}\sigma_{T_iT_{i+1}}(t)L_{T_iT_{i+1}}dt + \sigma_{T_iT_{i+1}}(t)L_{T_iT_{i+1}}(t)\,dW^{k+1}(t),$$

where, as explained before, $W^{k+1}(t)$ (assumed to be scalar for now) represents the Wiener process under the probability measure Q^{k+1}.

From the above we can note that $L_{T_iT_{i+1}}(t)$ is a martingale only with the numeraire $k+1 = i+1$ (Götsch [22]). Under numeraires with $k+1 \neq i+1$ the LIBOR rate has a drift, which depends on forward LIBOR rates (Brigo and Mercurio [11]).

4.4 Extension to Several Factors

The dynamics of forward rates derived above, can only be used to price derivatives whose payoffs can be decomposed into a set of independent payoffs which in turn is only dependent on a single forward rate (Götsch [22]). If however, the payoff depends on several forward rates at the same time, then the correlation between different forward rates affects the payoff and must therefore be considered (Brigo and Mercurio [11], Götsch [22] and Rebonato [47]).

We will consider two methods that can be used to model several factors. These will be similar to those discussed by Rebonato [47]. The first approach will model forward rates using n orthogonal Wiener processes. This approach will lead to a covariance matrix that is entirely expressed in terms of the volatility vectors. The second approach will use a similar methodology to that used in Section 3.4, i.e. we will introduce matrices that will allow the explicit modeling of correlation among different forward rates. These approaches are presented below.

4.4.1 Uncorrelated Factors

We will firstly consider the case in which we have n orthogonal Wiener processes (Götsch [22]). The dynamics of $L_{T_iT_{i+1}}(t)$ under Q^{i+1} is then given by

$$dL_{T_iT_{i+1}}(t) = \sigma_{T_iT_{i+1}}(t)L_{T_iT_{i+1}}(t)\,dW^{i+1}(t),$$

where $W^{i+1}(t)$ is the $n \times 1$ vector

$$W^{i+1}(t) = \begin{bmatrix} W_1^{i+1}(t) \\ \vdots \\ W_n^{i+1}(t) \end{bmatrix},$$

and $\sigma_{T_iT_{i+1}}(t)$ the $1 \times n$ vector

$$\sigma_{T_iT_{i+1}}(t) = [\sigma_{T_iT_{i+1},1}(t), \ldots, \sigma_{T_iT_{i+1},n}(t)].$$

The elements of the vector $\sigma_{T_iT_{i+1}}(t)$ contains the sensitivities of the forward rate $L_{T_iT_{i+1}}(t)$ towards the different orthogonal Wiener processes. It can be seen that the covariance matrix between the different forward rates is given by (Rebonato [47])

$$\Sigma = \sigma\sigma^{'}. \tag{4.4.1}$$

Consider, as in the previous section, the case where the numeraire is changed to the zero coupon bond with maturity T_i. Then we have from Equation (3.4.6) that

$$\begin{aligned} m_L^i\,dt &= d\ln L_{T_iT_{i+1}}(t)\,d\ln(1+\alpha_{T_iT_{i+1}}L_{T_iT_{i+1}}(t)), \\ &= \frac{\alpha_{T_iT_{i+1}}L_{T_iT_{i+1}}(t)}{1+\alpha_{T_iT_{i+1}}L_{T_iT_{i+1}}(t)}\sigma_{T_iT_{i+1}}(t)(dW^i)(dW^i)'\sigma_{T_iT_{i+1}}(t)', \\ &= \frac{\alpha_{T_iT_{i+1}}L_{T_iT_{i+1}}(t)}{1+\alpha_{T_iT_{i+1}}L_{T_iT_{i+1}}(t)}\sigma_{T_iT_{i+1}}(t)D[1]\sigma_{T_iT_{i+1}}(t)'\,dt, \end{aligned}$$

where $D[1]$ denotes the diagonal matrix

$$\begin{bmatrix} 1 & 0 & \ldots & 0 \\ 0 & 1 & \ldots & 0 \\ \vdots & \vdots & \ddots & \vdots \\ 0 & 0 & \ldots & 1 \end{bmatrix}.$$

Hence, we have that

$$m_L^i = \frac{\alpha_{T_iT_{i+1}}L_{T_iT_{i+1}}(t)\sum_{q=1}^{n}\sigma_{T_iT_{i+1},q}(t)\sigma_{T_iT_{i+1},q}(t)}{1+\alpha_{T_iT_{i+1}}L_{T_iT_{i+1}}(t)}.$$

Given above, and the assumption that forward LIBOR rates are lognormally distributed under the associated forward measure, we have that

$$\begin{aligned} dL_{T_iT_{i+1}}(t) &= \frac{\alpha_{T_iT_{i+1}} L_{T_iT_{i+1}}(t) \sum_{q=1}^{n} \sigma_{T_iT_{i+1},q}(t)\sigma_{T_iT_{i+1},q}(t)}{1+\alpha_{T_iT_{i+1}} L_{T_iT_{i+1}}(t)} L_{T_iT_{i+1}}(t)dt \\ &+ \sigma_{T_iT_{i+1}}(t) L_{T_iT_{i+1}}(t)\, dW^{i}(t). \end{aligned}$$

Using above technique repeatedly, the process for $L_{T_iT_{i+1}}(t)$ under Q^{k+1}, where $k+1<i+1$, will be given by

$$dL_{T_iT_{i+1}}(t) = \sum_{j=k+1}^{i} \frac{\alpha_{T_jT_{j+1}} L_{T_jT_{j+1}}(t) \sum_{q=1}^{n} \sigma_{T_jT_{j+1},q}(t)\sigma_{T_iT_{i+1},q}(t)}{1+\alpha_{T_jT_{j+1}} L_{T_jT_{j+1}}(t)} L_{T_iT_{i+1}}(t)dt$$
$$+ \sigma_{T_iT_{i+1}}(t) L_{T_iT_{i+1}}(t)\, dW^{k+1}(t).$$

Following similar arguments we can derive the dynamics of $L_{T_iT_{i+1}}(t)$ for the case where $k+1>i+1$. The results are summarized in the following theorem (Brigo and Mercurio [11]).

Theorem 4.4.1 (Forward LIBOR Dynamics Assuming Uncorrelated Wiener Processes - Brigo and Mercurio [11]) *Given above assumptions, we obtain that the dynamics of $L_{T_iT_{i+1}}(t)$ under the forward measure T_{k+1} in the three cases $k+1<i+1$, $k+1=i+1$ and $k+1>i+1$ are, respectively,*

$k+1<i+1, t\le T_{k+1}$:

$$\begin{aligned} &dL_{T_iT_{i+1}}(t) = \\ &\sum_{j=k+1}^{i} \frac{\alpha_{T_jT_{j+1}} L_{T_jT_{j+1}}(t) \sum_{q=1}^{n} \sigma_{T_jT_{j+1},q}(t)\sigma_{T_iT_{i+1},q}(t)}{1+\alpha_{T_jT_{j+1}} L_{T_jT_{j+1}}(t)} L_{T_iT_{i+1}}(t)dt \\ &+ \sigma_{T_iT_{i+1}}(t) L_{T_iT_{i+1}}(t)\, dW^{k+1}(t), \end{aligned}$$

$k+1=i+1, t\le T_i$:

$$dL_{T_iT_{i+1}}(t) = \sigma_{T_iT_{i+1}}(t) L_{T_iT_{i+1}}(t)\, dW^{k+1}(t),$$

$k+1>i+1, t\le T_i$:

$$\begin{aligned} &dL_{T_iT_{i+1}}(t) = \\ &-\sum_{j=k+1}^{i} \frac{\alpha_{T_jT_{j+1}} L_{T_jT_{j+1}}(t) \sum_{q=1}^{n} \sigma_{T_jT_{j+1},q}(t)\sigma_{T_iT_{i+1},q}(t)}{1+\alpha_{T_jT_{j+1}} L_{T_jT_{j+1}}(t)} L_{T_iT_{i+1}}(t)dt \\ &+ \sigma_{T_iT_{i+1}}(t) L_{T_iT_{i+1}}(t)\, dW^{k+1}(t), \end{aligned}$$

where $W^{k+1}(t)$ represents the uncorrelated Wiener process under the probability measure Q^{k+1}.

4.4.2 Correlated Factors

Now consider the case in which we have n correlated Wiener processes. The dynamics of $L_{T_iT_{i+1}}(t)$ under Q^{i+1} is then given by

$$dL_{T_iT_{i+1}}(t) = \sigma_{T_iT_{i+1}}(t)L_{T_iT_{i+1}}(t)\, dW^{i+1}_{T_iT_{i+1}}(t),$$

where the scalar $W^{i+1}_{T_iT_{i+1}}(t) = C_{T_iT_{i+1}}\overline{W}^{i+1}(t)$. The vector $\overline{W}^{i+1}(t)$ is defined as a $n \times 1$ vector of uncorrelated Wiener processes and is given by

$$\overline{W}^{i+1}(t) = \begin{bmatrix} \overline{W}^{i+1}_1(t) \\ \vdots \\ \overline{W}^{i+1}_n(t) \end{bmatrix}.$$

Note that the volatility $\sigma_{T_iT_{i+1}}(t)$ in this setting is assumed to be a deterministic scalar process.

It is worth mentioning again that the $n \times n$ matrix C was included to model correlation among the different forward rates. The correlation matrix in this setting will be given by (see Rebonato [47] and Section A.5))

$$\rho = CC'. \tag{4.4.2}$$

Consider the case where the numeraire is changed to the zero coupon bond with maturity T_i. Then we have from Equation (3.4.6) that

$$\begin{aligned} m^i_L\, dt &= d\ln L_{T_iT_{i+1}}(t)\, d\ln(1+\alpha_{T_iT_{i+1}}L_{T_iT_{i+1}}(t)), \\ &= \frac{\alpha_{T_iT_{i+1}}L_{T_iT_{i+1}}(t)}{1+\alpha_{T_iT_{i+1}}L_{T_iT_{i+1}}(t)}\sigma_{T_iT_{i+1}}(t)(dW^i_{T_iT_{i+1}})(dW^i_{T_iT_{i+1}})'\sigma_{T_iT_{i+1}}(t), \\ &= \frac{\alpha_{T_iT_{i+1}}L_{T_iT_{i+1}}(t)}{1+\alpha_{T_iT_{i+1}}L_{T_iT_{i+1}}(t)}\sigma_{T_iT_{i+1}}(t)\rho_{L(i,i+1);L(i,i+1)}\sigma_{T_iT_{i+1}}(t)\, dt, \end{aligned}$$

where $\rho_{L(i,i+1);L(i,i+1)}$ is the instantaneous correlation between $L_{T_iT_{i+1}}(t)$ and $L_{T_iT_{i+1}}(t)$. Hence, we have that

$$m^i_L = \frac{\rho_{L(i,i+1);L(i,i+1)}\alpha_{T_iT_{i+1}}L_{T_iT_{i+1}}(t)\sigma_{T_iT_{i+1}}(t)}{1+\alpha_{T_iT_{i+1}}L_{T_iT_{i+1}}(t)}\sigma_{T_iT_{i+1}}(t).$$

Given above, and the assumption that forward LIBOR rates are lognormally distributed under the associated forward measure, we have that

$$\begin{aligned} &dL_{T_iT_{i+1}}(t) = \\ &\frac{\rho_{L(i,i+1);L(i,i+1)}\alpha_{T_iT_{i+1}}L_{T_iT_{i+1}}(t)\sigma_{T_iT_{i+1}}(t)}{1+\alpha_{T_iT_{i+1}}L_{T_iT_{i+1}}(t)}\sigma_{T_iT_{i+1}}(t)L_{T_iT_{i+1}}(t)dt \\ &+ \sigma_{T_iT_{i+1}}(t)L_{T_iT_{i+1}}(t)\, dW^i(t). \end{aligned}$$

Using above technique repeatedly, the process for $L_{T_iT_{i+1}}(t)$ under Q^{k+1}, where $k+1 < i+1$, will be given by

$$dL_{T_iT_{i+1}}(t) =$$
$$\sum_{j=k+1}^{i} \frac{\rho_{L(i,i+1);L(j,j+1)}\alpha_{T_jT_{j+1}}L_{T_jT_{j+1}}(t)\sigma_{T_jT_{j+1}}(t)}{1+\alpha_{T_jT_{j+1}}L_{T_jT_{j+1}}(t)}\sigma_{T_iT_{i+1}}(t)L_{T_iT_{i+1}}(t)dt$$
$$\sigma_{T_iT_{i+1}}(t)L_{T_iT_{i+1}}(t)\,dW^{k+1}(t).$$

Following similar arguments we can derive the dynamics of $L_{T_iT_{i+1}}(t)$ for the case where $k+1 > i+1$. The results are summarized in the following theorem (Brigo and Mercurio [11]).

Theorem 4.4.2 (Forward LIBOR Dynamics Assuming Correlated Wiener Processes - Brigo and Mercurio [11]) *Given above assumptions, we obtain that the dynamics of $L_{T_iT_{i+1}}(t)$ under the forward measure T_{k+1} in the three cases $k+1 < i+1$, $k+1 = i+1$ and $k+1 > i+1$ are, respectively,*

$k+1 < i+1, t \leq T_{k+1}$:

$$dL_{T_iT_{i+1}}(t) =$$
$$\sum_{j=k+1}^{i} \frac{\rho_{L(i,i+1);L(j,j+1)}\alpha_{T_jT_{j+1}}L_{T_jT_{j+1}}(t)\sigma_{T_jT_{j+1}}(t)}{1+\alpha_{T_jT_{j+1}}L_{T_jT_{j+1}}(t)}\sigma_{T_iT_{i+1}}(t)L_{T_iT_{i+1}}(t)dt$$
$$+\,\sigma_{T_iT_{i+1}}(t)L_{T_iT_{i+1}}(t)\,dW^{k+1}(t),$$

$k+1 = i+1, t \leq T_i$:

$$dL_{T_iT_{i+1}}(t) = \sigma_{T_iT_{i+1}}(t)L_{T_iT_{i+1}}(t)\,dW^{k+1}(t),$$

$k+1 > i+1, t \leq T_i$:

$$dL_{T_iT_{i+1}}(t) =$$
$$-\sum_{j=k+1}^{i} \frac{\rho_{L(i,i+1);L(j,j+1)}\alpha_{T_jT_{j+1}}L_{T_jT_{j+1}}(t)\sigma_{T_jT_{j+1}}(t)}{1+\alpha_{T_jT_{j+1}}L_{T_jT_{j+1}}(t)}\sigma_{T_iT_{i+1}}(t)L_{T_iT_{i+1}}(t)dt$$
$$+\,\sigma_{T_iT_{i+1}}(t)L_{T_iT_{i+1}}(t)\,dW^{k+1}(t),$$

where $W^{k+1}(t)$ represents the correlated Wiener process under the probability measure Q^{k+1}.

Chapter 5

Volatility Modeling

The previous chapter showed that the dynamics of forward LIBOR rates are expressed in terms of the instantaneous volatility and correlation functions. From this it is evident that these two functions play an important role in the LIBOR market model. This chapter will consider different possible volatility specifications that can be grouped into two main categories, namely piecewise-constant and parametric.

Rebonato [47] points out that the market for instantaneous volatilities is incomplete (discussed in Section 2.4.2). This implies that we cannot imply unique volatility functions from the market and hence are forced to make certain assumptions regarding these functions. These assumptions will in turn have a significant impact on the valuation of exotic interest rate options (as well as the valuation of swaptions within the LMM framework) and hence it is important to make sure that the assumptions are financially plausible (Rebonato [47]).

In order to examine the properties of some of the volatility specifications, we need to define a concept called the term structure of volatilities and what it implies if the volatility specification is said to be time-homogeneous.

5.1 The Term Structure of Volatilities

The definition of the term structure of volatilities is as given by Brigo and Mercurio [11]. Let us consider the economy defined in Section 3.1, i.e. we have a set of times $\Omega = \{T_0, \ldots, T_M\}$ representing adjacent expiry-maturity pairs for a family of spanning forward rates.

Brigo and Mercurio [11] then defines the term structure of volatilities at time T_j as a graph of expiry times T_{h-1} against average volatilities $V(T_j, T_{h-1})$ of the forward rates $L_{T_{h-1}T_h}(t)$ up to that expiry time itself. In other words, we have that the term structure of volatilities at time $t = T_j$ is the graph of the points

$$\{(T_{j+1}, V(T_j, T_{j+1})), (T_{j+2}, V(T_j, T_{j+2})), \ldots, (T_{M-1}, V(T_j, T_{M-1}))\},$$

where for $h > j + 1$

$$V^2(T_j, T_{h-1}) = \frac{1}{\alpha_{T_j T_{h-1}}} \int_{T_j}^{T_{h-1}} \sigma^2_{T_{h-1}T_h}(t)\, dt. \tag{5.1.1}$$

The first obvious property of the term structure of volatilities, as defined above, is that different instantaneous volatility functions will imply different evolutions of the term structure of volatilities (Brigo and Mercurio [11]).

Secondly, note that the term structure of volatilities today is given by a graph consisting of forward rate expiries vs. market observable Black volatilities (Brigo and Mercurio [11] and Rebonato [47]). The Black volatilities are the caplet volatilities obtained from market quotations.

5.2 Time-Homogeneous Volatilities

Brigo and Mercurio [11] and Rebonato [47] defines the evolution of the term structure of volatilities as time-homogeneous if certain key characteristics of the current term structure is reflected in future term structures (in a strictly theoretical sense we would expect the term structure to remain exactly the same). These key characteristics can for example be the humped shape observable in caplet volatilities or the property that long term volatilities are lower than short term volatilities (depending on the current term structure). In general, if the term structure of volatilities is said to be time-homogeneous of nature, then we expect the bulk of the change to be in the level of volatilities.

These authors independently pointed out the importance of time-homogeneous volatilities. They mention that it is observable from market data that the shape of the term structure of volatilities can remain the same for significant time periods. Furthermore, Rebonato [47] mentions that the model can be extended to incorporate random changes in the term structure (will however not be considered in this thesis). Given above description and Equation (5.1.1), we have that the term structure of volatilities will be time-homogeneous if the instantaneous volatilities satisfy the following (Rebonato [47])

$$\int_{T_j}^{T_{h-1}} \sigma^2_{T_{h-1}T_h}(t)\, dt = \int_{T_j+\tau}^{T_{h-1}+\tau} \sigma^2_{T_{h-1}+\tau T_h+\tau}(t)\, dt. \tag{5.2.1}$$

It can easily be shown that this equation will be satisfied when the instantaneous volatility functions depend on the time to maturity of a specific forward rate (Rebonato [47]), i.e. if

$$\sigma_{T_{h-1}T_h}(t) = \sigma(T_{h-1} - t). \tag{5.2.2}$$

This is an important property and will be used frequently in the specification of time-homogeneous volatility functions. Recall that we mentioned earlier that

today's term structure of volatilities are given by the market caplet volatilities. Rebonato [47] points out that it is not always possible to find instantaneous volatility functions of the form given by Equation (5.2.2) that are consistent with today's caplet prices (and hence with today's market implied term structure of volatilities).

It is however possible to show that, given a volatility specification according to Equation (5.2.2), we will always be able to recover today's caplet prices if $T_i\sigma^2_{T_iT_{i+1}.\text{caplet}}$ is a strictly increasing function of T_i (Rebonato [47]). If these quantities are not strictly increasing, then the market imply a change in the shape of the term structure of volatilities.

The calibration difficulties discussed above relates to fact that we are trying to impose a certain financial criteria on the term structure of volatilities (i.e. a strictly time-homogeneous evolution). Without this assumption we will be able to recover caplet prices, however the evolution of the term structure might then be financially implausible.

It will be shown at a later stage that given the case where $T_i\sigma^2_{T_iT_{i+1}.\text{caplet}}$ is not a strictly increasing function of T_i, we can adjust the volatility specification in Equation (5.2.2) to ensure both the exact pricing of caplets as well as a time-homogeneous term structure (at least approximately). The calibration of such a structure will consist of two steps, one where we enforce time-homogeneity as best as possible and the next where we make the adjustments necessary for the correct pricing of today's caplets (Rebonato [47]).

We will now introduce different volatility specifications. It was mentioned earlier that the different volatility specifications will be divided into piecewise constant and parametric volatility structures. We will firstly consider piecewise constant volatilities as given by Brigo and Mercurio [11].

5.3 Piecewise Constant Volatility Structure

This section will define different types of piecewise constant volatility structures as given by Brigo and Mercurio [11]. Some of these specifications will then be used in later chapters where we calibrate the LIBOR market model to market data. These structures are also known as non-parametric volatility specifications (Gatarek, Bachert and Maksymiuk [21]).

5.3.1 General Structure

The most general piecewise constant volatility structure is presented in Table 5.1. Given the nature of this specification, we are not able to deduce any qualitative properties for the defined volatility functions. This is due to the fact that there exist an infinity of ways in which we can exactly recover today's term structure (Rebonato [47]). It is however important to notice the following properties of the structure at hand. Firstly, let us consider the expiry-maturity structure of the volatility functions. Each forward rate is assumed to be alive

in the time periods preceding its reset date. Following the reset date, the rate is fixed and hence the volatilities in these time periods are marked as "Dead". Secondly, it is evident that the integral in Equation (5.1.1) can now be replaced with a summation over the piecewise constant parts. Thirdly, as time approaches the reset date of the nearest forward rate, we will loose both the first row as well as the first column of the volatility matrix. This property can be used to determine if a volatility specification is time-homogeneous.

	Time: $t \in (0, T_0]$	$(T_0, T_1]$	$(T_1, T_2]$	...	$(T_{M-2}, T_{M-1}]$
$L_{T_0T_1}(t)$	$\sigma_{1,1}$	Dead	Dead	...	Dead
$L_{T_1T_2}(t)$	$\sigma_{2,1}$	$\sigma_{2,2}$	Dead	...	Dead
$\vdots$	...	...	...	...	...
$L_{T_{M-1}T_M}(t)$	$\sigma_{M,1}$	$\sigma_{M,2}$	$\sigma_{M,3}$	...	$\sigma_{M,M}$

Table 5.1: Piecewise constant volatility matrix for the most general instantaneous volatility specification.

As mentioned earlier, the structure specified in Table 5.1 is very general. We will now consider a series of assumptions that can be made on the entries of Table 5.1. This will in turn generate new volatility specifications which are a subset of the general specification. The details of these assumptions, as well as the implied properties, are presented below.

5.3.2 Dependence on Time to Maturity

The first assumption made by Brigo and Mercurio [11] on the entries of Table 5.1 is that the volatilities only depend on the time to maturity of the forward rate under consideration. This will result in the volatility matrix given in Table 5.2. Notice that this specification satisfies Equation (5.2.2) and hence we

	Time: $t \in (0, T_0]$	$(T_0, T_1]$	$(T_1, T_2]$	...	$(T_{M-2}, T_{M-1}]$
$L_{T_0T_1}(t)$	η_1	Dead	Dead	...	Dead
$L_{T_1T_2}(t)$	η_2	η_1	Dead	...	Dead
$\vdots$	...	...	...	...	...
$L_{T_{M-1}T_M}(t)$	η_M	η_{M-1}	η_{M-2}	...	η_1

Table 5.2: Piecewise constant volatility matrix where instantaneous volatilities depend on the time-to-maturity of the forward rate.

have that the term structure of volatilities will evolve in a time-homogeneous manner. This can also be seen through observing that the resulting volatility matrix, following a reset in the nearest expiry forward rate, is effectively the same as the original volatility matrix (Brigo and Mercurio [11]). The only

difference between the two matrices is that the new matrix will contain one less forward rate (assuming we do not introduce a new forward rate). This change is observed in the tail of the term structure (Brigo and Mercurio [11]).

Recall from the previous section that it will not always be possible to fit this structure to a market caplet term structure. We will only be able to use this in the case where the quantities $T_i\sigma^2_{T_iT_{i+1}.\text{caplet}}$ is a strictly increasing function of T_i. When this is not the case the procedure will produce imaginary forward rate volatilities (Rebonato [47]). This will be illustrated in later calibration examples.

5.3.3 Dependence on Maturity

The second assumption made by Brigo and Mercurio [11] on the entries of Table 5.1 is that the volatilities only depend on the maturity of the considered forward rate. This will result in the volatility matrix given in Table 5.3.

	Time: $t \in (0, T_0]$	$(T_0, T_1]$	$(T_1, T_2]$	...	$(T_{M-2}, T_{M-1}]$
$L_{T_0T_1}(t)$	s_1	Dead	Dead	...	Dead
$L_{T_1T_2}(t)$	s_2	s_2	Dead	...	Dead
$\vdots$	...	...	...	...	...
$L_{T_{M-1}T_M}(t)$	s_M	s_M	s_M	...	s_M

Table 5.3: Piecewise constant volatility matrix where instantaneous volatilities depend on the maturity of the forward rate.

This volatility specification does not result in a time-homogeneous evolution of the term structure. We can see this through removing the first row and column and noticing that the resulting matrix is different from the first. The structure can however be fitted to any initial term structure. This advantage is, however, overshadowed by its lack of financial plausibility and hence is unlikely to be implemented in practice (Rebonato [47]).

5.3.4 Separable Volatilities

The volatility specifications presented thus far only consisted of single factors. The final two assumptions made by Brigo and Mercurio [11] on the entries of Table 5.1 are intended to extend the range of defined factors.

These specifications are derived from volatility specifications with factors representing dependence on time and time to maturity. The only difference is the addition of the parameters indicated with Φ. When applying Equation (5.1.1) to these structures, it is easy to see that the Φ parameters can be taken outside of the summation. This is one of the properties that renders these as separable structures.

Given above, these structures then allow for the exact recovery of market observable caplet prices. This can be achieved through expressing the Φ's in terms of the Ψ's and the market caplet volatilities. The parameters Ψ, together with the instantaneous correlation of forward rates, can then be used in the calibration to swaption prices (Brigo and Mercurio [11] and Rebonato [47]). Furthermore, note that the second formulation consists of a time-homogeneous component (i.e. the Ψ parameters). It was shown by both Brigo and Mercurio [11] and Rebonato [47] that the parameters Φ need to be as constant as possible (across maturities) in order to allow a time-homogeneous evolution of the term structure of volatilities.

	Time: $t \in (0, T_0]$	$(T_0, T_1]$	$(T_1, T_2]$	...	$(T_{M-2}, T_{M-1}]$
$L_{T_0T_1}(t)$	$\Phi_1\Psi_1$	Dead	Dead	...	Dead
$L_{T_1T_2}(t)$	$\Phi_2\Psi_1$	$\Phi_2\Psi_2$	Dead	...	Dead
$\vdots$	...	...	...	...	...
$L_{T_{M-1}T_M}(t)$	$\Phi_M\Psi_1$	$\Phi_M\Psi_2$	$\Phi_M\Psi_3$	...	$\Phi_M\Psi_M$

Table 5.4: Piecewise constant volatility matrix where instantaneous volatilities can be separated into forward rate specific and time dependent components.

	Time: $t \in (0, T_0]$	$(T_0, T_1]$	$(T_1, T_2]$	...	$(T_{M-2}, T_{M-1}]$
$L_{T_0T_1}(t)$	$\Phi_1\psi_1$	Dead	Dead	...	Dead
$L_{T_1T_2}(t)$	$\Phi_2\psi_2$	$\Phi_2\psi_1$	Dead	...	Dead
$\vdots$	...	...	...	...	...
$L_{T_{M-1}T_M}(t)$	$\Phi_M\psi_M$	...	...	...	$\Phi_M\psi_1$

Table 5.5: Piecewise constant volatility matrix where instantaneous volatilities can be separated into forward rate specific and time-to-maturity components.

The five tables conclude the piecewise constant models for instantaneous volatilities as presented by Brigo and Mercurio [11]. We will illustrate in later chapters how these can be applied to market data. The fact that these are piecewise constant does reduce some of the computational requirements as the integrals in Equation (5.1.1) can simply be replaced with summations. Next we will consider different parametric forms as given by Rebonato [47].

5.4 Parametric Volatility Structure

Parametric volatility structures differ from piecewise constant structures in the sense that we introduce continuous functions, dependent on only a few parameters, for the instantaneous volatilities of forward rates. One of the

more detailed accounts of parametric volatility specifications can be found in the book by Rebonato [47]; hence the material in this section will mainly follow the arguments of the author. Later chapters relating to the calibration of the model will then show how we can apply these functional forms to real market data. Practical examples are given in the work by Brigo and Mercurio [11] and Gatarek, Bachert and Maksymiuk [21].

5.4.1 General Structure

Rebonato [47] starts his study through introducing different possible volatility structures for instantaneous forward rates. These structures are expressed as products of different functions (the functions are chosen to represent different key dependencies). The exact specification of these functions will be presented and discussed at a later stage.

Given above discussion, we will divert slightly from Rebonato [47] and firstly introduce two classes of volatility functions. The first class consists of only a single function, dependent on either time, time to maturity or the maturity of the forward rate. These basic functions are presented below.

$$\sigma_{T_{k-1}T_k}(t) = g(t), \tag{5.4.1}$$
$$\sigma_{T_{k-1}T_k}(t) = f(T_{k-1}), \tag{5.4.2}$$
$$\sigma_{T_{k-1}T_k}(t) = h(T_{k-1} - t). \tag{5.4.3}$$

The second class consists of different possible combinations of the functions defined above. This class is necessary since these volatility functions, when used in isolation, have some undesirable properties (we will discuss these properties in the rest of the section). Hence, through carefully using structures dependent on a combination of these functions, we will be able to create more accurate and robust volatility specifications.

We will, for the purpose of the discussion, subdivide the second class into two more categories. These categories were determined on the basis of the required computational effort when calibrating to the market. The first part will allow us to separate the different components during integration and is given by

$$\sigma_{T_{k-1}T_k}(t) = g(t)f(T_{k-1}), \tag{5.4.4}$$
$$\sigma_{T_{k-1}T_k}(t) = h(T_{k-1} - t)f(T_{k-1}). \tag{5.4.5}$$

As can be seen from above, this is possible since only one of the functions are dependent on time. With the rest of the functions this will not be the case, and hence we will have more complex integrals when calibrating to the market (Rebonato [47] suggest piecewise constant approximations for some of the function in the integral in order to simplify calculations). The functions

are presented below.

$$\sigma_{T_{k-1}T_k}(t) = h(T_{k-1}-t)g(t), \tag{5.4.6}$$
$$\sigma_{T_{k-1}T_k}(t) = h(T_{k-1}-t)g(t)f(T_{k-1}). \tag{5.4.7}$$

The rest of the chapter will consider the implied properties of the term structure given different specifications. We will also introduce some of the parametric forms that can be used for the functions defined above.

5.4.2 Dependence on Time

These are defined as instantaneous volatilities which are only dependent on time. The structure is given by Equation (5.4.1) as

$$\sigma_{T_{k-1}T_k}(t) = g(t),$$

for some purely time dependent function $g(t)$. This then implies that all active forward rates will have the same volatility at a specific point in time. Due to the fact that volatilities can change at each time step, we have that the volatility structure is not time-homogeneous. Furthermore, Rebonato [47] mentions that this structure is only consistent with certain term structures of volatilities.

5.4.3 Dependence on Maturity

This type of volatility specification assigns volatilities to forward rates according to their maturity dates. The structure is given by Equation (5.4.2) as

$$\sigma_{T_{k-1}T_k}(t) = f(T_{k-1}),$$

for some real valued function f. Similar to its piecewise constant counterpart, we have that any term structure can be recovered exactly, however the term structure of volatilities will not evolve in a time-homogeneous manner. Furthermore, Rebonato [47] points out that this specification implies that the volatility of forward rates remain the same throughout the duration of its life. This is a financially undesirable property.

5.4.4 Dependence on Time to Maturity

The structure is given by Equation (5.4.3) as

$$\sigma_{T_{k-1}T_k}(t) = h(T_{k-1}-t),$$

for some real valued function h. This function is in the form of Equation (5.2.2) and hence we know that it will ensure a time-homogeneous evolution of the term structure. It was however mentioned earlier that we will only be able to get an exact fit to the current structure if $T_i\sigma^2_{T_iT_{i+1}.\text{caplet}}$ is a strictly

increasing function of T_i. Note that above specification is expressed in terms of a general function h, i.e. no structural assumptions were made, and hence the piecewise constant approach by Brigo and Mercurio [11] (defined in Table 5.2) and the functional approach by Rebonato [47] are still relatively in line.

This is due to the fact that both processes are still essentially non-parametric (the function h is defined as an arbitrary function from the universe of functions dependent on the time to maturity of a forward rate). As soon as we assign a specific parametric form to the function h, then the approaches between Brigo and Mercurio [11] and Rebonato [47] start to differ more significantly. The approach by Rebonato [47], although still time-homogeneous, will not be guaranteed of an exact fit to the initial term structure (Rebonato [47]).

5.4.5 Separable Volatilities

The general functional definitions are given by Equations (5.4.4) - (5.4.5) as

$$\begin{aligned}\sigma_{T_{k-1}T_k}(t) &= g(t)f(T_{k-1}),\\ \sigma_{T_{k-1}T_k}(t) &= h(T_{k-1}-t)f(T_{k-1}),\end{aligned}$$

where the functions $h(T_{k-1}-t), g(t)$ and $f(T_{k-1})$ are as defined in the previous sections. The piecewise equivalents of these structures were discussed in Section 5.3.4 and hence we will only highlight a couple of important facts. Firstly, only the latter specification can result in a time-homogeneous evolution of the term structure of volatilities (Brigo and Mercurio [11] and Rebonato [47]). Secondly, in order for this to be the case, the forward rate dependent components need to be approximately constant (Brigo and Mercurio [11] and Rebonato [47]). This will then imply a calibration strategy in which we fit the time-homogeneous function to the initial term structure (explained in Section 5.4.4 that this will not always be exact even if $T_i\sigma^2_{T_iT_{i+1}.\text{caplet}}$ is a strictly increasing function of T_i). The forward rate component can then be used as a final correction. This is different to the calibration strategy that can be used for the first structure.

5.4.6 Multi-Time Dependence

The remaining functional forms are expressed in terms of more than one function with some sort of time dependence. These are given by Equations (5.4.6) - (5.4.7) as

$$\begin{aligned}\sigma_{T_{k-1}T_k}(t) &= h(T_{k-1}-t)g(t),\\ \sigma_{T_{k-1}T_k}(t) &= h(T_{k-1}-t)g(t)f(T_{k-1}),\end{aligned}$$

where the functions $h(T_{k-1}-t), g(t)$ and $f(T_{k-1})$ are as defined in the previous sections. Although more complex than the previous specifications, Rebonato

[47] points out that these specifications are very useful for calibration purposes. Furthermore, he explains how these structures can be calibrated in two and three steps respectively, with each step financially plausible. The calibration of these structures will be discussed in more detail at a later stage.

5.4.7 Specifying the Different Functions

This section will specify the functions $h(T_{k-1}-t), g(t)$ and $f(T_{k-1})$.

In the calibration algorithms that will be considered, we will require that the function $f(T_{k-1})$ should be as constant as possible (a brief description was given in Section 5.4.5).

Next, Rebonato [47] suggests the following parametric form for the time-homogeneous function $h(T_{k-1}-t)$

$$h(T_{k-1}-t) = [a + b(T_{k-1}-t)]\exp[-c(T_{k-1}-t)] + d. \tag{5.4.8}$$

Figure 5.1 displays some of the attainable shapes for different sets of parameters.

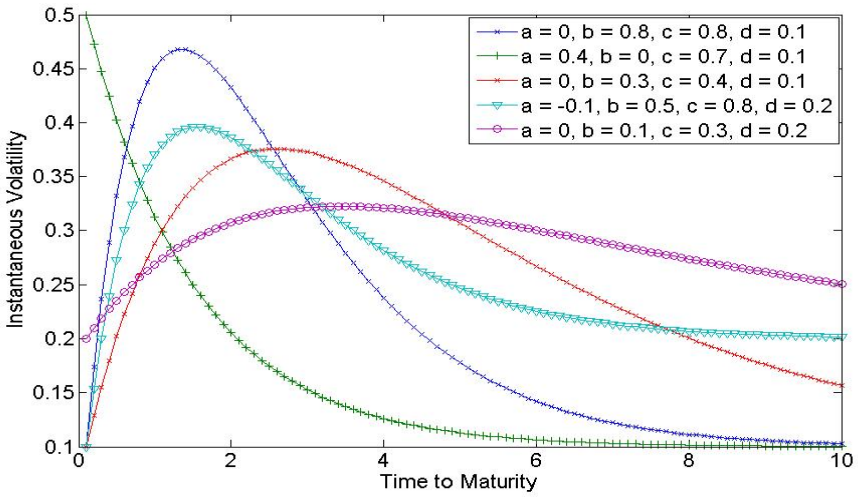

Figure 5.1: Rebonato's time-homogeneous instantaneous volatility function for different sets of parameters.

In theory, there are a number of different functions that one can use to describe this portion of the instantaneous volatility function. Rebonato [47] motivated the above choice as follows:

Firstly, this function can be shown to be compatible with a number of different term structure shapes. In particular, the function can produce instantaneous volatility functions that are compatible with normal (humped)

and stressed market conditions (monotonically decreasing). Secondly, its parameters lend themselves to easy interpretations. Finally, it allows for an easy analytical solution of Equation (4.1.5), which in turn simplifies calibration procedures.

Note that the following conditions must be satisfied at the end of a calibration process

$$a + d > 0, \tag{5.4.9}$$
$$d > 0, \tag{5.4.10}$$
$$c > 0. \tag{5.4.11}$$

The first two properties ensure positive volatilities as time to maturity approaches zero and infinity. The third condition is necessary to prevent volatilities from exploding.

The final parametric form that we will consider, relates to the purely time dependent component. Rebonato [47] suggests the following form for the function $g(t)$

$$g(t) = \left[\sum_{i=1}^{n} \epsilon_i \sin\left(\frac{t\pi i}{\text{Mat}} + \epsilon_{i+1}\right)\right] \exp(-\epsilon_{n+1} t). \tag{5.4.12}$$

Figure 5.2 displays some of the attainable shapes for different sets of parameters.

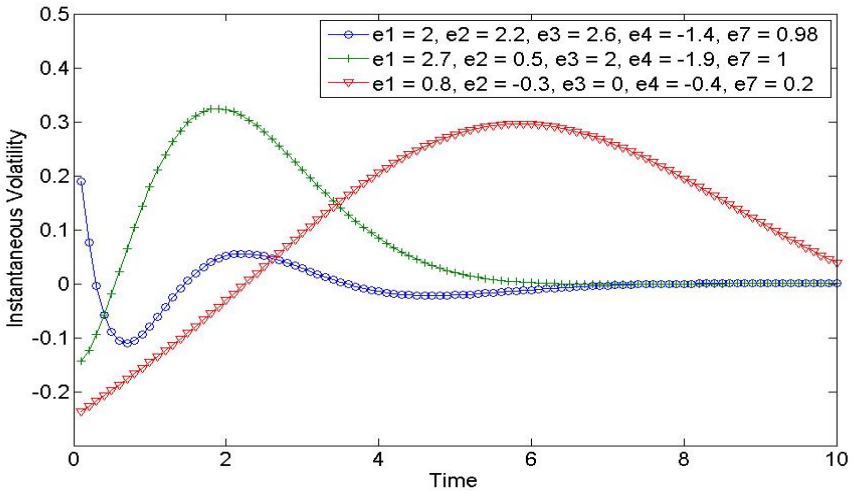

Figure 5.2: Rebonato's time dependent instantaneous volatility function for different sets of parameters.

Within this specification, it is recommended to keep n relatively low (Rebonato [47]). Furthermore, note that "Mat" indicates the longest caplet maturity. The choice of this functional form can briefly be motivated as follows:

This function will typically be used to explain the differences (or residuals) between the market observable term structure of volatilities and the term structure obtained through fitting the time homogeneous component. As a result, Rebonato [47] suggested a function that is a linear combination of a small number of sine waves and a multiplicative exponentially decaying term.

This structure also allows for a number of financially plausible shapes. For instance, we can choose the parameters to reflect decaying volatility as time passes (as we exit the credit crisis) or to display an increase of volatility in the near future followed by a steady decline (expected monetary policy decisions in short to medium term).

The functional form however exposes the model to negative forward rate volatilities (not discussed in book by Rebonato [47] even though the results obtained by the author implied negative volatilities). This is due to the oscillating nature of the function. Hence, although this might improve the calibration to a given input term structure (integrating the square of this function), we can expect this property to have a significant impact on the pricing of more complex derivatives. Alternatively, we can use the absolute of this function for pricing purposes. This will result in the same calibration error, however will ensure positive volatilities at all time steps.

5.5 Swap Rate Volatilities

It was already mentioned that the LIBOR and swap market models are not compatible. This then considerably increases the computational requirements when valuing vanilla swaptions. As a result we are left with calibration routines that will involve Monte Carlo simulations which are far from optimal.

Various authors however introduced possible analytical approximations for swaption prices within the LIBOR market model framework (see work by Brigo and Mercurio [11] for more details). This thesis will make use of the Rebonato [47] approximation formula for swaption volatilities. In order to get an idea of how this formula was derived, notice that we can write the swap rate given by Equation (4.2.1) as a linear combination of forward rates (with stochastic weights). This fact is used by various authors, see for example Brigo and Mercurio [11], Gatarek, Bachert and Maksymiuk [21] and Rebonato [47] and is given below for a swap starting at time s and ending at time N.

$$SR_{s,N}(t) = \sum_{i=s+1}^{N} w_i(t) L_{T_{i-1}T_i}(t), \tag{5.5.1}$$

where

$$w_i(t) = \frac{\alpha_{T_{i-1}T_i} B(t,T_i)}{\sum_{k=s+1}^{N} \alpha_{T_{k-1}T_k} B(t,T_k)}. \tag{5.5.2}$$

Through the use of above equations and assuming that all forward rates and weights w_i are fixed at their current values (these assumptions are not made

all at once but at different parts of the derivation), Rebonato [47] obtained the following volatility approximation formula (Brigo and Mercurio [11] and Rebonato [47]):

$$V^2_{s,N}T_s = \sum_{i,j=s+1}^{N} \overline{w}_i \overline{w}_j \int_0^{T_s} \sigma_{T_iT_{i+1}}(t)\sigma_{T_jT_{j+1}}(t)\rho_{L(i,i+1);L(j,j+1)}\, dt, \tag{5.5.3}$$

where

$$\overline{w}_i = \frac{w_i(0)L_{T_{i-1}T_i}(0)}{SR_{s,N}(0)}. \tag{5.5.4}$$

Hence, we have that the swap rate volatilities are expressed as a linear combinations of the forward rate terminal covariances (terminal covariance terms will be discussed in the next chapter). One important point to note from the above equation is that swaption volatilities will be dependent on the shape of the instantaneous volatility functions of forward rates (Rebonato [47]). This is not the case with caplets.

Gatarek, Bachert and Maksymiuk [21] refer to this approach as the linear pricing approach within the LIBOR market model framework and represent the weights defined in Equation (5.5.4) in the following equivalent form

$$R^i_{s,N}(0) = \frac{B(0,T_{i-1}) - B(0,T_i)}{B(0,T_s) - B(0,T_N)}. \tag{5.5.5}$$

Chapter 6

Correlation Modeling

This chapter will focus on the modeling of instantaneous correlations. Rebonato [47] mentions that the modeling of instantaneous correlation functions is more difficult than that of instantaneous volatilities. This is mainly due to the fact that no vanilla instruments are determined purely by the correlation between forward rates. Rebonato [47] further points out that even swaptions, which are the only vanilla instruments dependent on correlation, are determined by a combination of instantaneous volatilities and correlations (this was shown at the end of the previous chapter).

The structure of the chapter will be similar to the previous one. We start with some key definitions and requirements and then move on to introduce and explain some of the different correlation structures.

6.1 Terminal Correlation

Terminal correlations can be defined as the correlation between different forward rates at some future time T_1 (Brigo and Mercurio [11]). Brigo and Mercurio [11] points out that the calculation of terminal correlations in the LIBOR market model consists of solving the following equation

$$\frac{\text{cov}(L_{T_{i-1}T_i}(T_1), L_{T_{j-1}T_j}(T_1))}{\sqrt{\text{var}(L_{T_{i-1}T_i}(T_1))\text{var}(L_{T_{j-1}T_j}(T_1))}}, \tag{6.1.1}$$

where the forward rates are specified according to Proposition 4.4.2 and the covariance and variance terms are calculated under the appropriate measure. This type of calculation will definitely require Monte Carlo simulations and hence will be computationally intensive. Fortunately, as with the swaption volatilities there are some approximations available. Brigo and Mercurio [11] shows that given similar assumptions to those used in the calculation of swaption volatilities, we can obtain the T_1 terminal correlation between the forward

rates $L_{T_1T_2}$ and $L_{T_2T_3}$ as

$$\text{Corr}(L_{T_1T_2}(T_1), L_{T_2T_3}(T_1)) = \frac{\int_0^{T_1} \sigma_{T_1T_2}(t)\sigma_{T_2T_3}(t)\rho_{L(1,2);L(2,3)}\,dt}{\sqrt{\int_0^{T_1} \sigma_{T_1T_2}(t)^2\,dt}\sqrt{\int_0^{T_1} \sigma_{T_2T_3}(t)^2\,dt}}. \quad (6.1.2)$$

This then clearly shows a link between terminal correlations and the swaption volatilities provided at the end of the previous chapter. Note however that both instantaneous volatilities, as well as instantaneous correlations, will affect the terminal correlations (Rebonato [47]).

6.2 Required Correlation Properties

Before we can proceed to defining different possible correlation structures, we need to specify what properties these structures should adhere to. This will be divided into two sub-categories, i.e. mathematical and financial requirements.

6.2.1 Mathematical Requirements

From a mathematical point of view we know that the following properties should hold (Rebonato [47])

- $\rho_{i,i} = 1$ for all i
- $-1 \leq \rho_{i,j} \leq 1$ for all i, j combinations
- The correlation matrix should be symmetric
- The correlation matrix should be positive definite

6.2.2 Financial Requirements

Above requirements are however not enough to ensure a correct correlation matrix. Brigo and Mercurio [11] and Rebonato [47] make mention of some of the numerical studies done in the literature, illustrating some of the possible features. A short summary of their results, for an instantaneous correlation matrix ρ, is presented below.

- We can expect mainly positive correlations
- Correlation surfaces can show a change in convexity as the maturity of forward rates increase
- The closer the maturities between two forward rates the higher the correlation between these rates, i.e. two short-term rates should be more correlated than a short-term rate and one expiring in say twenty years.

- Correlation should be an increasing function of the tenor of adjacent rates, i.e. long-term rates should for example be more correlated than short-term rates.
- It would be favourable if the choice of the instantaneous correlation function result in a time-homogeneous behaviour.

A full rank $N \times N$ instantaneous correlation matrix has $N(N-1)/2$ elements that need to be estimated (Götsch [22]). This can result in complex practical implementation if the set of data consists of a large number of forward rates. We will consider two approaches to reduce the number of required calculations as mentioned by Brigo and Mercurio [11] and Götsch [22]. The first approach considers a full rank correlation matrix, but then through the use of a parametric function, reduces the number of elements that we should estimate to the number of parameters. The second approach reduces the number of elements through reducing the rank of the correlation matrix. The structure of the rest of the chapter will mainly follow that of Götsch [22].

6.3 Full Rank with Reduced Number of Parameters

As mentioned above, this type of specification firstly considers a full rank correlation matrix and then reduces the number of elements to be estimated through the use of a parametric function. There are a number of different parametric functions available in the literature.

Firstly, we will consider the parametric function as proposed by Schoenmakers and Coffey. Details are given below.

6.3.1 Schoenmakers and Coffey

They start by considering a finite sequence of positive real numbers (Brigo and Mercurio [11])

$$1 = c_1 < c_2 < \ldots < c_N, \tag{6.3.1}$$

where

$$\frac{c_1}{c_2} < \frac{c_2}{c_3} < \ldots < \frac{c_{N-1}}{c_N}. \tag{6.3.2}$$

They then assume that the correlation between between $L_{T_{i-1}T_i}$ and $L_{T_{j-1}T_j}$ is equal to

$$\rho_{i,j}(c) = \frac{c_i}{c_j}, \quad i \leq j, \quad i,j = 1,\ldots,N. \tag{6.3.3}$$

Brigo and Mercurio [11] mention that the resulting correlation matrix is full rank, symmetric and positive definite. This approach can be presented in Table 6.1 below (Götsch [22])

Note that Equations (6.3.1)-(6.3.3) have some significant implications. Firstly, the elements will range from 0 to 1 and hence the specification will

	$L_{T_1T_2}$	$L_{T_2T_3}$	$L_{T_3T_4}$	$L_{T_4T_5}$
$L_{T_1T_2}$	1	$\frac{c_1}{c_2}$	$\frac{c_1}{c_3}$	$\frac{c_1}{c_4}$
$L_{T_2T_3}$	$\frac{c_1}{c_2}$	1	$\frac{c_2}{c_3}$	$\frac{c_2}{c_4}$
$L_{T_3T_4}$	$\frac{c_1}{c_3}$	$\frac{c_2}{c_3}$	1	$\frac{c_3}{c_4}$
$L_{T_4T_5}$	$\frac{c_1}{c_4}$	$\frac{c_2}{c_4}$	$\frac{c_3}{c_4}$	1

Table 6.1: Schoenmakers and Coffey model implied correlation matrix.

result in positive correlations as required at the start of the chapter. Secondly, we have that the closer the maturities between two forward rates the higher the correlation between these rates. This can be seen from (Götsch [22])

$$\frac{c_1}{c_2} > \frac{c_1}{c_3} > \frac{c_1}{c_4}$$

and

$$\frac{c_2}{c_3} > \frac{c_2}{c_4}.$$

Thirdly, we have that correlation is an increasing function of the tenor of adjacent rates. See for example (Götsch [22])

$$\frac{c_1}{c_2} < \frac{c_2}{c_3} < \frac{c_3}{c_4}$$

and

$$\frac{c_1}{c_3} < \frac{c_2}{c_4}.$$

Furthermore, we have that the number of parameters are equal to N instead of $N(N-1)/2$. Rebonato [47] mentions that it is due to this fact that the approach is called semi-parametric.

Schoenmakers and Coffey mentions that it is always possible to characterize above elements with a finite sequence of nonnegative numbers $\Delta_2, \ldots, \Delta_N$ as (Brigo and Mercurio [11])

$$c_i = exp\left[\sum_{j=2}^{i} j\Delta_j + \sum_{j=i+1}^{N} (i-1)\Delta_j\right]. \tag{6.3.4}$$

From above equation, one can formulate different parameterizations through different assumptions regarding the Δ parameters. As an example, we will consider the two parameter case in which all the Δ's are set to zero except the last two (Brigo and Mercurio [11] and Rebonato [47]). This is presented by the following equation

$$\rho_{i,j} = \exp\left[-\frac{|i-j|}{N-1}\left(-\ln\rho_\infty + \eta\frac{N-1-i-j}{N-2}\right)\right],$$

where

$$\eta = \Delta_{N-1}(N-1)(N-2)/2.$$

There are a number of different assumptions proposed by Schoenmakers and Coffey that can for example lead to specifications involving more parameters. We will however restrict our attention to the simple two parameter case presented above.

Rebonato [47] mentions that one of the biggest advantages of the different Schoenmakers and Coffey parameterizations is the fact that the correlation matrix will always be positive definite. This is a very favourable property during the calibration phase (do not need to ensure at each step of calibration algorithm that the resulting matrix will be positive definite).

6.3.2 Rebonato's Parametric Forms

Rebonato [47] specifies three different time-homogeneous parametric forms. These will be discussed below. Note however that unlike the specifications by Schoenmakers and Coffey, these will not guarantee positive definite correlation matrices and hence this condition needs to be checked during the calibration of the model.

The first parametric specification proposed by Rebonato [47] is given by

$$\rho_{i,j}(t) = \rho_\infty + (1-\rho_\infty)\exp[-\beta|T_i - T_j|]. \tag{6.3.5}$$

Rebonato [47] mentions that this specification is desirable from a numerical point of view due to the fact that it is independent of time. This specification however has the disadvantage that correlations are only dependent on the difference in expiry times between two different forward rates. Hence, two short-term rates will have the same correlation as two long-term rates given the difference in expiry times of the two sets are the same. This is financially undesirable as long-term rates are typically more correlated than short-term rates (Brigo and Mercurio [11]). This specification also does not allow for a change in convexity (Rebonato [47]).

The second parametric specification proposed by Rebonato [47] is given by

$$\rho_{i,j}(t) = \rho_\infty + (1-\rho_\infty)\exp[-\beta|(T_i - t)^\gamma - (T_j - t)^\gamma|]. \tag{6.3.6}$$

Rebonato [47] showed that this specification allows for all of the required properties mentioned in Section 6.2.2 (obviously depending on the choice of γ, as it can be shown that for $\gamma = 1$ we get the first specification). The biggest drawback of this approach, as mentioned earlier, is that it does not guarantee a positive definite correlation matrix.

The third parametric specification proposed by Rebonato [47] is given by

$$\rho_{i,j}(t) = \rho_\infty + (1-\rho_\infty)\exp[-\beta|T_i - T_j| + \alpha\max(T_i, T_j)]. \tag{6.3.7}$$

This approach can then be shown to have the same time independence as the first approach, while maintaining some of the financial properties of the second approach (Rebonato [47]). Similar to the previous specification, this parametric form does not guarantee a positive definite correlation matrix.

The application of these parametric forms, to the South African market, is presented in Section 10.5.1.

6.4 Reduced-Rank Specifications

It was previously mentioned that a full rank correlation matrix has $N(N-1)/2$ elements that we need to estimate during the calibration of the model. We then considered introducing parametric forms in order to reduce the number of variables to the number of parameters. This section will consider a method in which we reduce the rank of the correlation matrix. This will then automatically reduce the number of elements we need to estimate. The theory presented in this section will mainly follow the work by Brigo and Mercurio [11] and Götsch [22].

6.4.1 General Concept

Consider an $N \times N$ correlation matrix ρ. We want to examine different methods of determining a $m-$rank $N \times m$ matrix B such that the new correlation matrix ρ^B will have a rank m which is smaller than N (Brigo and Mercurio [11]). The new correlation matrix will then be presented by

$$\rho^B = BB'. \tag{6.4.1}$$

This matrix B is then in line with Section A.5 and can be used to create a new correlated Wiener process given independent random shocks.

6.4.2 Different Specifications

This section will consider some of the different possible reduced rank methodologies. The first approach will be based on an angle formulation, while the other approach will focus more on the eigenvalues and eigenvectors of the original matrix.

6.4.2.1 Rebonato's Angles Formulation

We will firstly consider the specification as suggested by Rebonato [47]. Rebonato [47] suggested that each of the entries in B are given as a certain combination of angles, resulting in ones on the diagonal of the instantaneous correlation matrix. Furthermore, Brigo and Mercurio [11] mention that the resulting correlation matrix will be positive semi definte as well as symmetric. This section will consider a two- and three-factor model. Rebonato [47] mentions that this should be sufficient for most practical applications.

The specification of the matrix B for a two-factor model is presented below (Rebonato [47])

$$\begin{aligned} b_{i,1} &= \sin\theta_i, \\ b_{i,2} &= \cos\theta_i. \end{aligned}$$

From above and some trigonometric identities we obtain that the correlations in the two-factor model are given by

$$\rho_{i,j} = \cos(\theta_i - \theta_j). \tag{6.4.2}$$

Notice that even within this reduced rank specification there are still a number of parameters that we need to estimate. Brigo and Mercurio [11] mention that this can be reduced further through introducing a sub-parameterization for the θ parameters. They however caution against this type of approach when calibrating to a large swaption matrix. Rebonato [47] presents the following sub-parameterization example

$$\theta_i = a + bT_i \tag{6.4.3}$$

and mentions that such a sub-parameterization will always lead to the same correlation for equally spaced forward rates (irrespective of the expiries of the individual forward rates). In order to eliminate this we need to consider non-linear parametric forms.

Next, let us consider a three-factor model. The specification of the matrix B is presented below (Rebonato [47])

$$\begin{aligned} b_{i,1} &= \cos\theta_i \sin\phi_i, \\ b_{i,2} &= \sin\theta_i \sin\phi_i, \\ b_{i,3} &= \cos\phi_i. \end{aligned}$$

From above and some trigonometric identities we obtain that the correlations in the three-factor model are given by

$$\rho_{i,j} = \cos(\phi_i - \phi_j) - \sin\phi_i \sin\phi_j[1 - \cos(\theta_i - \theta_j)]. \tag{6.4.4}$$

Rebonato [47] points out that this specification is not, unlike the two-factor model, purely dependent on a difference between two angles. Hence, we will no longer be forced to use non-linear sub-parameterizations.

Note that the above approach is typically used when we try and imply correlations from a market swaption matrix. Brigo and Mercurio [11] mention that the above approach can also be used when we want to reduce the rank of an exogenously given correlation matrix (proposed by Rebonato and Jaeckel [50]). They describe the approach as follows.

Firstly, decide on an angle formulation (examples of two- and three-factor models are presented above). Then find the angle parameters that will minimize the following function

$$\sum_{i,j=1}^{N} (\rho_{i,j} - \rho_{i,j}(\theta))^2, \tag{6.4.5}$$

where $\rho_{i,j}$ indicate the exogenously given correlation matrix. It is important to note that we have no constraints due to the fact that the resulting matrix will always be symmetric, positive semidefinite and have ones on the diagonal (Brigo and Mercurio [11] and Rebonato [47]).

6.4.2.2 Using Eigenvalues and Eigenvectors

Given the fact that we are reducing the rank of the correlation matrix, it is natural to expect some methodology that is aimed at retaining only the most important driving factors. This approach will be discussed below. Before we proceed, consider the following mathematical results as given by Brigo and Mercurio [11].

From the properties of correlation matrices, we know that the correlation matrix ρ should be symmetric and positive definite. Then, according to Burden and Faires [14], we can decompose the matrix into the following form

$$\rho = PHP',$$

where P is a real orthogonal matrix such that $P'P = PP' = I_N$. The matrix H is a diagonal matrix of the positive eigenvalues of ρ. The columns of P are in turn the associated eigenvectors of ρ. Brigo and Mercurio [11] then show that if we define the matrix Λ such that

$$H = \Lambda\Lambda',$$

then we can decompose the correlation matrix ρ as

$$\rho = AA',$$

where

$$A = P\Lambda.$$

This immediately results in the following rank reduction methodology. Firstly, start by decomposing the exogenously given correlation matrix into its eigenvalues and eigenvectors. We can then set up a matrix B similar to matrix A in which we only use the most significant eigenvectors and eigenvalues (hence approach also called zeroing of smallest eigenvalues). From this we can then obtain the intermediate matrix ρ^{interm} according to Equation (6.4.1) as

$$\rho^{\text{interm}} = BB'. \tag{6.4.6}$$

Finally, Brigo and Mercurio [11] mention that in order to ensure ones on the diagonal, we have to scale the correlation entries as given below

$$\rho^B_{i,j} = \frac{\rho^{\text{interm}}_{i,j}}{\sqrt{\rho^{\text{interm}}_{i,i}\rho^{\text{interm}}_{j,j}}}. \tag{6.4.7}$$

This will provide us with the $m-$rank approximation $\rho^B_{i,j}$ of the matrix ρ (Brigo and Mercurio [11]).

6.5 Exogenous Correlation Matrix

This section will consider the estimation of a correlation matrix using historical data. As pointed out in the literature, these matrices might display some unwanted properties due to issues with the statistical estimation (Brigo and Mercurio [11]). Brigo and Mercurio [11] and Rebonato [47] recommend the fitting of a parametric form onto the historical matrix in order to smooth out some of the noise.

In order to illustrate this process, we will assume that we have a set of market forward rates (either obtained directly or derived from a set of zero coupon bonds). Note that interpolation might affect the end results.

We will consider the historical estimation technique as given by Götsch [22]. Firstly, the approach assumes that the log-returns of the forward rates are normally distributed. Next, in order to calculate sample correlations, we need to calculate sample means and sample covariances. Hence, we have that

$$\hat{\mu}_i = \frac{1}{x}\sum_{k=0}^{x-1} \ln\left[\frac{L_{T_iT_{i+1}}(t_{k+1})}{L_{T_iT_{i+1}}(t_k)}\right],$$

$$\hat{V}_{i,j} = \frac{1}{x}\sum_{k=0}^{x-1}\left[\left(\ln\left(\frac{L_{T_iT_{i+1}}(t_{k+1})}{L_{T_iT_{i+1}}(t_k)}\right) - \mu_i\right)\left(\ln\left(\frac{L_{T_jT_{j+1}}(t_{k+1})}{L_{T_jT_{j+1}}(t_k)}\right) - \mu_j\right)\right],$$

where x is the number of observed log-returns for each rate. Hence, we can now write the estimated correlation element as

$$\hat{\rho}_{i,j} = \frac{\hat{V}_{i,j}}{\sqrt{\hat{V}_{i,i}}\sqrt{\hat{V}_{j,j}}}. \tag{6.5.1}$$

Brigo and Mercurio [11] mention that the results should remain relatively the same when its sample size or its time positioning is changed. The fact that the results should remain relatively the same given a different time positioning is in line with the time-homogeneous requirement of Rebonato [47]. We can now use this matrix either directly in the calibration process, or fit it to a plausible parametric form.

This methodology was applied to the South African market in Section 8.5. Within this section, we explain some of the practical difficulties associated with such an approach. The resultant correlation matrix was then used in different calibration algorithms in Chapter 10.

Chapter 7

European Market Data

This chapter will consider the inputs to the LIBOR Market Model under consideration. We will start the discussion by presenting some of the existing examples available in the literature from which we will discuss key concepts such as caplet volatility stripping from quoted cap volatilities. These arguments will then be extended to the South African market in the next chapter.

The data given in this chapter is presented in the book by Gatarek, Bachert and Maksymiuk [21]. Apart from the actual bootstrapping of the discount factors, they present a very detailed account of the steps necessary to bootstrap caplet volatilities from quoted cap volatilities. This chapter will present these ideas and replicate the results.

7.1 Actual Market Inputs

The data set considered by Gatarek, Bachert and Maksymiuk [21] represents market prices as on 21 January 2005 and consists of discount factors, at-the-money (ATM) cap volatilities and ATM swaption volatilities. All rates are denominated in EUR. This thesis will mainly consider the calibration to ATM cap and swaption volatilities, with an extension to the SABR model in Chapter 11. The reader is referred to the work by Brigo and Mercurio [11], Björk [4] and Rebonato [47] for further possible extensions of the model beyond these approaches.

7.1.1 Discount Factors

The discount factors are assumed to be bootstrapped from underlying benchmark rates and was not illustrated by the authors. The resulting values are presented in Table 7.1. A detailed description of a typical bootstrap procedure will be presented for the South African market.

7.1.2 Cap Volatilities

The cap data set, as presented by Gatarek, Bachert and Maksymiuk [21], consists of ATM cap volatilities with expiries from $1Y$ out to $20Y$ and is given in Table 7.1.

Tenor T_i	Date	Discount factor $B(0,T_i)$	Cap volatility $\sigma_{T_0T_i.\text{cap}}$
$t=0$	2005/01/21	1.0000000	N/A
T_0	2005/01/25	0.9997685	N/A
T_{SN}	2005/01/26	0.9997107	N/A
T_{SW}	2005/02/01	0.9993636	N/A
T_{2W}	2005/02/08	0.9989588	N/A
T_{1M}	2005/02/25	0.9979767	N/A
T_{2M}	2005/03/25	0.9963442	N/A
T_{3M}	2005/04/25	0.9945224	N/A
T_{6M}	2005/07/25	0.9890361	N/A
T_{9M}	2005/10/25	0.9832707	N/A
T_{1Y}	2006/01/25	0.9772395	0.1641
T_{2Y}	2007/01/25	0.9507588	0.2137
T_{3Y}	2008/01/25	0.9217704	0.2235
T_{4Y}	2009/01/26	0.8908955	0.2188
T_{5Y}	2010/01/25	0.8589736	0.2127
T_{6Y}	2011/01/25	0.8262486	0.2068
T_{7Y}	2012/01/25	0.7928704	0.2012
T_{8Y}	2013/01/25	0.7595743	0.1958
T_{9Y}	2014/01/27	0.7261153	0.1905
T_{10Y}	2015/01/26	0.6942849	0.1859
T_{12Y}	2017/01/25	0.6348348	0.1806
T_{15Y}	2020/01/27	0.5521957	0.1699
T_{20Y}	2025/01/27	0.4345583	0.1567

Table 7.1: Discount factors and ATM cap volatilities obtained from the European market for business date 2005/01/21 (Gatarek, Bachert and Maksymiuk [21]).

This set of data is a typical example of what one can expect to observe in the market and highlights the important fact that it is not always possible to obtain volatilities for all possible caplets. Instead, one will typically observe a number of cap volatilities (which may be limited as well - for example no short term cap volatilities as illustrated in the market presented above) from which you will have to deduce the underlying caplet volatilities.

Market quoted cap volatilities are typically termed flat volatilities. These can be explained as the volatility that will yield the cap price when applied to each of the underlying caplets (Hull [32]). This concept is essential for caplet stripping and will be discussed in the following section.

It is useful to consider the shape of the cap volatility structure and hence is presented in Figure 7.1. From the figure, it is evident that the input volatilities exhibit a humped shape with the peak in the $3Y$ area. Rebonato [47] describes

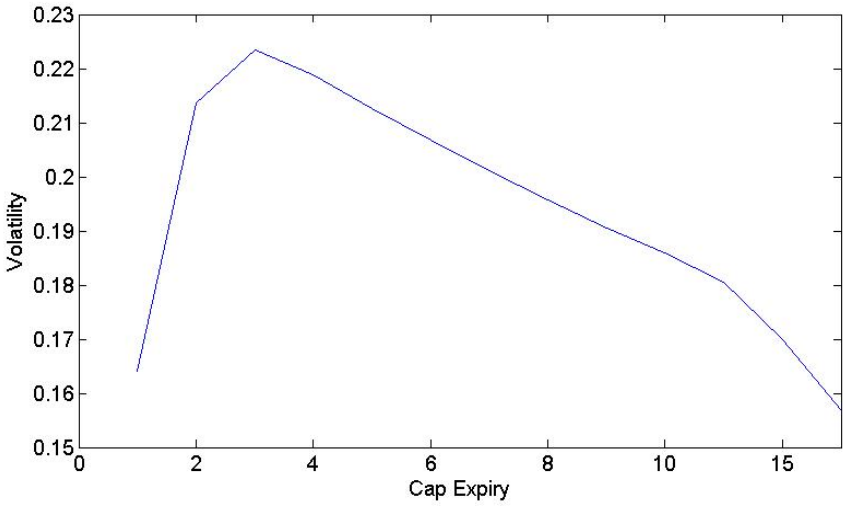

Figure 7.1: ATM cap volatilities obtained from the European market for business date 2005/01/21 (Gatarek, Bachert and Maksymiuk [21]).

this as a shape associated with normal market conditions as opposed to extreme market volatility. Under such conditions, one would experience less unexpected monetary actions and hence lower volatilities at the very short end of the curve. Rebonato [47] then explains that the longer term volatilities are less sensitive to the daily arrival of economic news (as long as result in non-structural changes). This then explains the lower volatilities associated with the longer end of the curve. The highest volatilities under normal market conditions are recorded in the intermediate maturities. This area of the curve usually represents market expectations regarding monetary rate decisions and have been shown to be very volatile throughout time.

7.1.3 Swaption Volatilities

The next set of market data that we will consider is the set of ATM swaption volatilities which can typically be used to determine the correlation between different forward rates (later chapters will discuss the difficulties associated with such an approach). This is due to the fact that the payoff of swaptions are dependent on several forward rates at a time and hence dependent on the joint dynamics of forward rates. Rebonato [47] advocates the use of cap prices for volatility calibration and the use of swaption prices for correlation modeling. This is partly based on the observation that the implied volatility term structure of forward rates tend to exhibit the same qualitative features when calibrated to either the swaption or cap market.

The ATM swaption volatilities are represented in Table 7.2. The rows of the table represent the option expiries while the columns represent the underlying

swap maturities. Within this context, the start date of the underlying swap always coincides with the expiry date of the option. Hence, if the option expiry and underlying maturity are both equal to $1Y$, then this represents an option to enter into a one year swap in one year's time.

	Option Expiry/Underlying Maturity									
	1Y	2Y	3Y	4Y	5Y	6Y	7Y	8Y	9Y	10Y
1Y	0.2270	0.2300	0.2210	0.2090	0.1960	0.1860	0.1760	0.1690	0.1630	0.1590
2Y	0.2240	0.2150	0.2050	0.1940	0.1830	0.1740	0.1670	0.1620	0.1580	0.1540
3Y	0.2090	0.2010	0.1900	0.1800	0.1700	0.1630	0.1580	0.1550	0.1520	0.1500
4Y	0.1950	0.1870	0.1770	0.1680	0.1600	0.1550	0.1510	0.1480	0.1470	0.1450
5Y	0.1820	0.1740	0.1650	0.1580	0.1510	0.1480	0.1450	0.1430	0.1420	0.1400
6Y	0.1746	0.1674	0.1590	0.1524	0.1462	0.1436	0.1410	0.1394	0.1384	0.1368
7Y	0.1672	0.1608	0.1530	0.1468	0.1414	0.1392	0.1370	0.1358	0.1348	0.1336
8Y	0.1598	0.1542	0.1470	0.1412	0.1366	0.1348	0.1330	0.1322	0.1312	0.1304
9Y	0.1524	0.1476	0.1410	0.1356	0.1318	0.1304	0.1290	0.1286	0.1276	0.1272
10Y	0.1450	0.1410	0.1350	0.1300	0.1270	0.1260	0.1250	0.1250	0.1240	0.1240

Table 7.2: ATM swaption volatilities obtained from the European market for business date 2005/01/21 (Gatarek, Bachert and Maksymiuk [21]).

The swaption volatilities are given by the surface in Figure 7.2 (contours were included to illustrate the smoothness of the curve beyond the initial peak).

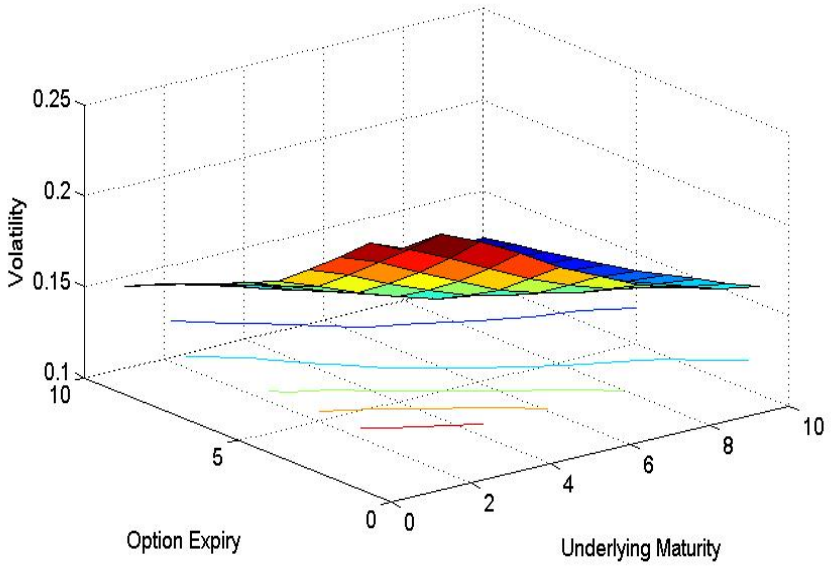

Figure 7.2: ATM swaption volatilities obtained from the European market for business date 2005/01/21 (Gatarek, Bachert and Maksymiuk [21]).

7.1.4 Historical Correlations

The authors Gatarek, Bachert and Maksymiuk [21] also presented calculated historical correlations. The estimations were performed on a historical Reuters data set containing observed rates from 29 October 1999 to 20 January 2005. Their results are presented below.

	3-6M	6-9M	9M-1Y	1-2Y	2-3Y	3-4Y	4-5Y	5-6Y	6-7Y	7-8Y	8-9Y	9-10Y
3M-6M	1	0.128	0.214	0.159	0.223	0.2	0.155	0.082	0.046	0.02	0.074	-0.008
6M-9M	0.128	1	-0.072	0.179	0.199	0.2	0.215	0.065	0.062	0.056	0.069	-0.025
9M-1Y	0.214	-0.072	1	-0.016	0.202	0.164	0.126	0.05	0.041	0.115	0.023	-0.004
1Y-2Y	0.159	0.179	-0.016	1	0.513	0.379	0.354	0.259	0.134	0.124	0.155	-0.005
2Y-3Y	0.223	0.199	0.202	0.513	1	0.208	0.194	0.168	0.128	0.204	0.059	0.002
3Y-4Y	0.2	0.2	0.164	0.379	0.208	1	0.149	0.142	0.164	0.072	0.11	0.013
4Y-5Y	0.155	0.215	0.126	0.354	0.194	0.149	1	-0.176	0.133	0.019	0.161	-0.01
5Y-6Y	0.082	0.065	0.05	0.259	0.168	0.142	-0.176	1	-0.121	0.26	0.055	0.007
6Y-7Y	0.046	0.062	0.041	0.134	0.128	0.164	0.133	-0.121	1	-0.128	0.062	0.015
7Y-8Y	0.02	0.056	0.115	0.124	0.204	0.072	0.019	0.26	-0.128	1	-0.359	-0.011
8Y-9Y	0.074	0.069	0.023	0.155	0.059	0.11	0.161	0.055	0.062	-0.359	1	-0.709
9Y-10Y	-0.008	-0.025	-0.004	-0.005	0.002	0.013	-0.01	0.007	0.015	-0.011	-0.709	1

Table 7.3: Historical forward rate correlations, based on observed rates from the European market, for the time period 1999/10/29 - 2005/01/20 (Gatarek, Bachert and Maksymiuk [21]).

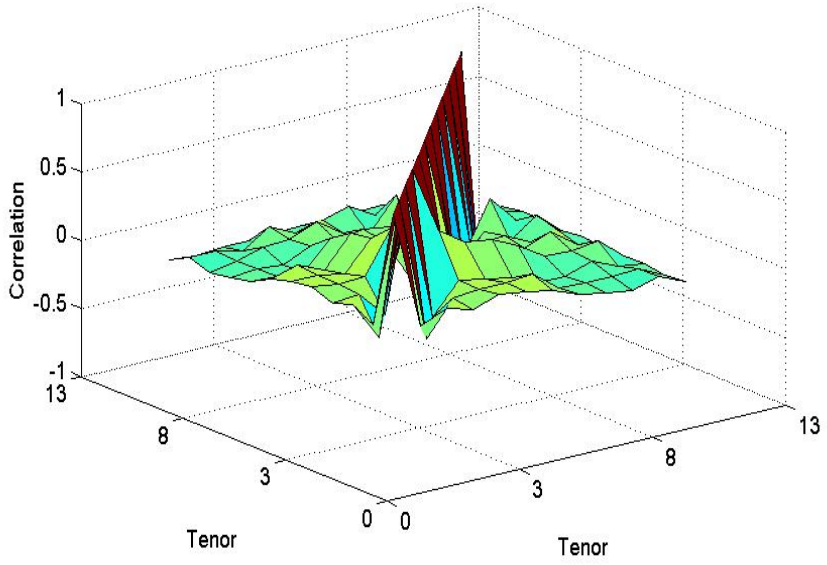

Figure 7.3: Historical forward rate correlations, based on observed rates from the European market, for the time period 1999/10/29 - 2005/01/20 (Gatarek, Bachert and Maksymiuk [21]).

From above it appears that there is a considerable amount of noise within the estimated correlations. Firstly, note that there is a number of negative correlations, which according to Brigo and Mercurio [11] and Rebonato [47] is a financially undesirable property. Secondly, due to the erratic movements in correlations, it is hard to get a feel of what the matrix is implying. This in turn can create difficulties when we try and calibrate the model.

In order to consider the implied properties of the given correlation matrix in more detail, we will examine the first three rows of the correlation matrix in isolation. These are presented in Figure 7.4 below.

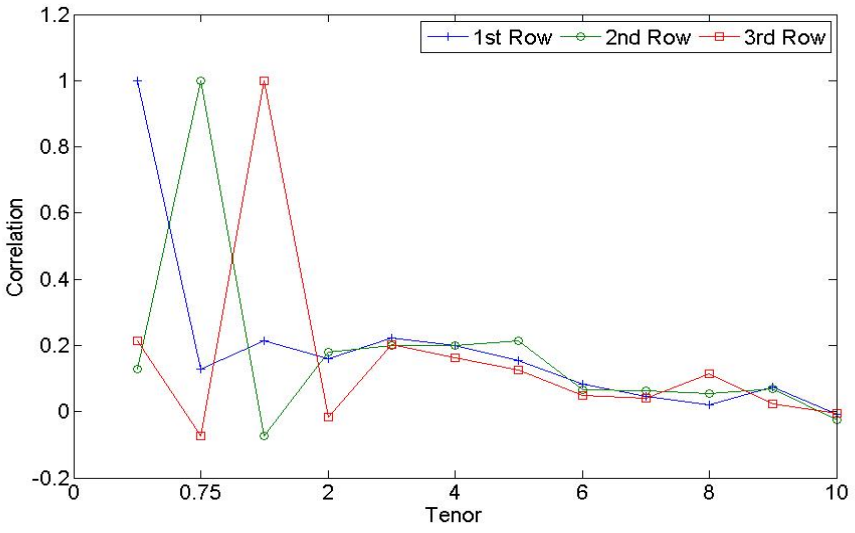

Figure 7.4: Graphical representation of the first three rows of Table 7.3.

From Figure 7.4 it is evident that the correlation surface experiences a change in convexity as the reset times of the forward rates increase (Rebonato [47]). This observation can play an important part in the determination of an appropriate parametric form used in the modeling of correlations. Furthermore, the correlations are decreasing functions of reset time. The latter property implies, for example, that a short and long term rate are less correlated than two short term rates. This is a financially desirable property.

We can also infer from the above graph that correlations seem to approach a negative level as the reset time increases. This is an undesirable property.

It should, however, be noted that some of the undesirable features mentioned above can be due to the use of unevenly spaced forward rates. The data set consists of three monthly forward rates up and till one year and yearly forward rates further out. The impact of this will be considered in the section relating to the South African market.

7.2 Caplet Stripping

Consider the quoted ATM cap volatilities presented in Table 7.1. In order to determine the dynamics of forward LIBOR rates in the LMM,we need a methodology for stripping caplet volatilities from the quoted cap volatilities. The first obvious question arising when we attempt to determine caplet volatilities, is the question of what strikes we should use for the quoted caps (Gatarek, Bachert and Maksymiuk [21]).

Firstly, we know that a T_{i-1} caplet is said to be ATM when its strike price $X = X_i$ is equal to the current value of the underlying forward rate. As mentioned in Section 2.1.2, a cap is a collection of caplets with a common strike X. Each caplet would however be ATM for a different strike X_i. We can select a single rate that takes into account all the forward rates of the underlying caplets. This rate is called the forward swap rate and will be used in the determination of strikes for ATM caps in the next section (Gatarek, Bachert and Maksymiuk [21]).

7.2.1 ATM Strikes for Caps

A forward swap rate is per definition the rate of the fixed leg of an interest rate swap that will ensure that the present value of the fixed leg will be equal to the present value of the floating leg of the swap. Consider an interest rate swap that starts at T_s and ends at T_N. Then, according to Equation (4.2.1), we have that forward swap rate is given by (proof provided in Appendix B.1)

$$SR_{s,N}(T_0) = \frac{B(T_0, T_s) - B(T_0, T_N)}{\sum_{i=s+1}^{N} B(T_0, T_i)\alpha_{T_{i-1}T_i}}.$$

The forward swap rate $SR_{s,N}(T_0)$, as given above, will be used to determine strikes for ATM caps. The concept of calculating forward swap rates is illustrated in the following example as given by Gatarek, Bachert and Maksymiuk [21].

The example will be aimed at replicating some of the results obtained by the authors and examining the calculations in more detail. This will then be extended in the following chapter to the South African market.

Example 7.2.1 In this example, we will compute the ATM strikes of a series of caps maturing from one year up to 20 years. We will assume that ATM cap options starts at date T_0 and have 3-monthly resets. Resets occur at the start of each period and payments at the end. Rates reset against the 3-month LIBOR rate. Given that caps start at T_0, we will need to adjust the discount factors in Table 7.1 to reflect discount factors up to time T_0 instead of time $t = 0$. This is a simple calculation and is given by the following equation

$$B(T_0, T_i) = B(0, T_i)/B(0, T_0). \tag{7.2.1}$$

The table below illustrates the process of computing ATM strikes for caps with maturities from 1 year up to 20 years

Time T_i	Date	Year fraction act/360 $\alpha_{T_{i-1}T_i}$	Disc factor (DF) $B(T_0,T_i)$	Spot Rate	Year fraction *DF $\alpha_{T_{i-1}T_i} * B(T_0,T_i)$	Cum Sum $\sum_{j=6M}^{i} \alpha_{T_{j-1}T_j} B(T_0,T_j)$	Difference of DF $B(T_0,T_{3M}) - B(T_0,T_i)$	Forward swap rate (ATM cap strike) $SR_{3M,i}(T_0)$
3M	2005/04/25	0.2500	0.9948					
6M	2005/07/25	0.2528	0.9893		0.2501	0.2501	0.0055	2.194%
9M	2005/10/25	0.2556	0.9835		0.2513	0.5014	0.0113	2.245%
1Y	2006/01/25	0.2556	0.9775	0.0227	0.2498	0.7512	0.0173	2.301%
1Y 3M	2006/04/25	0.2500	0.9713	0.0233	0.2428	0.9940	0.0235	2.361%
1Y 6M	2006/07/25	0.2528	0.9648	0.0239	0.2439	1.2379	0.0299	2.419%
1Y 9M	2006/10/25	0.2556	0.9580	0.0245	0.2448	1.4827	0.0367	2.478%
2Y	2007/01/25	0.2556	0.9510	0.0251	0.2430	1.7258	0.0438	2.536%
2Y 3M	2007/04/25	0.2500	0.9441	0.0256	0.2360	1.9618	0.0507	2.583%
2Y 6M	2007/07/25	0.2528	0.9369	0.0261	0.2368	2.1986	0.0578	2.629%
2Y 9M	2007/10/25	0.2556	0.9295	0.0266	0.2376	2.4362	0.0652	2.677%
3Y	2008/01/25	0.2556	0.9220	0.0271	0.2356	2.6718	0.0728	2.724%
3Y 3M	2008/04/25	0.2528	0.9145	0.0275	0.2312	2.9030	0.0802	2.764%
3Y 6M	2008/07/25	0.2528	0.9069	0.0279	0.2293	3.1322	0.0878	2.804%
3Y 9M	2008/10/27	0.2611	0.8989	0.0284	0.2347	3.3669	0.0958	2.845%
4Y	2009/01/26	0.2528	0.8911	0.0288	0.2253	3.5922	0.1037	2.885%
4Y 3M	2009/04/27	0.2528	0.8833	0.0292	0.2233	3.8155	0.1115	2.922%
4Y 6M	2009/07/27	0.2528	0.8753	0.0296	0.2213	4.0367	0.1194	2.958%
4Y 9M	2009/10/26	0.2528	0.8673	0.0300	0.2192	4.2559	0.1275	2.995%
5Y	2010/01/25	0.2528	0.8592	0.0304	0.2172	4.4731	0.1356	3.031%
5Y 3M	2010/04/26	0.2528	0.8511	0.0307	0.2151	4.6883	0.1436	3.064%
5Y 6M	2010/07/26	0.2528	0.8430	0.0311	0.2131	4.9014	0.1518	3.096%
5Y 9M	2010/10/25	0.2528	0.8348	0.0315	0.2110	5.1124	0.1600	3.129%
6Y	2011/01/25	0.2556	0.8264	0.0318	0.2112	5.3236	0.1683	3.162%
7Y	2012/01/25	0.2556	0.7931	0.0332	0.2027	6.1404	0.2017	3.285%
8Y	2013/01/25	0.2556	0.7598	0.0344	0.1942	6.9255	0.2350	3.393%
9Y	2014/01/27	0.2611	0.7263	0.0356	0.1896	7.6788	0.2685	3.496%
10Y	2015/01/26	0.2528	0.6944	0.0366	0.1755	8.3930	0.3003	3.578%
11Y	2016/01/25	0.2528	0.6646	0.0373	0.1680	9.0763	0.3302	3.638%
12Y	2017/01/25	0.2556	0.6350	0.0380	0.1623	9.7331	0.3598	3.696%
13Y	2018/01/25	0.2556	0.6069	0.0386	0.1551	10.3590	0.3879	3.744%
14Y	2019/01/25	0.2556	0.5794	0.0392	0.1481	10.9569	0.4154	3.791%
15Y	2020/01/27	0.2611	0.5523	0.0398	0.1442	11.5302	0.4424	3.837%
16Y	2021/01/25	0.2528	0.5275	0.0402	0.1333	12.0729	0.4673	3.871%
17Y	2022/01/25	0.2556	0.5032	0.0406	0.1286	12.5923	0.4915	3.903%
18Y	2023/01/25	0.2556	0.4797	0.0410	0.1226	13.0875	0.5150	3.935%
19Y	2024/01/25	0.2556	0.4569	0.0415	0.1168	13.5594	0.5378	3.967%
20Y	2025/01/27	0.2611	0.4347	0.0419	0.1135	14.0122	0.5601	3.997%

Table 7.4: Computing ATM strikes for caps from the European market data of 2005/01/21 (Gatarek, Bachert and Maksymiuk [21]).

The table is mostly in the same format as given by Gatarek, Bachert and Maksymiuk [21], however all values were physically replicated which resulted in small rounding differences. An extra column was included to illustrate the intermediate spot rate values necessary for the calculation of unknown discount

factors. Below we will consider some simple examples illustrating the different techniques used.

Firstly note that time T_0, as specified in Table 7.1, is 2005/01/25. The calculations are as follows:

$T_i = 3\text{M}$

$$\begin{aligned}
\text{Year Fraction} &= \text{DaysBetween}(2005/04/25,2005/01/25)/360 \\
&= 90/360 \\
&= 0.25000. \\
\text{Disc Factor} &= B(0,T_{3M})/B(0,T_0) \\
&= 0.9945224/0.9997685 \\
&= 0.9947527.
\end{aligned}$$

$T_i = 6\text{M}$

$$\begin{aligned}
\text{Year Fraction} &= \text{DaysBetween}(2005/07/25,2005/04/25)/360 \\
&= 91/360 \\
&= 0.25278. \\
\text{Disc Factor} &= B(0,T_{6M})/B(0,T_0) \\
&= 0.9890361/0.9997685 \\
&= 0.9892651. \\
\text{Year Fraction} \times \text{DF} &= 0.25278 \times 0.9892651 \\
&= 0.2500642. \\
\text{Cumulative Sum} &= \text{Year Fraction} \times \text{DF} \\
&= 0.2500642. \\
\text{Difference of DF} &= B(T_0,T_{3M}) - B(T_0,T_{6M}) \\
&= 0.9947527 - 0.9892651 \\
&= 0.0054876. \\
\text{Forward Swap Rate} &= (\text{Difference of DF})/(\text{Cumulative Sum}) \\
&= 0.0054876/0.2500642 \\
&= 2.19\%.
\end{aligned}$$

Also note that Table 7.4 contains discount factors for periods other than those given as inputs in Table 7.1. These discount factors were obtained through using linear interpolation between the associated spot rates. We will briefly illustrate this process below:

Let us consider the calculation of the discount factor for maturity T_{1Y3M}. From Table 7.4 we have that

$$B(T_0,T_{1Y}) = 0.9774658$$

and

$$B(T_0, T_{2Y}) = 0.9509789.$$

Using these discount factors we can calculate the following spot rates (used annual compounding and day count convention of act/360)

$$z(T_0, T_{1Y}) = 0.0227343$$

$$z(T_0, T_{2Y}) = 0.0250972.$$

Applying linear interpolation to above zero rates yield

$$z(T_0, T_{1Y3M}) = 0.0233170.$$

Finally, we can convert above rate to the discount factor

$$B(T_0, T_{1Y3M}) = 0.9712885$$

which, given rounding, is equivalent to the value given in Table 7.4.

This concludes the calculation of ATM strikes for the quoted caps. We will now consider the calculation of caplet volatilities given the quoted cap volatilities.

7.2.2 Stripping Caplet Volatilities from Cap Quotes

Before we proceed, let us consider how quoted cap volatilities should be interpreted. We will follow arguments given by Brigo and Mercurio [11] and Gatarek, Bachert and Maksymiuk [21]. We know from Section 2.1.2 that the price of a cap is equal to the sum of the prices of the underlying caplets. The market quoted cap volatility is the average volatility, that when applied to all underlying caplets, will give you the market price of the cap (Hull [32]). Hence, for a cap starting at T_0 with quarterly resets starting at T_{3M}, we have that

$$\text{Cap}^{MKT}(T_0, T_j, X, \sigma_{T_0T_j.\text{cap}}) = \sum_{i=3M}^{j-1} \text{Cpl}^{Black}(T_0, T_i, T_{i+1}, X, \sigma_{T_0T_j.\text{cap}}).$$

Brigo and Mercurio [11] point out that this formula results in some inconsistencies as a T_i maturity caplet will have different volatilities when determined from different caps. In order to eliminate these inconsistencies, we need to have

$$\begin{aligned} &\sum_{i=3M}^{j-1} \text{Cpl}^{Black}(T_0, T_i, T_{i+1}, X, \sigma_{T_0T_j.\text{cap}}) \\ &= \sum_{i=3M}^{j-1} \text{Cpl}^{Black}(T_0, T_i, T_{i+1}, X, \sigma_{T_iT_{i+1}.\text{caplet}}). \end{aligned} \tag{7.2.2}$$

Given the preliminary calculations, we can now move on to consider the stripping methodology as presented by Gatarek, Bachert and Maksymiuk [21].

Example 7.2.2

Firstly, notice that the volatility data given in Table 7.1 only starts at $T = 1Y$. This then implies some difficulties in the use of Equation (7.2.2) since we do not have cap volatilities for each of the periods prior to one year. In order to facilitate the caplet stripping procedure, Gatarek, Bachert and Maksymiuk [21] points out that it is common practice to assume constant volatilities for the caps with expiries less than a year (given these volatilities are not observable in the market). This is given by the equation below

$$\sigma_{T_0T_{6M}.\text{cap}} = \sigma_{T_0T_{9M}.\text{cap}} = \sigma_{T_0T_{1Y}.\text{cap}}.$$

The cap maturing at $t = T_{6M}$ consists of only one caplet, i.e. the caplet spanning the time period $T_{3M} - T_{6M}$, and hence we have that the volatility of this caplet is equal to the volatility of the cap. Next we can consider the calculation of the volatility of the caplet spanning the time period $T_{6M} - T_{9M}$. We know that the cap with maturity $t = T_{9M}$ consists of both the $T_{3M} - T_{6M}$ and $T_{6M} - T_{9M}$ caplets. Using Equation (7.2.2), we obtain

$$\begin{aligned}
&\text{Cpl}^{Black}(T_0, T_{3M}, T_{6M}, X, \sigma_{T_0T_{9M}.\text{cap}}) \\
+&\text{Cpl}^{Black}(T_0, T_{6M}, T_{9M}, X, \sigma_{T_0T_{9M}.\text{cap}}) \\
=&\text{Cpl}^{Black}(T_0, T_{3M}, T_{6M}, X, \sigma_{T_{3M}T_{6M}.\text{caplet}}) \\
&\text{Cpl}^{Black}(T_0, T_{6M}, T_{9M}, X, \sigma_{T_{6M}T_{9M}.\text{caplet}}).
\end{aligned}$$

Given that $\sigma_{T_0T_{9M}.\text{cap}}$ and $\sigma_{T_{3M}T_{6M}.\text{caplet}}$ equals 0.1641, we have that

$$\sigma_{T_{6M}T_{9M}.\text{caplet}} = 0.1641.$$

Similarly, we can obtain the volatility of the caplet spanning the time period $T_{9M} - T_{1Y}$ as

$$\sigma_{T_{9M}T_{1Y}.\text{caplet}} = 0.1641.$$

In order to calculate caplet volatilities for broken periods above 1 year, we firstly need to obtain cap volatilities for these periods as only cap volatilities for full years are taken directly from the market. This is done through using linear interpolation. For example, consider the following (Gatarek, Bachert and Maksymiuk [21] assumed quarterly year fractions of exactly 0.25, this can be changed to ACT/360)

$$\begin{aligned}
&\sigma_{T_0T_{1y3M}.\text{cap}} \\
=&0.25 \times (\sigma_{T_0T_{2y}.\text{cap}} - \sigma_{T_0T_{1y}.\text{cap}}) + \sigma_{T_0T_{1y}.\text{cap}} \\
=&0.25 \times (0.2137 - 0.1641) + 0.1641 \\
=&0.1765
\end{aligned}$$

and

$$\begin{aligned}
&\sigma_{T_0T_{1y6M}.\text{cap}} \\
=&0.5 \times (\sigma_{T_0T_{2y}.\text{cap}} - \sigma_{T_0T_{1y}.\text{cap}}) + \sigma_{T_0T_{1y}.\text{cap}} \\
=&0.5 \times (0.2137 - 0.1641) + 0.1641 \\
=&0.1889.
\end{aligned}$$

Similar calculations show that

$$\sigma_{T_0T_{1y9M}.\text{cap}} = 0.2013.$$

Given these cap volatilities, we can calculate the volatilities $\sigma_{T_{1Y}T_{1Y3M}.\text{caplet}}$, $\sigma_{T_{1Y3M}T_{1Y6M}.\text{caplet}}$ and $\sigma_{T_{1Y6M}T_{1Y9M}.\text{caplet}}$ using Equation (7.2.2).

We will now illustrate the calculation of the volatility $\sigma_{T_{1Y}T_{1Y3M}.\text{caplet}}$. The terms of Equation (7.2.2) where obtained as follows:

Using cap volatility

$$\begin{aligned}
&\text{Cpl}^{Black}(T_0, T_{3M}, T_{6M}, X, \sigma_{T_0T_{1Y3M}.\text{cap}}) = 0.00005756 \\
&\text{Cpl}^{Black}(T_0, T_{6M}, T_{9M}, X, \sigma_{T_0T_{1Y3M}.\text{cap}}) = 0.00021627 \\
&\text{Cpl}^{Black}(T_0, T_{9M}, T_{1Y}, X, \sigma_{T_0T_{1Y3M}.\text{cap}}) = 0.00043742 \\
&\text{Cpl}^{Black}(T_0, T_{1Y}, T_{1Y3M}, X, \sigma_{T_0T_{1Y3M}.\text{cap}}) = 0.00068103.
\end{aligned}$$

Using caplet volatility

$$\begin{aligned}
&\text{Cpl}^{Black}(T_0, T_{3M}, T_{6M}, X, \sigma_{T_{3M}T_{6M}.\text{caplet}}) = 0.00004782 \\
&\text{Cpl}^{Black}(T_0, T_{6M}, T_{9M}, X, \sigma_{T_{6M}T_{9M}.\text{caplet}}) = 0.00019635 \\
&\text{Cpl}^{Black}(T_0, T_{9M}, T_{1Y}, X, \sigma_{T_{9M}T_{1Y}.\text{caplet}}) = 0.00041210,
\end{aligned}$$

where X, according to Table 7.4, is equal to 2.361%. Subtracting the sum of the caplet prices derived using caplet volatilities from the sum of the caplet prices derived using the cap volatility, we obtain

$$\text{Cpl}^{Black}(T_0, T_{1Y}, T_{1Y3M}, X, \sigma_{T_{1Y}T_{1Y3M}.\text{caplet}}) = 0.00073601.$$

The final step in the calculation is to use a numeric algorithm to obtain the volatility for which above equation will hold. This was obtained as

$$\sigma_{T_{1Y}T_{1Y3M}.\text{caplet}} = 0.2015.$$

Repeating above process, produced the following results

$$\begin{aligned}
\sigma_{T_{1Y3M}T_{1Y6M}.\text{caplet}} &= 0.2189, \\
\sigma_{T_{1Y6M}T_{1Y9M}.\text{caplet}} &= 0.2365,
\end{aligned}$$

and

$$\sigma_{T_{1Y9M}T_{2Y}.\text{caplet}} = 0.2550.$$

The complete set of results, as given in the book by Gatarek, Bachert and Maksymiuk [21], is given in the table below.

Tenor T_i	Cap Volatility $\sigma_{T_0T_i.\text{cap}}$	Caplet Volatility $\sigma_{T_{i-1}T_i.\text{caplet}}$	Time Homogeneity Test $\sigma^2_{T_{i-1}T_i.\text{caplet}}\alpha_{T_0T_{i-1}}$
6M	0.1641	0.1641	0.0067
9M	0.1641	0.1641	0.0135
1Y	0.1641	0.1641	0.0204
1Y 3M	0.1765	0.2015	0.0412
1Y 6M	0.1889	0.2189	0.0606
1Y 9M	0.2013	0.2365	0.0849
2Y	0.2137	0.2550	0.1153
2Y 3M	0.2162	0.2213	0.0993
2Y 6M	0.2186	0.2255	0.1159
2Y 9M	0.2211	0.2298	0.1336
3Y	0.2235	0.2342	0.1528
3Y 3M	0.2223	0.2098	0.1339
3Y 6M	0.2212	0.2084	0.1431
3Y 9M	0.2200	0.2073	0.1524
4Y	0.2188	0.2055	0.1608
5Y	0.2127	0.1938	0.1811
6Y	0.2068	0.1859	0.2014
7Y	0.2012	0.1781	0.2171
8Y	0.1958	0.1700	0.2272
9Y	0.1905	0.1621	0.2331
10Y	0.1859	0.1569	0.2437
11Y	0.1833	0.1650	0.2969
12Y	0.1806	0.1602	0.3058
13Y	0.1770	0.1450	0.2720
14Y	0.1735	0.1380	0.2655
15Y	0.1699	0.1316	0.2592
16Y	0.1673	0.1352	0.2922
17Y	0.1646	0.1300	0.2871
18Y	0.1620	0.1243	0.2780
19Y	0.1593	0.1184	0.2664
20Y	0.1567	0.1133	0.2571

Table 7.5: ATM caplet volatilities obtained from European cap volatilities for business date 2005/01/21 (Gatarek, Bachert and Maksymiuk [21]).

Consider the caplet volatility structure as given in Table 7.5. This implies a similar humped shape as the one presented in Figure 7.1 for cap volatilities. The biggest difference is however in the variability of caplet volatilities vs. that of the associated cap volatilities. Gatarek, Bachert and Maksymiuk [21] points out that this is simply due to the fact that cap volatilities are representative

of average caplet volatilities. The caplet volatility structure is presented in the figure below.

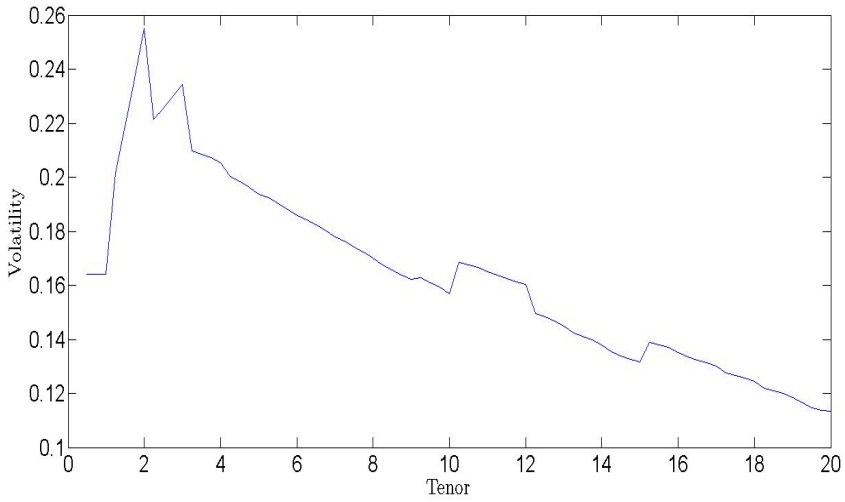

Figure 7.5: ATM caplet volatilities obtained from European cap volatilities for business date 2005/01/21 (Gatarek, Bachert and Maksymiuk [21]).

Next, let us consider the last column of Table 7.5. This is presented in the figure below.

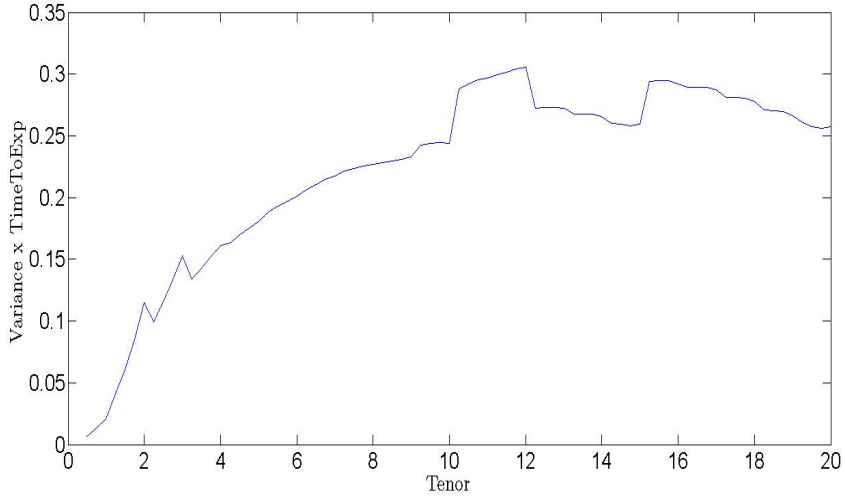

Figure 7.6: Time homogeneity test derived from European ATM caplet volatilities for business date 2005/01/21 (Gatarek, Bachert and Maksymiuk [21]).

As discussed in Chapter 5, it will always be possible to recover today's caplet prices for a volatility specification according to Equation (5.2.2) if $T_i\sigma^2_{T_iT_{i+1}.\text{caplet}}$ is a strictly increasing function of T_i.

From Figure 7.6 it is clearly evident that this is not the case. The impact of this characteristic on the calibration of the model will be considered in a later chapter.

Chapter 8

South African Market Data

This chapter will move on to consider how we can obtain similar inputs from the South African market. Topics covered, will range from different data sources to the bootstrapping of curves and volatilities. This will illustrate why some of the modeling assumptions made in the previous chapters are applicable to the South African market.

8.1 Actual Market Inputs

The purpose of this chapter is largely to illustrate how we can apply the techniques derived in the previous chapters to the South African market. Given this motivation, I have decided to follow a slightly different approach in the sourcing of the relevant market data. Instead of taking market data from Reuters (or similar sources) as illustrated by Gatarek, Bachert and Maksymiuk [21], this chapter will rather be based on the market data of a certain South African investment bank. This will not only allow the analysis of the real life market views and assumptions made by SA traders, but will also help to eliminate the noise associated with illiquid prices. It is important to note that these prices are submitted to price testing processes on a weekly basis and hence can be assumed to be a relatively accurate reflection of the data available on sources such as Reuters and Bloomberg.

Although we will be using actual trader inputs for calculation purposes, it will be illustrated how similar market data can be obtained from trading sources such as Reuters or Bloomberg.

8.1.1 Benchmark Rates

Benchmark rates will be defined as the benchmark instruments used as input variables in the construction of an interest rate yield curve. These rates are typically JIBAR rates, FRAs and swaps depending on the type of yield curve and the market under consideration. The yield curve to be considered in this

section will consist of a $3M$ JIBAR rate, 3 monthly FRAs and interest rate swaps exchanging fixed cash flows for floating cash flows linked to $3M$ JIBAR. Consequently, this curve is typically referred to as a three-month ZAR interest rate curve. Similar curves can be constructed to more accurately price and risk manage instruments that have resets occurring at time intervals other than three-months.

The available data set ranges from 2005/01/03 until 2009/12/31, with the data for 2009/12/31 presented in the table below.

No.	Benchmark Instrument	Rate
1	JIBAR 3M	7.229
2	FRA 3x6	7.090
3	FRA 6x9	7.110
4	FRA 9x12	7.280
5	FRA 12x15	7.510
6	FRA 15x18	7.860
7	FRA 18x21	8.822
8	FRA 21x24	8.620
9	IRS 3Y	8.035
10	IRS 4Y	8.342
11	IRS 5Y	8.520
12	IRS 6Y	8.637
13	IRS 7Y	8.712
14	IRS 8Y	8.760
15	IRS 9Y	8.790
16	IRS 10Y	8.787
17	IRS 12Y	8.737
18	IRS 15Y	8.567
19	IRS 20Y	8.297
20	IRS 25Y	8.057
21	IRS 30Y	7.837

Table 8.1: Benchmark instruments obtained from a South African investment bank for business date 2009/12/31.

It is worth mentioning how to interpret some of these rates. All rates defined above are typically given using simple compounding convention.

The Johannesburg Interbank Agreed Rate (JIBAR) is a daily reference rate based on interest rates at which banks borrow unsecured funds from other banks in the South African interbank market. This rate is determined through taking an average of a series of quotes following the elimination of certain outliers. These rates are available for different time periods, for example one-month, three-month, six-month, nine-month and twelve-month (Gumbo [23]).

The FRAs in turn are defined as forward rates for a specific three month time period, whereas swap rates are defined as the fixed rates that will ensure swaps to price back to zero.

In order to understand these market variables and how they behave under different market circumstances, we will consider graphs of these rates for different interest rate cycles. An interest rate cycle will in turn be defined as the different time periods relating to the hiking or cutting of interest rates based on economic variables and the mandate of the Reserve Bank of South Africa. These time periods can be seen through looking at the history of the repo rate, defined as the rate at which banks can borrow money from the Reserve Bank. The repo rate, for various historical dates, is presented in the table below (Reserve Bank website [53]).

Date	Repo Rate	Change (in bps)
1999/11/25	12.00	
2000/01/14	11.75	-25
2000/10/17	12.00	25
2001/06/15	11.00	-100
2001/09/05	10.00	-100
2001/09/21	9.50	-50
2002/01/16	10.50	100
2002/03/15	11.50	100
2002/06/14	12.50	100
2002/09/13	13.50	100
2003/06/13	12.00	-150
2003/08/15	11.00	-100
2003/09/11	10.00	-100
2003/10/17	8.50	-150
2003/12/12	8.00	-50
2004/08/13	7.50	-50
2005/04/14	7.00	-50
2006/06/08	7.50	50
2006/08/03	8.00	50
2006/10/13	8.50	50
2006/12/08	9.00	50
2007/06/08	9.50	50
2007/08/17	10.00	50
2007/10/12	10.50	50
2007/12/07	11.00	50
2008/04/11	11.50	50
2008/06/13	12.00	50
2008/12/12	11.50	-50
2009/02/06	10.50	-100
2009/03/25	9.50	-100
2009/05/04	8.50	-100
2009/05/29	7.50	-100
2009/08/14	7.00	-50

Table 8.2: South African repo rate history for the time period 1999/11/25 - 2009/12/31.

Hence, we can observe five interest rate cycles (three cutting and two hiking

cycles). These are presented in Figure 8.1 below.

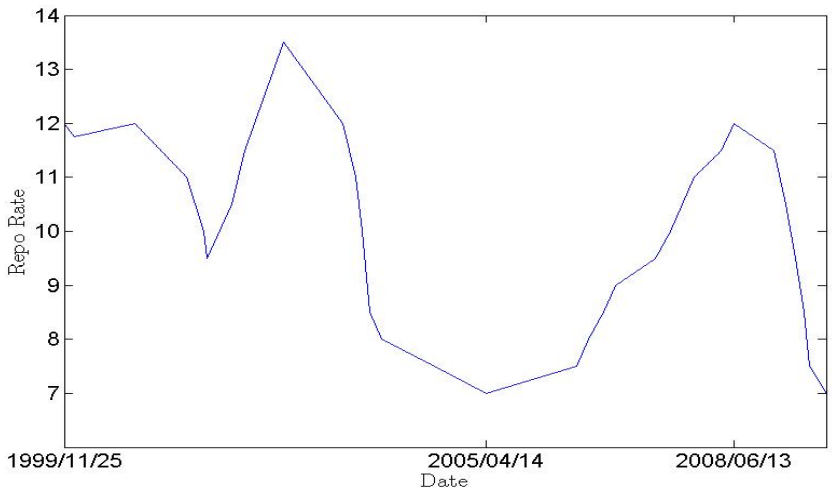

Figure 8.1: South African repo rate for the period 1999/11/25 - 2009/12/31.

Given the history we have at our disposal, we will analyze the movements present in the time periods 2005/01/03 - 2008/06/13 and 2008/06/14 - 2009/12/31.

The first time period relates to a rate hiking cycle. The benchmark rates associated with this cycle is presented in the figure below.

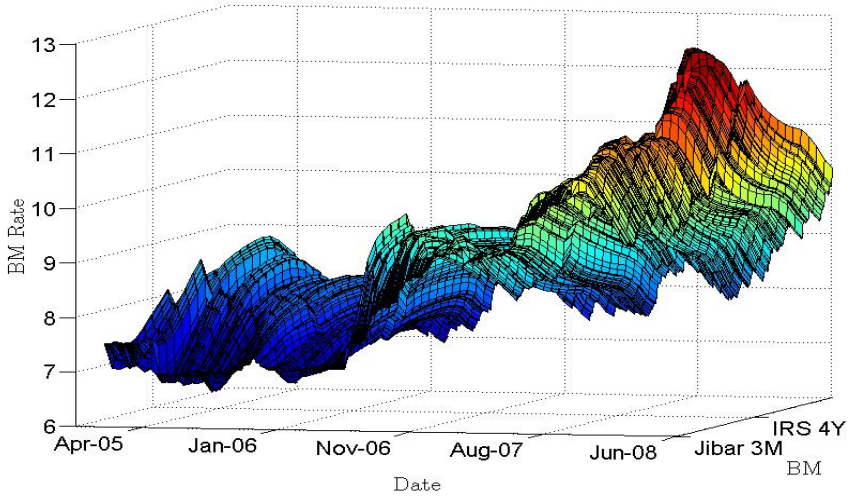

Figure 8.2: Benchmark rates obtained from a South African investment bank for the time period 2005/01/03 - 2008/06/13. This relates to a rate hiking cycle.

Figure 8.2 displays a clear increase in the level of benchmark rates, as well as an inversion in benchmark rates. By the latter we mean that short term rates appear to rise at a faster pace than longer term rates (also known as a bear inversion). This is reflective of expected rate hikes in the short term followed by lower rates in the longer term. Lower long term rates typically reflect the expectation that the monetary policy was successfully implemented (for example inflation within target range). Another point to note is that the change in level and shape (i.e. inversion of rates) started to appear roughly between Jan-06 and Nov-06 (see Figure 8.2). According to Table 8.2, this is exactly the time period in which we experienced the first hike of the new cycle.

The second time period relates to a rate cutting cycle. The benchmark rates associated with this cycle is presented in the figure below.

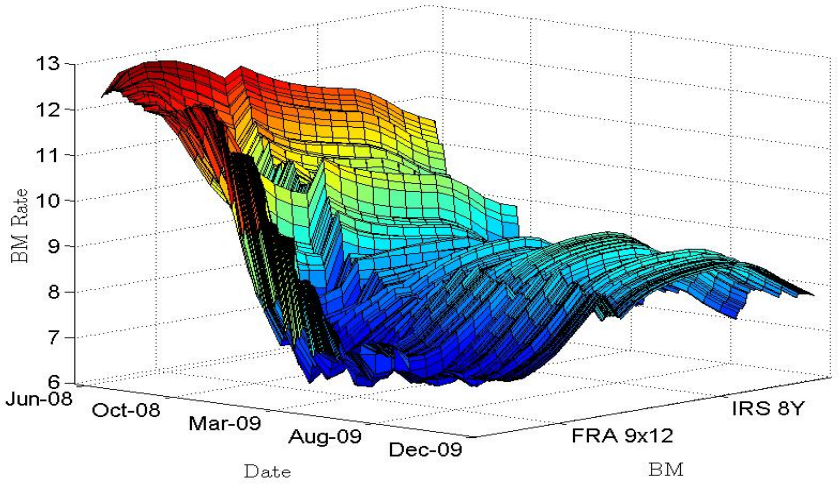

Figure 8.3: Benchmark rates obtained from a South African investment bank for the time period 2008/06/14 - 2009/12/31. This relates to a rate cutting cycle.

In contrast to the previous curve, Figure 8.3 is characterized by a decrease in the level of benchmark rates, while exhibiting a steepening of rates. This is known as a bull steepener (i.e. short term rates appear to be falling faster than longer term rates).

These two cycles represent some of the key interest rate movements observable in the market. Principal component analysis of these benchmarks are shown in the graphs below and are in line with the comments made above.

Figure 8.4 represents the first three vectors obtained from a principal component analysis on the data of cycle 1. The first two components, in order of importance, represent a parallel upward shift in rates as well as an inversion in rates (bear inversion).

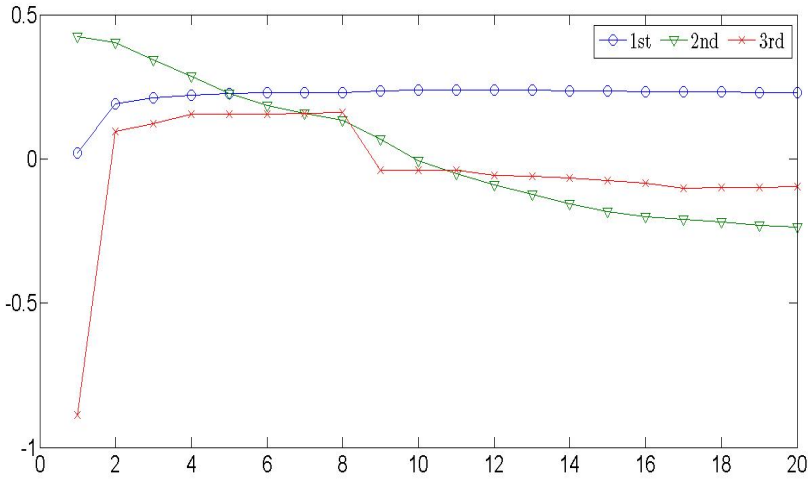

Figure 8.4: Results obtained from PCA when applied to the data presented in Figure 8.2. This relates to a rate hiking cycle.

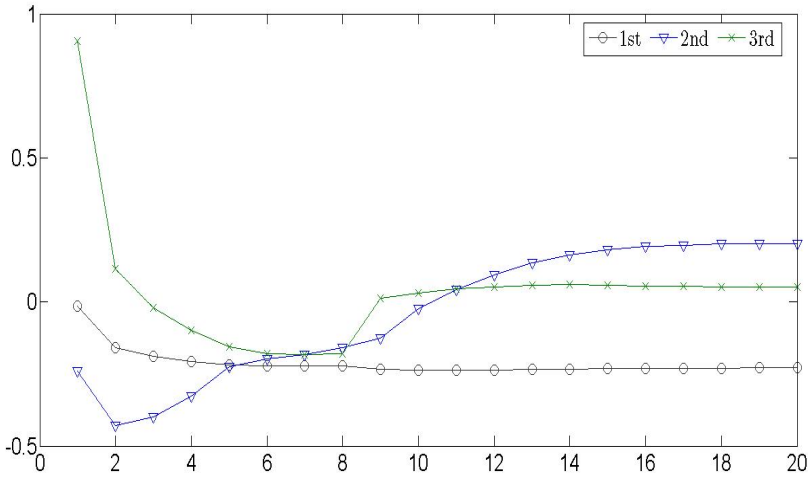

Figure 8.5: Results obtained from PCA when applied to the data presented in Figure 8.3. This relates to a rate cutting cycle.

Figure 8.5 in turn represents the first three vectors resulting from a principal component analysis on the data of cycle 2. The first two components, in order of importance, represent a parallel downward shift in rates as well as a steepening in rates (bull steepening).

Above benchmark rates can independently be sourced from Bloomberg or Reuters. Figure 8.6 illustrates the different JIBAR quotes available on

Bloomberg.[1] This confirms the observation made by Gumbo [23], i.e. JIBAR rates are typically quoted for the time periods one-month, three-month, six-month, nine-month and twelve-month.

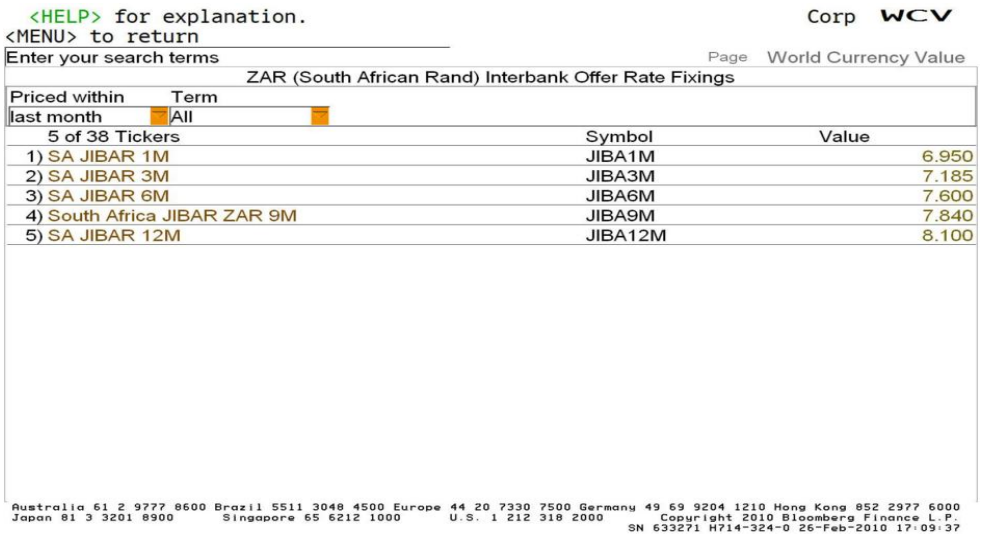

Figure 8.6: Example of extracting South African JIBAR rates from Bloomberg.

Next, Figure 8.7 shows the FRA quotations available on Bloomberg. Note from below that there are several FRAs available in the market. This thesis will, however, only consider the FRAs with forward time periods of three months. This is due to the fact that we will mainly focus on the modeling of three-monthly forward rates.

Similar results can be obtained for the other forward rates (and through using the associated x-month JIBAR rate and swaps with resetting intervals of x-months). It will also be shown at a later stage how we can convert three-month volatilities to different tenors which will consequently add some flexibility to the model.

Figure 8.8 presents the swap rates as quoted on Bloomberg. Similar to the rates illustrated in the previous figures, we have a number of quotations available in the market.

These screen prints illustrate how the data used in this section is typically presented in the market. For each of these quotes, it is possible to obtain historical data for a user specified time interval. It is, however, important to confirm what the day count conventions and compounding methodologies are before the data is used. This will be made more clear in later sections when we need to calculate forward rates and forward rate volatilities.

[1] In order to obtain the data from Bloomberg, one needs to use the command WCV ZAR <GO>. Once this command is entered, the user will be presented with a number of ZAR interest rate quotes.

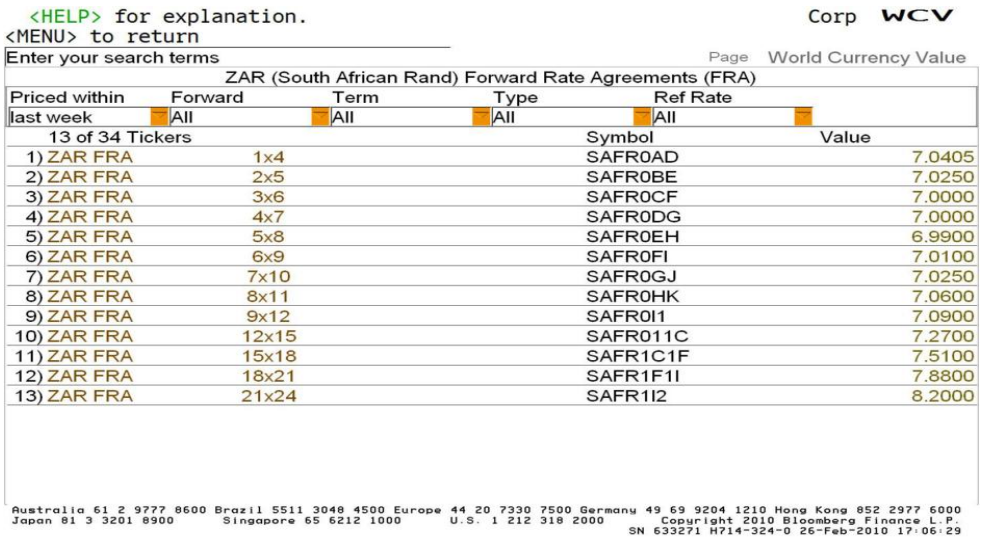

<HELP> for explanation. Corp WCV
<MENU> to return
Enter your search terms Page World Currency Value

ZAR (South African Rand) Forward Rate Agreements (FRA)

Priced within	Forward	Term	Type	Ref Rate
last week	All	All	All	All

13 of 34 Tickers		Symbol	Value
1) ZAR FRA	1x4	SAFR0AD	7.0405
2) ZAR FRA	2x5	SAFR0BE	7.0250
3) ZAR FRA	3x6	SAFR0CF	7.0000
4) ZAR FRA	4x7	SAFR0DG	7.0000
5) ZAR FRA	5x8	SAFR0EH	6.9900
6) ZAR FRA	6x9	SAFR0FI	7.0100
7) ZAR FRA	7x10	SAFR0GJ	7.0250
8) ZAR FRA	8x11	SAFR0HK	7.0600
9) ZAR FRA	9x12	SAFR0I1	7.0900
10) ZAR FRA	12x15	SAFR011C	7.2700
11) ZAR FRA	15x18	SAFR1C1F	7.5100
12) ZAR FRA	18x21	SAFR1F1I	7.8800
13) ZAR FRA	21x24	SAFR1I2	8.2000

Australia 61 2 9777 8600 Brazil 5511 3048 4500 Europe 44 20 7330 7500 Germany 49 69 9204 1210 Hong Kong 852 2977 6000
Japan 81 3 3201 8900 Singapore 65 6212 1000 U.S. 1 212 318 2000 Copyright 2010 Bloomberg Finance L.P.
SN 633271 H714-324-0 26-Feb-2010 17:06:29

Figure 8.7: Example of extracting South African FRA rates from Bloomberg.

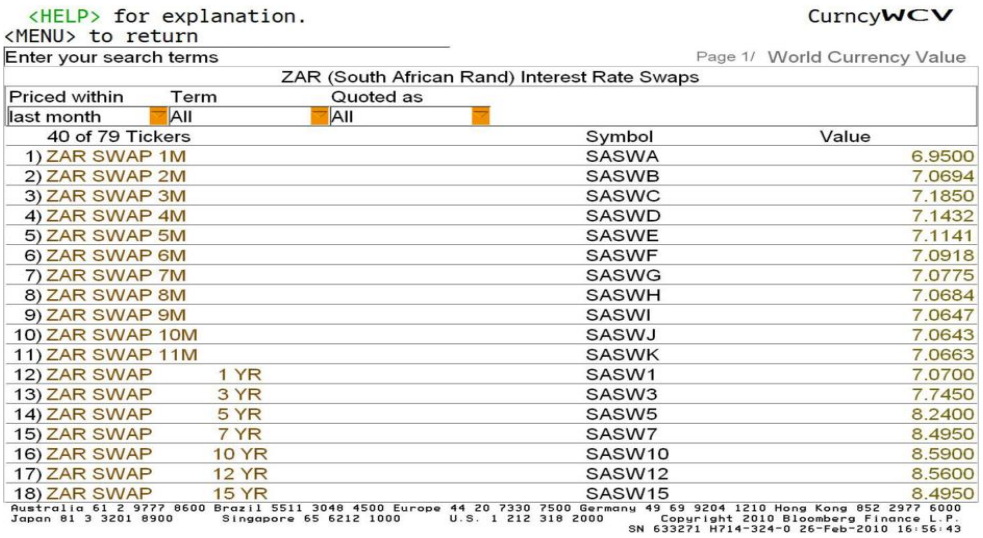

<HELP> for explanation. CurncyWCV
<MENU> to return
Enter your search terms Page 1/ World Currency Value

ZAR (South African Rand) Interest Rate Swaps

Priced within	Term	Quoted as
last month	All	All

40 of 79 Tickers		Symbol	Value
1) ZAR SWAP	1M	SASWA	6.9500
2) ZAR SWAP	2M	SASWB	7.0694
3) ZAR SWAP	3M	SASWC	7.1850
4) ZAR SWAP	4M	SASWD	7.1432
5) ZAR SWAP	5M	SASWE	7.1141
6) ZAR SWAP	6M	SASWF	7.0918
7) ZAR SWAP	7M	SASWG	7.0775
8) ZAR SWAP	8M	SASWH	7.0684
9) ZAR SWAP	9M	SASWI	7.0647
10) ZAR SWAP	10M	SASWJ	7.0643
11) ZAR SWAP	11M	SASWK	7.0663
12) ZAR SWAP	1 YR	SASW1	7.0700
13) ZAR SWAP	3 YR	SASW3	7.7450
14) ZAR SWAP	5 YR	SASW5	8.2400
15) ZAR SWAP	7 YR	SASW7	8.4950
16) ZAR SWAP	10 YR	SASW10	8.5900
17) ZAR SWAP	12 YR	SASW12	8.5600
18) ZAR SWAP	15 YR	SASW15	8.4950

Australia 61 2 9777 8600 Brazil 5511 3048 4500 Europe 44 20 7330 7500 Germany 49 69 9204 1210 Hong Kong 852 2977 6000
Japan 81 3 3201 8900 Singapore 65 6212 1000 U.S. 1 212 318 2000 Copyright 2010 Bloomberg Finance L.P.
SN 633271 H714-324-0 26-Feb-2010 16:56:43

Figure 8.8: Example of extracting South African swap rates from Bloomberg.

8.1.2 Cap and Caplet Volatilities

This section will present the ATM cap and caplet volatilities as obtained from one of the South African investment banks. The volatilities changed from a mixture of caplet (in short term) and cap volatilities (longer term) to a set consisting of only caplet volatilities from 0 to 10.25 years (driven by changes in business processes and trader views). The caplet volatilities, for business date 2009/12/31, is presented in Table 8.3.

The calculation of the time homogeneity factors, as presented in the table below, was based on the assumptions that T_0 =2009/12/31 and that the three-monthly time periods are given by equal fractions of 0.25.

Tenor T_i	Caplet Volatility $\sigma_{T_{i-1}T_i.\text{caplet}}$	Time Homogeneity Test $\sigma^2_{T_{i-1}T_i.\text{caplet}}\alpha_{T_0T_{i-1}}$
6M	0.12518	0.00392
9M	0.13991	0.00979
1Y	0.15458	0.01792
1Y 3M	0.16334	0.02668
1Y 6M	0.16497	0.03402
1Y 9M	0.16657	0.04162
2Y	0.16786	0.04931
2Y 3M	0.17250	0.05951
2Y 6M	0.16773	0.06330
2Y 9M	0.16299	0.06641
3Y	0.15850	0.06909
3Y 3M	0.15747	0.07439
3Y 6M	0.15416	0.07724
3Y 9M	0.15031	0.07908
4Y	0.14625	0.08021
4Y 3M	0.14731	0.08680
4Y 6M	0.14408	0.08823
4Y 9M	0.14084	0.08926
5Y	0.13752	0.08983
5Y 3M	0.13702	0.09387
5Y 6M	0.13575	0.09675
5Y 9M	0.13447	0.09945
6Y	0.13311	0.10188
6Y 3M	0.13422	0.10809
6Y 6M	0.13305	0.11064
6Y 9M	0.13193	0.11314
7Y	0.13070	0.11531
7Y 3M	0.13150	0.12105
7Y 6M	0.13045	0.12337
7Y 9M	0.12939	0.12556
8Y	0.12834	0.12765
8Y 3M	0.12878	0.13267
8Y 6M	0.12776	0.13466
8Y 9M	0.12663	0.13630
9Y	0.12576	0.13839
9Y 3M	0.12778	0.14695
9Y 6M	0.12687	0.14889
9Y 9M	0.12605	0.15094
10Y	0.12495	0.15222
10Y 3M	0.12677	0.16071

Table 8.3: ATM caplet volatilities obtained from a South African investment bank, for business date 2009/12/31, following a caplet stripping procedure.

The caplet volatility structure, as given in Table 8.3, clearly implies a

humped shape with the peak in the $2Y$ region. This is similar to the behaviour of volatilities in the European market and is presented in Figure 8.9 below.

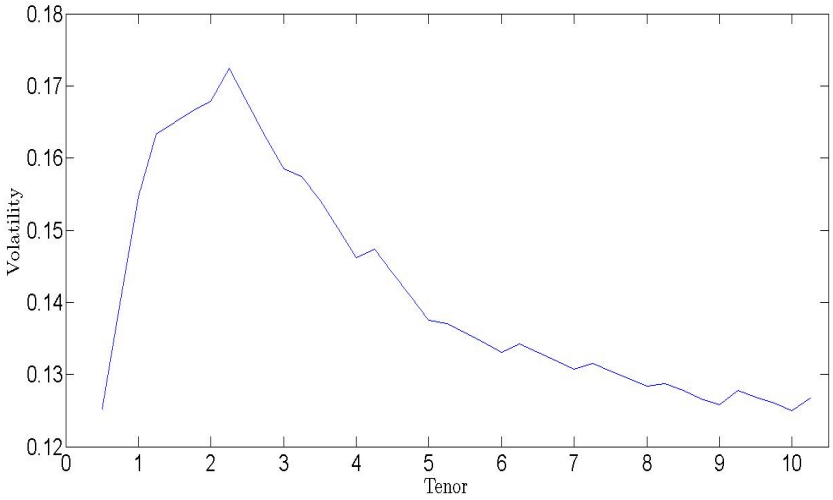

Figure 8.9: ATM caplet volatilities obtained from a South African investment bank, for business date 2009/12/31, following a caplet stripping procedure.

Next, we will consider the time homogeneity test. This is presented in Figure 8.10 below.

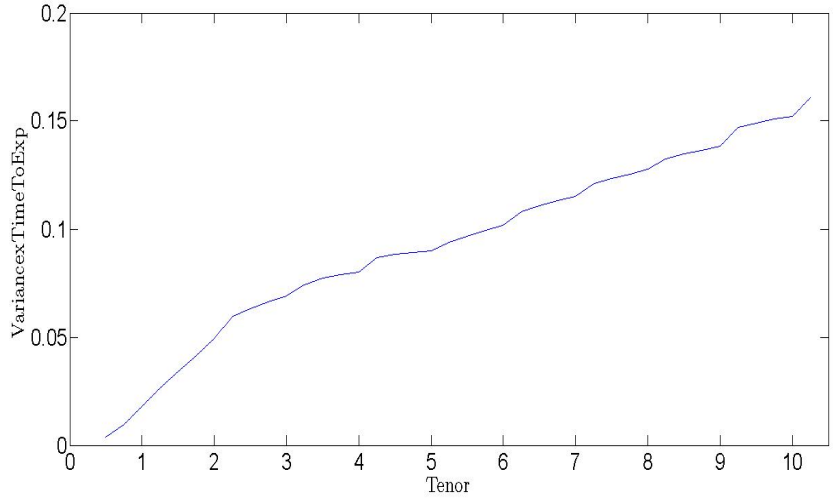

Figure 8.10: Time homogeneity test derived from South African ATM caplet volatilities for business date 2009/12/31.

From the figure above and Table 8.3, it is evident that this function is strictly increasing and hence we can expect the shape of term structure of volatilities to remain the same over time.

Before we proceed any further, it is worth repeating some of the properties associated with the volatility behaviour presented in Figure 8.9. It was mentioned earlier that this type of behaviour is typically observed under normal market conditions (Rebonato [47]). This represents uncertainty in the medium term which typically relates to expected monetary rate decisions. The lower volatilities observed in the short- and longer term maturities reflect the low probabilities associated with unexpected monetary rate decisions (in the short-term) and economic news that may result in structural changes (in the longer-term, such as a change in inflation targeting). Historical analysis presented later in the chapter will also consider the other end of this spectrum, i.e. volatility behaviour in more volatile time periods.

The above examples specifically relate to business date 2009/12/31. The available set of volatilities only consists of weekly volatilities from 2009/05/06 to 2009/12/31. No historical caplet volatilities could be obtained from either Bloomberg or Reuters.

The granularity of the available volatilities differ through time (reflecting changes in business processes etc.) and can be divided into two periods. The volatilities for the last three months in the data set consists of three monthly caplet volatilities up to $10Y$ as illustrated in Table 8.3. This level of granularity is not available in the market and was obtained through a caplet volatility stripping procedure.

The volatility data of the first five months consists of caplet volatilities up to two years and cap volatilities for time periods $3Y$, $4Y$, $5Y$ and $10Y$. In order to illustrate the above, we will consider the volatility data for business date 2009/08/12. This is presented in Table 8.4 below.

Tenor T_i	Cap Volatility $\sigma_{T_0T_i.\text{cap}}$	Caplet Volatility $\sigma_{T_{i-1}T_i.\text{caplet}}$
6M		0.20303
9M		0.20692
1Y		0.20765
1Y 3M		0.20605
1Y 6M		0.20562
1Y 9M		0.20475
2Y		0.20128
3Y	0.20229	
4Y	0.19502	
5Y	0.18734	
10Y	0.17608	

Table 8.4: ATM cap and caplet volatilities obtained from a South African investment bank for business date 2009/08/12.

It will be illustrated later in the chapter how we can obtain three-monthly caplet volatilities, from the quotes given above, using a caplet stripping algorithm. This analysis will, however, be preceded with the bootstrapping of rates from the input benchmark rates. This part is necessary for the calculation of discount factors (and consequently the ATM swap strikes).

To conclude this section, we will take a look at the volatility data available on Bloomberg. Figure 8.11 illustrates the different available cap/caplet quotes.[2]

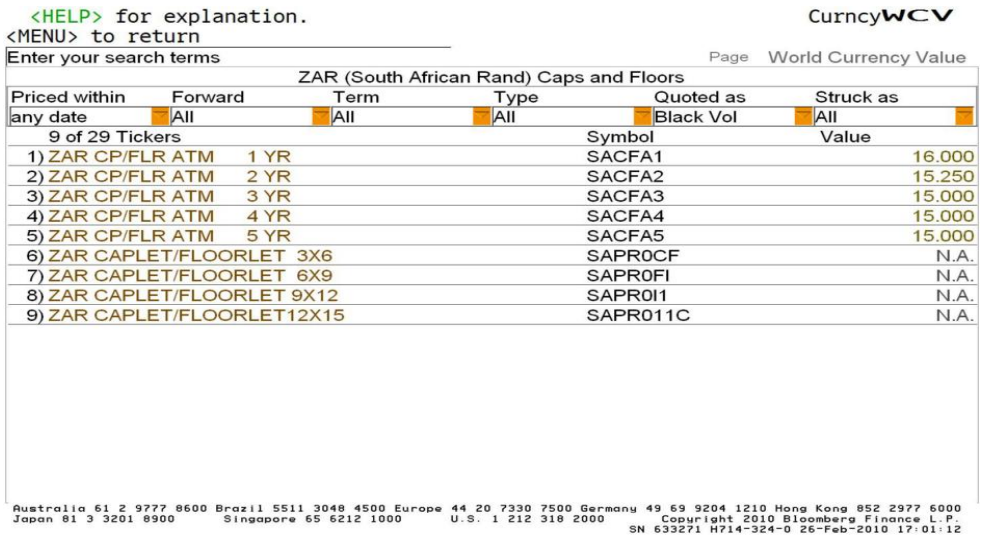

Figure 8.11: Example of extracting South African ATM cap and caplet volatilities from Bloomberg.

This thesis is mainly aimed at calibrating to ATM cap and caplet volatilities, hence the "Struck as" field should be chosen to reflect ATM options. Also note that the volatilities used in this setup are Black or lognormal volatilities. The user has the option of making this choice (see Figure 8.11). If it is only possible to obtain normal volatilities (hence not Black or lognormal), then we need to find a way to convert these volatilities to Black volatilities. The paper by Hagan [25] provides a relationship between the two types of volatilities.

8.1.3 Swaption Volatilities

This section will consider the set of available ATM swaption volatilities. Similar to the cap and caplet volatilities, the data set will consist of weekly spaced ATM swaption volatilities (obtained from one of the SA investment banks)

[2] In order to obtain the data from Bloomberg, we can use the same command WCV ZAR <GO>. Once this command is entered, the user can select the required volatilities from the list presented.

from 2009/05/06 to 2009/12/31. The volatilities for business date 2009/12/31 is presented in the table below.

	Option Expiry/Underlying Maturity							
	1Y	2Y	3Y	4Y	5Y	10Y	15Y	20Y
1M	0.14000	0.14250	0.14000	0.14000	0.13750	0.14000	0.14750	0.15750
3M	0.15500	0.15500	0.15000	0.14750	0.14500	0.14500	0.15250	0.16250
6M	0.16000	0.15750	0.15250	0.15000	0.14750	0.14500	0.15250	0.16250
1Y	0.17250	0.16000	0.16000	0.15750	0.15500	0.16000	0.16750	0.17750
2Y	0.15500	0.14250	0.14750	0.14500	0.14750	0.15750	0.16500	0.17500
5Y	0.14250	0.13000	0.13500	0.13250	0.13500	0.16250	0.17000	0.18000
10Y	0.14250	0.14000	0.15500	0.15750	0.16500	0.21500	0.22250	0.23250

Table 8.5: ATM swaption volatilities obtained from a South African investment bank for business date 2009/12/31.

The rows of the table above represent the option expiries while the columns represent the underlying swap maturities. Within this context, the start date of the underlying swap always coincides with the expiry date of the option. Table 8.5 is graphically presented in the figure below.

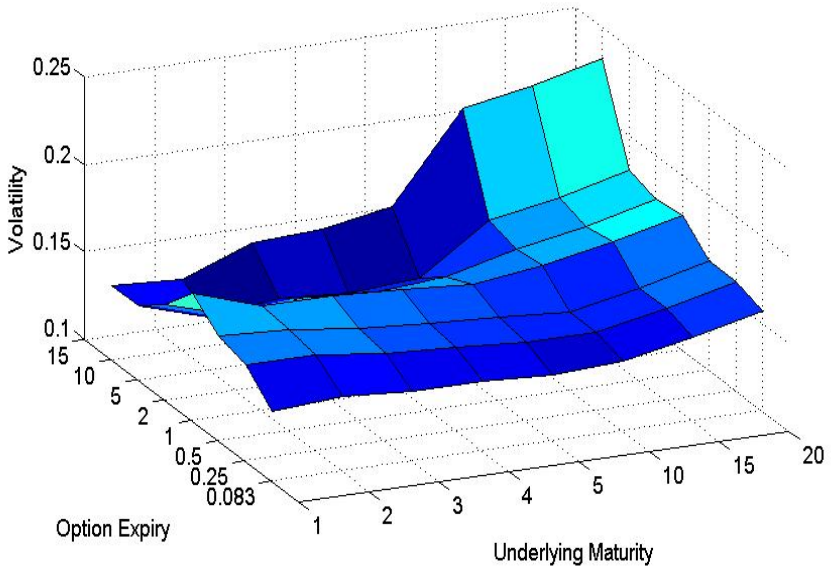

Figure 8.12: ATM Swaption volatilities obtained from a South African investment bank for business date 2009/12/31.

It was mentioned previously that these can and will be used to determine the correlation between different forward rates given the fact that a swap rate is dependent on several forward rates. Rebonato [47] advocates the use of cap

prices for volatility calibration and the use of swaption prices for correlation modeling. This is partly based on the observation that the implied volatility term structure of forward rates tend to exhibit the same qualitative features when calibrated to either the swaption or cap market (although there will be differences in the actual level of the implied volatilities).

Please note that the available volatility data is somewhat limited. More data points can be added to increase the accuracy of estimated correlations (given of course that the extra points do not create noise due to illiquidity or even overlapping terms). Due to the difficulties associated with the sourcing of accurate historical swaption volatilities, we will base future calculations on the data set introduced in this section.

Some of the available swaption volatilities, as given by Bloomberg, are presented in the figure below.[3]

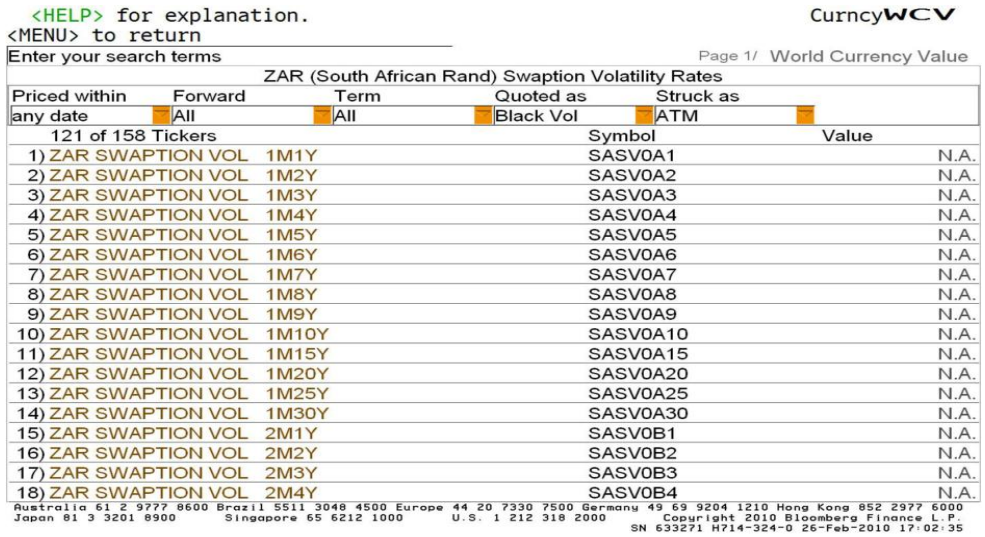

<HELP> for explanation. CurncyWCV
<MENU> to return
Enter your search terms Page 1/ World Currency Value

ZAR (South African Rand) Swaption Volatility Rates

Priced within	Forward	Term	Quoted as	Struck as
any date	All	All	Black Vol	ATM

121 of 158 Tickers		Symbol	Value
1) ZAR SWAPTION VOL	1M1Y	SASV0A1	N.A.
2) ZAR SWAPTION VOL	1M2Y	SASV0A2	N.A.
3) ZAR SWAPTION VOL	1M3Y	SASV0A3	N.A.
4) ZAR SWAPTION VOL	1M4Y	SASV0A4	N.A.
5) ZAR SWAPTION VOL	1M5Y	SASV0A5	N.A.
6) ZAR SWAPTION VOL	1M6Y	SASV0A6	N.A.
7) ZAR SWAPTION VOL	1M7Y	SASV0A7	N.A.
8) ZAR SWAPTION VOL	1M8Y	SASV0A8	N.A.
9) ZAR SWAPTION VOL	1M9Y	SASV0A9	N.A.
10) ZAR SWAPTION VOL	1M10Y	SASV0A10	N.A.
11) ZAR SWAPTION VOL	1M15Y	SASV0A15	N.A.
12) ZAR SWAPTION VOL	1M20Y	SASV0A20	N.A.
13) ZAR SWAPTION VOL	1M25Y	SASV0A25	N.A.
14) ZAR SWAPTION VOL	1M30Y	SASV0A30	N.A.
15) ZAR SWAPTION VOL	2M1Y	SASV0B1	N.A.
16) ZAR SWAPTION VOL	2M2Y	SASV0B2	N.A.
17) ZAR SWAPTION VOL	2M3Y	SASV0B3	N.A.
18) ZAR SWAPTION VOL	2M4Y	SASV0B4	N.A.

Australia 61 2 9777 8600 Brazil 5511 3048 4500 Europe 44 20 7330 7500 Germany 49 69 9204 1210 Hong Kong 852 2977 6000
Japan 81 3 3201 8900 Singapore 65 6212 1000 U.S. 1 212 318 2000 Copyright 2010 Bloomberg Finance L.P.
SN 633271 H714-324-0 26-Feb-2010 17:02:35

Figure 8.13: Example of extracting South African ATM swaption volatilities from Bloomberg.

One important aspect of swaption quotations is the resetting periods of the underlying swaps. This determines what type of forwards (for example monthly, three-monthly, semi-annual, etc.) are needed in order to determine the value of the swap at any point in time. In the data presented until thus far, we assumed three-monthly caplet volatilities which indirectly implies the use of three-monthly forward rates. Should the resetting periods of the underlying swaps not be equal to three-months, then we will have to adjust the three-monthly caplet volatilities in order to calibrate to both markets simultaneously (see Brigo and Mercurio [11] and Gatarek, Bachert and Maksymiuk [21]). This

[3] Once again the command WCV ZAR <GO> can be used.

will have a significant impact on the calibration of the model to market inputs. The exact methodology, that can be used for the above mentioned conversion, will be illustrated in a later chapter.

Another point worth mentioning is the actual liquidity of some of these option trades. Although caps and swaptions are vanilla option trades, discussions with an option trader revealed that the actual number of prices shown in the market on a daily basis are fairly limited. This remark then confirms the numerous statements made by Rebonato [47] regarding volatility and correlation modeling within the LIBOR market model. The author mentioned that we should strive to obtain volatility and correlation parameterizations that best fit market volatilities, while reflecting trader views (the "reflection of trader views" is essentially needed to complete the market).

8.2 Curve Bootstrapping

The work by Gatarek, Bachert and Maksymiuk [21] provide the reader with the necessary discount factors needed for calibration purposes, with no real detail given as to what assumptions were made in the bootstrapping of these rates (given in Table 7.1).

This section will consider the bootstrapping of rates from the benchmark instruments provided in Section 8.1.1. This process is an important part in the calibration of the model and will result in the necessary discount factors and ATM strikes. Another important aspect of this process, is that we will be able to derive three-monthly (or any other term, we however focus on three-monthly forward rates) forward rates from the benchmark rates. This is important given the fact that the LIBOR market model actually consists of the modeling of forward rates. From these rates, we will then be able to deduce historical volatilities and correlations which will be used at a later stage.

The benchmark instruments that we will use are presented in Table 8.1 and consist of a $3M$ JIBAR rate, 3 monthly FRAs and interest rate swaps exchanging fixed cash flows for floating cash flows linked to $3M$ JIBAR. Consequently, this curve is typically referred to as a three-month ZAR interest rate curve. As mentioned earlier, we can construct similar curves to better price and risk instruments that have resets occurring at time intervals other than three-months.

Assuming a 0-day settlement procedure, we have that the first part of the curve is automatically obtained, i.e. we have the 0-$3M$ rate equal to the $3M$ JIBAR rate, and then we have three-monthly forward rates thereafter out until 2-years.

In order to obtain three-monthly forward rates for the $2Y$ to $3Y$ time period, we will need to introduce the 3-year swap rate to the current set of equations. Firstly, recall that the $3Y$ par swap rate can be defined as the fixed rate such that the present value of the floating leg of the swap will equal the

present value of the fixed leg of the swap. This then implies that the $3Y$ swap rate contains some information regarding the unknown forward rates for the time period under consideration. The valuation of a $3Y$ swap is presented in Table 8.6.

Cum YF	Forw Rate (Simple)	Swap Rate	Comp Fact	DF	Proj Float	PV Float	Proj Fixed	PV Fixed	Spot Rate (Simple)	Spot Rate (Annual)
0.25	0.07229	0.08035	1.01807	0.98225	0.01807	0.01775	0.02009	0.01973	0.07229	0.07427
0.50	0.07090	0.08035	1.03612	0.96514	0.01773	0.01711	0.02009	0.01939	0.07224	0.07354
0.75	0.07110	0.08035	1.05453	0.94829	0.01778	0.01686	0.02009	0.01905	0.07271	0.07337
1.00	0.07280	0.08035	1.07373	0.93134	0.01820	0.01695	0.02009	0.01871	0.07373	0.07373
1.25	0.07510	0.08035	1.09389	0.91417	0.01878	0.01716	0.02009	0.01836	0.07511	0.07443
1.50	0.07860	0.08035	1.11538	0.89655	0.01965	0.01762	0.02009	0.01801	0.07692	0.07551
1.75	0.08220	0.08035	1.13830	0.87850	0.02055	0.01805	0.02009	0.01765	0.07903	0.07683
2.00	0.08620	0.08035	1.16283	0.85997	0.02155	0.01853	0.02009	0.01727	0.08142	0.07835
2.25		0.08035					0.02009			
2.50		0.08035					0.02009			
2.75		0.08035					0.02009			
3.00		0.08035					0.02009			

Table 8.6: Cash Flows of a $3Y$ IRS using rates for business date 2009/12/31.

The first column of Table 8.6 indicates the cumulative year fractions. Note that equal time intervals of 0.25 (given rates reset every three months) were assumed in order to simplify historical calculations. Testing of this assumption for a particular working day showed a maximum impact of less than one basis point. Furthermore, the forward (simple compounding) and swap rates were taken directly from Table 8.1. The calculations of the rest of the entries in the second row of Table 8.6 are presented below.

The compounding factor (Comp Fact) was defined as the factor needed to grow one Rand from time today until the end of the period indicated by the cumulative year fraction (Cum YF) column. Hence, we have for Cum YF$= 0.5$ that

$$\begin{aligned} \text{Comp Fact}(0.5) &= \text{Comp Fact}(0.25) \times [1 + \text{Forw Rate}(0.5) \times 0.25] \\ &= 1.01807 \times [1 + 0.0709 \times 0.25] \\ &= 1.03612. \end{aligned}$$

The factors calculated above are typically used in the calculation of discount factors. The process of obtaining a discount factor for Cum YF$= 0.5$ is illustrated below

$$\begin{aligned} \text{DF}(0.5) &= 1/\text{Comp Fact}(0.5) \\ &= 1/1.03612 \\ &= 0.96514. \end{aligned}$$

Next, we need to calculate the present values of the projected cash flows (where we have available forward rates) using the results obtained above.

$$\begin{aligned}
\text{PV Float}(0.5) &= \text{Proj Float}(0.5) \times \text{DF}(0.5) \\
&= 0.0709 \times 0.25 \times 0.96514 \\
&= 0.01711, \\
\text{PV Fixed}(0.5) &= \text{Proj Fixed}(0.5) \times \text{DF}(0.5) \\
&= 0.08035 \times 0.25 \times 0.96514 \\
&= 0.01939.
\end{aligned}$$

Under normal market circumstances, where all forward rates are available, these calculations should be sufficient to determine present values for each of the underlying cash flows. Table 8.6, however, illustrates the fact that we have four unknown rates compared with the one condition that the present value of the fixed leg of the swap (consisting of a number of individual cash flows) should equal the present value of the float leg of the swap. Hence, in order to solve for the four unknown forward rates, we will have to introduce some assumptions given the fact that there are an infinite number of solutions that will ensure that the swap prices back to zero. In curve construction, these assumptions are typically in the form of different interpolation techniques.

In order to simplify calculations we will focus our attention on linear interpolation. Hagan and West [27] mention that the interpolation can be applied to different types of rates, for example discount factors and spot rates. We will only consider linear interpolation on spot interest rates. The front office system used by the investment bank introduced earlier in this chapter also perform interpolations on spot interest rates as opposed to discount factors. Furthermore, this front office system performs all of its curve calculations in the annual compounding space, even if its inputs are quoted in simple terms. Hence, before we can proceed any further, we need to have a look at the calculation of the spot rates presented in Table 8.6.

$$\begin{aligned}
\text{Spot Rate}_{\text{S}}(0.5) &= (\text{Comp Fact}(0.5) - 1)/\text{Cum YF}(0.5) \\
&= (1.03612 - 1)/0.5 \\
&= 0.07224.
\end{aligned}$$

This rate can then be annualized for calculation purposes (in order to keep in line with front office system).

The examples given above explain the calculation of the elements of Table 8.6. In order to extend the table over the remaining few time periods, we will need to follow the process as presented by Hagan and West [27]. The first step of the process is to choose an arbitrary annual spot interest rate

for Cum YF= 3. Next, apply linear interpolation between Cum YF= 2 and Cum YF= 3 to obtain annual spot rates for the unknown time periods. From these estimates we will be able to work backwards through the table to obtain present values for both the swap legs.

Once this is done, we need to apply a root finding routine to solve for the $3Y$ annual spot interest rate such that the swap prices back to zero. The goal seek functionality in excel was used to obtain the results presented in the table below.

Cum YF	Forw Rate (Simple)	Swap Rate	Comp Fact	DF	Proj Float	PV Float	Proj Fixed	PV Fixed	Spot Rate (Simple)	Spot Rate (Annual)
0.25	0.07229	0.08035	1.01807	0.98225	0.01807	0.01775	0.02009	0.01973	0.07229	0.07427
0.50	0.07090	0.08035	1.03612	0.96514	0.01773	0.01711	0.02009	0.01939	0.07224	0.07354
0.75	0.07110	0.08035	1.05453	0.94829	0.01778	0.01686	0.02009	0.01905	0.07271	0.07337
1.00	0.07280	0.08035	1.07373	0.93134	0.01820	0.01695	0.02009	0.01871	0.07373	0.07373
1.25	0.07510	0.08035	1.09389	0.91417	0.01878	0.01716	0.02009	0.01836	0.07511	0.07443
1.50	0.07860	0.08035	1.11538	0.89655	0.01965	0.01762	0.02009	0.01801	0.07692	0.07551
1.75	0.08220	0.08035	1.13830	0.87850	0.02055	0.01805	0.02009	0.01765	0.07903	0.07683
2.00	0.08620	0.08035	1.16283	0.85997	0.02155	0.01853	0.02009	0.01727	0.08142	0.07835
2.25	0.08686	0.08035	1.18808	0.84169	0.02172	0.01828	0.02009	0.01691	0.08359	0.07961
2.50	0.08923	0.08035	1.21459	0.82332	0.02231	0.01837	0.02009	0.01654	0.08583	0.08087
2.75	0.09160	0.08035	1.24240	0.80489	0.02290	0.01843	0.02009	0.01617	0.08815	0.08212
3.00	0.09396	0.08035	1.27159	0.78642	0.02349	0.01847	0.02009	0.01580	0.09053	0.08338

Table 8.7: Cash Flows of a $3Y$ IRS using known and bootstrapped rates for business date 2009/12/31.

Similarly, the results for the $4Y$ swap quotation are presented below.

Cum YF	Forw Rate (Simple)	Swap Rate	Comp Fact	DF	Proj Float	PV Float	Proj Fixed	PV Fixed	Spot Rate (Simple)	Spot Rate (Annual)
0.25	0.07229	0.08342	1.01807	0.98225	0.01807	0.01775	0.02086	0.02049	0.07229	0.07427
0.50	0.07090	0.08342	1.03612	0.96514	0.01773	0.01711	0.02086	0.02013	0.07224	0.07354
0.75	0.07110	0.08342	1.05453	0.94829	0.01778	0.01686	0.02086	0.01978	0.07271	0.07337
1.00	0.07280	0.08342	1.07373	0.93134	0.01820	0.01695	0.02086	0.01942	0.07373	0.07373
1.25	0.07510	0.08342	1.09389	0.91417	0.01878	0.01716	0.02086	0.01907	0.07511	0.07443
1.50	0.07860	0.08342	1.11538	0.89655	0.01965	0.01762	0.02086	0.01870	0.07692	0.07551
1.75	0.08220	0.08342	1.13830	0.87850	0.02055	0.01805	0.02086	0.01832	0.07903	0.07683
2.00	0.08620	0.08342	1.16283	0.85997	0.02155	0.01853	0.02086	0.01794	0.08142	0.07835
2.25	0.08686	0.08342	1.18808	0.84169	0.02172	0.01828	0.02086	0.01755	0.08359	0.07961
2.50	0.08923	0.08342	1.21459	0.82332	0.02231	0.01837	0.02086	0.01717	0.08583	0.08087
2.75	0.09160	0.08342	1.24240	0.80489	0.02290	0.01843	0.02086	0.01679	0.08815	0.08212
3.00	0.09396	0.08342	1.27159	0.78642	0.02349	0.01847	0.02086	0.01640	0.09053	0.08338
3.25	0.09194	0.08342	1.30081	0.76875	0.02298	0.01767	0.02086	0.01603	0.09256	0.08428
3.50	0.09363	0.08342	1.33126	0.75117	0.02341	0.01758	0.02086	0.01567	0.09465	0.08519
3.75	0.09532	0.08342	1.36298	0.73368	0.02383	0.01748	0.02086	0.01530	0.09680	0.08609
4.00	0.09701	0.08342	1.39604	0.71631	0.02425	0.01737	0.02086	0.01494	0.09901	0.08699

Table 8.8: Cash Flows of a $4Y$ IRS using known and bootstrapped rates for business date 2009/12/31.

Through applying above procedure to the remainder of the benchmark instruments in Table 8.1, we obtain the following

Cum YF	Spot Rate (Simple)	Forw Rate (Simple)	Spot Rate (Annual)	Forw Rate (Annual)
0.25	0.07229	0.07229	0.07427	0.07427
0.50	0.07224	0.07090	0.07354	0.07281
0.75	0.07271	0.07110	0.07337	0.07302
1.00	0.07373	0.07280	0.07373	0.07481
1.25	0.07511	0.07510	0.07443	0.07724
1.50	0.07692	0.07860	0.07551	0.08095
1.75	0.07903	0.08220	0.07683	0.08477
2.00	0.08142	0.08620	0.07835	0.08903
2.25	0.08359	0.08686	0.07961	0.08973
2.50	0.08583	0.08923	0.08087	0.09226
2.75	0.08815	0.09160	0.08212	0.09479
3.00	0.09053	0.09396	0.08338	0.09733
3.25	0.09256	0.09194	0.08428	0.09515
3.50	0.09465	0.09363	0.08519	0.09697
3.75	0.09680	0.09532	0.08609	0.09878
4.00	0.09901	0.09701	0.08699	0.10059
4.25	0.10080	0.09269	0.08751	0.09596
4.50	0.10263	0.09367	0.08804	0.09702
4.75	0.10451	0.09466	0.08856	0.09807
5.00	0.10644	0.09564	0.08909	0.09913
5.25	0.10817	0.09317	0.08944	0.09647
5.50	0.10994	0.09382	0.08979	0.09718
5.75	0.11175	0.09448	0.09014	0.09788
6.00	0.11361	0.09513	0.09049	0.09858
6.25	0.11530	0.09278	0.09071	0.09606
6.50	0.11704	0.09319	0.09094	0.09650
6.75	0.11881	0.09361	0.09116	0.09695
7.00	0.12061	0.09403	0.09138	0.09739
7.25	0.12231	0.09212	0.09152	0.09535
7.50	0.12405	0.09238	0.09165	0.09563
7.75	0.12581	0.09263	0.09179	0.09590
8.00	0.12762	0.09289	0.09193	0.09617
8.25	0.12934	0.09138	0.09201	0.09456
8.50	0.13110	0.09153	0.09209	0.09472
8.75	0.13290	0.09168	0.09217	0.09488
9.00	0.13472	0.09183	0.09225	0.09504
9.25	0.13632	0.08760	0.09220	0.09052
9.50	0.13794	0.08751	0.09215	0.09043
9.75	0.13958	0.08743	0.09211	0.09033
10.00	0.14125	0.08734	0.09206	0.09024

Table 8.9: Bootstrapped spot and forward rates for business date 2009/12/31.

It is worth briefly discussing the effect of linear interpolation on the bootstrapped rates. Hagan and West [27] points out that the interpolation method used in the bootstrapping process plays an integral part in the procedure as a whole. Consequently, we can expect different interest rate behaviours for different interpolation methods used. Some of the key factors influenced by the type of interpolation method are, for example, the stability of forward rates

and the distribution of risk between different input variables. To illustrate this concept, consider the graph of the three-monthly forward rates (annual compounding) presented in Table 8.9.

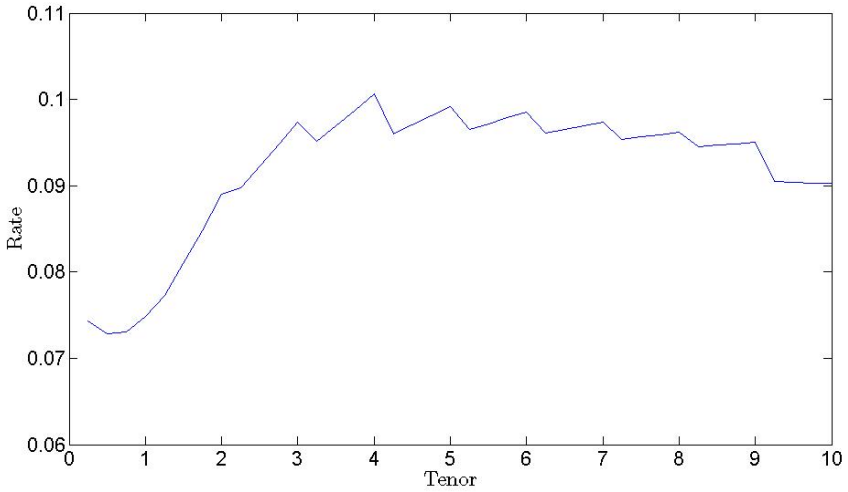

Figure 8.14: Bootstrapped forward rates for business date 2009/12/31 using linear interpolation.

Switching the interpolation to Hermite, we obtain the graph below.

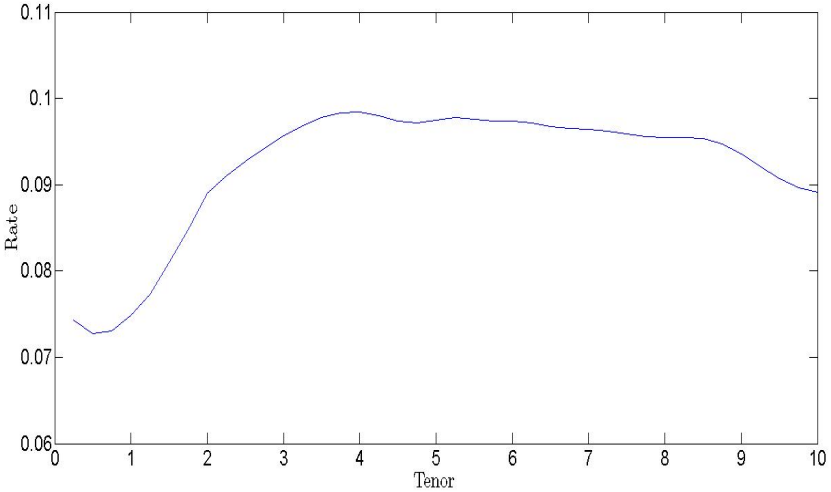

Figure 8.15: Bootstrapped forward rates for business date 2009/12/31 using Hermite interpolation.

The effect of linear interpolation between different tenors are clearly visible in the above graphs, i.e. non-smooth forward rates (even though a similar plot of the annual spot rates given in Table 8.9 would yield a smooth curve).

The latter interpolation method (results obtained from front office trading system) clearly results in smoother forward rates. One drawback of Hermite interpolation is that the risk is not localized, i.e. a bump in one of the benchmark instruments may influence a number of bootstrapped rates. In practice there are, however, a number of factors to consider before deciding on the interpolation method. The reader is referred to the article by Hagan and West [27] for more details.

In order to briefly analyze the historical behaviour of three-monthly forward rates, we will consider the historical forward rates over the same interest rate cycles defined in Section 8.1. The required forward rates were obtained through applying the same bootstrapping techniques to the historical set of benchmark rates. The resultant rates are presented below.

The three-monthly forward rates (using linear interpolation), for the rate hiking cycle between 2005/01/03 and 2008/06/13, are presented in the graph below (benchmark equivalent presented in Figure 8.2).

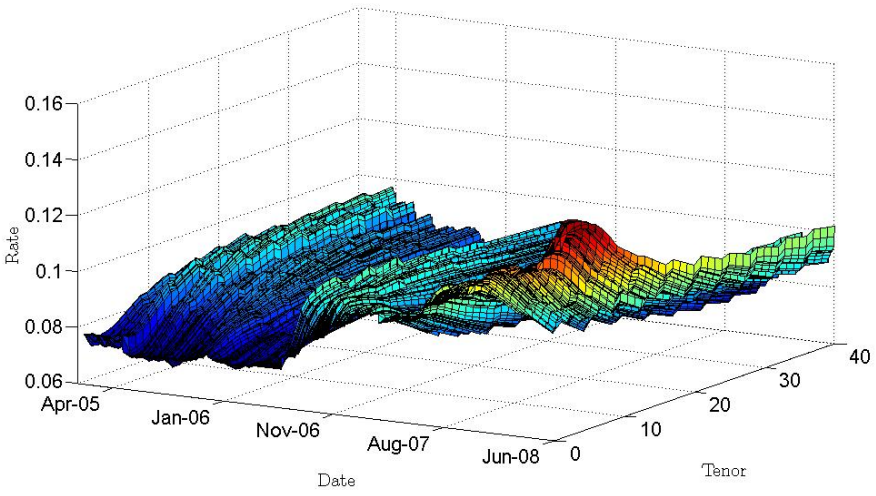

Figure 8.16: Historical forward rates bootstrapped from South African benchmark instruments for the time period 2005/01/03 - 2008/06/13. This relates to a rate hiking cycle.

From above it is evident that the forward rates behave similar to the underlying benchmark instruments in a rate hiking cycle, i.e. a net increase in the level of rates while exhibiting an inverting behaviour over time.

Next, let us consider the behaviour of the three-monthly forward rates under a rate cutting cycle (benchmark equivalent presented in Figure 8.3).

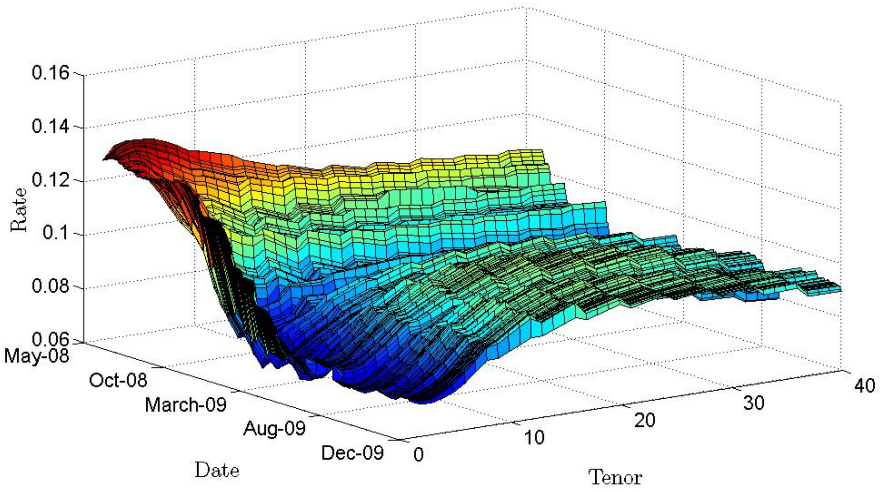

Figure 8.17: Historical forward rates bootstrapped from South African benchmark instruments for the time period 2008/06/14 - 2009/12/31. This relates to a rate cutting cycle.

This time period was defined earlier as the historical days between 2008/06/14 and 2009/12/31. Similar to the previous case, the rates in Figure 8.17 exhibit properties that are in line with those of the underlying benchmark rates, i.e. a net decrease in the level of rates while exhibiting a steepening behaviour over time.

This concludes the section on the bootstrapping of interest rates from historical benchmark rates. The history of the three-monthly interest rates in this section will be used at a later stage to estimate both historical volatilities as well as historical correlations between forward rates.

8.3 Caplet Stripping

Caplet stripping was considered in detail in Section 7.2, hence this section will only briefly touch on some of the required calculations necessary for such a procedure and then present the results obtained when applied to the South African market.

Section 8.1.2 provided the reader with a clear description of the cap and caplet data available in the market as well as the data obtained from a South African investment bank. Furthermore, we stated that actual trader inputs will be used in this project as opposed to data obtained from the market. This will allow us to examine the historical views of a particular set of traders which may be more informative than analyzing the data from the market as a whole. The accuracy of this particular set of data is ensured through regular price testing practices within the investment bank under consideration.

It was mentioned earlier that the granularity of the available volatilities differ through time and can consequently be divided into two periods.

The volatilities for the last three months in the data set consists of three monthly caplet volatilities out to $10Y$ as illustrated in Table 8.3. This level of granularity was obtained through a caplet volatility stripping procedure.

In contrast to above, the volatility data of the first five months consists of caplet volatilities out to two years and cap volatilities for time periods $3Y$, $4Y$, $5Y$ and $10Y$. An example of this was presented in Table 8.4. The lack of granularity in this data set will require the use of a caplet stripping procedure.

8.3.1 ATM Strikes for Caps

One of the key elements in a caplet stripping algorithm is the calculation of the strikes associated with the quoted volatilities. Given that we only consider ATM volatilities, we need to calculate the ATM strikes of caps. It was motivated in Section 7.2 that these strikes can be represented by forward swap rates.

Note that these are forward rates and hence should not be confused with the ATM swap rates used as inputs to the bootstrapping procedure. Given we consider caps made up of three-monthly caplets, we need the swap rates starting in three-months time.

The forward swap rates were calculated for each of the historical days from the bootstrapped forward rates. In order to avoid repetition, the calculation of these rates will be assumed to be the same as given in Section 7.2.1.

8.3.2 Stripping Caplet Volatilities from Cap Quotes

Section 7.2.2 illustrated how we can bootstrap caplet volatilities from cap quotes. Applying these same techniques to the South African market data resulted in Figure 8.18.

We can draw some interesting conclusions from Figure 8.18. Firstly, note the decrease in the level of volatilities. This is in line with greater uncertainty in the market during the start of 2009 which was driven by the global credit crisis of 2007/2008 (numerous papers were written with regards to the sub prime crisis, see for instance Alfaro and Kanczuk [1] and Gwinner and Sanders [24] for extentions to emerging markets).

Secondly, it is important to note the different shapes of the volatility term structure. This is important given the fact that we need to decide on different parametric volatility structures in the calibration process (given we use a parametric calibration algorithm). Figure 8.18 clearly confirms the comments made by Rebonato [47] regarding volatility behaviour under different market circumstances.

Volatility behaviour in periods of uncertainty represents an inverted structure (as can be seen for the first couple of months). Rebonato [47] attributes

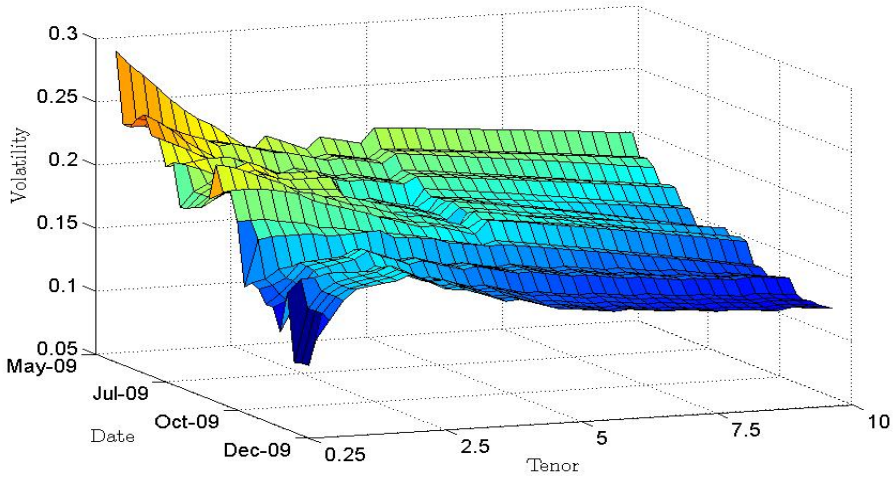

Figure 8.18: Historical market implied ATM caplet volatilities, calculated through applying the caplet stripping algorithm of Section 7.2.2 to the set of cap and caplet volatilities obtained from a South African investment bank.

the high volatility at the short-end of the curve to a constant analysis of expected forward rates.

At the opposite side of the spectrum, we have that volatilities in periods of less uncertainty typically represents a humped term structure. Rebonato [47] points out that under normal market conditions, we have that volatilities in the short-medium term are influenced by the arrival of financial news (such as inflation prints etc. and the impact on the interest rate cycle). Short- and long-term rates are typically more stable under these market conditions.

8.4 Historical Volatilities

The previous section looked at how we can imply forward rate volatilities from market quotations. These implied volatilities, along with the assumed lognormal property of forward rates, can then be used to determine market expectations of future interest rates (see for example the article by the Bank of Montreal [43]).

In order to examine the realized volatility of forward rates, we need to perform some sort of calculation on historical forward rates. There are a number of different calculations available in the literature, for example equally weighted, exponentially weighted, ARCH and GARCH processes etc. We will focus our attentions on the equally weighted technique.

Rebonato [47] refers to a historical analysis performed by Dodds [18] in which the author used constant-maturity three-month forward rates. We will try and replicate the results in this section.

The term constant-maturity, is found throughout the literature when sourcing information regarding the historical estimation of volatilities (or correlations) within the LMM framework. This is due to the model assumptions made regarding the underlying variables and should not be confused with market observable constant time-to-maturities (Brigo and Mercurio [11]).

Before we can proceed to the calculation of historical volatilities, we first need to calculate the constant maturity forward rates. Given the definition of the LMM, we need to obtain historical data of rates that start out as a specific forward rate and approach the $3M$ JIBAR rate as it approaches maturity (or reset time). This is needed, since the pricing of an option will need to reflect such behaviour as opposed to the behaviour of constant time-to-maturity forward rates observable in the market (in order to accurately reflect the cost of hedging). The following procedure was followed:

- Set the forward rate under consideration equal to the $3M$ JIBAR rate for t equal to today
- For each subsequent day in the historical data set, calculate this 3-month rate as we move away from today
- Repeat this process until the start of the respective forward rates are reached, i.e. 91 days for a 3×6 FRA, 182 days for a 6×9 FRA etc.
- Calculate the log returns of the rates obtained in the previous steps
- Calculate the volatilities of these returns (see Section 6.5) and scale these to annual volatilities through using the factor $\sqrt{252}$ (assuming 252 working days in a year) as proposed by Hull [32]
- Repeat above procedure for different historical starting points in order to get a feel of the distribution of calculated volatilities

There are a number of calculations involved in above procedure. These will be briefly described in this section.

The bootstrapping procedure described in Section 8.2, yielded spot rates with maturities (stated in year fractions) of $0.25, 0.5, \ldots, 10$. This immediately poses a problem for calculating forward rates as we start moving away from today. This is due to the fact that the rate with maturity 3M from today, is a forward rate as we start to move away from today. Hence, we need to interpolate spot rates between the rates obtained through the bootstrapping procedure. This was done through using linear interpolation and the introduction of an overnight point to anchor the interpolations at $t = 0$ (actually an 1-day point, however assumed to be 0-day in order to simplify calculations). This rate is observable in the market and was taken from the same set of trader inputs.

In order to illustrate this procedure, let us consider the calculation of the rates used in the volatility estimation of the 3×6 forward rate. The spot rates obtained from the bootstrapping procedure (simple compounding) as well as the overnight point (assumed to be 0-day), are presented in Table 8.10.

	Spot Rate Tenor		
	0	0.25	0.5
2009/12/31	0.06659	0.07229	0.07224
2009/12/30	0.06690	0.07229	0.07224
⋮	⋮	⋮	⋮
2009/08/21	0.06662	0.07121	0.07016

Table 8.10: An extract of the South African spot rate data used in the historical calculation of a constant maturity 3×6 forward rate.

The forward rates Forw Rate(0)...Forw Rate(91), are then calculated as illustrated below.

$$\begin{aligned} \text{Forw Rate}(0) &= \text{Spot Rate}(0.25) \\ &= 0.07229. \end{aligned}$$

Next, we need to calculate the rate over the exact same time period, one day into the history. In order to do this we need to interpolate two spot rates that will be used in the calculation of the forward rate with expiry 0.25 years from 2009/12/31. This can be obtained as follows at t =2009/12/30.

$$\begin{aligned} \text{Spot Rate}(0{+}1\text{d}) &= \text{Spot Rate}(0) \\ &+ (\text{Spot Rate}(0.25) - \text{Spot Rate}(0)) \times \frac{\frac{1}{365}}{0.25} \\ &= 0.06690 + (0.07229 - 0.06690) \times \frac{\frac{1}{365}}{0.25} \\ &= 0.06696. \end{aligned}$$

Similarly, we can calculate Spot Rate(0.25+1d) as

$$\begin{aligned} \text{Spot Rate}(0.25{+}1\text{d}) &= \text{Spot Rate}(0.25) \\ &+ (\text{Spot Rate}(0.5) - \text{Spot Rate}(0.25)) \times \frac{\frac{1}{365}}{0.25} \\ &= 0.07229 + (0.07224 - 0.07229) \times \frac{\frac{1}{365}}{0.25} \\ &= 0.07229. \end{aligned}$$

From these rates we can calculate the next forward rate in our vector as

$$\begin{aligned}\text{Forw Rate}(1) &= \left[\frac{1+\text{Spot Rate}(0.25{+}1\text{d})\times(0.25+\frac{1}{365})}{1+\text{Spot Rate}(0{+}1\text{d})\times(0+\frac{1}{365})}-1\right]\times\frac{1}{0.25}\\ &= \left[\frac{1+0.07229\times(0.25+\frac{1}{365})}{1+0.06696\times(0+\frac{1}{365})}-1\right]\times\frac{1}{0.25}\\ &= 0.07233.\end{aligned}$$

Repeating above procedure, it is evident that the calculated forwards should approach the 3×6 forward rate at 2009/08/21. These forward rates are presented in the table below.

Day	Rate	Day	Rate	Day	Rate
2009/12/31	0.07229	2009/11/16	0.07166	2009/10/02	0.07083
2009/12/30	0.07233	2009/11/13	0.07189	2009/10/01	0.07092
2009/12/29	0.07238	2009/11/12	0.07196	2009/09/30	0.07095
2009/12/28	0.07242	2009/11/11	0.07186	2009/09/29	0.07070
2009/12/24	0.07247	2009/11/10	0.07193	2009/09/28	0.07073
2009/12/23	0.07251	2009/11/09	0.07186	2009/09/25	0.07070
2009/12/22	0.07255	2009/11/06	0.07199	2009/09/23	0.07014
2009/12/21	0.07258	2009/11/05	0.07244	2009/09/22	0.06999
2009/12/18	0.07263	2009/11/04	0.07245	2009/09/21	0.06905
2009/12/17	0.07266	2009/11/03	0.07247	2009/09/18	0.06909
2009/12/15	0.07271	2009/11/02	0.07259	2009/09/17	0.06901
2009/12/14	0.07273	2009/10/30	0.07287	2009/09/16	0.06932
2009/12/11	0.07277	2009/10/29	0.07319	2009/09/15	0.06923
2009/12/10	0.07278	2009/10/28	0.07360	2009/09/14	0.06926
2009/12/09	0.07281	2009/10/27	0.07366	2009/09/11	0.06927
2009/12/08	0.07283	2009/10/26	0.07372	2009/09/10	0.06925
2009/12/07	0.07285	2009/10/23	0.07315	2009/09/09	0.06898
2009/12/04	0.07289	2009/10/22	0.07289	2009/09/08	0.06898
2009/12/03	0.07284	2009/10/21	0.07234	2009/09/07	0.06907
2009/12/02	0.07286	2009/10/20	0.07228	2009/09/04	0.06925
2009/12/01	0.07284	2009/10/19	0.07217	2009/09/03	0.06942
2009/11/30	0.07284	2009/10/16	0.07206	2009/09/02	0.06969
2009/11/27	0.07284	2009/10/15	0.07204	2009/09/01	0.06972
2009/11/26	0.07238	2009/10/14	0.07200	2009/08/31	0.06939
2009/11/25	0.07225	2009/10/13	0.07184	2009/08/28	0.06896
2009/11/24	0.07200	2009/10/12	0.07186	2009/08/27	0.06868
2009/11/23	0.07203	2009/10/09	0.07194	2009/08/26	0.06849
2009/11/20	0.07210	2009/10/08	0.07144	2009/08/25	0.06821
2009/11/19	0.07206	2009/10/07	0.07149	2009/08/24	0.06802
2009/11/18	0.07203	2009/10/06	0.07098	2009/08/21	0.06792
2009/11/17	0.07198	2009/10/05	0.07086		

Table 8.11: Historical evolution of a constant maturity 3×6 forward rate in the South African market.

The data in Table 8.11 is graphically presented in Figure 8.19 below. From this graph we can see a clear decrease in volatility as we approach the more deterministic 3-month JIBAR rate (left-hand side of graph). This is in contrast with the model assumption of constant volatilities.

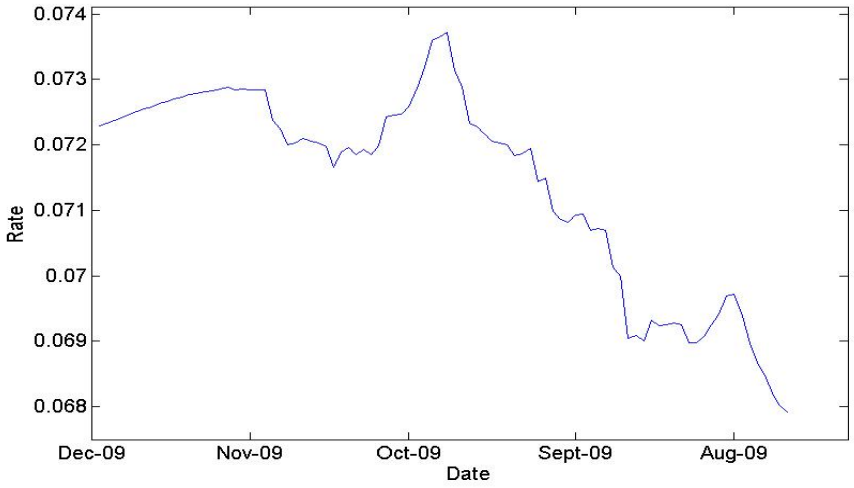

Figure 8.19: Historical evolution of a constant maturity 3×6 forward rate in the South African market.

Calculating the volatility of the log of returns of above rates will yield a realized (actual) volatility for the latest 3×6 forward rate. Note, however, that these volatilities only provide us a history of realized volatilities of certain forward rates and may be different from market expectations or implied volatilities. One point clearly visible in above calculation, is that we are estimating the volatility of a forward rate starting today and expiring 3-months from today with a volatility of a rate starting 3-months ago and expiring today. This indicates that although we have an indication of the realized volatilities for a certain 3-month forward rate, our volatility estimation is more weighted towards today's 3-month JIBAR rate than towards today's 3×6 forward rate.

Irrespective of above arguments it is important to analyze historical realized volatilities and how these compare with the market or implied volatilities.

The procedure discussed in this section was applied to 10 forward rates, ranging from 3×6 to 30×33, and across 300 historical days. The calculation was capped at 9 forward rates in order to allow the inclusion of more historical days (which are necessary to get a feel for the distribution of the volatilities). The results of this analysis are presented in Figures 8.20 - 8.21 below.

From Figure 8.20 we can draw some relationships between the market implied and historical volatilities. Note, for example, the clearly visible "humped" shape of the term structure and how the peak of the volatilities approach

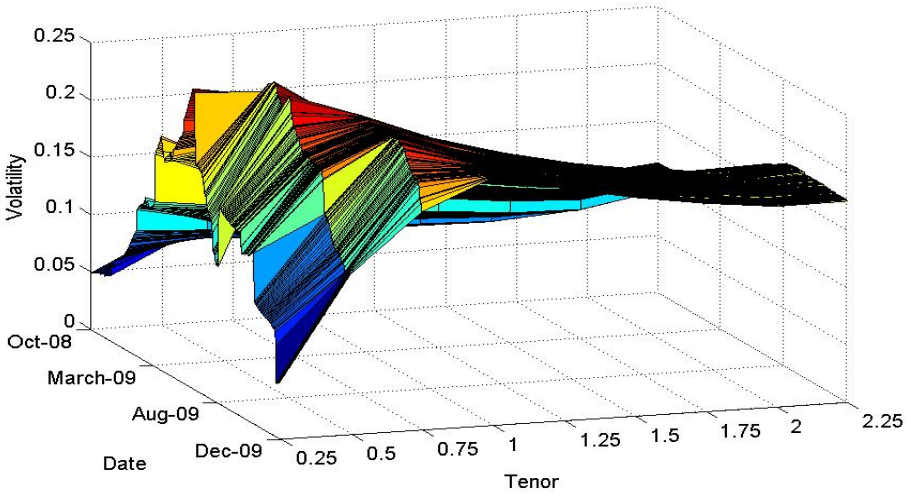

Figure 8.20: Historical implied ATM caplet volatilities calculated from bootstrapped forward rates, with the first historical date towards the reader.

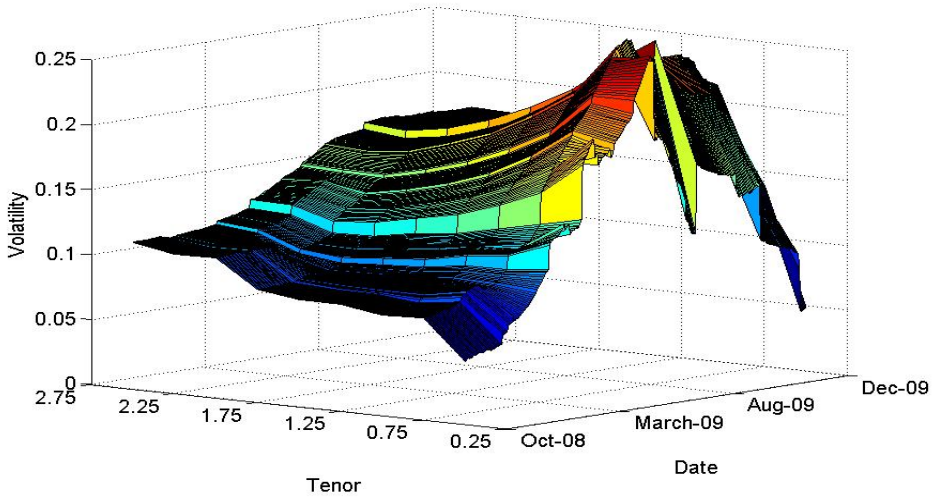

Figure 8.21: Historical implied ATM caplet volatilities calculated from bootstrapped forward rates, with the last historical date towards the reader.

shorter tenors as we move into a more volatile period. Furthermore, there is a clear change in the level of volatilities as we move through the different historical days. The peak in volatilities for 2009/12/31 however appears to be in the $1Y$ region vs. $2Y$ for the market obtained volatilities. This difference can partly be due to the lag in data used for this calculation (peak in implied volatilities where observable in shorter tenors up until 3-months prior

to 2009/12/31).

Figure 8.21 was obtained through rotating Figure 8.20 by 180 degrees. Notice the slightly increased volatilities at the front end of the graph. This type of behaviour is unexpected since we always expected either a "humped" or decreasing shape. Looking at the actual data, it appears as though this type of behaviour starts on 2009/02/05. Comparing this with Table 8.2, we can see that this is just after the series of 100bp cuts in the Repo rate.

Following above arguments and the ease of obtaining implied volatilities from the market, it is always advisable to rather use the latter in the pricing of options. The study presented in this section does however confirm some of the properties observable in implied volatilities. Furthermore, these volatilities provide more insight regarding the actual riskiness associated with each of the forward rates.

8.5 Historical Correlations

We will now move on to consider the calculation of historical correlations between different forward rates. Similar to the previous section we need to base our calculations on constant maturity forward rates. The calculation method used in this section is a slight variation from the method used in the previous section. The procedure followed is explained below.

- Set the forward rates under consideration equal to the rates that these variables will approach as we reach the first reset date (i.e. the reset date of the forward with the shortest expiry date). For example, if we assume that we start at t equal to today and we want to calculate the realized correlation between the 3×6 and 6×9 forward rates, then we will need to set these variables equal to the 3M JIBAR and 3×6 rate for t equal to today.
- For each subsequent day in the historical data set, calculate these forward rates as we move away from today
- Repeat this process until the start of the respective forward rates are reached (note that these will all start on the same day). This will equate to 91 days if the first reset date equates to 3-months from inception, 182 days if 6-months from inception etc.
- Calculate the log returns of the rates obtained in the previous steps
- Calculate the correlations between these returns (see Section 6.5)
- Repeat above procedure for different historical starting points

There are some issues regarding the estimation of historical correlations that we need to consider before moving on to the actual results. Firstly, Rebonato

[47] pointed out that market segmentation might create some noise within the correlation estimates. This is due to the fact that we are using FRA and JIBAR rates to construct the short end of the curve while using par swap rates to construct the longer end. Rebonato [47] mentions that there are typically different market participants in these markets which may result in different interest rate behaviours.

Secondly, we used linear interpolation in our bootstrapping procedure. It was illustrated in Figures 8.14 and 8.15 that this can have a significant impact on the smoothness of forward rates. Hence, we can expect this to result in some noise as we move into the swap space (short term forwards were bootstrapped exactly without the use of interpolation - ignoring the calculation of historical constant maturity forward rates).

Thirdly, we need to decide on an adequate historical period used in the calculation process. The assumption made in this section was that we will set this period equal to the time to expiry of the shortest forward rate (did not make sense to use less data and cannot move past the start of the first forward). This period can then be extended through using longer dated forward rates.

In order to illustrate the results, let us firstly consider the correlations between the short term rates (as with the historical volatility calculations). This then eliminates difficulties obtained with market segmentation (ignoring the $3M$ JIBAR point) as well as interpolation within the bootstrapping procedure. The results are presented in the table below.

	3M-6M	6M-9M	9M-12M	12M-15M	15M-18M	18M-21M	21M-24M
3M-6M	1.0000	0.7008	0.6411	0.5489	0.5148	0.5184	0.5202
6M-9M	0.7008	1.0000	0.9435	0.8722	0.8290	0.8189	0.8116
9M-12M	0.6411	0.9435	1.0000	0.9691	0.9364	0.9271	0.9145
12M-15M	0.5489	0.8722	0.9691	1.0000	0.9868	0.9787	0.9704
15M-18M	0.5148	0.8290	0.9364	0.9868	1.0000	0.9965	0.9895
18M-21M	0.5184	0.8189	0.9271	0.9787	0.9965	1.0000	0.9944
21M-24M	0.5202	0.8116	0.9145	0.9704	0.9895	0.9944	1.0000

Table 8.12: Forward rate correlations between short term forward rates for business date 2009/12/31. These were obtained using historically calculated constant maturity forwards from the South African market.

From Table 8.12 it is clearly visible that the obtained correlation matrix adheres to most of the requirements stipulated in Sections 6.2.1-6.2.2. In particular note that all correlations are positive, correlations decrease as we move from the diagonal downwards (one or two exceptions, disappears when using longer history) and that longer term rates are more correlated than shorter term rates. This matrix is presented in Figure 8.22 below.

Notice from the figure the smoothness of the correlation surface. This is in line with the comments made at the start of the section.

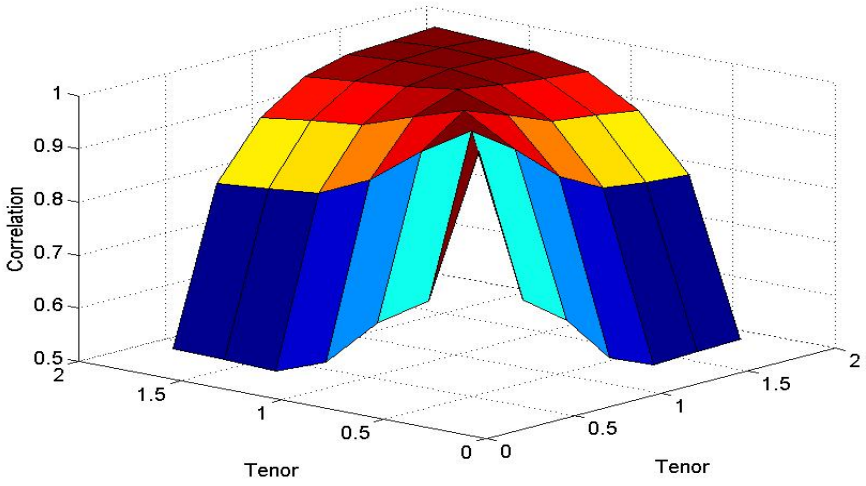

Figure 8.22: Forward rate correlations between short term forward rates for business date 2009/12/31. These were obtained using historically calculated constant maturity forwards from the South African market.

Moving the correlation calculations to start just after the series of 100bp cuts in the Repo rate (as discussed in the previous section), resulted in significantly higher correlations for the first two forward rates. This once again illustrates that the shorter term forwards are much more sensitive to interest rate decisions than the longer term rates.

Next, let us consider extending this calculation until the first swap rate (i.e. $3Y$ swap). The resultant correlation surface is presented in Figure 8.23 below.

The introduction of the $3Y$ IRS clearly added some noise to the surface. As explained earlier, this can be due to both market segmentation as well as linear interpolation during the bootstrapping routine. Similar to the previous results, the matrix did display most of the properties in Sections 6.2.1-6.2.2. Furthermore, extending the history used from 91 to 365 days, did reduce some of the noise.

Finally, calculating the forward rates over a spectrum of 30 forward rates resulted in the Figure 8.24.

This figure was obtained using 365 days of history for each of the forward rates. Also, note that the correlation surface includes all forward rates from $1Y$ out to 8.5 years. This surface does exhibit more noise than the others.

Finally, given the difficulties associated with the estimation of an exogenous correlation surface, we will fit a parametric form to this matrix before we attempt any calibration procedures.

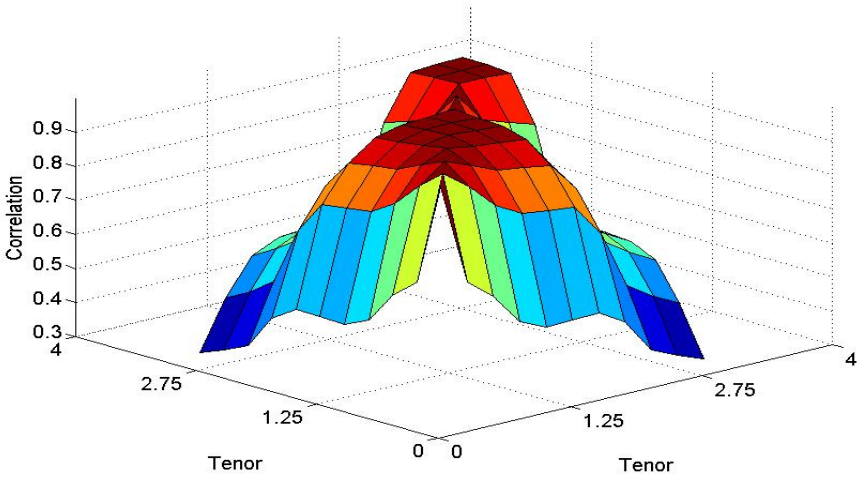

Figure 8.23: Forward rate correlations between forward rates out until $3Y$. These were obtained using historically calculated constant maturity forwards from the South African market. Results presented for business date 2009/12/31.

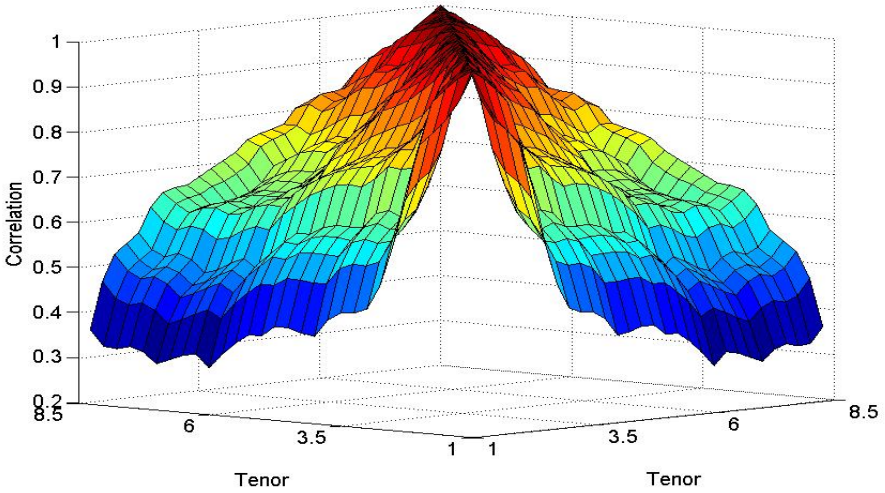

Figure 8.24: Forward rate correlations between some of the longer term forward rates. These were obtained using historically calculated constant maturity forwards from the South African market. Results presented for business date 2009/12/31.

Chapter 9

Volatility Calibration

This chapter will mainly focus on the calibration of volatility parameters to market data. Similar to the specifications provided in Chapter 5, we will divide this chapter into two main categories, i.e. parametric and non-parametric specifications.

The non-parametric calibration will mainly follow the work by Brigo and Mercurio [11] and Gatarek, Bachert and Maksymiuk [21] and will illustrate the ease at which we can calibrate this type of specification to a given set of market data. This ease of calibration may however result in financially implausible results and hence should be applied with care. Irrespective of the shortcomings of this approach, it is useful to illustrate some of the possible issues that may be encountered while calibrating the model.

Rebonato [47] in contrast favours parametric calibration techniques. This is mainly motivated by the possibility to enforce certain financial properties on the resulting volatilities and hence restricts the degrees of freedom inherent in the process.

The above mentioned techniques will be applied to both the European (as given by Gatarek, Bachert and Maksymiuk [21]) as well as South African market and the results will be presented.

9.1 Non-Parametric Volatility Calibration

We will firstly consider the non-parametric calibration of volatilities as given in the work by Brigo and Mercurio [11] and Gatarek, Bachert and Maksymiuk [21]. Using Table 5.1 we can re-write Equation (4.1.5) as

$$\sigma^2_{T_{i-1}T_i,\text{caplet}} = \frac{1}{T_{i-1}} \int_0^{T_{i-1}} \sigma^2_{T_{i-1}T_i}(t)dt \tag{9.1.1}$$

$$= \frac{1}{T_{i-1}} \sum_{j=1}^{i} \alpha_{T_{j-2}T_{j-1}} \sigma^2_{ij}. \tag{9.1.2}$$

This is the most general volatility specification of Tables 5.1-5.5 and will be used to derive similar results for the rest of the volatility specifications.

9.1.1 Volatilities Depending on Time to Maturity

Let us now consider volatilities that are dependent on the time to maturity of the forward rate under consideration. Using Table 5.2, we can write Equation (9.1.2) as follows

$$\sigma^2_{T_{i-1}T_i.\text{caplet}} = \frac{1}{T_{i-1}} \sum_{j=1}^{i} \alpha_{T_{j-2}T_{j-1}} \eta^2_{i-j+1}. \tag{9.1.3}$$

This equation allows for a very simplistic calibration algorithm. In order to illustrate this, let us consider a couple of different calibration scenarios.

Firstly, let us consider the calibration to the shortest dated caplet, i.e. set $i = 1$. Applying Equation (9.1.3), we obtain

$$\sigma^2_{T_0T_1.\text{caplet}} = \frac{1}{T_0} \alpha_{0T_0} \eta^2_1 \tag{9.1.4}$$

and hence we have that

$$\eta^2_1 = \frac{1}{\alpha_{0T_0}} T_0 \sigma^2_{T_0T_1.\text{caplet}}. \tag{9.1.5}$$

Next, let us consider the calibration to the second caplet quote, i.e. set $i = 2$. Applying Equation (9.1.3), we obtain

$$\sigma^2_{T_1T_2.\text{caplet}} = \frac{1}{T_1} \left(\alpha_{0T_0} \eta^2_2 + \alpha_{T_0T_1} \eta^2_1 \right) \tag{9.1.6}$$

and hence we have that

$$\eta^2_2 = \frac{1}{\alpha_{0T_0}} \left(T_1 \sigma^2_{T_1T_2.\text{caplet}} - \alpha_{T_0T_1} \eta^2_1 \right). \tag{9.1.7}$$

Extending the results to the rest of the caplets follow a similar procedure and hence not presented. The ease of calibration for this particular model is impressive. Note however that the resulting volatility from Equation (9.1.7) can be imaginary if

$$T_1 \sigma^2_{T_1T_2.\text{caplet}} < \frac{\alpha_{T_0T_1}}{\alpha_{0T_0}} T_0 \sigma^2_{T_0T_1.\text{caplet}}, \tag{9.1.8}$$

which, assuming equally spaced time intervals, equates to requiring that the quantity $T_{i-1}\sigma^2_{T_{i-1}T_i.\text{caplet}}$ is a strictly increasing function of i. This ties back to comments made in Section 5.2, i.e. we need this condition to hold in order to fit a time homogeneous model to a given set of market data.

9.1.2 Volatilities Depending on Maturity

We will now consider the case where the instantaneous volatilities are assumed to be dependent on the time to maturity of the considered forward rate. Using Table 5.3, we can write Equation (9.1.2) as follows

$$\sigma^2_{T_{i-1}T_i.\text{caplet}} = s_i^2. \tag{9.1.9}$$

This specification ensures an exact fit to any set of caplet volatilities, which is in contrast with the specification considered in the previous section. Furthermore, as pointed out by Brigo and Mercurio [11], we have that this is not a time-homogeneous volatility specification (except for flat term structures) given that the term structure changes following each reset.

This concludes the piecewise constant structures that will be considered in this chapter. The next chapter will extend above discussions to the separable cases presented by Tables 5.4 and 5.5. These structures will be used for the simultaneous calibration to cap and swaption prices given the extra degrees of freedom.

9.2 Parametric Volatility Calibration

This section will consider some of the parametric volatility calibrations as presented in the text by Rebonato [47]. As mentioned earlier, this method is preferred over its non-parametric counterparts mainly due to the ability to enforce certain financial properties on the resulting model implied volatilities.

The most important property that we will enforce during the calibration process is the principle of time-homogeneous term structures, i.e. we expect the term structure of volatilities at any future date to look the same as the structure implied by the market today (this is time-homogeneity in its strictest form, if we relax this condition slightly then we would require that certain key properties are at least preserved at future time instances).

Note that we mentioned in Section 5.2 that we can obtain a time-homogeneous function $h(T_{k-1} - t)$ that will fit a given market term structure exactly given $T_i\sigma^2_{T_iT_{i+1}.\text{caplet}}$ is a strictly increasing function of T_i. Rebonato [47] however makes the very important observation that, although there exist such a function h, this will not hold for all functions h. Hence, if we specify h by Equation (5.4.8), then there exists a possibility that the we will not be able to price back exactly to all the given inputs. In order to price back exactly, we will need to introduce an additional component that is dependent on the forward rate under consideration.

Although time-homogeneity is a very desirable property (mainly due to difficulty for trader to express views on future term structures), there might be cases where a trader has a strong view that the shape of the term structure will change at a certain future instance. In order to incorporate this possible change in our deterministic volatility setup, Rebonato [47] suggests a simultaneous

calibration to both term structures (current as well as future expected term structure).

The various different parametric specifications were defined in Chapter 5. We will however only consider some of these in order to illustrate some of the key calibrating principles.

9.2.1 Separable Volatility Specification

The first specification was introduced by Rebonato [47] in order to allow for exact fitting to given market caplet prices while ensuring a time homogeneous evolution of the term structure. This specification is given by Equation (5.4.5) and is presented below

$$\sigma_{T_{k-1}T_k}(t) = h(T_{k-1} - t)f(T_{k-1}).$$

The calibration algorithm firstly fits the time homogeneous part, i.e. the function h, as closely as possible to the given term structure. This will ensure that most of the explanatory burden is placed on this component. In order to achieve this, we need solve for the set of parameters of the function h that will result in a minimum for the objective function

$$\chi^2 = \sum_{j=1}^{n} \eta_j^2, \tag{9.2.1}$$

where

$$\eta_j^2 = \left[\sigma^2_{T_{j-1}T_j.\text{caplet}} T_{j-1} - \int_0^{T_{j-1}} h(T_{j-1} - t)^2 \, dt\right]^2. \tag{9.2.2}$$

The remainder of the calibration will then consist of determining the forward rate specific components, i.e. the function f, that will ensure the exact pricing of the input caplet prices. Given this function is independent of time, we know that we can move it outside the integral when integrating over time. Hence, we have from Equations (4.1.5) and (5.4.5)

$$f(T_{j-1})^2 = \frac{\sigma^2_{T_{j-1}T_j.\text{caplet}} T_{j-1}}{\int_0^{T_{j-1}} h(T_{j-1} - t)^2 \, dt}. \tag{9.2.3}$$

Note that the second part of the calibration algorithm is necessary even if $T_i\sigma^2_{T_iT_{i+1}.\text{caplet}}$ is a strictly increasing function of T_i (due to function parameterization as discussed above). Furthermore, this will allow the exact pricing of caplet prices for the cases in which $T_i\sigma^2_{T_iT_{i+1}.\text{caplet}}$ is not a strictly increasing function of T_i. Rebonato [47] points out that although the model recovers the caplet prices exactly, there is a risk that the resulting function f might distort the time homogeneous behaviour obtained in the previous step. This then implies that f should be as close to unity as possible.

If the function obtained in the second step is not constantly close to unity, then the procedure failed to calibrate the proposed time homogeneous behaviour to the set of market data.

9.2.2 Multi-Time Dependence Volatility Specification

It was mentioned in the previous section that there might be cases in which the forward rate volatility component can be significantly different from unity. This then implies a rejection in the time homogeneous assumption given the two components are working against each other. There is, however, a way in which we can preserve the time homogeneous property while recovering the exact caplet prices (or at least to a better degree than the previous approach). This improvement is obtained through the introduction of a time dependent function to the volatility specification. The parametric form is given by Equation (5.4.7) and presented below

$$\sigma_{T_{k-1}T_k}(t) = h(T_{k-1} - t)g(t)f(T_{k-1}).$$

Similar to the process described in the previous section, Rebonato [47] proposed a three-step procedure to calibrate the specification presented above.

The first step is to fit the time homogeneous component. This is given by Equations (9.2.1) and (9.2.2). The next step consists of explaining as much as possible of the remaining differences using the time dependent function $g(t)$. In order to achieve this, we need to solve for the set of parameters of the function g that will result in a minimum for the objective function

$$\chi^2 = \sum_{j=1}^{n} \eta_j^2, \tag{9.2.4}$$

where

$$\eta_j^2 = \left[\sigma^2_{T_{j-1}T_j.\text{caplet}} T_{j-1} - \int_0^{T_{j-1}} \left(h(T_{j-1} - t)g(t)\right)^2 \, dt\right]^2. \tag{9.2.5}$$

The remainder of the calibration will then consist of determining the forward rate specific components, i.e. the function f, that will ensure the exact pricing of the input caplet prices. Following the same arguments, we can obtain

$$f(T_{j-1})^2 = \frac{\sigma^2_{T_{j-1}T_j.\text{caplet}} T_{j-1}}{\int_0^{T_{j-1}} \left(h(T_{j-1} - t)g(t)\right)^2 \, dt}. \tag{9.2.6}$$

Although this procedure should lead to a smoother function f, we still need to check this property in the calibration process in order to ensure that a time homogeneity term structure is enforced.

9.3 European Market Results

This section will consider the application of above techniques to the European market data set. Similar arguments and results were presented by Gatarek, Bachert and Maksymiuk [21]. These arguments will then be extended to the South African market in the following section.

9.3.1 Volatilities Depending on Time to Maturity

We will start the discussion with the first non-parametric volatility specification, i.e. the case where we assume that the volatilities are only dependent on time to maturity. The examples below will illustrate the ease with which we can obtain the necessary model calibration to the data presented in Table 7.5 (assuming equal time intervals of 0.25).

Example 9.3.1
Let us consider the calculation of the first parameter of Table 5.2. The formula for this parameter was derived in Section 9.1.1 and is given by Equation (9.1.5). Applying this to the market data presented in Table 7.5 results in the following

$$\begin{aligned}\eta_1 &= sqrt\left(\frac{1}{\alpha_{0T_{3M}}} T_{3M}\sigma^2_{T_{3M}T_{6M}.caplet}\right)\\ &= \sigma_{T_{3M}T_{6M}.caplet}\\ &= 0.1641.\end{aligned}$$

Example 9.3.2
Next, let us consider the calculation of the instantaneous volatility η_2. Using Equation (9.1.7) and Table 7.5, we can write

$$\begin{aligned}\eta_2 &= sqrt\left(\frac{1}{\alpha_{0T_{3M}}}\left(T_{6M}\sigma^2_{T_{6M}T_{9M}.caplet} - \alpha_{T_{3M}T_{6M}}\eta_1^2\right)\right)\\ &= sqrt\left(\frac{1}{0.25}\left(0.5\times 0.1641^2 - 0.25\times 0.1641^2\right)\right)\\ &= 0.1641.\end{aligned}$$

Example 9.3.3
Similarly, we can calculate the instantaneous volatility η_3 as illustrated below

$$\begin{aligned}\eta_3 &= sqrt\left(\frac{1}{\alpha_{0T_{3M}}}\left(T_{9M}\sigma^2_{T_{9M}T_{1Y}.caplet} - \alpha_{T_{3M}T_{6M}}\eta_2^2 - \alpha_{T_{6M}T_{9M}}\eta_1^2\right)\right)\\ &= sqrt\left(\frac{1}{0.25}\left(0.5\times 0.1641^2 - 0.25\times 0.1641^2\right)\right)\\ &= 0.1641.\end{aligned}$$

Given the simplicity of the calculations, there is no need to present more examples relating to the calculation of the parameters of Table 5.2. Extending this approach to the rest of the parameters consists of determining η_i through the use of Equation (9.1.3) and the given set of market data.

The more important aspect to consider in this section is the behaviour of the calculated forward rate volatilities. Given the variance plot in Figure 7.6, we know from previous discussions that it might not be possible to enforce the time-homogeneous volatility structure onto the given set of market data. Furthermore, from this figure it is evident that this type of unfavourable behaviour will start around the $2Y$ area.

The full set of results is given in the Table 9.1 below (same format as Table 5.2). Note the errors returned by the process from time $2Y$. This is

	$(0, T_{3M}]$	$(T_{3M}, T_{6M}]$	$(T_{6M}, T_{9M}]$	...	$(T_{19.75Y}, T_{20Y}]$
$L_{T_{3M}T_{6M}}(t)$	0.1641	Dead	Dead	...	Dead
$L_{T_{6M}T_{9M}}(t)$	0.1641	0.1641	Dead	...	Dead
$L_{T_{9M}T_{1Y}}(t)$	0.1641	0.1641	0.1641	...	Dead
$L_{T_{1Y}T_{1.25Y}}(t)$	0.2856	0.1641	0.1641	...	Dead
$L_{T_{1.25Y}T_{1.5Y}}(t)$	0.2778	0.2856	0.1641	...	Dead
$L_{T_{1.5Y}T_{1.75Y}}(t)$	0.3101	0.2778	0.2856	...	Dead
$L_{T_{1.75Y}T_{2Y}}(t)$	0.3458	0.3101	0.2778	...	Dead
$L_{T_{2Y}T_{2.25Y}}(t)$	error!	0.3458	0.3101	...	Dead
$\vdots$	...	...	...	...	...
$L_{T_{19.75Y}T_{20Y}}(t)$	error!	error!	error!	...	0.1641

Table 9.1: Piecewise constant volatilities obtained from European market data when instantaneous volatilities depend on the time-to-maturity of the forward rate. Results presented for business date 2005/01/21.

in line with the comments made earlier and hence illustrates the need for the variance function to be strictly increasing. It is important to mention some properties regarding the evolution of the term structure of volatilities under this specification. From Table 9.1 and Definition 5.1 it is evident that, ignoring the shortening of the tail, the term structure evolves in a time-homogeneous manner (Brigo and Mercurio [11]). From a financial point of view, it can be argued that this is more appealing than a deformation at the short-end of the structure.

9.3.2 Volatilities Depending on Maturity

The calibration of volatilities under this specification was discussed in Section 9.1.2. Furthermore, it was shown that the entire calibration process is given

by Equation (9.1.9). This then implies that any term structure can be fitted exactly to any given set of market data.

The results from calibrating the model to the market data given in Table 7.5 is presented below (same format as Table 5.3). Brigo and Mercurio [11]

	$(0, T_{3M}]$	$(T_{3M}, T_{6M}]$	$(T_{6M}, T_{9M}]$	...	$(T_{19.75Y}, T_{20Y}]$
$L_{T_{3M}T_{6M}}(t)$	0.1641	Dead	Dead	...	Dead
$L_{T_{6M}T_{9M}}(t)$	0.1641	0.1641	Dead	...	Dead
$L_{T_{9M}T_{1Y}}(t)$	0.1641	0.1641	0.1641	...	Dead
$L_{T_{1Y}T_{1.25Y}}(t)$	0.2015	0.2015	0.2015	...	Dead
$L_{T_{1.25Y}T_{1.5Y}}(t)$	0.2189	0.2189	0.2189	...	Dead
$L_{T_{1.5Y}T_{1.75Y}}(t)$	0.2365	0.2365	0.2365	...	Dead
$L_{T_{1.75Y}T_{2Y}}(t)$	0.2550	0.2550	0.2550	...	Dead
$L_{T_{2Y}T_{2.25Y}}(t)$	0.2213	0.2213	0.2213	...	Dead
$\vdots$	...	...	...	...	...
$L_{T_{19.75Y}T_{20Y}}(t)$	0.1133	0.1133	0.1133	...	0.1133

Table 9.2: Piecewise constant volatilities obtained from European market data when instantaneous volatilities depend on the maturity of the forward rate. Results presented for business date 2005/01/21.

mentions that this specification is less desirable given that the head of the term structure falls away as we move through time. Hence, even though we are guaranteed of an exact fit, we have that the disadvantage associated with the evolution of the term structure far outweighs the ease of calibration.

9.3.3 Separable Volatility Specification

The previous two volatility specifications can be classified as piecewise constant non-parametric volatility specifications. We will now move on to parametric specifications as proposed by Rebonato [47]. The calibration strategy that will be used was described in detail in Section 9.2.1.

In order to illustrate the calibration process, we will consider the results obtained at each of the different steps. The first step of the calibration consists of minimizing Equation (9.2.2). This then immediately requires the modeler to choose a specific parametric form for the time homogeneous function h. We will use the parametric form given by Equation (5.4.8) (recommended by Rebonato [47]). Details regarding this calculation is briefly discussed below.

The minimization of this function was performed in Matlab using the function *lsqnonlin* (function for nonlinear least-squares problems). In order to ensure a "more" global solution, the process employed 50 different starting points generated randomly from a uniform distribution. The reader is referred

to texts by Rardin [46] and Snyman [55] for more information regarding different optimization routines and the reason for using multiple starting points. Integration was performed numerically using the Matlab defined function *quad* (see text by Burden and Faires [14] for more information regarding numerical integration). This was used, irrespective of the available analytical solution, in order to allow more complex volatility specifications. The Matlab code for this calculation is provided in Section C.1.1.1.

Let us now consider the results obtained from this first step of the calibration process. The reported minimum of the objective function is 0.001596. The parameters of the function h resulting in this minimum is given as

$$\begin{aligned} a &= -0.047580, \\ b &= 0.471041, \\ c &= 1.044462, \\ d &= 0.112314. \end{aligned}$$

In order to illustrate the accuracy of this first fit, we will consider the graph of the model implied volatility term structure against the market input term structure. This is presented in Figure 9.1 below.

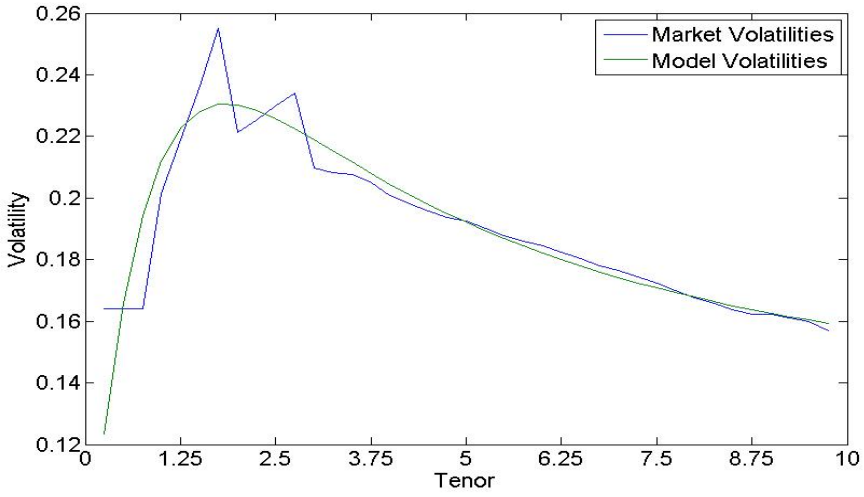

Figure 9.1: Term structure of volatilities obtained through fitting Rebonato's time homogeneous function to the set of European ATM caplet volatilities. Results presented for business date 2005/01/21.

The results presented in this section are slightly better than those obtained by Gatarek, Bachert and Maksymiuk [21]. This difference is expected to be

due to the year fractions used in their algorithm. The authors started these at 0.5 as opposed to the first reset time, i.e. 0.25.

Note from above the complexity associated with the fit. It is impossible to get an exact fit to the caplet term structure given the erratic volatility behaviour and the smoothness of function h. In order to achieve this we will need to introduce forward rate specific components. These are defined as the function f in Equation (9.2.3) and are presented in the figure below.

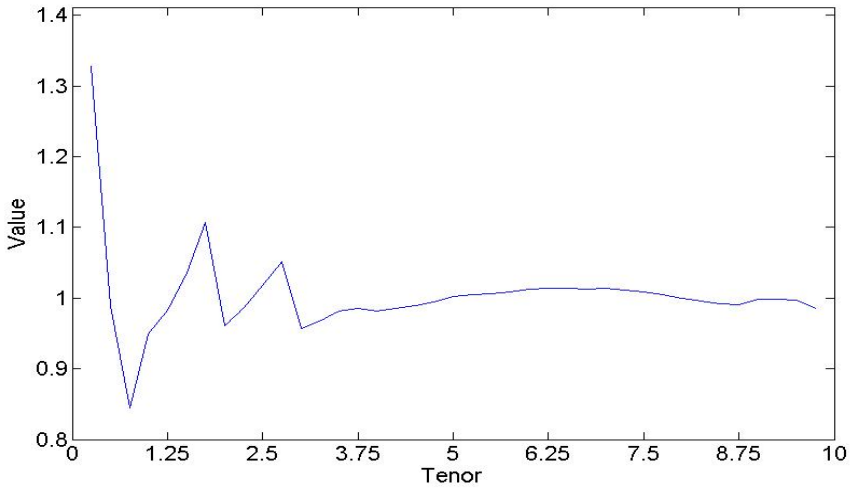

Figure 9.2: Implied forward rate specific components following the fitting of Rebonato's time homogeneous function to the set of European ATM caplet volatilities. Results presented for business date 2005/01/21.

Apart from the first scaling factor in Figure 9.2, the factors appear to be reasonably close to one (comparing to results obtained by Rebonato [47] in similar studies). It is also evident from the previous two figures that the biggest scaling factors are needed in the short end. This is in line with the erratic caplet behaviour in this area.

Next, let us consider the evolution of term structure over time as implied by the model. This is important given the fact that this implies future hedging costs (and consequently the price of the derivative under consideration). Hence, it is essential that this evolution should be in line with trader expectations (given the market incompleteness).

In order to obtain a graph reflecting the evolution of the term structure of volatilities, it was assumed that the scaling factors in Figure 9.2 tend to 1 as maturities increase. Furthermore, the term structure of volatilities was calculated at each of the different reset times, i.e. in fractions of 0.25. This is presented in Figure 9.3 below (the Matlab code used for this calculation is presented in Section C.1.1.1)

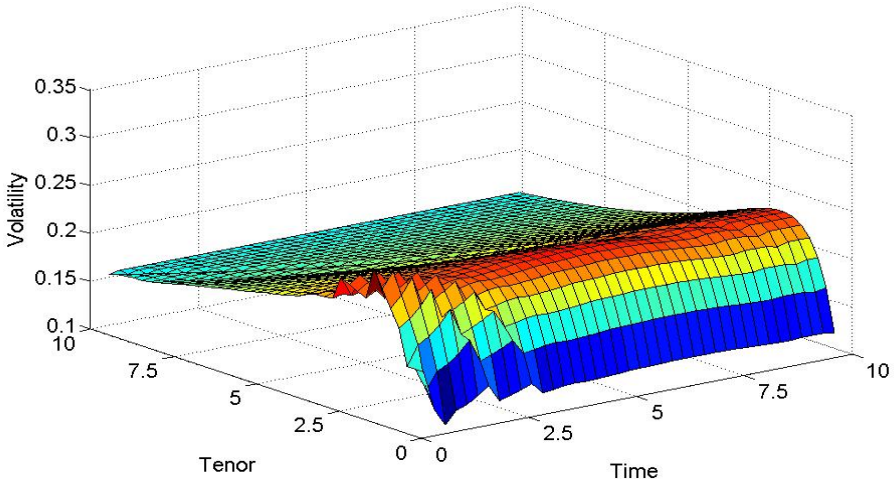

Figure 9.3: Model implied term structure evolution following the two step fitting methodology outlined in this section. Results presented for the European market and were obtained through calibrating to the market term structure of 2005/01/21.

Note from above the evolution of the term structure as we move through time. In its strictest sense, it can probably be argued that there is some change in the term structure as time progresses. These changes are, however, short lived and mainly concentrated in the short term (in line with what predicted by scaling factors in Figure 9.2). There is however a much stronger case for time homogeneity. This can for example be seen by noting that the general shape of the term structure is obtained across the bulk of the different time steps (even in short-term we maintain a humped shape). This confirms the success the calibration methodology in ensuring a time homogeneous evolution while pricing back exactly to the given set of caplet prices. The obtained results are very promising given the complexities associated with the input volatilities, i.e. variances not strictly increasing.

9.3.4 Multi-Time Dependence Volatility Specification

We will now consider the calibration using the three-step approach as proposed by Rebonato [47]. The first step of this process consist of the fitting of a time homogeneous function to the set of caplet volatilities. This process was already performed in the previous section and the results presented. According to the arguments presented in Section 9.2.2, we will need to fix the parameters of the time homogeneous function at these values.

The next step is then to add a time dependent component in order to explain as much as possible of the remaining differences. This was done through specifying the function g according to (5.4.12) with n set equal to 4.

Note however that due to the oscillating nature of the function g, we were forced to change the numerical integration function to *quadgk*. Equation (9.2.5) was consequently minimized using the code provided in Section C.1.1.2. Similarly to the previous section, the algorithm employed multiple starting points in order to get closer to a global minimum. This was set to 100, although this appeared to be over conservative.

The addition of a time dependent component resulted in a better fit between market and implied volatilities. The minimum of the objective function consequently reduced further to 0.001231. The parameters of the function g resulting in this minimum is given as

$$\begin{aligned}
\epsilon_1 &= -1.283060, \\
\epsilon_2 &= 0.428639, \\
\epsilon_3 &= -0.364465, \\
\epsilon_4 &= -0.254697, \\
\epsilon_5 &= 1.715605, \\
\epsilon_6 &= -0.031785.
\end{aligned}$$

In order to illustrate the accuracy of the fit, we will once again consider graphs of the different results. The first figure displays the model implied volatilities against the market input term structure. This is presented in Figure 9.4 below.

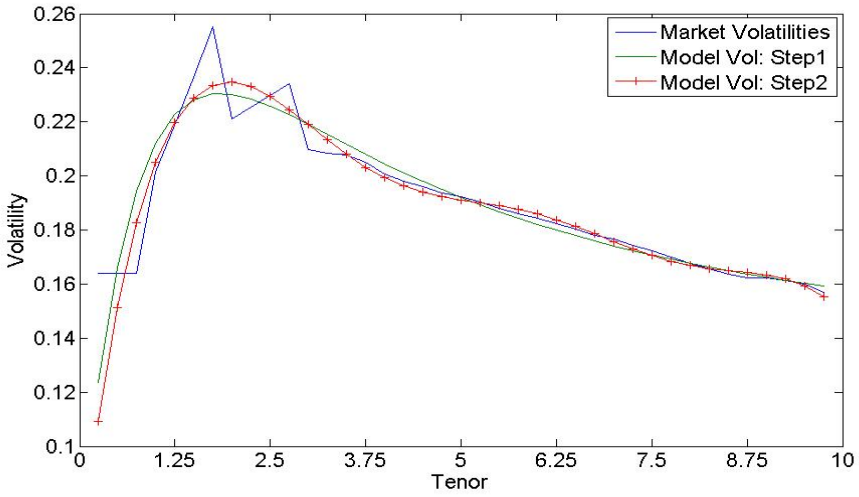

Figure 9.4: Term structure of volatilities obtained when adding an additional time dependent function to the instantaneous volatility specification. Results presented for the European market and were obtained through calibrating to the market term structure of 2005/01/21.

The results presented in the figure above illustrates a general improvement in the fit of the volatilities. This came at the price of a less accurate approximation for the first caplet volatility. Note however the oscillating nature of the new specification. From this it is clearly evident that the inclusion of such a time dependent component can significantly increase the accuracy of the calibration. Although we paid a price in the very short end (will fall away after first reset), it should be noted that the input volatilities are not that well behaved. Comparing these volatilities with those used by Rebonato [47], it is clear that these almost represent a worst case scenario. In practice it is advisable to try and use smoother input volatilities for calibration purposes.

In order to achieve the exact pricing of market caplets, we will once again need to introduce forward rate specific components. These are defined as the function f in Equation (9.2.6) and are presented in the figure below.

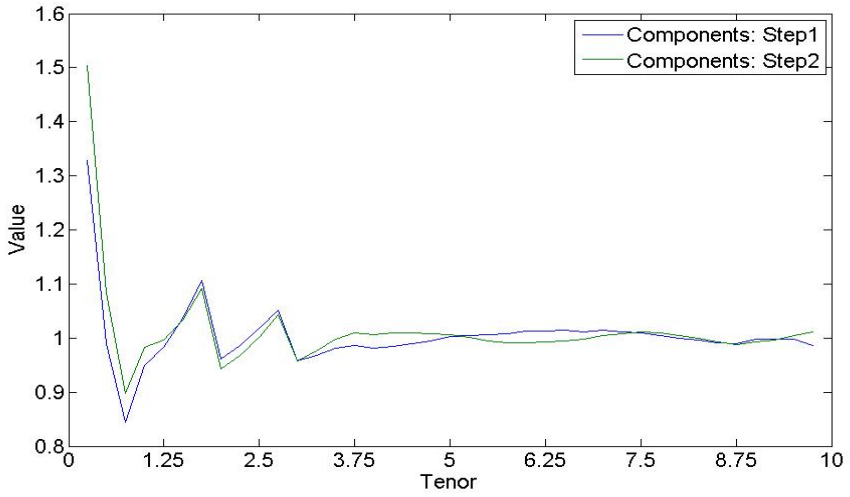

Figure 9.5: Implied forward rate specific components following the introduction of a time dependent component into the instantaneous volatility specification. Results presented for the European market and were obtained through calibrating to the market term structure of 2005/01/21.

The figure above confirm some of the previous comments, i.e. improvements across most of the expiries and a significant reduction in the accuracy at the very short end. The implied term structure evolution is very similar to the one given in Figure 9.3 and hence not presented again. This was expected given the results displayed in the previous two figures. Although not optimal, this is mainly due to the significant amount of noise experienced in the short end of the term structure (this type of behaviour limits the explanatory power of the additional parameters). The evolution of the term structure under

this specification will not be included in this section. This will however be considered in the section relating to the South African market.

9.4 South African Market Results

This section will move on to consider the results obtained when similar calibration algorithms are applied to the South African market. The calibration process is however significantly dependent on accurate market data. The process of obtaining reasonable market data can essentially be classified as a field on its own (investment banks typically have entire teams to manage this process). Some of the steps involved in such a process was discussed in Chapter 8.

9.4.1 Volatilities Depending on Time to Maturity

We will once again start the discussion with the first non-parametric volatility specification, i.e. the case where we assume that the volatilities are only dependent on time to maturity. The required calibration can be obtained through applying the techniques discussed in Section 9.1.1 to the set of market data given in Table 8.3. The full set of results for the parameters of Table 5.2 is given below.

Variable	Value	Variable	Value	Variable	Value	Variable	Value
η_1	0.1252	η_{11}	0.1034	η_{21}	0.1072	η_{31}	0.0914
η_2	0.1532	η_{12}	0.1457	η_{22}	0.1040	η_{32}	0.1417
η_3	0.1804	η_{13}	0.1067	η_{23}	0.0986	η_{33}	0.0892
η_4	0.1872	η_{14}	0.0858	η_{24}	0.1576	η_{34}	0.0809
η_5	0.1713	η_{15}	0.0673	η_{25}	0.1010	η_{35}	0.0914
η_6	0.1743	η_{16}	0.1624	η_{26}	0.0999	η_{36}	0.1851
η_7	0.1754	η_{17}	0.0755	η_{27}	0.0932	η_{37}	0.0881
η_8	0.2020	η_{18}	0.0644	η_{28}	0.1515	η_{38}	0.0906
η_9	0.1231	η_{19}	0.0477	η_{29}	0.0965	η_{39}	0.0716
η_{10}	0.1116	η_{20}	0.1271	η_{30}	0.0936	η_{40}	0.1842

Table 9.3: Parameters of Table 5.2 as obtained from South African market data. Results presented for business date 2009/12/31.

Above given results can then be summarized into a similar format as the results given in Section 9.3.1. This is presented in Table 9.4 below.

One significant difference between the results presented in this section vs. those presented in Section 9.3.1 is the fact that all the parameters are well defined (i.e. no square roots of negative values encountered). This is due to the strictly increasing nature of the function $T_i\sigma^2_{T_iT_{i+1}.\text{caplet}}$ (concept explained in Section 9.1.1). Within this specific example, we achieved exact re-pricing of market caplets as well as a time homogeneous term structure of volatilities.

	$(0, T_{3M}]$	$(T_{3M}, T_{6M}]$	$(T_{6M}, T_{9M}]$	...	$(T_{10Y}, T_{10.25Y}]$
$L_{T_{3M}T_{6M}}(t)$	0.1252	Dead	Dead	...	Dead
$L_{T_{6M}T_{9M}}(t)$	0.1532	0.1252	Dead	...	Dead
$L_{T_{9M}T_{1Y}}(t)$	0.1804	0.1532	0.1252	...	Dead
$L_{T_{1Y}T_{1.25Y}}(t)$	0.1872	0.1804	0.1532	...	Dead
$L_{T_{1.25Y}T_{1.5Y}}(t)$	0.1713	0.1872	0.1804	...	Dead
$L_{T_{1.5Y}T_{1.75Y}}(t)$	0.1743	0.1713	0.1872	...	Dead
$L_{T_{1.75Y}T_{2Y}}(t)$	0.1754	0.1743	0.1713	...	Dead
$L_{T_{2Y}T_{2.25Y}}(t)$	0.2020	0.1754	0.1743	...	Dead
$\vdots$	...	...	...	...	...
$L_{T_{10Y}T_{10.25Y}}(t)$	0.1842	0.0716	0.0906	...	0.1252

Table 9.4: Piecewise constant volatilities obtained from South African market data when instantaneous volatilities depend on the time-to-maturity of the forward rate. Results presented for business date 2009/12/31.

These results were however only achievable due to well behaved input volatilities. This type of dependency poses a risk for practical implementations and hence renders the approach as unattractive.

The evolution of the term structure, under this specification, is presented in the figure below

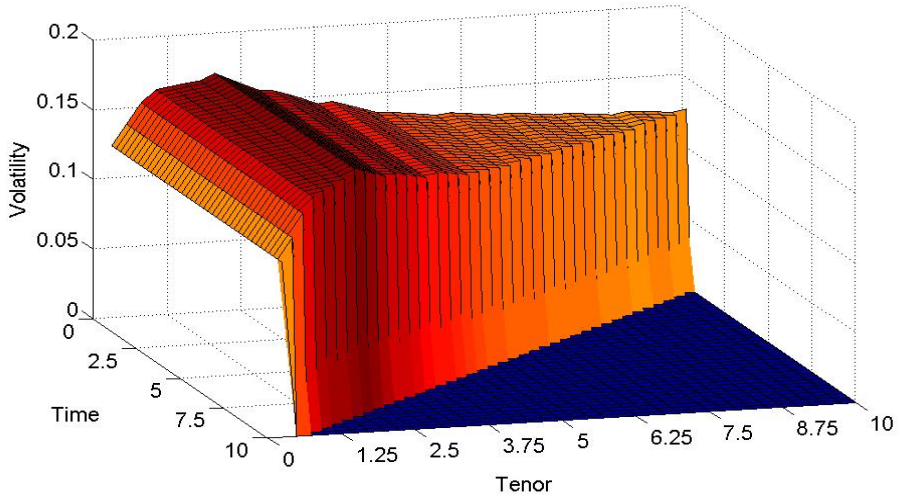

Figure 9.6: Model implied term structure evolution for piecewise constant volatilities dependent on the time-to-maturity of a forward rate. Results presented for the South African market and were obtained through calibrating to the market term structure of 2009/12/31.

This figure clearly illustrates the shortening of the tail of the term structure

as we move through time. It was mentioned earlier that this is a far more attractive property than when the head of the the term structure is affected (discussed in next section).

Given the simplicity of the calibration techniques we were able to perform the calculations in Excel. The Matlab code in Section C.1.2.1 illustrates the calculation of the term structure as we move through time (the reader can also reference this code to get the full set of results for techniques applied in this section).

9.4.2 Volatilities Depending on Maturity

This is the specification with the most straight forward calibration algorithm. Furthermore, it was shown that this specification always result in an exact fit to the current term structure. The entire calibration process is given by Equation (9.1.9). This process was discussed in Section 9.1.2 and results presented for the European market in Section 9.3.2. We will now extend the application the set of market data presented in Table 8.3.

The parameters can be read directly from Table 8.3, i.e. each row of Table 5.3 is given by the volatility of the associated forward rate. The results for this calibration is thus given by the table below.

	$(0, T_{3M}]$	$(T_{3M}, T_{6M}]$	$(T_{6M}, T_{9M}]$	...	$(T_{10Y}, T_{10.25Y}]$
$L_{T_{3M}T_{6M}}(t)$	0.1252	Dead	Dead	...	Dead
$L_{T_{6M}T_{9M}}(t)$	0.1399	0.1399	Dead	...	Dead
$L_{T_{9M}T_{1Y}}(t)$	0.1546	0.1546	0.1546	...	Dead
$L_{T_{1Y}T_{1.25Y}}(t)$	0.1633	0.1633	0.1633	...	Dead
$L_{T_{1.25Y}T_{1.5Y}}(t)$	0.1650	0.1650	0.1650	...	Dead
$L_{T_{1.5Y}T_{1.75Y}}(t)$	0.1666	0.1666	0.1666	...	Dead
$L_{T_{1.75Y}T_{2Y}}(t)$	0.1679	0.1679	0.1679	...	Dead
$L_{T_{2Y}T_{2.25Y}}(t)$	0.1725	0.1725	0.1725	...	Dead
$\vdots$	...	...	...	...	...
$L_{T_{10Y}T_{10.25Y}}(t)$	0.1268	0.1268	0.1268	...	0.1268

Table 9.5: Piecewise constant volatilities obtained from South African market data when instantaneous volatilities depend on the maturity of the forward rate. Results presented for business date 2009/12/31.

Irrespective of the ease at which we performed the calibration, we still have one significant shortcoming, i.e. the term structure does not evolve in a time homogeneous manner. This can easily be seen through having a look at the results presented in Table 9.5.

Notice, for instance, the change in the volatility of the nearest expiry forward rate as we move through time. This clearly illustrates the deformation in

the short end of the term structure. Hence, prices of interest rate derivatives (dependent on dynamics) may not adequately take into account the humped nature of the input volatilities (as this will clearly fall off as we move through time). The concepts discussed above are presented in Figure 9.7 below.

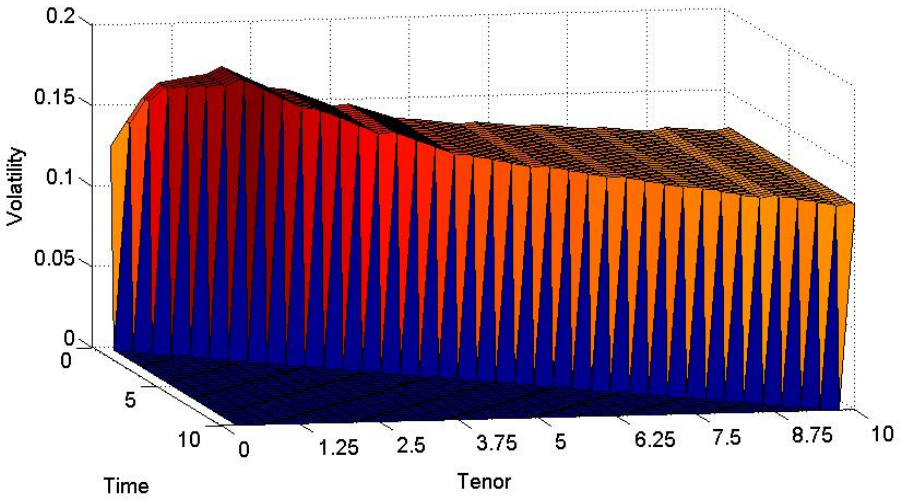

Figure 9.7: Model implied term structure evolution for piecewise constant volatilities dependent on the maturity of a forward rate. Results presented for the South African market and were obtained through calibrating to the market term structure of 2009/12/31.

These two sections conclude the examples relating to non parametric specifications.

9.4.3 Separable Volatility Specification

Let us now turn our attention to the parametric volatility specifications as proposed by Rebonato [47]. It was illustrated in section 9.3.3 how this technique was applied to the European market. This section will consider the calibration of this specification to the South African market.

Similar to the European market we will discuss the process in different steps. The first step of this calibration procedure consists of fitting the time homogeneous function 5.4.8 to the set of caplet volatilities given in Table 8.3. This is equivalent to minimizing Equation (9.2.2) where h is the function defined above. Results were obtained with ease in the European market through the use of a simple unconstrained minimization routine. Attempting the same unconstrained minimization routine in the South African market however resulted in mathematical as well as financial inconsistencies. This can largely be explained by the noise inherent in the volatility data which is clearly visible

in Figure 8.9. The inconsistencies as well as alternative solutions implemented are briefly discussed below.

One of the first problems encountered was the violation of some of the constraints given by Equations (5.4.9)-(5.4.11). A nonlinear constrained minimization routine was then employed (used the Matlab function *fmincon*).

Although this resolved the issue, the solution was still not optimal from a financial point of view. Rebonato [47] points out that the sum of the parameters a and d of function h should at least be approximately equal to the volatility of the shortest maturity caplet. This is due to the fact that the function approaches the quantity $a+d$ in the limit as time to maturity approaches zero. As a consequence this value was limited at 0.08, for the purpose of the example, however this should typically be determined by the trader.

Another important point to consider (as pointed out by Rebonato [47]), is the location of the hump in forward rate volatilities (note referring here to the actual forward rate volatilities and not Black volatilities). This was limited to the $1y$ area. These assumptions can typically be avoided (as with the European market) if the input volatilities are sufficiently smooth.

A final note on the first step is that the algorithm used the analytical formula, as given by Rebonato [47], for integrating the square of the instantaneous volatilities. This was used in order to speed up the required calculations. This formula is presented in the equation below.

$$\begin{aligned}\int \sigma^2_{T_{i-1}T_i}(t)\,dt &= \frac{1}{4c^3}(8ac^2d\,\exp[c(t-Ti)] + 4c^3d^2t \\ &- 8bcd\,\exp[c(t-Ti)](c(t-Ti)-1) \\ &+ \exp[c(2t-2Ti)]\{2a^2c^2 + 2abc(1+c(2Ti-2t)) \\ &+ b^2(1+2c^2(t-Ti)^2 + c(2Ti-2t))\}).\end{aligned}$$

The Matlab code used for the calibration is included in Section C.1.2.2. Similar to Section 9.3.3, the code made use of several randomly generated starting points in an attempt to find a global minimum. Results obtained through this calibration process are presented below.

The reported minimum of the objective function is 0.000320. This was obtained at the following parameter values of the function h

$$\begin{aligned}a &= -0.025783, \\ b &= 0.279814, \\ c &= 1.237841, \\ d &= 0.105783.\end{aligned}$$

Notice from above the following important points. Firstly, we have that all of the constraints in Equations (5.4.9)-(5.4.11) are satisfied. Next, we have

that the value of h as time to maturity approaches 0 is given by

$$\begin{aligned} \lim_{(T-t)\to 0} h &= a + d \\ &= 0.08. \end{aligned}$$

Finally, it can easily be seen from Equation (5.4.8) that the maximum of h is given at

$$\begin{aligned} \text{location of max} &= \frac{b - ca}{cb} \\ &= 0.90. \end{aligned}$$

In order to get a better feel of this we can consider a plot of the input data vs. the model implied values. Given the fit was performed in the variance space, we will use this graph in order to get an idea of the inherent residuals (only considered volatility plots for the European market in order to try and avoid repetition). This is presented in the figure below.

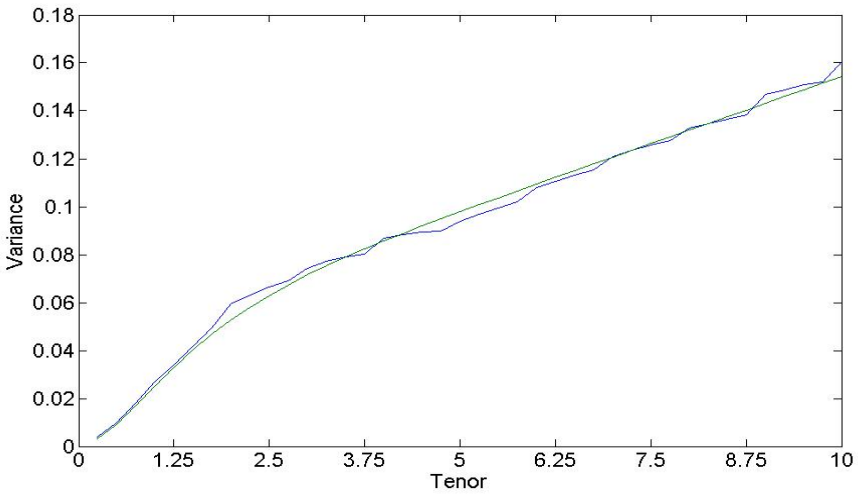

Figure 9.8: Variances obtained through fitting Rebonato's time homogeneous function to the set of South African ATM caplet volatilities. Results presented for business date 2009/12/31.

In statistics there are, however, a number of different methods that can be used to assist with this analysis. One alternative, would be to consider the sum of squared errors. This was already presented and amounted to 0.000320. Although useful, this can be a rather limited statistic as it does not provide any detail regarding the distribution of the errors.

Figure 9.8 above indicates some significant residuals. The impact of these on the associated volatility plot is depicted below.

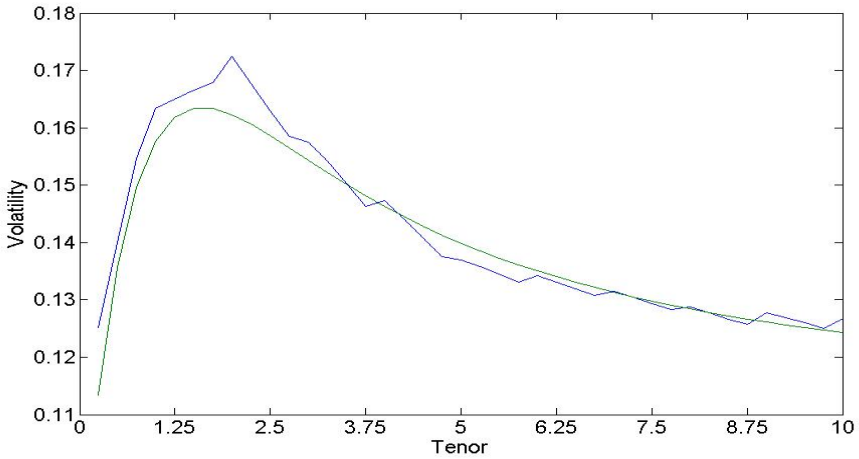

Figure 9.9: Term structure of volatilities obtained through fitting Rebonato's time homogeneous function to the set of South African ATM caplet volatilities. Results presented for business date 2009/12/31.

In order to achieve an exact fit to the input term structure we will need to introduce the forward rate specific components presented below.

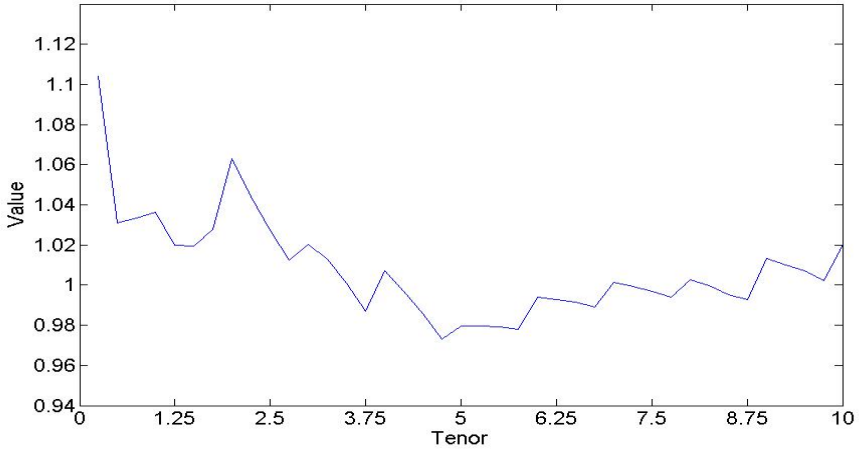

Figure 9.10: Implied forward rate specific components following the fitting of Rebonato's time homogeneous function to the set of South African ATM caplet volatilities. Results presented for 2009/12/31.

These are defined as the function f in Equation (9.2.3). The shortcomings of this first attempt is clearly visible in the above graphs. It can however be shown that the goodness of fit will increase as we relax some of the assumptions made (for example regarding short-term volatilities and location of hump). This is indicative of the noise present in the input data.

Irrespective of these results, we should keep in mind the intended purpose of this first step, i.e. to try and explain as much as possible of the volatility behaviour through the use of a time-homogeneous function. The accuracy of this fit will consequently be improved as we move on to the following step of the calibration process.

The forward rate components in the figure above are relatively close to one, however it is clearly evident that there is still some room for improvement (expect these components to be randomly distributed around 1 in a more accurate fit). Furthermore, these components appear to be slightly more volatile than those obtained in the European market. The biggest risk associated with the introduction of forward rate components is the possibility that these factors might disturb the time-homogeneous evolution of forward rates. Hence, we need to consider the evolution of the term structure over time to determine if the fit is financially justifiable or not. This is presented in Figure 9.11.

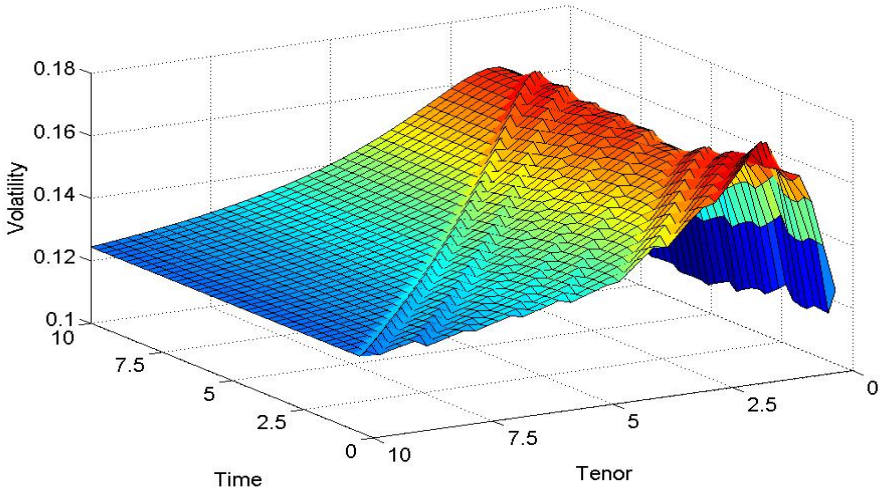

Figure 9.11: Model implied term structure evolution following the two step fitting methodology outlined in this section. Results presented for the South African market and were obtained through calibrating to the market term structure of 2009/12/31.

In order to obtain this graph it was assumed that the scaling factors in Figure 9.10 tend to 1 as maturities increase. Furthermore, the term structure of volatilities was calculated at each of the different reset times, i.e. in fractions

of 0.25. The Matlab code used for this calculation is presented in Section C.1.2.2.

This evolution clearly exhibits more changes as we move through time when compared with the results obtained from the European market. However, we still preserve the main volatility characteristics.

Another interesting comparison can be made through comparing the evolution just obtained with the one obtained in the non-parametric case, i.e. Figure 9.6 (note that Figure 9.11 should also represent a shortening in the tail of the term structure as we move through time, the example however assumed that the forward rate components approach 1). The term structures in the non-parametric case remain exactly the same as opposed to the slight changes in the parametric term structures. This is due to the introduction of the forward rate components.

9.4.4 Multi-Time Dependence Volatility Specification

Similar to Section 9.3.4 we will now consider the three-step approach as proposed by Rebonato [47]. This procedure is discussed in detail in Section 9.2.2. The first step was already performed in the previous section from which it was evident that there is a need for additional parameters in order to help explain market term structure.

These extra parameters will be obtained through including a time dependent function g in the instantaneous volatility specification and hence obtaining a new objective function 9.2.5. This function is defined in Equation (5.4.12). Furthermore, we will follow the parameterization of the European market and set n equal to 4. The results obtained for the optimization, using 2000 different starting points (increase due to more noise in input data), are presented and discussed below (Matlab code given in Section C.1.2.3).

The addition of a time dependent component resulted a better fit between market and implied volatilities. The minimum of the objective function reduced to 0.000080. The parameters of the function g resulting in this minimum is given as

$$\begin{aligned}
\epsilon_1 &= -4.92206,\\
\epsilon_2 &= -3.482772,\\
\epsilon_3 &= -1.493793,\\
\epsilon_4 &= 0.366691,\\
\epsilon_5 &= -0.828297,\\
\epsilon_6 &= 0.167607.
\end{aligned}$$

Let us now consider the accuracy of this fit through considering the same graphs as in the previous section. The first figure below illustrates the model implied variances against the market input variances.

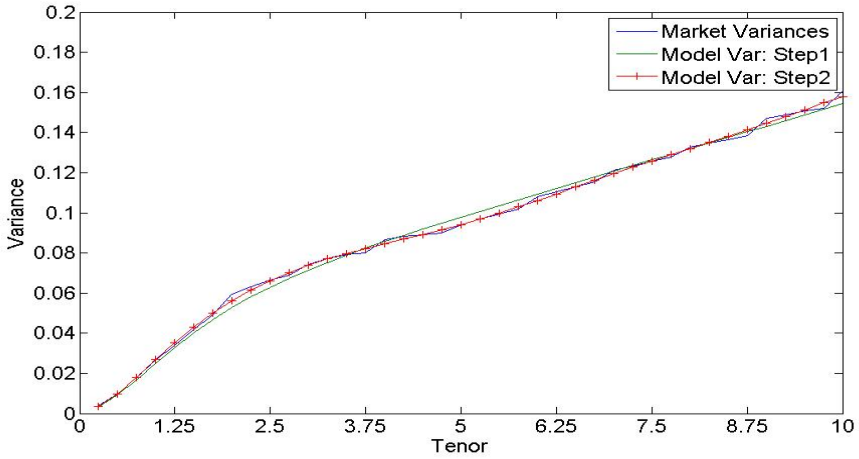

Figure 9.12: Variances obtained when adding an additional time dependent function to the instantaneous volatility specification. Results presented for business date 2009/12/31.

From above it is evident that the time dependent function provided the required flexibility. Note the way in which the new specification follows the curves in the market variances (reflective of the oscillating nature of the time dependent function). This behaviour resulted in much smaller residuals.

The associated volatility term structure is presented in Figure 9.13 below.

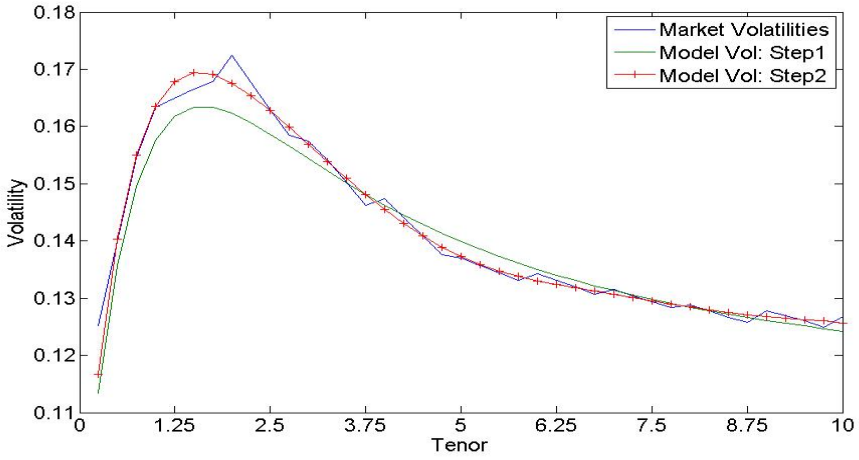

Figure 9.13: Term structure of volatilities obtained when adding an additional time dependent function to the instantaneous volatility specification. Results presented for the South African market and were obtained through calibrating to the market term structure as observed on 2009/12/31.

The volatility plot confirms the results seen in the variance space, i.e. a significant increase in the accuracy of the model. The final two graphs that we will consider, are presented below

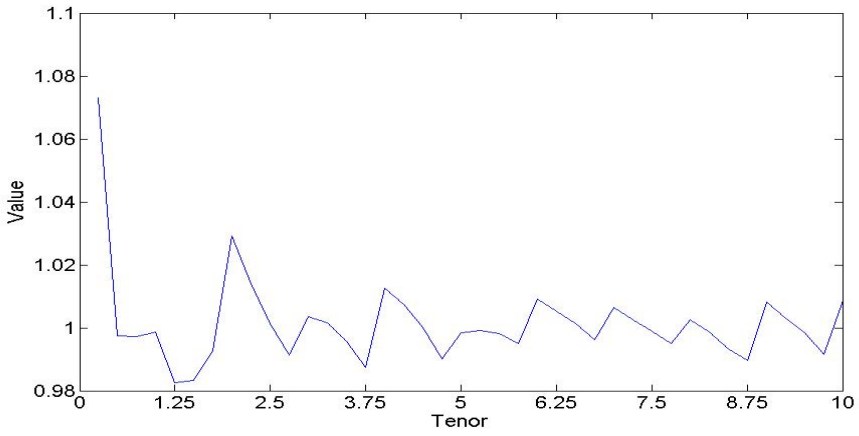

Figure 9.14: Implied forward rate specific components following the introduction of a time dependent component into the instantaneous volatility specification. Results presented for the South African market and were obtained through calibrating to the market term structure of 2009/12/31.

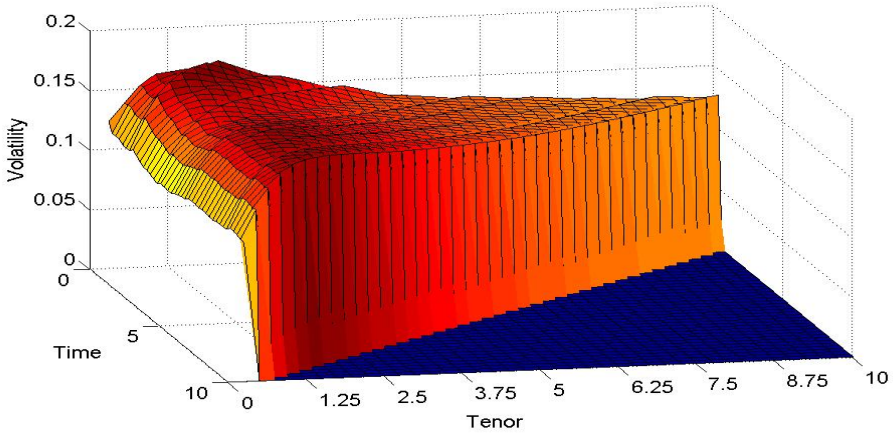

Figure 9.15: Model implied term structure evolution following the introduction of a time dependent component into the instantaneous volatility specification. Results presented for the South African market and were obtained through calibrating to the market term structure of 2009/12/31.

Figure 9.14 represents the corrections required to price back exactly to market inputs and are defined as the function f in Equation (9.2.6).

This figure clearly illustrates the accuracy of the fit. This can be seen from the random distribution of the residuals around 1 and the fact that the residuals mainly range between 0.98 and 1.02. The introduction of the time dependent component was clearly beneficial and explained most of the remaining variance irrespective of the noise inherent in the input data.

Finally, consider the model implied evolution of the term structure of volatilities, as given in Figure 9.15. This represents the behaviour of all three factors inherent in the instantaneous volatility specification as we move through time. The Matlab code for this calculation is given in Section C.1.2.3

The evolution appears to be sufficiently well behaved. Furthermore, the preservation of the humped structure remains in tact as we move through time. Hence, despite the noise inherent in input data, we still managed to obtain satisfactory results. Note that no assumptions were made regarding forward rate specific components as we move through time, hence the resulting evolution will illustrate a shortening in the tail of the term structure.

Chapter 10

Joint Calibration

The previous chapter dealt with the estimation of volatility parameters from market data. This fully described the calibration procedure for simple instruments such as caps or floors. Unfortunately, some products may depend on several forward rates at a time or even on both forward and swap rates. Hence, we will need to extend our techniques to incorporate co-movements between different market variables. This will be achieved through the inclusion of correlations into our calibration procedures.

Correlation is one of the more difficult concepts to incorporate into a model. This is largely due to the difficulty of obtaining accurate estimates from market prices. Previous chapters illustrated the ease with which volatilities can be obtained from observable vanilla prices. Market data restrictions renders this approach implausible when attempting to obtain similar market data for correlation calculations. European swaptions, for example, is one of the traded products that may actually contain information regarding the correlations between different forward rates. However, when considering the swaption volatility approximation formula it is evident that the shape of the instantaneous volatility functions also play a significant role in the pricing of swaptions, resulting in different implied correlations for different instantaneous volatility functions (Rebonato [47]). Hence, in order to imply correlations from market data we would typically need actively traded correlation derivatives. To my knowledge, these are not currently available in the South African market and hence we are forced to obtain correlations from historical rate movements as well as trader estimates.

Alternatively, Rebonato [47] mentioned that actively traded serial options would be able to complete the instantaneous volatility market (serial options were discussed in Section 2.4.2). Once these functions are determined, we would then be able to imply correlations through taking views regarding the price congruence between the different markets. Restrictions in liquidity however renders this approach implausible.

Given these points, we will consider calibration algorithms in which we

obtain volatility parameters from market data and correlation parameters through market analysis. These will range from the joint calibration of forward rates, i.e. same state variables, to the joint calibration of cap and swaption prices. Each of these techniques are based on a certain set of assumptions, driven by market incompleteness, and it is important to consider these in detail before deciding on which approach to implement.

10.1 Preliminary Calculations and Definitions

There are some final calculations that we need to perform in order to transform our market data into a format that can be used in our calibration algorithms.

The first required calculation relates to correlations. The historical estimation of correlations were presented in Section 8.5. From the results obtained it was clear that the estimated correlation matrix contained some noise which can have a negative impact on the calibration procedure. Furthermore, this is a historical estimate and hence will not reflect market views of future expected correlations. Given this, and the general complexity of obtaining such a matrix, it is hence recommended to rather use this as an estimation tool as opposed to a direct input. As a consequence, we will consider an approach that can be used to obtain exogenous correlation inputs given a historically estimated correlation matrix and trader expectations.

The second calculation can be used to convert caplet and swaption volatilities to the same payment frequency. This type of calculation is not required within the South African market and hence was merely presented for completeness purposes. Each of the above mentioned points will be discussed in the following sections and possible solutions will be proposed.

10.1.1 Correlation Smoothing

The objective is to fit some functional correlation structure to the estimated correlation matrix. These types of functional forms were discussed in Section 6.3 and represent specifications with full rank and a reduced number of parameters. Fitting such a structure typically consists of the minimization of some penalty function representing the differences between the exogenous correlation matrix and the functional form for a particular choice of parameters. Alternatively, Brigo and Mercurio [11] proposed a method in which the parameters can be obtained through inspection. Brigo and Mercurio [11] called this technique the pivot matrix approach given the fact that some of the key elements of the correlation matrix are exactly obtained during the fitting procedure. This is achieved through inverting the parametric forms in order to express the parameters in terms of these key elements (pivots).

The current chapter will however make use of the former approach in which we fit a specific parametric form to the historically estimated correlation matrix. We will use the parametric forms given by Equations (6.3.5)-(6.3.6), i.e.

$$\rho_{i,j}(t) = \rho_\infty + (1-\rho_\infty)\exp[-\beta|T_i - T_j|]$$

and

$$\rho_{i,j}(t) = \rho_\infty + (1-\rho_\infty)\exp[-\beta|(T_i - t)^\gamma - (T_j - t)^\gamma|].$$

Given the particular choice of correlation function, it is important to ensure that the long term level as well as the correlation matrix itself is well defined.

Another important point to consider is the impact of the smoothing on the associated eigenvectors and eigenvalues. From a financial point of view we would prefer these to remain relatively the same. Note that this is purely a financial requirement. For pricing purposes it is the actual correlations that matters as opposed to the implied eigenvectors and eigenvalues (Rebonato [47]).

The trader can alternatively try and obtain different correlation matrices for different sets of parameters should she feel that these are not a correct representation of the current market. It is however recommended to use some parametric form in the estimation process given the difficulty of obtaining market indications of these quantities.

10.1.2 Volatility Conversions

When performing a joint calibration between complementary instruments, one can encounter a scenario where the payment frequencies of observed cap/floor prices are different to the payment frequency of observed swaption prices. This type of discrepancy is only visible in some of the foreign markets and does not currently affect our local market. It is, however, important to briefly consider a technique that can be used to align the different payment conventions. This conversion will take place in the volatility space and is discussed below.

Suppose, for instance, we have a scenario in which the cap frequency is semi-annual, whereas the swaption frequency is annual. The approach will then start through expressing annual forward rates in terms of semi-annual forward rates. Given these expressions, we can then derive the appropriate annual volatilities through using Taylor expansions. As an example, consider an approximation derived by Brigo and Mercurio [11] for the three time instants $0 < T_1 < T_2 < T_3$, all six months spaced.

$$V^2_{T_1,T_3} = \sum_{i,j=1}^{2} u_i u_j \sigma_{T_i T_{i+1}.\text{caplet}} \sigma_{T_j T_{j+1}.\text{caplet}} \rho_{L(i,i+1);L(j,j+1)},$$

where

$$u_i(t) = \frac{1}{L_{T_1,T_3}(t)} \left(\frac{L_{T_i T_{i+1}}(t)}{2} + \frac{L_{T_1 T_2}(t) L_{T_2 T_3}(t)}{4} \right).$$

Within our example, V_{T_1,T_3} represents the resultant Black swaption volatility of the forward swap rate $SR_{T_1,T_3}(t)$.

10.1.3 Forward Rate Dynamics

Before we proceed to the next sections, it is important to point out that we will be working with forward rates as defined in Section 4.4.2. Hence, we have that the dynamics of the forward rate expiring at time T_i under the measure Q^T is given by

$$dL_{T_iT_{i+1}}(t) = \ldots dt + \sigma_{T_iT_{i+1}}(t)L_{T_iT_{i+1}}(t)C_{T_iT_{i+1}}d\overline{W}(t), \tag{10.1.1}$$

where the vector $\overline{W}(t)$ is defined as a $n \times 1$ vector of uncorrelated Wieners. The row vector $C_{T_iT_{i+1}}$ was included in order to model correlation between different forwards. This specification, as recommended by Rebonato [47], then allows the market observable volatility component to be separated from the component used for correlation modeling. This will be at the center of some of our calibration techniques. In closing, we will present this formulation in vector form as

$$\frac{dL}{L} = \ldots dt + \sigma C d\overline{W}, \tag{10.1.2}$$

where σ is the diagonal matrix containing volatilities of the different forward rates, i.e.

$$\sigma = \begin{bmatrix} \sigma_{T_1T_1} & 0 & \ldots & 0 \\ 0 & \sigma_{T_2T_2} & \ldots & 0 \\ \vdots & \vdots & \ddots & \vdots \\ 0 & 0 & \ldots & \sigma_{T_nT_n} \end{bmatrix}, \tag{10.1.3}$$

and the matrix C is chosen such that (see Sections 4.4.2 and A.5 for more details)

$$\rho = CC'.$$

10.2 Calibrating to Caplet Prices and Exogenous Forward Rate Correlation Matrix

This approach will typically be used when the exotic product will be hedged using caplets. Within this setup, the trader would want to recover the prices of hedging instruments exactly, while obtaining a best possible fit to the exogenous correlation matrix. The first question that might arise is why do we even have to use a calibration procedure in this setup when the volatility parameters are already determined. Rebonato [47] points out that this is mainly when we want to reduce the dimensionality of the problem.

This then immediately takes us to the second part of Chapter 6, i.e. reduced rank correlation specifications. We will show how the concepts, discussed in Sections 6.4.2.1 and 6.4.2.2, can be used in creating different calibration routines.

The routines described in the following sections are both based on the forward rate dynamics given by Equation (10.1.2). As a result, we have that the incorporation of correlations are independent of the volatility calibration. Hence, we will assume volatility parameters derived in the previous chapter and will mainly focus on determining the matrix C.

10.2.1 Hull and White PCA Approach

The approach suggested by Hull and White [31] makes use of the property that a correlation matrix can be decomposed into eigenvalues and eigenvectors using the relationships as discussed in Section 6.4.2.2. As a result, we can obtain the following simple expression for the matrix C should we want to retain as many factors as forward rates

$$C = P\Lambda, \tag{10.2.1}$$

where the matrix P is the resultant eigenvector matrix and the matrix Λ is a diagonal matrix containing the square root of the respective eigenvalues.

It is however seldom practical to work with a model in which the number of factors are equal the number of forward rates. Hull and White [31] suggested that we only retain the most significant eigenvectors. These can be determined through using the following formula to obtain the significance of each eigenvector

$$\text{PercExpl} = \frac{h_i}{\sum_{j=1}^{n} h_i}, \tag{10.2.2}$$

where h_i represents the i'th eigenvalue and n represents the number of eigenvalues. The user can then construct a new matrix C through using the chosen eigenvectors and eigenvalues.

Note however the following important point. We are reducing the rank of the problem and hence the resulting matrix C will not have unit rows as required in Section A.5. As a result, we will have to apply a final scaling in order to preserve this property. This is easily achieved through using the following relationship

$$c_{ij}^{\text{new}} = \frac{c_{ij}^{\text{interm}}}{\sqrt{\sum_{j=1}^{n} \left(c_{ij}^{\text{interm}}\right)^2}}, \tag{10.2.3}$$

where the matrix C^{interm} represents the unscaled matrix consisting out of the chosen eigenvectors and values.

The main advantage of this approach is that we can easily obtain forward rate dynamics that are consistent with PCA and hence this approach has a very nice financial appeal. Furthermore, the calibration to volatilities and correlations are independently performed.

10.2.2 Rebonato's Approach

The algorithm described in the previous section lacks one property, i.e. the approach can result in correlation matrices that are different from the original input matrix. This can result in significant pricing implications. Rebonato [47] proposed a methodology in which the matrix C is chosen in such a way as to most accurately reflect the input correlation matrix.

The approach is based on the angular formulation presented in Section 6.4.2.1. Within this approach, we have that the matrix C should be defined as

$$c_{ik}(t) = \cos\theta_{ik}(t) \prod_{j=1}^{k-1} \sin\theta_{ij}(t), k = 1, \ldots, s-1, \tag{10.2.4}$$

$$c_{ik}(t) = \prod_{j=1}^{k-1} \sin\theta_{ij}(t), k = s. \tag{10.2.5}$$

Above parameterization will automatically ensure unit rows for the matrix C. Given this property, we will have a calibration routine that is only concerned with finding the set of angles that minimizes the differences between the model and input correlation matrices. Consequently, the procedure collapses into an unconstrained minimization problem. The associated penalty function is given by the following equation (Rebonato [47])

$$\chi^2 = \sum_{j,k=1}^{N} \left(\rho_{j,k}^{\text{input}} - \rho_{j,k}^{\text{model}}\right), \tag{10.2.6}$$

where N represents the number of forward rates. Following the calibration procedure it is then advisable to compare the principle components of the new matrix with that of the original matrix.

10.3 Calibrating to Swaption Prices and Exogenous Forward Rate Correlation Matrix

This section presents some of the calibration procedures that can be used in order to incorporate swaption prices in the LMM framework. In all of the procedures we will use an exogenously given correlation matrix. Brigo and Mercurio [11] also considered the alternative formulation, i.e. calibrating to swaption prices using the first separable structure presented in Section 5.4.5. This allowed for the calibration to swaption prices through solving for the optimal correlations as well as the time-to-maturity components of the volatility specification. The authors however obtained unsatisfactory results and instead recommended an approach where the volatility specification is more general and in which the correlations are exogenously given. This is in line with the comments made by Rebonato [47] regarding the insensitivity of swaption prices

to instantaneous correlations, as well as the possible lack of price congruence between the two different markets.

10.3.1 Cascade Calibration

Cascade Calibration was originally developed by Brigo and Mercurio [11], [10] and is designed to provide an exact calibration to swaption prices given the volatility specification in Table 5.1 and an exogenous correlation matrix. This approach is based on inverting Rebonato's swaption formula given in Equation (5.5.3). Adjusting this formula to incorporate the volatility structure presented in Table 5.1, we obtain

$$V^2_{\alpha,\beta} \approx \sum_{i,j=\alpha+1}^{\beta} \frac{w_i(0)w_j(0)L_i(0)L_j(0)\rho_{i,j}}{T_\alpha SR^2_{\alpha,\beta}(0)} \sum_{h=0}^{\alpha} \tau_{h-1,h}\sigma_{i,h+1}\sigma_{j,h+1}, \tag{10.3.1}$$

where

$$w_i(t) = \frac{\tau_{i-1,i}B(t,T_i)}{\sum_{i=s+1}^{N}\tau_{k-1,k}B(t,T_k)}. \tag{10.3.2}$$

Notice a slightly shortened notation and a change in weights. These changes were made in order to simplify upcoming equations as well as to align with the work of the developers.

We will start by considering the first version of this approach, i.e. the calibration to the upper triangle of the swaption input matrix. An example of such a matrix is presented in the table below (as previous, rows represent expiries whereas columns represent underlying maturities), with $T_0 = 1y$.

	$1y$	$2y$	$3y$	$4y$	$5y$	$6y$	$7y$
$1y$	$V_{0,1}$	$V_{0,2}$	$V_{0,3}$	$V_{0,4}$	$V_{0,5}$	$V_{0,6}$	$V_{0,7}$
$2y$	$V_{1,2}$	$V_{1,3}$	$V_{1,4}$	$V_{1,5}$	$V_{1,6}$	$V_{1,7}$	
$3y$	$V_{2,3}$	$V_{2,4}$	$V_{2,5}$	$V_{2,6}$	$V_{2,7}$		
$4y$	$V_{3,4}$	$V_{3,5}$	$V_{3,6}$	$V_{3,7}$			
$5y$	$V_{4,5}$	$V_{4,6}$	$V_{4,7}$				
$6y$	$V_{5,6}$	$V_{5,7}$					
$7y$	$V_{6,7}$						

Using Equation (10.3.1), we can now derive a one-to-one relationship between swaption volatilities given above and the associated forward rate volatilities presented in Table 5.1.

An important observation to make from the tables presented is that each swaption, as we move from left to right, is dependent on one (and only one) more forward rate. Hence, as we move from left to right in the swaption matrix,

it will be possible to invert Equation (10.3.1) in such a way as to obtain the volatility of the newly included forward rate. Similarly, as we move from top to bottom within the swaption matrix, we have a scenario where the swaption is dependent on one (and only one) more section of the instantaneous volatility function, i.e. one more column in the forward rate volatility matrix. Following each of these steps, it will be possible to solve for the missing instantaneous volatility using an elementary second order polynomial. Note, however, that the approach requires the user to firstly determine all the possible instantaneous volatilities for a given row (using left to right approach) before moving on to the next row (and then again proceeding from left to right as before). This can be seen more clearly through considering specific examples. The reader is referred to Brigo and Mercurio [11] for more details.

From the previous discussion, it is clear that the calibration algorithm will amount to solving $\sigma_{\beta,\alpha+1}$ at each step. This value can be explicitly obtained from Equation (10.3.1) as follows

$$
\begin{aligned}
&T_\alpha SR^2_{\alpha,\beta}(0)V^2_{\alpha,\beta} \approx \\
&\sum_{i,j=\alpha+1}^{\beta} w_i(0)w_j(0)L_i(0)L_j(0)\rho_{i,j}\sum_{h=0}^{\alpha}\tau_{h-1,h}\sigma_{i,h+1}\sigma_{j,h+1} \\
&= \sum_{i,j=\alpha+1}^{\beta-1} w_i(0)w_j(0)L_i(0)L_j(0)\rho_{i,j}\sum_{h=0}^{\alpha}\tau_{h-1,h}\sigma_{i,h+1}\sigma_{j,h+1} \\
&+ w_\beta(0)^2L_\beta(0)^2\sum_{h=0}^{\alpha}\tau_{h-1,h}\sigma^2_{\beta,h+1} \\
&+ 2\sum_{j=\alpha+1}^{\beta-1} w_\beta(0)w_j(0)L_\beta(0)L_j(0)\rho_{\beta,j}\sum_{h=0}^{\alpha}\tau_{h-1,h}\sigma_{\beta,h+1}\sigma_{j,h+1} \\
&= \sum_{i,j=\alpha+1}^{\beta-1} w_i(0)w_j(0)L_i(0)L_j(0)\rho_{i,j}\sum_{h=0}^{\alpha}\tau_{h-1,h}\sigma_{i,h+1}\sigma_{j,h+1} \\
&+ 2\sum_{j=\alpha+1}^{\beta-1} w_\beta(0)w_j(0)L_\beta(0)L_j(0)\rho_{\beta,j}\sum_{h=0}^{\alpha-1}\tau_{h-1,h}\sigma_{\beta,h+1}\sigma_{j,h+1} \\
&+ 2\sum_{j=\alpha+1}^{\beta-1} w_\beta(0)w_j(0)L_\beta(0)L_j(0)\rho_{\beta,j}\tau_{\alpha-1,\alpha}\sigma_{j,\alpha+1}\sigma_{\beta,\alpha+1} \\
&+ w_\beta(0)^2L_\beta(0)^2\sum_{h=0}^{\alpha-1}\tau_{h-1,h}\sigma^2_{\beta,h+1} \\
&+ w_\beta(0)^2L_\beta(0)^2\tau_{\alpha-1,\alpha}\sigma^2_{\beta,\alpha+1}.
\end{aligned}
$$

Notice that the last and third last expressions are the only ones containing the variable $\sigma_{\beta,\alpha+1}$. These can consequently be grouped into the following simple quadratic equation

$$A_{\alpha,\beta}\sigma_{\beta,\alpha+1}^2 + B_{\alpha,\beta}\sigma_{\beta,\alpha+1} + C_{\alpha,\beta} = 0, \tag{10.3.3}$$

where the coefficients of the quadratic equation are defined as below

$$\begin{aligned}
A_{\alpha,\beta} &= w_\beta(0)^2 L_\beta(0)^2 \tau_{\alpha-1,\alpha}, \\
B_{\alpha,\beta} &= 2\sum_{j=\alpha+1}^{\beta-1} w_\beta(0) w_j(0) L_\beta(0) L_j(0) \rho_{\beta,j} \tau_{\alpha-1,\alpha} \sigma_{j,\alpha+1}, \\
C_{\alpha,\beta} &= \sum_{i,j=\alpha+1}^{\beta-1} w_i(0) w_j(0) L_i(0) L_j(0) \rho_{i,j} \sum_{h=0}^{\alpha} \tau_{h-1,h} \sigma_{i,h+1} \sigma_{j,h+1} \\
&+ 2\sum_{j=\alpha+1}^{\beta-1} w_\beta(0) w_j(0) L_\beta(0) L_j(0) \rho_{\beta,j} \sum_{h=0}^{\alpha-1} \tau_{h-1,h} \sigma_{\beta,h+1} \sigma_{j,h+1} \\
&+ w_\beta(0)^2 L_\beta(0)^2 \sum_{h=0}^{\alpha-1} \tau_{h-1,h} \sigma_{\beta,h+1}^2 \\
&- T_\alpha S R_{\alpha,\beta}^2(0) V_{\alpha,\beta}^2.
\end{aligned}$$

This concludes the first part of this section. Brigo and Mercurio [11] summarized this approach in the following algorithm.

Algorithm 10.3.1 ***(Cascade Calibration Algorithm (CCA) - Brigo and Mercurio [11])*** *The calibration to the upper triangle of a swaption matrix can be achieved through the steps described below.*

1. *Select the number s of rows in the swaption matrix that are of interest for the calibration*
2. *Set $\alpha = 0$*
3. *Set $\beta = \alpha + 1$*
4. *Solve Equation (10.3.3) in $\sigma_{\beta,\alpha+1}$. Since both $A_{\alpha,\beta}$ and $B_{\alpha,\beta}$ are strictly positive, if we assume positive instantaneous correlations, then Equation (10.3.3) has at most one positive solution, namely*

$$\sigma_{\beta,\alpha+1} = \frac{-B_{\alpha,\beta} + \sqrt{B_{\alpha,\beta}^2 - 4A_{\alpha,\beta}C_{\alpha,\beta}}}{2A_{\alpha,\beta}}$$

if and only if $C_{\alpha,\beta} < 0$.

5. *Increase β by one. If $\beta \leq s$, then go back to point 4, otherwise increase α by one.*

6. *If $\alpha < s$ go back to 3, otherwise stop.*

The algorithm just presented can only be used to calibrate to the upper triangle of the swaption matrix. As a result, we will only be able to obtain the upper half of the forward rate volatilities displayed in Table 5.1. In order to illustrate the concept, we will present, as an example, the forward rate volatilities that can be determined through Algorithm 10.3.1 when applied to the example 7×7 swaption matrix given earlier in this section. This is given in the table below.

	$(0,1y]$	$(1y,2y]$	$(2y,3y]$	$(3y,4y]$	$(4y,5y]$	$(5y,6y]$	$(6y,7y]$
$L_1(t)$	$\sigma_{1,1}$	Dead	Dead	Dead	Dead	Dead	Dead
$L_2(t)$	$\sigma_{2,1}$	$\sigma_{2,2}$	Dead	Dead	Dead	Dead	Dead
$L_3(t)$	$\sigma_{3,1}$	$\sigma_{3,2}$	$\sigma_{3,3}$	Dead	Dead	Dead	Dead
$L_4(t)$	$\sigma_{4,1}$	$\sigma_{4,2}$	$\sigma_{4,3}$	$\sigma_{4,4}$	Dead	Dead	Dead
$L_5(t)$	$\sigma_{5,1}$	$\sigma_{5,2}$	$\sigma_{5,3}$	$\sigma_{5,4}$	$\sigma_{5,5}$	Dead	Dead
$L_6(t)$	$\sigma_{6,1}$	$\sigma_{6,2}$	$\sigma_{6,3}$	$\sigma_{6,4}$	$\sigma_{6,5}$	$\sigma_{6,6}$	Dead
$L_7(t)$	$\sigma_{7,1}$	$\sigma_{7,2}$	$\sigma_{7,3}$	$\sigma_{7,4}$	$\sigma_{7,5}$	$\sigma_{7,6}$	$\sigma_{7,7}$

Brigo and Morini [12] and Morini [40] did however propose an extension of this technique that can be used to calibrate to the remainder of the swaption volatilities, i.e. those presented in bold in the matrix below

	$1y$	$2y$	$3y$	$4y$	$5y$	$6y$	$7y$
$1y$	$V_{0,1}$	$V_{0,2}$	$V_{0,3}$	$V_{0,4}$	$V_{0,5}$	$V_{0,6}$	$V_{0,7}$
$2y$	$V_{1,2}$	$V_{1,3}$	$V_{1,4}$	$V_{1,5}$	$V_{1,6}$	$V_{1,7}$	$\mathbf{V_{1,8}}$
$3y$	$V_{2,3}$	$V_{2,4}$	$V_{2,5}$	$V_{2,6}$	$V_{2,7}$	$\mathbf{V_{2,8}}$	$\mathbf{V_{2,9}}$
$4y$	$V_{3,4}$	$V_{3,5}$	$V_{3,6}$	$V_{3,7}$	$\mathbf{V_{3,8}}$	$\mathbf{V_{3,9}}$	$\mathbf{V_{3,10}}$
$5y$	$V_{4,5}$	$V_{4,6}$	$V_{4,7}$	$\mathbf{V_{4,8}}$	$\mathbf{V_{4,9}}$	$\mathbf{V_{4,10}}$	$\mathbf{V_{4,11}}$
$6y$	$V_{5,6}$	$V_{5,7}$	$\mathbf{V_{5,8}}$	$\mathbf{V_{5,9}}$	$\mathbf{V_{5,10}}$	$\mathbf{V_{5,11}}$	$\mathbf{V_{5,12}}$
$7y$	$V_{6,7}$	$\mathbf{V_{6,8}}$	$\mathbf{V_{6,9}}$	$\mathbf{V_{6,10}}$	$\mathbf{V_{6,11}}$	$\mathbf{V_{6,12}}$	$\mathbf{V_{6,13}}$

This will then also enable us to determine the remainder of the forward rate volatilities and hence complete the calibration. Extending this approach to the rest of the matrix is however not an automatic process. Multiple unknowns are encountered every time the last column of the swaption matrix is reached (with exception of the first). As a result, they suggested setting all the unknowns in these scenarios equal to the same value which will then allow us to determine the volatilities presented in bold in the matrix below.

	$(0,1y]$	$(1y,2y]$	$(2y,3y]$	$(3y,4y]$	$(4y,5y]$	$(5y,6y]$	$(6y,7y]$
$L_1(t)$	$\sigma_{1,1}$	Dead	Dead	Dead	Dead	Dead	Dead
$L_2(t)$	$\sigma_{2,1}$	$\sigma_{2,2}$	Dead	Dead	Dead	Dead	Dead
$L_3(t)$	$\sigma_{3,1}$	$\sigma_{3,2}$	$\sigma_{3,3}$	Dead	Dead	Dead	Dead
$L_4(t)$	$\sigma_{4,1}$	$\sigma_{4,2}$	$\sigma_{4,3}$	$\sigma_{4,4}$	Dead	Dead	Dead
$L_5(t)$	$\sigma_{5,1}$	$\sigma_{5,2}$	$\sigma_{5,3}$	$\sigma_{5,4}$	$\sigma_{5,5}$	Dead	Dead
$L_6(t)$	$\sigma_{6,1}$	$\sigma_{6,2}$	$\sigma_{6,3}$	$\sigma_{6,4}$	$\sigma_{6,5}$	$\sigma_{6,6}$	Dead
$L_7(t)$	$\sigma_{7,1}$	$\sigma_{7,2}$	$\sigma_{7,3}$	$\sigma_{7,4}$	$\sigma_{7,5}$	$\sigma_{7,6}$	$\sigma_{7,7}$
$L_8(t)$	$\sigma_{\mathbf{8,1}}$	$\sigma_{\mathbf{8,2}}$	$\sigma_{\mathbf{8,3}}$	$\sigma_{\mathbf{8,4}}$	$\sigma_{\mathbf{8,5}}$	$\sigma_{\mathbf{8,6}}$	$\sigma_{\mathbf{8,7}}$
$L_9(t)$	$\sigma_{\mathbf{9,1}}$	$\sigma_{\mathbf{9,2}}$	$\sigma_{\mathbf{9,3}}$	$\sigma_{\mathbf{9,4}}$	$\sigma_{\mathbf{9,5}}$	$\sigma_{\mathbf{9,6}}$	$\sigma_{\mathbf{9,7}}$
$L_{10}(t)$	$\sigma_{\mathbf{10,1}}$	$\sigma_{\mathbf{10,2}}$	$\sigma_{\mathbf{10,3}}$	$\sigma_{\mathbf{10,4}}$	$\sigma_{\mathbf{10,5}}$	$\sigma_{\mathbf{10,6}}$	$\sigma_{\mathbf{10,7}}$
$L_{11}(t)$	$\sigma_{\mathbf{11,1}}$	$\sigma_{\mathbf{11,2}}$	$\sigma_{\mathbf{11,3}}$	$\sigma_{\mathbf{11,4}}$	$\sigma_{\mathbf{11,5}}$	$\sigma_{\mathbf{11,6}}$	$\sigma_{\mathbf{11,7}}$
$L_{12}(t)$	$\sigma_{\mathbf{12,1}}$	$\sigma_{\mathbf{12,2}}$	$\sigma_{\mathbf{12,3}}$	$\sigma_{\mathbf{12,4}}$	$\sigma_{\mathbf{12,5}}$	$\sigma_{\mathbf{12,6}}$	$\sigma_{\mathbf{12,7}}$
$L_{13}(t)$	$\sigma_{\mathbf{13,1}}$	$\sigma_{\mathbf{13,2}}$	$\sigma_{\mathbf{13,3}}$	$\sigma_{\mathbf{13,4}}$	$\sigma_{\mathbf{13,5}}$	$\sigma_{\mathbf{13,6}}$	$\sigma_{\mathbf{13,7}}$

This technique was labeled by the authors as the "equal multiple unknowns" assumption. The assumption can easily be incorporated into the previously derived results and can be expressed mathematically as

$$\sigma_{\beta,\alpha+1} = \sigma_{\beta,\alpha} = \ldots = \sigma_{\beta,1} \; for \; \beta = s + \alpha.$$

From the above equation, we can derive the following expression for $\sigma_{\beta,\alpha+1}$ in the case where $\beta = s + \alpha$

$$\begin{aligned}
&T_\alpha SR^2_{\alpha,\beta}(0)V^2_{\alpha,\beta} \approx \\
&= \sum_{i,j=\alpha+1}^{\beta-1} w_i(0)w_j(0)L_i(0)L_j(0)\rho_{i,j}\sum_{h=0}^{\alpha}\tau_{h-1,h}\sigma_{i,h+1}\sigma_{j,h+1} \\
&+ 2\sum_{j=\alpha+1}^{\beta-1} w_\beta(0)w_j(0)L_\beta(0)L_j(0)\rho_{\beta,j}\sum_{h=0}^{\alpha-1}\tau_{h-1,h}\sigma_{j,h+1}\sigma_{\beta,\alpha+1} \\
&+ 2\sum_{j=\alpha+1}^{\beta-1} w_\beta(0)w_j(0)L_\beta(0)L_j(0)\rho_{\beta,j}\tau_{\alpha-1,\alpha}\sigma_{j,\alpha+1}\sigma_{\beta,\alpha+1} \\
&+ w_\beta(0)^2L_\beta(0)^2\sum_{h=0}^{\alpha-1}\tau_{h-1,h}\sigma^2_{\beta,\alpha+1} \\
&+ w_\beta(0)^2L_\beta(0)^2\tau_{\alpha-1,\alpha}\sigma^2_{\beta,\alpha+1}.
\end{aligned}$$

Above expressions can then be grouped into the following quadratic equation

$$A^*_{\alpha,\beta}\sigma^2_{\beta,\alpha+1} + B^*_{\alpha,\beta}\sigma_{\beta,\alpha+1} + C^*_{\alpha,\beta} = 0, \tag{10.3.4}$$

where the coefficients of the quadratic equation are defined as below

$$\begin{aligned}
A^*_{\alpha,\beta} &= w_\beta(0)^2 L_\beta(0)^2 \tau_{\alpha-1,\alpha} + w_\beta(0)^2 L_\beta(0)^2 \sum_{h=0}^{\alpha-1} \tau_{h-1,h}, \\
B^*_{\alpha,\beta} &= 2 \sum_{j=\alpha+1}^{\beta-1} w_\beta(0) w_j(0) L_\beta(0) L_j(0) \rho_{\beta,j} \tau_{\alpha-1,\alpha} \sigma_{j,\alpha+1} \\
&+ 2 \sum_{j=\alpha+1}^{\beta-1} w_\beta(0) w_j(0) L_\beta(0) L_j(0) \rho_{\beta,j} \sum_{h=0}^{\alpha-1} \tau_{h-1,h} \sigma_{j,h+1}, \\
C^*_{\alpha,\beta} &= \sum_{i,j=\alpha+1}^{\beta-1} w_i(0) w_j(0) L_i(0) L_j(0) \rho_{i,j} \sum_{h=0}^{\alpha} \tau_{h-1,h} \sigma_{i,h+1} \sigma_{j,h+1} \\
&- T_\alpha SR^2_{\alpha,\beta}(0) V^2_{\alpha,\beta}.
\end{aligned}$$

This concludes the second part of this section. Brigo and Mercurio [11] summarized this approach in the following algorithm.

Algorithm 10.3.2 ***(Rectangular Cascade Calibration Algorithm (RCCA) - Brigo and Mercurio [11])*** *The calibration to the entire swaption matrix can be achieved through extending Algorithm 10.3.1 using the two steps presented below.*

1. *At point* 5 *replace the condition* $\beta \leq s$ *with* $(\beta - \alpha) \leq s$.
2. *Point* 4 *should be changed to reference Equation (10.3.4) every time the last column of the swaption matrix is reached (with exception of the first), i.e. when* $\beta = s + \alpha$

The rest of the algorithm remains unchanged.

The algorithms introduced in this section provided us with tools that can be used to recover market swaption prices exactly given an exogenous correlation matrix. Unfortunately, given its non-parametric and unconstrained principles, it is clear that the instantaneous volatilities are expected to take up the slack in order to obtain correct swaption pricing. Brigo and Mercurio [11] mentioned that this can lead to negative or even imaginary values for the calibrated instantaneous volatilities. The authors contributed these errors to irregularity and illiquidity in the input swaption matrix. It was found that these can be eliminated through the use of suitable data manipulating techniques (whether smoothing, interpolating missing entries or rank reduction etc.). However, these manipulations can be problem specific and hence does not provide a robust solution that can be used across different types of market

inputs. Furthermore, these types of adjustments will go against the main principle underlying these methods, i.e. the exact pricing to market swaption prices given an exogenous correlation matrix. As a result, Brigo and Morini [13] and Morini [41] developed a robust extension of the previous algorithms which is solely dependent on the input market data and does not require any data manipulation (at least in most of the cases). This method will be considered in the last part of this section.

The new proposed methodology makes use of endogenous interpolation based only on pure market data. This allows the calibration to swaption matrices that may contain missing rows, for example the swaption matrix presented for the South African market in Table 8.5. In order to achieve this the algorithm firstly make assumptions regarding volatilities that are entirely undetermined due to the missing swaptions data, i.e. volatilities that are not contained in any of the preceding or following market observable swaptions. Typical assumptions made are those presented in Tables 5.2-5.3, i.e. dependence on either time-to-maturity or maturity of the forward rate under consideration. Following this assumption, the usual "equal multiple unknowns" assumption is employed when moving to the next observable swaption price.

The concepts described above will be illustrated through the use of some examples. Let us revisit the upper triangle swaption matrix presented earlier in this section. Using Equation (10.3.3), we can obtain the following dependence structure for the first three swaptions in the matrix (format similar to that given by Brigo and Mercurio [11])

	$1y$	$2y$	$3y$	$4y$
$1y$	$V_{0,1}$ $\sigma_{1,1}$	$V_{0,2}$ $\sigma_{1,1}\sigma_{2,1}$	$V_{0,3}$ $\sigma_{1,1}\sigma_{2,1}\sigma_{3,1}$	$V_{0,4}$ $\sigma_{1,1}\sigma_{2,1}\sigma_{3,1}\sigma_{4,1}$
$2y$	$V_{1,2}$ $\sigma_{2,1}$ $\sigma_{2,2}$	$V_{1,3}$ $\sigma_{2,1}\sigma_{3,1}$ $\sigma_{2,2}\sigma_{3,2}$	$V_{1,4}$ $\sigma_{2,1}\sigma_{3,1}\sigma_{4,1}$ $\sigma_{2,2}\sigma_{3,2}\sigma_{4,2}$	
$3y$	$V_{2,3}$ $\sigma_{3,1}$ $\sigma_{3,2}$ $\sigma_{3,3}$	$V_{2,4}$ $\sigma_{3,1}\sigma_{4,1}$ $\sigma_{3,2}\sigma_{4,2}$ $\sigma_{3,3}\sigma_{4,3}$		
$4y$	$V_{3,4}$ $\sigma_{4,1}$ $\sigma_{4,2}$ $\sigma_{4,3}$ $\sigma_{4,4}$			

Note the following from above matrix. If the swaption quotations relating to row 2 were missing, then we would be faced with the scenario that the

entry $\sigma_{2,2}$ does not appear in any rows preceding or following the second one. Hence, only row 2 can be used to determine this entry. This then forces the assumption relating to time-to-maturity or maturity of the associated forward. All of the other unknowns in row 2 does appear in the following row and hence can be determined using the "equal multiple unknowns" assumption.

This concludes the final part of this section. Brigo and Mercurio [11] summarized this approach in the following algorithm.

Algorithm 10.3.3 ***(Rectangular Cascade Calibration with Endogenous Interpolation Algorithm (RCCAEI) - Brigo and Mercurio [11])*** *With reference to Equations (10.3.3) and (10.3.4), we must follow the steps:*

1. *Select the number s of rows in the swaption matrix that are of interest for the calibration, including those non quoted. The final row must be available from the market. Then define K as the set of missing maturities.*

2. *Set $\alpha = 0$;*

3. a) *If $a \in K$, define m as the first market quoted maturity higher than α. Then set*

$$\sigma_{j,m+1} = \sigma_{j,m} = \cdots = \sigma_{j,\alpha+1} =: \sigma_j \text{ for all } j\text{: } m+1 \leq j < s+\alpha, \tag{10.3.5}$$

   that is we assume that all the involved forward rates have constant volatility in the period. Set $\gamma = \alpha$ and then $\alpha = m$.

   b) *If $\alpha \notin K$, set $\gamma = \alpha$.*

   Set $\beta = \alpha + 1$

4. a) *If $\gamma \in K$, solve in σ_β Equation (10.3.3) after adjusting to take into account Constraint (10.3.5).*

   b) *If $\gamma \notin K$, solve in $\sigma_{\beta,\alpha+1}$ Equation (10.3.3).*

5. *Increase β by 1. If $\beta < s + \gamma$ go back to point 4. If $s + \gamma \leq \beta \leq s + \alpha$, set*

$$\sigma_{\beta,\alpha+1} = \sigma_{\beta,\alpha} = \cdots = \sigma_{\beta,1}$$

   and solve in $\sigma_{\beta,\alpha+1}$ Equation (10.3.4). Increase α by 1.

6. *If $\alpha < s$, go back to point 3, otherwise stop.*

10.4 European Market Results

This section will only consider the application of the cascade calibration algorithms to the set of European data as given by Brigo and Mercurio [11]. The

aim is to highlight some of their results and to illustrate that the implemented algorithms provide answers consistent with that of the authors. Furthermore, it will provide useful insight into the dependence of these algorithms on the granularity of the input volatilities.

10.4.1 Market Data

Let us firstly consider the data as given by the authors. The initial forward curve is given by

Reset	Rate
0	0.046900
1y	0.050114
2y	0.055973
3y	0.058387
4y	0.060027
5y	0.061315
6y	0.062779
7y	0.062747
8y	0.062926
9y	0.062286
10y	0.063009
11y	0.063554
12y	0.064257
13y	0.064784
14y	0.065312
15y	0.063976
16y	0.062997
17y	0.06184
18y	0.060682
19y	0.05936

Table 10.1: Forward rates obtained from the European market for business date 2000/05/16 (Brigo and Mercurio [11]).

This set of forwards includes the spot rate, i.e. the rate reset occurs today. This is necessary for the calculation of discount factors used in the cascade calibration algorithm. The procedures required to obtain such a curve were described in detail in previous chapters.

Next, we will introduce the set of swaption prices. These are presented in the table below.

The authors mentioned that they could not obtain quotations for swaption maturities of $6, 8$ and 9 years, and hence replaced these with linear interpolation (expressed in bold, necessary for the first two cascade calibration algorithms).

The final set of data that we need in order to implement the cascade calibration algorithms, is the exogenous correlation matrix. These were defined in

	1y	2y	3y	4y	5y	6y	7y	8y	9y	10y
1y	0.1800	0.1670	0.1540	0.1450	0.1380	0.1340	0.1300	0.1260	0.1240	0.1220
2y	0.1810	0.1620	0.1450	0.1350	0.1270	0.1230	0.1200	0.1170	0.1150	0.1130
3y	0.1780	0.1550	0.1370	0.1250	0.1170	0.1140	0.1110	0.1080	0.1060	0.1040
4y	0.1670	0.1430	0.1260	0.1150	0.1080	0.1050	0.1030	0.1000	0.0980	0.0960
5y	0.1540	0.1320	0.1180	0.1090	0.1040	0.1040	0.0990	0.0960	0.0940	0.0920
6y	**0.1470**	**0.1265**	**0.1125**	**0.1035**	**0.0980**	**0.0975**	**0.0940**	**0.0915**	**0.0900**	**0.0885**
7y	0.1400	0.1210	0.1070	0.0980	0.0920	0.0910	0.0890	0.0870	0.0860	0.0850
8y	**0.1367**	**0.1173**	**0.1033**	**0.0947**	**0.0890**	**0.0880**	**0.0860**	**0.0843**	**0.0833**	**0.0823**
9y	**0.1333**	**0.1137**	**0.0997**	**0.0913**	**0.0860**	**0.0850**	**0.0830**	**0.0817**	**0.0807**	**0.0797**
10y	0.1300	0.1100	0.0960	0.0880	0.0830	0.0820	0.0800	0.0790	0.0780	0.0770

Table 10.2: ATM swaption volatilities obtained from the European market for business date 2000/05/16 (Brigo and Mercurio [11]).

terms of a Rebonato rank-two correlation structure, with corresponding angles given by

Reset	Angle
1y	0.0147
2y	0.0643
3y	0.1032
4y	0.1502
5y	0.1969
6y	0.2239
7y	0.2771
8y	0.2950
9y	0.3630
10y	0.3810
11y	0.4217
12y	0.4836
13y	0.5204
14y	0.5418
15y	0.5791
16y	0.6496
17y	0.6679
18y	0.7126
19y	0.7659

Table 10.3: Angles associated with a Rebonato rank-two correlation structure. Results presented for business date 2000/05/16 (Brigo and Mercurio [11]).

10.4.2 Cascade Calibration

We will now move on to briefly consider some of the results when implementing the algorithms presented in Section 10.3.1. The first set of results that we will consider is that obtained through applying Algorithm 10.3.1, i.e. the calibration to the upper half of the swaption volatilities presented in the previous section.

The volatilities obtained from implementing this algorithm were found to be exactly the same as those given by Brigo and Mercurio [11] when replacing the missing swaption volatilities with manually interpolated values (as opposed to the rounded values given in the work by the authors). The resultant forward rate volatilities are presented in the table below.

0.1800	-	-	-	-	-	-	-	-	-
0.1548	0.2039	-	-	-	-	-	-	-	-
0.1285	0.1559	0.2329	-	-	-	-	-	-	-
0.1178	0.1042	0.1656	0.2437	-	-	-	-	-	-
0.1091	0.0988	0.0973	0.1606	0.2483	-	-	-	-	-
0.1131	0.0734	0.0781	0.1009	0.1618	0.2627	-	-	-	-
0.1040	0.0984	0.0502	0.0737	0.1128	0.1633	0.2633	-	-	-
0.0940	0.1052	0.0938	0.0319	0.0864	0.0969	0.1684	0.2731	-	-
0.1065	0.0790	0.0857	0.0822	0.0684	0.0536	0.0921	0.1763	0.2848	-
0.1013	0.0916	0.0579	0.1030	0.1514	-0.0316	0.0389	0.0845	0.1634	0.2777

Table 10.4: Forward rate volatilities obtained through applying the CCA technique to the European market data presented in this section. Results obtained for business date 2000/05/16.

Extending the calculations to the rest of the swaption matrix we can obtain the remainder of the forward rate volatilities. This can be achieved through making use of Algorithm 10.3.2. The results of such an implementation is presented in the table below.

0.1800	-	-	-	-	-	-	-	-	-
0.1548	0.2039	-	-	-	-	-	-	-	-
0.1285	0.1559	0.2329	-	-	-	-	-	-	-
0.1178	0.1042	0.1656	0.2437	-	-	-	-	-	-
0.1091	0.0988	0.0973	0.1606	0.2483	-	-	-	-	-
0.1131	0.0734	0.0781	0.1009	0.1618	0.2627	-	-	-	-
0.1040	0.0984	0.0502	0.0737	0.1128	0.1633	0.2633	-	-	-
0.0940	0.1052	0.0938	0.0319	0.0864	0.0969	0.1684	0.2731	-	-
0.1065	0.0790	0.0857	0.0822	0.0684	0.0536	0.0921	0.1763	0.2848	-
0.1013	0.0916	0.0579	0.1030	0.1514	-0.0316	0.0389	0.0845	0.1634	0.2777
0.0916	0.0916	0.0787	0.0431	0.0299	0.2088	-0.0383	0.0746	0.0948	0.1854
0.0827	0.0827	0.0827	0.0709	0.0488	0.0624	0.1561	-0.0103	0.0731	0.0911
0.0744	0.0744	0.0744	0.0744	0.0801	0.0576	0.0941	0.1231	-0.0159	0.0610
0.0704	0.0704	0.0704	0.0704	0.0704	0.1009	0.0507	0.0817	0.1203	-0.0210
0.0725	0.0725	0.0725	0.0725	0.0725	0.0725	0.1002	0.0432	0.0619	0.1179
0.0753	0.0753	0.0753	0.0753	0.0753	0.0753	0.0753	0.0736	0.0551	0.0329
0.0719	0.0719	0.0719	0.0719	0.0719	0.0719	0.0719	0.0719	0.0708	0.0702
0.0690	0.0690	0.0690	0.0690	0.0690	0.0690	0.0690	0.0690	0.0690	0.0680
0.0663	0.0663	0.0663	0.0663	0.0663	0.0663	0.0663	0.0663	0.0663	0.0663

Table 10.5: Forward rate volatilities obtained through applying the RCCA technique to the European market data presented in this section. Results obtained for business date 2000/05/16.

Note the negative entries in the above given tables. Brigo and Mercurio [11] mentioned that these negative values can be removed through using different input correlation structures or different methods of interpolating missing swaption volatilities. Irrespectively, it was mentioned that these type of solutions can be problem specific and hence does not provide a robust solution that can be used across different types of market inputs. Consequently, we will rather focus our attention in the remainder of the section on the more robust methodology given by algorithm 10.3.3. The results obtained, following the implementation of this algorithm, is presented in the table below.

0.1800	-	-	-	-	-	-	-	-	-
0.1548	0.2039	-	-	-	-	-	-	-	-
0.1285	0.1559	0.2329	-	-	-	-	-	-	-
0.1178	0.1042	0.1656	0.2437	-	-	-	-	-	-
0.1091	0.0988	0.0973	0.1606	0.2483	-	-	-	-	-
0.1131	0.0734	0.0781	0.1009	0.1618	0.2483	-	-	-	-
0.1040	0.0984	0.0502	0.0737	0.1128	0.2191	0.2191	-	-	-
0.0940	0.1052	0.0938	0.0319	0.0864	0.1373	0.1373	0.2191	-	-
0.1065	0.0790	0.0857	0.0822	0.0684	0.0754	0.0754	0.1373	0.2191	-
0.1013	0.0916	0.0579	0.1030	0.1514	0.0132	0.0132	0.1942	0.1942	0.1942
0.0916	0.0916	0.0787	0.0431	0.0299	0.0610	0.0610	0.1351	0.1351	0.1351
0.0827	0.0827	0.0827	0.0709	0.0488	0.1132	0.1132	0.0577	0.0577	0.0577
0.0744	0.0744	0.0744	0.0744	0.0801	0.0775	0.0775	0.0451	0.0451	0.0451
0.0704	0.0704	0.0704	0.0704	0.0704	0.0725	0.0725	0.0454	0.0454	0.0454
0.0774	0.0774	0.0774	0.0774	0.0774	0.0774	0.0774	0.0771	0.0771	0.0771
0.0752	0.0752	0.0752	0.0752	0.0752	0.0752	0.0752	0.0492	0.0492	0.0492
0.0711	0.0711	0.0711	0.0711	0.0711	0.0711	0.0711	0.0711	0.0711	0.0711
0.0685	0.0685	0.0685	0.0685	0.0685	0.0685	0.0685	0.0685	0.0685	0.0685
0.0660	0.0660	0.0660	0.0660	0.0660	0.0660	0.0660	0.0660	0.0660	0.0660

Table 10.6: Forward rate volatilities obtained through applying the RCCAEI technique to the European market data presented in this section. Results obtained for business date 2000/05/16.

This calibration algorithm resulted in only real and positive volatilities, illustrating the effectiveness of the approach. This is however not the only criteria that should be used in evaluating the accuracy of the approach. We will, similar to Brigo and Mercurio [11], consider the evolution of the term structure of volatilities, model implied caplet volatilities relative to market observable caplet volatilities and model implied swaption volatilities.

The evolution of the term structure of volatilities is presented in Figure 10.1 below. Please note that the lines showing the drop from the last volatility to the start of the $y-$axis can be ignored. The program used for plotting this figure unfortunately did not allow for the exclusion of these points. Irrespective of this, we can still get a good idea of the evolution of the term structure of volatilities as implied by the empirically efficient cascade calibration algorithm.

This evolution depicted in the figure is the same as the results displayed by Brigo and Mercurio [11].

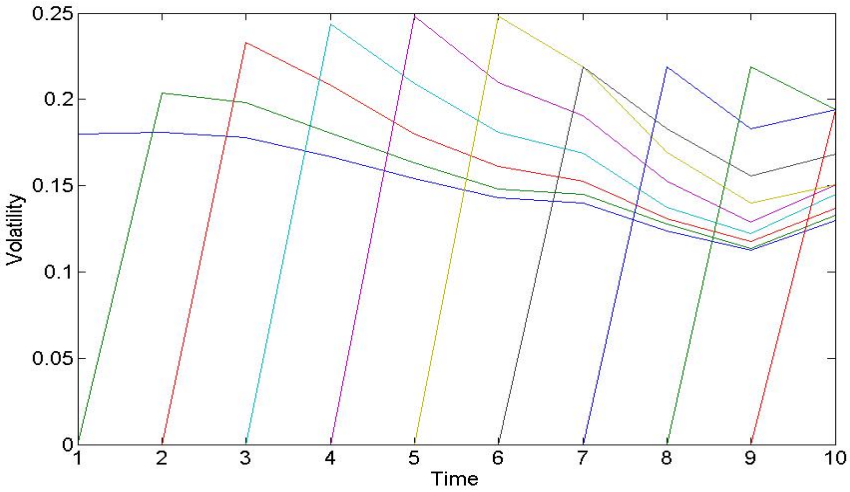

Figure 10.1: Term structure evolution as implied by the RCCAEI technique. Results presented for the European market and were obtained through calibrating to the market term structure of 2000/05/16.

The figure shows an initial slightly humped term structure. This then changes to a more inverted shape as we move through time (Brigo and Mercurio [11] pointed out that this can be due to the first column of the swaption matrix displaying volatilities that are higher than the rest). Also, note that the volatilities in the short end are expected to increase to just below 25%, which is considerably higher than the implied term structure at time zero.

Another fact to point out is that this evolution can be expected to be sensitive to the input correlation matrix. The authors, for example, showed that the evolution can be expected to be more smooth and well behaved when correlation structures of lower rank are used. Furthermore, alternative endogenous interpolation techniques might be used to try and improve the results.

The next figure that we will consider, is a graph depicting the market observable caplet structure on 16 May 2000 against the model implied caplet structure. This is presented in the Figure 10.2 below.

From Figure 10.2, it is evident that the cascade calibration algorithm implies lower caplet prices than the market (with some noise in the long end, would prefer this to be smoother for pricing and hedging purposes). This will change with different input correlations. This observation is also in line with findings by Rebonato [47] and points to the fact that the two markets might not be in line. Hence, it is very dangerous to implement calibration strate-

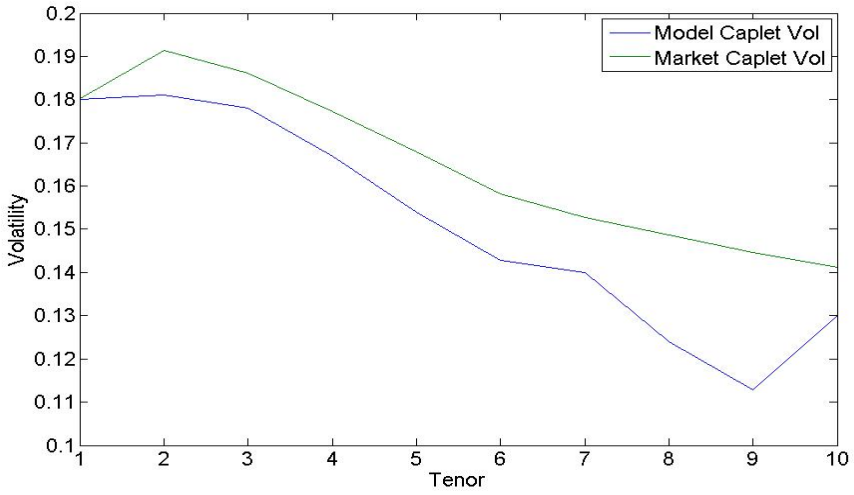

Figure 10.2: Term structure of volatilities as implied by the RCCAEI technique. Results presented for the European market and were obtained through calibrating to the market term structure as observed on 2000/05/16.

gies in which we assume a perfect congruence between caplet and swaption markets. Hence, the exclusion of such techniques from this thesis.

As a final result, we will present the model implied swaption prices for the missing rows of the input swaption matrix. These are expressed in bold in the matrix below.

	1y	2y	3y	4y	5y	6y	7y	8y	9y	10y
1y	0.1800	0.1670	0.1540	0.1450	0.1380	0.1340	0.1300	0.1260	0.1240	0.1220
2y	0.1810	0.1620	0.1450	0.1350	0.1270	0.1230	0.1200	0.1170	0.1150	0.1130
3y	0.1780	0.1550	0.1370	0.1250	0.1170	0.1140	0.1110	0.1080	0.1060	0.1040
4y	0.1670	0.1430	0.1260	0.1150	0.1080	0.1050	0.1030	0.1000	0.0980	0.0960
5y	0.1540	0.1320	0.1180	0.1090	0.1040	0.1040	0.0990	0.0960	0.0940	0.0920
6y	**0.1428**	**0.1322**	**0.1197**	**0.1099**	**0.1042**	**0.0983**	**0.0960**	**0.0937**	**0.0914**	**0.0902**
7y	0.1400	0.1210	0.1070	0.0980	0.0920	0.0910	0.0890	0.0870	0.0860	0.0850
8y	**0.1240**	**0.1067**	**0.1037**	**0.0978**	**0.0937**	**0.0898**	**0.0867**	**0.0855**	**0.0841**	**0.0829**
9y	**0.1128**	**0.1144**	**0.1050**	**0.0965**	**0.0904**	**0.0862**	**0.0849**	**0.0830**	**0.0818**	**0.0807**
10y	0.1300	0.1100	0.0960	0.0880	0.0830	0.0820	0.0800	0.0790	0.0780	0.0770

Table 10.7: ATM swaption volatilities implied by the RCCAEI approach for the missing rows of Table 10.2. Results presented for business date 2000/05/16.

These can then be presented to the trader for further validation. Brigo and Mercurio [11] mentioned that these volatilities displayed most of the required properties. Notice, however, some noise in the first two columns. This is driven by the forward rate volatilities determined outside of the model.

The Matlab code used in obtaining these results is presented in Section C.2.1.1.

10.5 South African Market Results

Applying the calibration techniques discussed in this chapter to the South African market is slightly more complicated than the algorithms presented for volatility calibration. This section will examine and discuss some of these complexities.

10.5.1 Correlation Smoothing

Before we present the results for the correlation smoothing technique, it is important to consider the eigenvectors of the correlation matrix that resulted in Figure 8.24. These are presented in Figure 10.3.

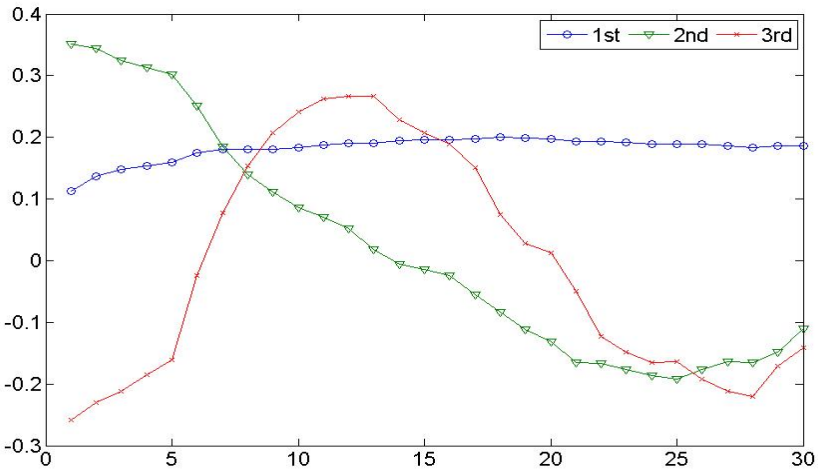

Figure 10.3: Eigenvectors of the historical correlation matrix presented in Figure 8.24. This correlation matrix was obtained using historically calculated constant maturity forwards from the South African market. Results presented for business date 2009/12/31.

This is very promising. We managed to obtain sensible principal components even with all the associated difficulties relating to the estimation of historical correlations. These three vectors will then account for 92% of all forward rate movements, should we decide to use this matrix as a direct input to the forward rate dynamics.

We will now move on to consider the fitting of the second parametric form onto the historically estimated correlation matrix as discussed in Section 10.1.1. This is the more flexible parametric form of the two and allow for different correlations depending on the expiries of the forward rates.

The fitting procedure was performed using a simple unconstrained minimization routine with initial starting point $x_0 = [0.1; 0.1; 0.1]$. This approach surprisingly resulted in a positive definite correlation matrix (which is not explicitly catered for in the parametric function) as well as a long term correlation level that is greater than zero. Although these results displayed the correct mathematical properties, it cannot be guaranteed that this will always be the case. The user should therefore always perform a check following the minimization routine or instead make use of a constrained minimization routine (which will affect performance). The results of the minimization routine are presented below.

$$\begin{aligned} f_{val} &= 1.5027, \\ \rho_\infty &= 0.1297, \\ \beta &= 10.4549, \\ \gamma &= 0.0580. \end{aligned}$$

From above, we have that the sum of the squared differences between the input and model correlation matrices amounts to 1.5027. This figure can further be reduced through making use of different optimization routines, exploring different starting points or even the use of a different parametric function. The resulting correlation surface is presented in the figure below.

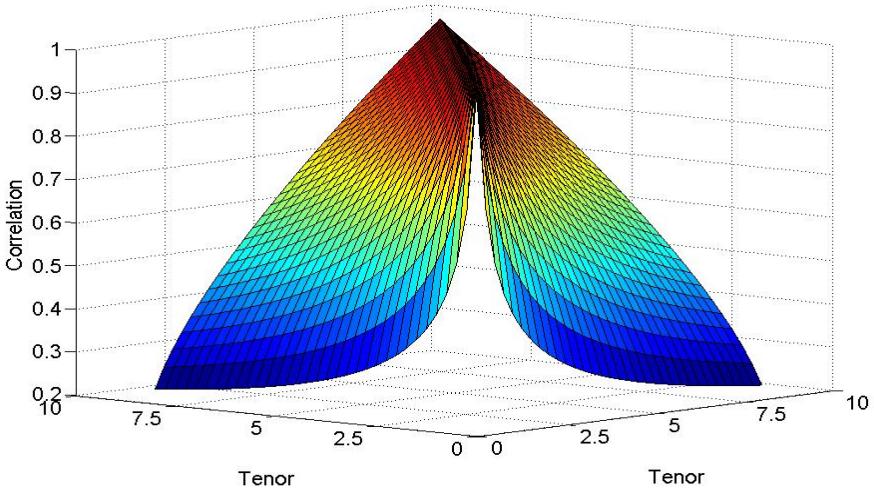

Figure 10.4: Correlation surface obtained when fitting Equation (6.3.6) to the historically estimated correlation surface given by Figure 8.24.

Note that the historically estimated correlation matrix only consisted of forward rates from 1y. This choice was made to include more historical points

in the correlation estimation procedure. Hence, we are left with a similarly spaced model implied correlation matrix. The implementations of this chapter will however require a full correlation matrix, i.e. a matrix starting at the 3m expiry. In order to obtain this, we will assume an endogenous interpolation technique (with the idea stemming from the technique used in Algorithm 10.3.3) which consists of estimating the short term correlations using the parameters obtained from the minimization routine (as opposed to using parameters that were obtained through calibrating to the entire correlation matrix).

The surface presented in Figure 10.4 is remarkably similar to the one presented in Figure 8.24. The interpolated values were found to compare well with the first row of Table 8.12, with bigger differences observed for the rest of the rows. This was to be expected, given the difference in estimation techniques. Alternatively, we can consider a global fit to the two historical data sets.

The correct approach will depend on the problem under consideration. There is one final check that we need to perform before making conclusions regarding the accuracy of the correlations. We need to be sure that the smoothed correlation matrix did not affect the eigenvectors in a financially undesirable way. These are presented in Figure 10.5 below.

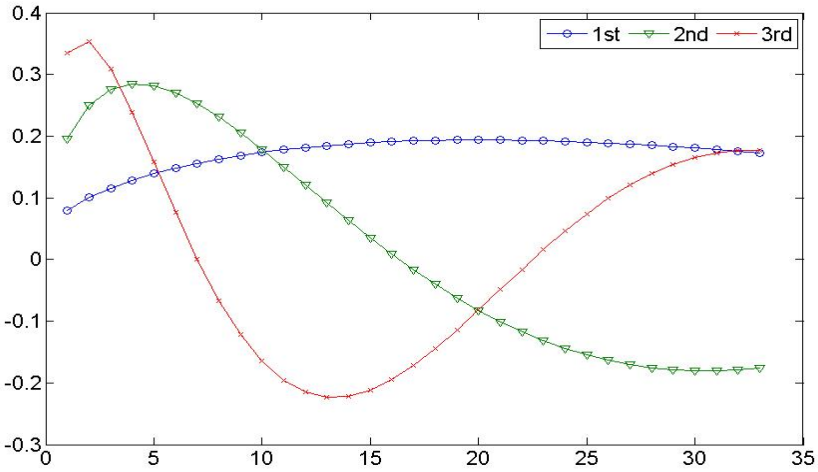

Figure 10.5: Eigenvectors of the correlation surface presented in Figure 10.4.

The most obvious change appears to be in the third eigenvector. Such a change is expected to have a minor financial implication since it is approximately a scalar multiple of the previously obtained third component. Irrespective of this, the example clearly states some of the risks associated with correlation smoothing. Furthermore, note that the explanatory power of these

components now reduced to 88%. This drop was found to be driven by the endogenous interpolation and not due to the smoothing.

In an attempt to remove the effect of the endogenous interpolation, we will follow the same procedure for the first parametric form given in Section 10.1.1. This is the simplest of the parametric functions and assume forward rates with the same difference in expiries to have the same correlations. Hence, the short term correlations are directly implied from the longer term forwards, i.e. those for which we do have estimates. The fitting procedure was performed using a simple unconstrained minimization routine with initial starting point $x_0 = [0.1; 0.1]$. The results of the minimization routine are presented below.

$$\begin{aligned} f_{val} &= 6.6428, \\ \rho_\infty &= 0.2844, \\ \beta &= 0.2194. \end{aligned}$$

The reduction in the quality of the fit is visible through considering the increase in the f_{val} value. This is clearly due to a loss in flexibility. Irrespective of this, we will show that this surface still has some promising features. The associated correlation surface, as implied by this parametric form, is given in Figure 10.6 below.

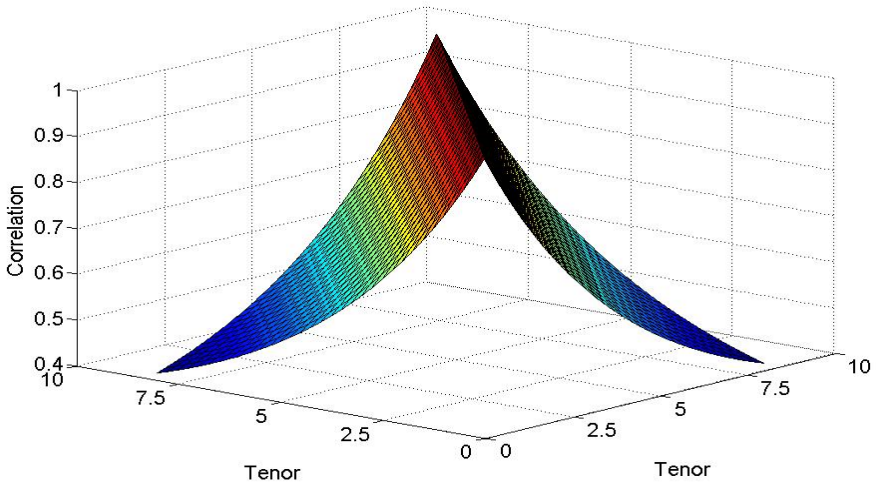

Figure 10.6: Correlation surface obtained when fitting Equation (6.3.5) to the historically estimated correlation surface given by Figure 8.24.

The eigenvectors associated with this parametric form is presented in the figure below.

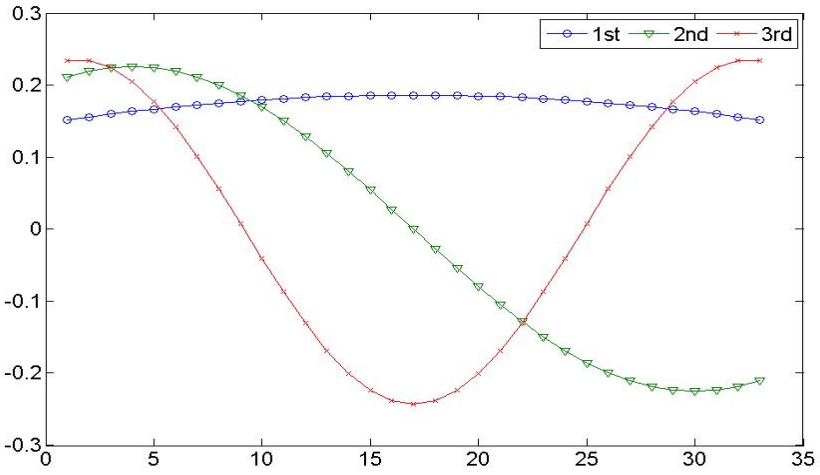

Figure 10.7: Eigenvectors of the correlation surface presented in Figure 10.6.

Once again we obtained financially desirable eigenvectors. Furthermore, the net explanatory power of these vectors amount to 90%, which is a slight increase from the previous parametric form. This increase can be seen to be driven by both, the elimination of the endogenous interpolation, as well as the change in the properties of the parametric form.

The differences between the two parametric forms are presented below.

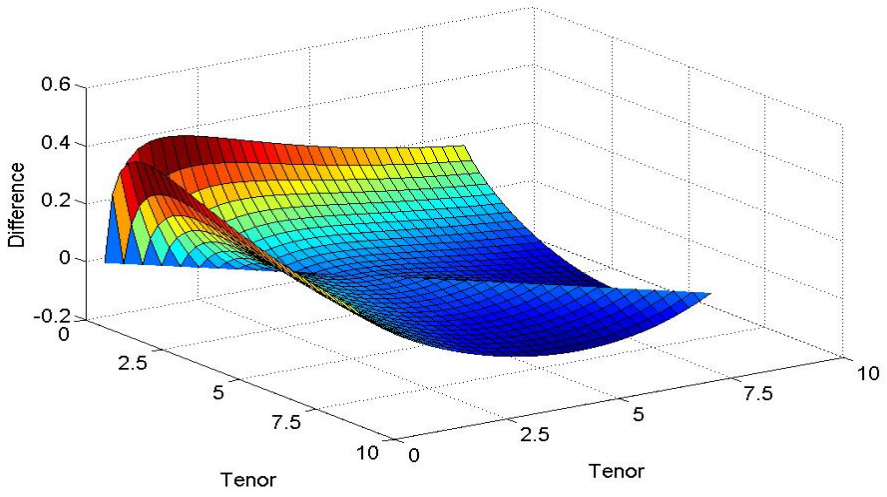

Figure 10.8: Difference in correlations implied by the two parametric correlation surfaces presented in this section.

From Figure 10.8, it is evident that the main differences are in the short end of the surface. Hence, the flexible form allows for the front forward rates to be less correlated with the remaining part of the curve (Rebonato [47]). This then ties back to the results presented in Table 8.12, indicating that these results may actually be a much better reflection of true correlations than initially thought. Hence, it may be worth while to consider a global fit to the historically estimated correlation matrix. This alternative will not be explored in this thesis.

10.5.2 Hull and White PCA Approach

This approach is very simple to implement. As discussed in Section 10.2.1 this is independent of the volatility calibration routine, hence we can assume the results of the previous chapter for this portion of the covariance elements. This section will in particular focus on the correlation component. The approach discussed can be extended to any input correlation surface. As a result, we will provide results for both parametric forms discussed in the previous section.

The important point to consider when implementing this approach, is how the model implied correlation matrix compare with the input correlation matrix. Big differences can result in substantial price differences for exotic products. This is irrespective of the financial requirement that the associated eigenvectors should resemble certain movements in forward rates (which are ensured by construction).

The trader is hence left with a decision of how many factors to include in the model. An exact match to any input correlation matrix can be obtained through retaining as many factors as forward rates. However, this will increase the complexity associated with the implementation of such a model.

These concepts are illustrated in the Table 10.8 below. The results were obtained through implementing the technique as discussed in Section 10.2.1.

From Table 10.8, it is clear that retaining all factors in the calibration process, results in an exact match to the correlations given by both of the parametric forms discussed in the previous section. This will then allow the pricing of interest rate derivatives that are exactly in line with market cap prices, as well as the input correlation matrix.

It is also clear that the simple parametric form, given by Equation (6.3.5), requires less factors to obtain a certain level of accuracy, when compared to the more complex parametric form given by Equation (6.3.6). In particular, the two parametric forms require 8 and 9 factors respectively in order to ensure a SSE below one.

The Matlab code used in obtaining these results is presented in Section C.2.2.1.

	Parametric Form 6.3.5		Parametric Form 6.3.6	
Factors	SSE	PercExpl	SSE	PercExpl
1	119.92823	0.71262	164.69991	0.68895
2	23.88608	0.84766	34.35219	0.82180
3	8.29204	0.90189	11.89556	0.87964
4	4.06408	0.92824	5.75012	0.91055
5	2.33962	0.94398	3.29640	0.93013
6	1.50528	0.95426	2.11850	0.94346
7	1.03547	0.96158	1.44651	0.95319
8	0.74947	0.96703	1.02700	0.96057
9	0.56149	0.97128	0.75375	0.96637
10	0.43242	0.97469	0.56647	0.97105
11	0.33968	0.97750	0.43296	0.97489
12	0.27118	0.97986	0.33553	0.97811
13	0.21907	0.98188	0.26274	0.98084
14	0.17869	0.98364	0.20715	0.98318
15	0.14676	0.98519	0.16426	0.98521
16	0.12119	0.98657	0.13071	0.98698
17	0.10047	0.98782	0.10416	0.98854
18	0.08308	0.98895	0.08299	0.98993
19	0.06865	0.98999	0.06600	0.99116
20	0.05658	0.99095	0.05231	0.99226
21	0.04641	0.99185	0.04123	0.99326
22	0.03783	0.99269	0.03226	0.99416
23	0.03054	0.99348	0.02501	0.99497
24	0.02437	0.99423	0.01912	0.99571
25	0.01912	0.99495	0.01440	0.99638
26	0.01470	0.99564	0.01062	0.99699
27	0.01098	0.99631	0.00759	0.99755
28	0.00788	0.99695	0.00521	0.99806
29	0.00535	0.99758	0.00337	0.99853
30	0.00333	0.99820	0.00199	0.99895
31	0.00178	0.99880	0.00100	0.99934
32	0.00068	0.99940	0.00035	0.99969
33	0.00000	1.00000	0.00000	1.00000

Table 10.8: HW correlation fitting results when applied to the South African market. Results presented for business date 2009/12/31.

10.5.3 Rebonato's Approach

In contrast to the previous approach, this methodology is based on an unconstrained minimization routine with the objective function representing the differences between the input and model implied correlations. It is hence expected to require fewer factors in order to ensure the levels of accuracy given by the Hull and White approach. This section will investigate the impact of the minimization routine on the required number of factors.

Applying the techniques discussed in Section 10.2.2, we obtained the results given in Table 10.9.

These were obtained using a simple unconstrained minimization routine

Factors		Parametric Form 6.3.5 Resulting SSE		Parametric Form 6.3.6 Resulting SSE	
2	21	18.21124	0.52209	25.10427	0.99136
3	22	4.98499	0.67150	7.49053	0.84814
4	23	2.10393	1.09102	3.16269	0.94371
5	24	1.67289	0.80979	2.08686	0.84162
6	25	1.47227	0.68983	1.20799	0.70774
7	26	1.00496	0.64900	1.25166	1.00807
8	27	0.93810	0.65704	1.22648	0.92205
9	28	0.49119	0.65884	0.87260	1.08829
10	29	0.64461	0.67001	0.89835	0.99713
11	30	0.86993	0.97389	0.89436	1.26849
12	31	0.75674	0.58837	0.98115	0.76049
13	32	0.74575	0.59666	0.70485	0.91472
14	33	0.92827	0.65863	1.03604	0.86343
15		0.64966		0.95153	
16		0.72071		0.84035	
17		0.79128		1.00380	
18		0.72682		0.81629	
19		0.78296		0.94895	
20		0.58681		0.86532	

Table 10.9: Rebonato correlation fitting results when applied to the South African market. Results presented for business date 2009/12/31.

with three different starting points. The process was found to be very time consuming, especially as we increase the number of factors. The results show an initial improvement over the Hull and White approach when the number of factors are low. However, this advantage seems to reduce quickly as we increase the required accuracy. Note from above that the same number of factors are required in order to ensure a SSE of below one. Also, note that the results does not appear to converge as we increase the number of factors. This is in contrast with the previous approach and is believed to be due to an insufficient optimization routine. Hence, it is evident that this approach is slightly more complicated to implement. Irrespective of these points, we still have that this approach can be very attractive when a small number of factors are required (consider for example the case in which two or three factors are retained).

Although not presented here (given we are working with the resultant SSE numbers), it is always necessary to examine and present the resultant correlation surfaces to the trader before making a choice regarding the actual method to use.

The Matlab code for this approach is given in Section C.2.2.2.

10.5.4 Cascade Calibration

The cascade calibration algorithms, introduced in Section 10.3.1 and implemented for the European market in Section 10.4.2, provided a nice way of obtaining forward rate volatilities given exogenous forward rate correlations and a set of swaption prices. In particular, it seemed like Algorithm 10.3.3 might be very useful, especially in the South African market were swaption volatilities are not that readily available.

This point requires some further discussion. Let us consider the required market inputs to these algorithms more closely. Each of these methodologies require input swaption volatilities with expiry and maturity increments set equal to the underlying reset frequency. For instance, in the examples relating to the European market, we had an underlying resetting frequency of one year. As a result, we needed swaption expiries and underlying swap maturities of $1y$ up to $10y$. Algorithm 10.3.3 then catered for instances in which we had some missing swaption expiries.

In the South African market, on the other hand, we have that caps and swaptions are based on 3-monthly interest rates. This then implies that we will need significantly more available swaption prices in order to implement the different cascade calibration algorithms. A typical set of available swaption prices is given in Table 8.5. This clearly illustrates the magnitude of the missing volatilities, i.e. we are not only missing a number of expiries, but also a number of underlying maturities. Note that Algorithm 10.3.3 does not cater for the latter part of the missing data by construction (i.e. using the endogenous interpolation technique) and hence will require even more simplifying assumptions.

The only way in which these algorithms can then be implemented in the South African market is through first interpolating the missing swaption volatilities (at least all of the missing maturities and then obtain the missing expiries through endogenous interpolation). However, we know that the outcome of the calibration algorithm will be significantly influenced by these assumptions, which will present us with the problem of finding an interpolation algorithm that most closely reflect the unobservable swaption volatilities (assuming such an algorithm exists). Hence, it is strongly recommended to first try and extend Table 8.5 as much as possible, which in practice can be a tedious task and must be weighted up against the advantages of implementing such an approach.

Given the issues discussed above, as well as the detailed implementation in Section 10.4.2, we will not pursue this problem any further.

Chapter 11

Extending the LMM to the SABR Model

The results obtained thus far have mainly focused around the deterministic volatility case. This allowed us to calibrate to the at-the-money term structure of instantaneous volatilities while enforcing some financial requirements.

Inherent in this approach is a constant volatility graph as we move across strikes for any particular expiry. This is, however, not optimal given the fact that market observable option prices tend to exhibit different implied volatilities for different strikes. Therefore it is essential that we consider possible adjustments of the model that can be used to incorporate this type of behaviour.

It was mentioned earlier in the project that the SABR model is a popular way in which to incorporate interest rate smiles. This approach is already being used in South Africa and from my understanding it is market standard internationally. The most significant drawback of this approach is the fact that it models each forward rate in isolation. Hence, there is no way to incorporate the joint dynamics between different forward rates and consequently cannot be used for the pricing of exotic interest rate options.

As a result, we will consider some of the recent work done by Rebonato [49] and Rebonato and White [52] in which they present extensions of the LIBOR Market Model that are compatible with the SABR implied option prices. Such an approach will then allow for the joint modeling of forward rates, while at the same time producing vanilla option prices that are consistent with the observed market prices.

Please note that this chapter will deviate slightly from the notation used throughout the thesis. This approach was followed in order to align the presented equations with those of the original authors. This allows for a simpler communication of the concepts to be discussed.

11.1 The SABR Volatility Model

The Stochastic Alpha Beta Rho (SABR) model, developed by Hagan *et al.* [26], is a stochastic volatility model that can be used to recover the dynamics of the volatility smile. Since its development, this approach has become the market standard internationally for the pricing of vanilla interest rate caps/floors and swaptions. This model specifies the following dynamics for the forward LIBOR rate.

$$df_t^T = \alpha_t^T \left(f_t^T\right)^{\beta_{SABR}^T} dz_t^T, \tag{11.1.1}$$

$$d\alpha_t^T = \nu^T \alpha_t^T dw_t^T, \tag{11.1.2}$$

$$E\left[dz_t^T dw_t^T\right] = \rho^T dt, \tag{11.1.3}$$

where, as indicated above, the parameters β_{SABR}, ν and ρ are expiry dependent. In order to ease the notation, we will omit this dependence in future equations. A brief discussion around the different parameters is presented below.

Hagan *et al.* [26] mentioned that it is typically difficult to obtain β through direct calibration to smile data, given the fact that the correlation parameter ρ affect the volatility curve in a similar way. Hence, this parameter is usually determined outside the model. Three popular and intuitive choices are $\beta = 1$ for stochastic lognormal, $\beta = 0$ for stochastic normal and $\beta = 0.5$ for stochastic CIR. Alternatively, this parameter can be estimated from historical data.

Once this choice is made, we then have that α controls the level of the overall height of the curve, ρ controls the amount of skew and ν controls the degree of smile.

The main result of the article by Hagan *et al.* [26] is an analytical formula that can be used to obtain Black implied volatilities, given the above set of parameters. This is presented below.

$$\sigma_{K,f} = \frac{\alpha}{(fK)^{(1-\beta)/2}\left\{1 + \frac{(1-\beta)^2}{24}\log^2 f/K + \frac{(1-\beta)^4}{1920}\log^4 f/K + \dots\right\}} \cdot \left(\frac{z}{x(z)}\right)$$

$$\cdot \left\{1 + \left[\frac{(1-\beta)^2}{24}\frac{\alpha^2}{(fK)^{1-\beta}} + \frac{1}{4}\frac{\rho\beta\nu\alpha}{(fK)^{(1-\beta)/2}} + \frac{2-3\rho^2}{24}\nu^2\right]T + \dots\right\}, \tag{11.1.4}$$

where

$$z = \frac{v}{\alpha}(fK)^{(1-\beta)/2}\log f/K, \tag{11.1.5}$$

and

$$x(z) = \log\left\{\frac{\sqrt{1-2\rho z + z^2} + z - \rho}{1-\rho}\right\}. \tag{11.1.6}$$

Note that the formula given above can be problematic for ATM options when implemented directly into a programming language. This is due to the fact that some of the terms need to be calculated in the limit as f approaches K. Hence, Hagan *et al.* [26] obtained the following formula for ATM implied volatilities.

$$\sigma(f,f) = \frac{\alpha}{f^{(1-\beta)}}\left\{1 + \left[\frac{(1-\beta)^2}{24}\frac{\alpha^2}{f^{(2-2\beta)}} + \frac{1}{4}\frac{\rho\beta\alpha\nu}{f^{(1-\beta)}} + \frac{2-3\rho^2}{24}\nu^2\right]T + \ldots\right. \tag{11.1.7}$$

Hagan *et al.* [26] mentioned that it might be more convenient to work with the ATM volatilities as opposed to the α parameters. These parameters can then be obtained through inverting Equation (11.1.7).

West [57], for instance, showed that such an inversion amounts to finding the appropriate root of the polynomial given below.

$$\frac{(1-\beta)^2 T}{24 f^{(2-2\beta)}}\alpha^3 + \frac{\rho\beta\nu T}{4 f^{(1-\beta)}}\alpha^2 + \left(1 + \frac{2-3\rho^2}{24}\nu^2 T\right)\alpha - \sigma(f,f)f^{(1-\beta)} = 0 \tag{11.1.8}$$

These are the main SABR concepts required for this chapter and hence concludes the extent to which this model will be analyzed. We will be more concerned with the calibration of the LMM to the SABR parameters. Consequently, we will assume these parameters as given (following the approaches of Rebonato [49] and Rebonato and White [52]). Similar to the market data presented in the previous chapters, these parameters were obtained from one of the South African investment banks and hence are reflective of actual trader views.

11.2 Caplet Volatility Data

Previous chapters specifically described some of the at-the-money term structures of instantaneous volatilities. It was mentioned that these differ from normal and stressed market conditions. Normal market conditions typically represents a humped term structure, whereas stressed conditions represents a decreasing level of volatilities as the tenor of the option increase.

We will now move on to consider similar graphs that will depict the observed interest rate smiles for the European and South African caplet markets. These are SABR implied surfaces and hence reflect traders views. Note that the European caplets used in this chapter resets every six months, while the South African market caplets resets every three months.

The smile surface for the European caplet market on 2009/12/31 is given in the Figure 11.1 below.

This graph already highlights some of the important points associated with observed option prices. Notice for instance the at-the-money term structure,

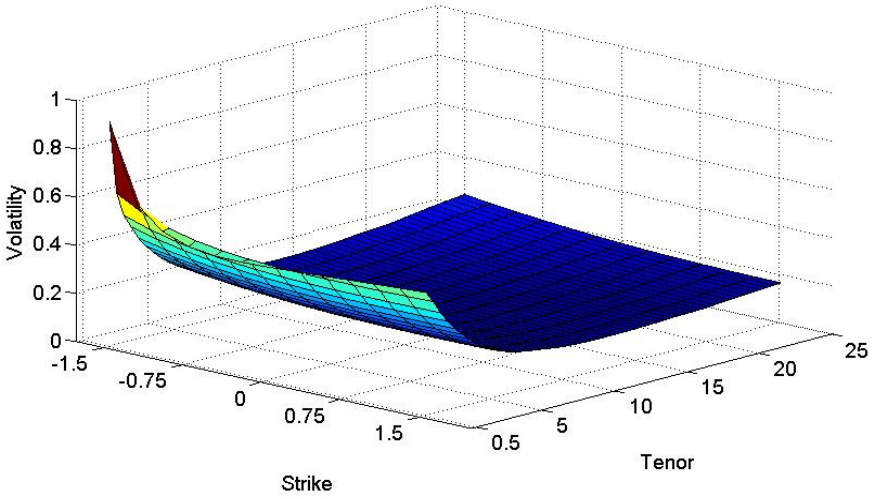

Figure 11.1: European caplet volatility surface obtained from a South African investment bank for business date 2009/12/31.

i.e. the volatilities across various terms when the strike is at the forward. This is reflective of an ATM term structure observable during periods of market stress, i.e. inverting (very slight hump at the short end of the curve).

Secondly, this graph exhibits a variation in volatilities as we move across different strikes. For this specific example, the graph is more in line with a skew type behaviour, i.e. higher volatilities for lower strikes. In particular, notice the high volatilities for strikes that are -1.5% from the current forward. This is in line with the market circumstances at the time, i.e. high level of volatilities and low rates (this also ties back to the inverted ATM shape).

Finally, note that the degree of smile/skew can differ as we move across different expiries.

We will now move on to consider a case that is reflective of normal market circumstances. This is presented in Figure 11.2 below, with data taken from 2007/05/30.

This graph displays the typical humped shape term structure for ATM volatilities. Furthermore, note the hockey stick type profile at the very short end. The rest of the arguments can be extrapolated from the previous figure.

In order to extend the results to the South African market, we present a similar graph for business date 2009/12/31 in Figure 11.3 below.

This surface has a much more pronounced smile than the European market. Furthermore, in contrast with the equivalent graph from the European market, we have that the ATM term structure is humped. Similarly, we will now consider a graph from a stressed period which was taken from business date 2009/02/25. This is given in Figure 11.4.

It is interesting to note that the two markets represents different term

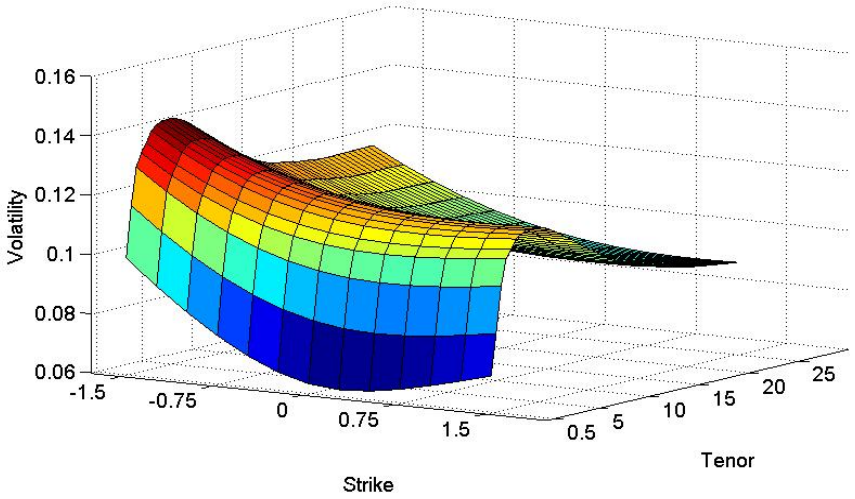

Figure 11.2: European caplet volatility surface obtained from a South African investment bank for business date 2007/05/30.

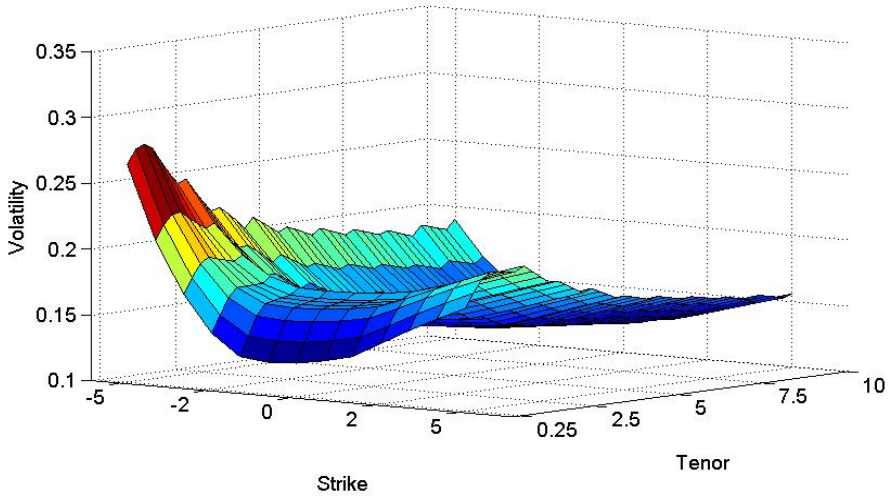

Figure 11.3: South African caplet volatility surface obtained from a South African investment bank for business date 2009/12/31.

structure behaviours at the same point in time. This is probably reflective of the credit crisis creating more volatility in the European market than in some of the emerging markets. However, all the figures presented in this section illustrated the important point that volatilities tend to differ for various strikes. The reasons for this type of behaviour are typically in the form of supply and demand, as well as, market behaviour in periods of severe stress.

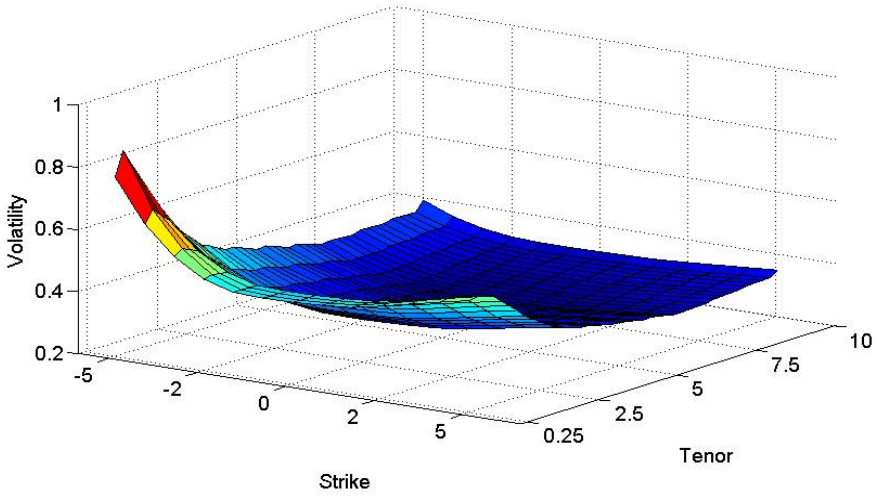

Figure 11.4: South African caplet volatility surface obtained from a South African investment bank for business date 2009/02/25.

11.3 Extending the LMM to SABR Caplet Prices

The first part of this chapter will be concerned with methods that can be used to extend the LMM to the SABR caplet prices. This is based on the work by Rebonato [49] and Rebonato and White [52]. In order to move on to the different calibration strategies, we firstly need to consider the underlying mathematical framework. This is briefly discussed below.

The associated LMM forward rate dynamics, under the terminal measure Q^T, is defined as

$$df_t^T = s_t^T (f_t^T)^{\beta_{LMM}^T} dz_t^T, \tag{11.3.1}$$

$$s_t^T = k_t^T g_t^T, \tag{11.3.2}$$

$$dk_t^T = k_t^T \mu_t^T dt + k_t^T h_t^T dw_t^T, \tag{11.3.3}$$

$$E\left[dz_t^T dw_t^T\right] = r^T dt, \tag{11.3.4}$$

where $g_t^T = g(T-t)$ and $h_t^T = h(T-t)$ are the time-homogeneous parametric functions given by Equation (5.4.8). Also note that the correction factors given by k_t^T are now assumed to be stochastic (recall that these were determined by Equation (9.2.3) in the deterministic case).

This specific choice of dynamics was mainly driven by financial requirements. The volatility component, for instance, were decomposed into the previously used separable structure which allowed for exact caplet pricing in the deterministic setting. The only difference now is that we allowed for the correction factors k_t^T to be stochastic, with the vol of vol given by a time homogeneous function $h_t^T = h(T-t)$.

The authors calculated the drift term of k_t^T for a variety of different numeraires and always found it to be very small and of minimal numerical significance. Hence, setting $\mu_t^T = 0$, we can obtain an expression for k_t^T as

$$k_t^T = k_0^T \exp\left[\int_0^t \left\{-\frac{1}{2}h^2(T-s)\,ds + h(T-s)dw_s\right\}\right]. \tag{11.3.5}$$

Both of the approaches that will be considered below, start with the following simple choices:

$$r = \rho, \tag{11.3.6}$$

$$\beta_{SABR} = \beta_{LMM}. \tag{11.3.7}$$

Hence, we are only left with task of finding the parameters for the time-homogeneous functions g_t^T and h_t^T.

11.3.1 Rebonato's Proposed Extension

Rebonato [49] originally proposed a simplistic way of obtaining the parameters of the functions g_t^T and h_t^T. This is briefly discussed below.

The first step of this approach is very similar to the technique discussed in Section 9.2.1. In theory, we should not be able to apply the same approach given the fact that the stochastic variable α_t^T does not have a single root-mean-squared value. Rebonato [49] suggests we rather approximate this quantity with the expectation at time 0 of α_t^T, i.e. α_0^T (approach derived through a heuristic argument that the deterministic portion of the volatility component should reflect current market data).

The calibration procedure then follows the process outlined in Section 9.2.1, i.e. we need to solve for the set of parameters of the function g that will result in a minimum for the objective function

$$\chi^2 = \sum_{j=1}^{n} \eta_j^2, \tag{11.3.8}$$

where

$$\eta_j^2 = \left[\left(\alpha_0^{T_j}\right)^2 T_j - \int_0^{T_j} \left(g_t^{T_j}\right)^2 dt\right]^2. \tag{11.3.9}$$

The initial values of $k_t^{T_j}$ are then chosen as the factors required for an exact fit to the quantities $\left(\alpha_0^{T_j}\right)^2 T_j$. As discussed in Section 9.2.1, we need these to be close to one in order for the calibration to be regarded as successful. Rebonato *et al.* [51] importantly pointed out that this will allow for a volatility function that is a stochastic perturbation of a deterministic function. Hence, on average, we will obtain a behaviour that is reflective of our financial assumptions (for

example a time-homogeneous volatility function that can either be humped or inverted).

Rebonato [49] suggested a similar way of obtaining the parameters of h_t^T, i.e. we need solve for the set of parameters of the function h that will result in a minimum for the objective function

$$\chi^2 = \sum_{j=1}^{n} \eta_j^2, \tag{11.3.10}$$

where

$$\eta_j^2 = \left[\left(\nu^{T_j}\right)^2 T_j - \int_0^{T_j} \left(h_t^{T_j}\right)^2 dt \right]^2. \tag{11.3.11}$$

Following the latter minimization, we also need to ensure that the model implied correction factors are close to one. Note that the vector ν^{T_j} are assumed to be externally given.

11.3.2 Rebonato and White Proposed Extension

Rebonato and White [52] pointed out that the previous methodology is strictly only correct in the limit as the volatility of volatility approaches zero, i.e. as the forward rate processes approach a deterministic state (only in this case will the terminal distributions of the two models be the same). Furthermore, note that the previous methodology calibrated the volatility and volatility of volatility functions independently.

Rebonato [49] and Rebonato and White [52] mentioned that this is not correct. The authors hence proposed an alternative methodology that depends on when the volatility and volatility of volatility are large or small.

This approximation was obtained through approximating SABR and LMM call prices in a stochastic volatility setting (with some simplifying assumptions) and then solving for the SABR-LMM parameters that will result in the same prices (up to certain degree of accuracy).

The first relationship obtained between the different parameters is surprisingly exactly the same as the one implied by Equation (11.3.9). This is presented below.

$$\left(\alpha_0^{T_j}\right)^2 T_j = \left(k_0^{T_j}\right)^2 \int_0^{T_j} g(t)^2 dt. \tag{11.3.12}$$

From this we can approximate the parameters of g as well as the initial values of $k_t^{T_j}$ using the approach described in the previous section.

The other relationship obtained between the different parameters depend on the interactions between the volatility and volatility of volatility functions.

This is presented below.

$$\frac{\left(\alpha_0^{T_j}\right)\left(\nu^{T_j}\right)^2 T_j^2}{2\left(k_0^{T_j}\right)^2} = \int_0^{T_j} \left(g_t^{T_j}\right)^2 \left(\hat{h}_t^{T_j}\right)^2 t dt, \tag{11.3.13}$$

where $\hat{h}_t^{T_j}$ is defined as the RMS value of $h_t^{T_j}$.

Using the parameters obtained for the functions g and $k_0^{T_j}$ in the first step, we then need to solve for the parameters of the function h that will result in a minimum for the objective function

$$\chi^2 = \sum_{j=1}^{n} \eta_j^2, \tag{11.3.14}$$

where

$$\eta_j^2 = \left[\frac{\left(\alpha_0^{T_j}\right)\left(\nu^{T_j}\right)^2 T_j^2}{2\left(k_0^{T_j}\right)^2} - \int_0^{T_j} \left(g_t^{T_j}\right)^2 \left(\hat{h}_t^{T_j}\right)^2 t dt\right]^2. \tag{11.3.15}$$

11.4 Extending the LMM to SABR Swaption Prices

Rebonato and White [52] also developed an analytical approximation for the implied swaption prices given the previously obtained SABR-LMM parameters. The authors mentioned that this approximation can then be used for the calibration to the swaption matrix as well as for studies relating to the congruence between the two markets.

The previous section provided approximations for the parameters of the forward rates in the SABR-LMM approach when fitted to individual caplet prices. In order to price swaptions (or any other product that is dependent on a number of forward rates at a time), we need to define the various correlations embedded within these dynamics. As a result, we will extend Equations (11.3.1)-(11.3.4) to the equations presented below

$$df_t^{T_i} = s_t^{T_i} (f_t^{T_i})^{\beta_{LMM}^{T_i}} dz_t^{T_i}, \tag{11.4.1}$$

$$s_t^{T_i} = k_t^{T_i} g_t^{T_i}, \tag{11.4.2}$$

$$dk_t^{T_i} = k_t^{T_i} \mu_t^{T_i} dt + k_t^{T_i} h_t^{T_i} dw_t^{T_i}, \tag{11.4.3}$$

$$E\left[dz_t^{T_i} dz_t^{T_j}\right] = \rho_{i,j} dt, \tag{11.4.4}$$

$$E\left[dw_t^{T_i} dw_t^{T_j}\right] = \theta_{i,j} dt, \tag{11.4.5}$$

$$E\left[dw_t^{T_i} dz_t^{T_j}\right] = \phi_{i,j} dt. \tag{11.4.6}$$

This then illustrates that the model will be fully specified once all the correlations are determined. Note that the elements on the diagonal of ϕ can be obtained from the techniques discussed in the previous section. The rest of the correlations can be determined outside of the model using some of the concepts described (at length) throughout this thesis.

The approximation of swaption prices, mentioned at the start of the section, will be obtained through approximating the SABR swaption parameters. From these parameters, we will then be able to obtain the approximate swaption implied volatilities using the Hagan *et al.* [26] formula.

Hence, let us explicitly state the SABR forward swap rate process. From Equations (11.1.1)-(11.1.3), we have that the dynamics of $SR_t^{\alpha\beta}$ is given by

$$dSR_t = (SR_t)^B \Sigma_t dZ_t, \tag{11.4.7}$$

$$d\Sigma_t = \Sigma_t V dZ_t', \tag{11.4.8}$$

$$E\left[dZ_t dZ_t'\right] = \Phi dt. \tag{11.4.9}$$

The following section will then be concerned with obtaining approximations for Σ_0, Φ, B and V as a function of the LMM-SABR parameters.

11.4.1 Rebonato and White Proposed Extension

The authors start by deriving an approximation of Σ_t using the same "freezing of weights" techniques originally proposed for swap rate volatilities in a LMM setup. This approximation is presented below.

$$\Sigma_t = \sqrt{\sum_{k,m=1}^{n_j} W_k^0 W_m^0 s_t^{T_k} s_t^{T_m} \rho_{k,m}}, \tag{11.4.10}$$

where

$$W_k^t = w_k \frac{\left(f_t^k\right)^{\beta_k}}{(SR_t)^B}. \tag{11.4.11}$$

Note the similarity between the values w_k, defined above, and the forward rate weights defined in Equation (5.5.2).

Rebonato and White [52] then followed the same approach as in Section 11.3.2 to obtain approximations for the parameters Σ_0 and V. These are given as

$$\Sigma_0 = \sqrt{\frac{1}{T}\sum_{i,j}\left(\rho_{ij} W_i^0 W_j^0 k_0^i k_0^j \int_0^T g^i g^j \, dt\right)}, \tag{11.4.12}$$

$$V = \frac{1}{\Sigma_0 T}\sqrt{2\sum_{i,j}\left(\rho_{ij}\theta_{i,j} W_i^0 W_j^0 k_0^i k_0^j \int_0^T g^i g^j \hat{h}_{ij}(t)^2 t \, dt\right)}, \tag{11.4.13}$$

where T indicates the swaption expiry while T_i indicates the expiry of the forward rate under consideration.

The only remaining sets of parameters are then the correlation between the swap rate and its volatility, Φ, and the swap rate exponents B.

The correlation parameter approximation derived in the reference paper is given by

$$\Phi = \sum_{i,j} \Omega_{ij} \phi_{ij}, \tag{11.4.14}$$

where

$$\Omega_{ij} = \frac{2\rho_{ij}\phi_{ij} W_i^0 W_j^0 k_0^i k_0^j \int_0^T g^i g^j \hat{h}(t)^2 t \, dt}{(V \Sigma_0 T)^2}. \tag{11.4.15}$$

As a final step, Rebonato and White [52] then approximate the parameters B with

$$B = \sum_{1,n_j} w_k B_k. \tag{11.4.16}$$

They motivate that the quality of this approximation will typically range between exact (for the normal case) to relatively good (in the lognormal case).

The approximations presented in this section can then be used to obtain the implied swaption SABR parameters given the associated SABR-LMM parameters. Such an approximation can be very useful in practice. It can for instance be used to check the congruence between the two markets or for identifying possible trading opportunities. However, in general, it is very important to be able to analyze the prices of one set of state variables given the prices of another.

Alternatively, we can also use these approximations to fit the forward rate parameters in such a way as to minimize the differences between the SABR swaption parameters observable in the market and the SABR swaption parameters implied by the model. This is similar to some of the concepts discussed in the previous chapters. The difficulty of implementing such an approach would be the number of free parameters caused by the large amount of correlations. We should always be able to obtain SABR parameters to a pre-defined degree of accuracy, however this can be at the price of realistic and financially acceptable correlations. Another approach would be to first solve for the parameters of the time-homogeneous functions that will provide SABR parameters as close as possible to their market values given a set of exogenous correlations. We should then just ensure that the solution is as time-homogeneous as possible (forward rate components close to one).

Chapter 12

Conclusion

It was mentioned, at the start of this document, that the current market methodology for the pricing of vanilla interest rate options in the South African market, is the standard Black model with some sort of smile adjustment (which appears to be in the form of the SABR model). The most significant drawback of this approach is the fact that it models each forward rate in isolation. Therefore, there is no way to incorporate the joint dynamics between different forward rates and consequently cannot be used for the pricing of exotic interest rate options (Rebonato [49]). Even simple interest rate derivatives, such as Bermudan swaptions, will fall outside this framework.

It was mentioned that one alternative to the current approach would be to turn to different possible short rate models. As a result, we considered a number of different short rate models in Chapter 2. These, however, resulted in a number of different limitations. The first obvious limitation is that short rate models are based on the assumption that the dynamics of the entire yield curve is only driven by the instantaneous short rate. In the case of single-factor models, we only have one source of uncertainty implying perfectly correlated rates. In order to improve correlation modeling we need to add additional factors to the model, which consequently add more complexity to the model. Furthermore, the instantaneous short rate is not a directly observable market variable. This then complicates the calibration and implementation of these models and hence reduces some of its financial appeal (Hunt and Kennedy [33]).

We then turned our attention to the LIBOR market model with deterministic volatilities (will comment later in this section on the extension to the SABR volatility model). This choice was mainly motivated by some of the properties associated with this model. For instance, it allows us to price exotic options in such a way that is internally consistent with the Black framework (Rebonato [47]); i.e., it will allow the pricing of exotic options in such a way that is internally consistent with the current market methodology for ATM vanilla options. This was argued to be an extremely important point,

given the fact that exotic options traders will typically look at hedging their positions with vanilla interest rate options. Hence, it is imperative to have a model that implies the correct prices of these hedging instruments.

Another favourable aspect of this model relates to its financial appeal. Instead of having a model that is based on unobservable rates, we have that the state variables in the LIBOR market model are discretely compounded forward rates (Rebonato [47]). These are market observable rates and are assumed to be lognormally distributed (in the deterministic volatility setting and under their associated T-forward measures (Björk [4])). This then allows for the pricing of caplets and hence caps (can be generalized to floorlets and hence floors) that is consistent with the Black [5] framework.

We also introduced the swap market model. The state variables in this model were defined as discretely compounded forward swap rates (Rebonato [47]). Similar to the LIBOR market model, these are market observable rates and are assumed to be lognormally distributed (in the deterministic volatility setting and under their associated swap rate measures (Björk [4])). This then allows for the pricing of swaptions in a manner that is consistent with the Black [5] framework.

At this point in the project we started referring to some of the important concepts emphasized throughout the thesis. One of these are, that the LIBOR and swap market models are not compatible (mentioned by a number of authors; see for example Brigo and Mercurio [11], Björk [4] and Rebonato [47]). This can be seen through noting that a swap rate can be expressed as a linear combination of forward rates with stochastic weights (Rebonato [47]). Hence, the pricing of swaptions in the LIBOR market model will not be consistent with the Black [5] framework (similar result can be derived for the pricing of caps/floors in the swap market model). This then implies that one has to decide, based on the problem at hand, which one of the models to work with. We focused our attention on the LIBOR market model. From above it is evident that this will imply simple calibration to cap/floor prices and we will have to use approximations for the calibration to swaption prices (Brigo and Mercurio [11], Björk [4]).

This then also pointed to the fact that different forward rates cannot be martingales under the same measure. Hence, we needed to introduce a mechanism for modeling the the joint dynamics of several forward rates. This is due to the fact that the payoff of some derivatives, like interest rate swaptions (or more exotic options), are dependent on more than one forward rate at the same time. Hence, we introduced the concept of no-arbitrage dynamics under different forward measures. In particular, these were obtained for a number of different possible scenarios. This analysis started with a scalar Wiener process and gradually extended the derivations to several factors, where the Wiener processes were assumed to be correlated.

The forward rate dynamics, as described above, were found to be expressed entirely in terms of its associated instantaneous covariance elements. Within

this setup, we then know that the calibration of this model will be based on the determination of these elements. Björk [4] mentioned that these quantities should be determined by the market, which will then allow for the pricing of derivatives under the market implied measure. The question, however, remains if these covariance functions can be uniquely determined. This will then imply an unique measure and hence unique exotic prices. Rebonato [47] argued that this is not possible and hence the market for instantaneous covariances is incomplete.

This then implied that the user of the model will have to make some financially justifiable assumptions regarding the covariance structure of the model (Rebonato [47]). Hence, we introduced two chapters relating to the modeling of instantaneous volatilities and correlations. Within these chapters, we investigated various types of modeling choices, and motivated the use of the different types of specifications. In general, we favoured approaches that allowed for a time-homogeneous evolution in the term structure of volatilities. Forward rate specific or time dependent components were also introduced in order to allow for the exact pricing of market observable ATM options.

The reason for opting for time-homogeneous volatility specifications, was based on on the view that the term structure of volatilities should remain approximately the same as we move through time (in a deterministic volatility setting, will later consider the extension to the stochastic volatility setting). Alternatively, it was also mentioned that it is possible to calibrate to two different term structures. In this scenario, the one term structure will then represent the current term structure of volatilities, whereas the other term structure will reflect some future scenario (Rebonato [47]). In this setup, we can then assign different weights to the different term structures to reflect the order of importance. Such an approach was not implemented in this thesis, however is in essence a very simplistic example of extending the LMM to a stochastic volatility setting.

Such discussions then started to highlight some of the limitations embedded in our current approach. Given the fact that future volatilities and consequently future term structures reflect future hedging costs, we should have an approach that can reflect the correct future expected behaviour (Rebonato and White [51]). Irrespective of this, we have that our current simplistic model already identified some of the possible desirable features that an accurate model should have. The next point, would be to include different volatilities as we move across different strikes. This will be discussed later in this section.

Turning our attention now to correlations, it was motivated that we will focus our attention on historically estimated correlation matrices. From this, we can then perform the necessary rank reduction procedures (in order to simplify Monte Carlo simulations) and/or fit an appropriate parametric form if the input data contained a considerable amount of noise.

The decision to work with exogenously given correlation matrices, was motivated by the difficulty of obtaining accurate correlation estimates from

market inputs. Rebonato [47] mentioned that this task is very complex, even within a liquid interest rate market. European swaptions, for example, is one of the traded products that may actually contain information regarding the correlations between different forward rates. However, when considering the swaption volatility approximation formula it is evident that the shape of the instantaneous volatility functions also play a significant role in the pricing of swaptions, resulting in different implied correlations for different instantaneous volatility functions (Rebonato [47]). Hence, in order to imply correlations from market data we would typically need actively traded correlation derivatives. To my knowledge, these are not currently available in the South African market and hence we are forced to obtain correlations from historical rate movements as well as trader estimates.

Alternatively, Rebonato [47] mentioned that actively traded serial options would be able to complete the instantaneous volatility market (serial options were discussed in Section 2.4.2). Once these functions are determined, we would then be able to imply correlations through taking views regarding the price congruence between the different markets. Restrictions in liquidity however renders this approach implausible.

At this point, most of the theoretical concepts relating to the deterministic volatility LMM were defined and discussed. Next, we moved on to consider if we actually have the required data inputs in the South African market to implement such an approach. Within this context, we considered market inputs as obtained from one of the South African investment banks. This type of approach not only allowed for the analysis of the real life market views and assumptions as made by SA traders, but also helped to eliminate the noise associated with illiquid prices (these prices are submitted to price testing processes on a weekly basis and hence can be assumed to be a relatively accurate reflection of the data available on sources such as Reuters and Bloomberg). Although we mainly considered actual trader inputs, it was also illustrated how to obtain similar market data from trading sources such as Reuters or Bloomberg.

Following the sourcing of the relevant market data, we also considered key procedures required to transform the obtained market data into the required format. These included curve bootstrapping (for which we briefly discussed the effect of different interpolation techniques), as well as, a caplet stripping procedure. From these we were able to obtain the required caplet volatilities from market cap volatilities. The curve bootstrapping methodology was then used on the historical data set in order to obtain historical forward rates. These were then in turn used for the historical estimation of implied caplet volatilities, as well as, the correlations between different constant maturity forward rates (note that we calculated the correlations for constant maturity forwards, this is due to the model assumptions regarding the underlying variables and should not be confused with market observable constant time-to-maturities (Brigo and Mercurio [11])).

The historical caplet volatilities were provided for pure analysis purposes and were not used in any calibration routines. This, however, allowed us to draw some interesting relationships between the market implied and historical volatilities. Both term structures, for instance, reflected a "humped" shape for normal time periods, vs. an inverted shape during more volatile periods. The most significant difference between the two different term structures, related to the timing difference at any point in time, i.e. the historical estimation is always backward looking, whereas the market implied volatilities are forward looking.

Similarly, we obtained financially desirable historical correlations. The estimates did display some noise, which was expected to be due to linear interpolation and market segmentation. It was then argued that we should first fit a parametric form to this matrix before using in practical applications (given this matrix is broadly in line with trader expectations).

With these market inputs to our disposal, we then moved to the actual calibration of the model. The analysis started with the volatility portions of the instantaneous covariance functions. We illustrated in which cases some of the piecewise constant volatility specifications resulted in imaginary volatilities (was only found in the European market, for the case where instantaneous volatilities depend on the time-to-maturity of the forward rate under consideration). This scenario was explained and we did consider available techniques to identify such scenarios. The remainder of the volatility specifications were implemented successfully, and allowed for the exact pricing of the input caplet volatilities in all scenarios. Note that we only considered the calibration to caplet prices. These results can easily be extended to an input swaption matrix, given an exogenous correlation matrix and Rebonato's [47] approximate swaption volatility formula. Following each of the calibration procedures, we considered the market implied term structures. These were found to be time-homogeneous (with small noise for parametric functions due to the used forward rate specific components, as well as, the time dependent functions) for most of the volatility specifications (only exception relates to the piecewise constant volatility specification where volatilities depend on the maturity of the forward rate). We also illustrated that the accuracy of parametric volatility functions were significantly improved when we included time dependent components.

Next, we moved on to the joint calibration of different forward rates. These applications were based on the fact that we can separate the market observable volatility component from the component used for correlation modeling (Rebonato [47]). As a result, we required exogenously given correlation matrices. For the European market, we used the correlation matrix as provided by Brigo and Mercurio [11]. On the other hand, we used the historically estimated correlation matrix (described earlier) as the exogenous correlation matrix for the South African market.

Before using this historically estimated correlation matrix, we firstly ex-

amined its implied eigenvectors. These implied sensible principal components, even with all the associated difficulties relating to the estimation of historical correlations. These factors were in line with movements observable in a rate hiking scenario. This analysis was performed in order to ensure that the evolution of forward rates will be in line with market expectations. Next, we fitted different parametric forms to this matrix in order to smooth out some of the noise inherent in this matrix. Following the smoothing process, we still obtained sensible principal components, irrespective of the parametric form. We also used this opportunity, to examine some of the differences implied by the two parametric forms. The main differences between the two parametric forms, for this particular example, were found to be in the short end of the curve. This was due to the fact that the more flexible form allowed for the front forward rates to be less correlated with the remaining part of the curve (as opposed to the simpler form where correlations are only dependent on the difference in expiry times between two different forward rates).

Regarding the actual calibration routines, we considered three different approaches. Two of the approaches were based on rank reduction techniques, while the other was based on the calibration to a swaption volatility matrix, assuming piecewise constant instantaneous volatilities.

The two rank reduction techniques were easily applied within the South African market. We assumed in this calibration, the results obtained from the calibration to caplet volatilities. The remainder of the calibration algorithm then consisted of incorporating the exogenously given matrix into the forward rate dynamics. As discussed earlier in the thesis, no additional calibration is required (within this particular forward rate based setup where we have already determined the instantaneous volatility functions and assume an exogenously given correlation matrix) if we are not concerned with the dimensionality of the forward rate dynamics (Rebonato [47]). However, for practical applications, we need to consider ways in which to reduce the associated dimensionality.

The first method used here, was the Hull and White [31] approach which only retains certain eigenvectors of the correlation matrix (depending on the desired accuracy). The important point to consider when implementing this approach, is how the model implied correlation matrix compare with the input correlation matrix. Big differences can result in substantial price differences for exotic products. This is irrespective of the financial requirement that the associated eigenvectors should resemble certain movements in forward rates (which are ensured by construction). It was also illustrated that the simple parametric form required less factors to obtain a certain level of accuracy, when compared to the more complex parametric form. The results of this approach were obtained with minimal computational time.

The other rank reduction technique we considered, was based on Rebonato's [47] angular formulation. This approach focus on the specification of forward rate dynamics, that most accurately reflect the input correlation matrix. In contrast to the previous approach, this methodology is based on an

unconstrained minimization routine with the objective function representing the differences between the input and model implied correlations. It is hence expected to require fewer factors in order to ensure the levels of accuracy given by the Hull and White approach. This process was, however, found to be very time consuming, especially as we increase the number of factors. The results show an initial improvement over the Hull and White approach when the number of factors are low. However, this advantage seemed to reduce quickly as we increase the required accuracy.

The final joint calibration technique that we considered, as mentioned above, was based on the calibration to a swaption volatility matrix, assuming piecewise constant instantaneous volatilities. This type of calibration was introduced by Brigo and Mercurio [11], which resulted in a series of different cascade calibration algorithms. Each calibration algorithm, was developed to improve on the previous one. We implemented these calibration algorithms to the European market and matched the results of the authors.

In particular, it seemed like the final algorithm proposed by the authors might be very useful, especially in the South African market were swaption volatilities are not that readily available. Upon further analysis, it was found that each of these methodologies require input swaption volatilities with expiry and maturity increments set equal to the underlying reset frequency. For instance, in the examples relating to the European market, we had an underlying resetting frequency of one year. As a result, we needed swaption expiries and underlying swap maturities of $1y$ up to $10y$. The final algorithm then catered for instances in which we had some missing swaption expiries.

In the South African market, on the other hand, we have that caps and swaptions are based on 3-monthly interest rates. This then implies that we will need significantly more available swaption prices in order to implement the different cascade calibration algorithms. Through examining the market available swaption volatility matrix, it was found that we are not only missing a number of expiries, but also a number of underlying maturities. The final algorithm proposed by Brigo and Mercurio [11] does not cater for the latter part of the missing data by construction and hence will require even more simplifying assumptions.

The only way in which these algorithms can then be implemented in the South African market is through first interpolating the missing swaption volatilities (at least all of the missing maturities and then obtain the missing expiries through endogenous interpolation). However, we know that the outcome of the calibration algorithm will be significantly influenced by these assumptions, which will present us with the problem of finding an interpolation algorithm that most closely reflect the unobservable swaption volatilities (assuming such an algorithm exists). Hence, it was strongly recommended to first try and extend the input swaption matrix as much as possible, which in practice can be a tedious task and must be weighted up against the advantages of implementing such an approach. Given these issues, as well as the detailed

implementation for the European market data, we did not pursue this problem any further.

In the final chapter of this thesis, we briefly considered extending our approach to incorporate observable interest rate smiles (stochastic volatility setting). This then provided us with the final required adjustment, to ensure that the model implied hedging costs are more in line with that realized in the market.

The focus in this chapter was based on the SABR model (although there are a number of alternative approaches). This choice was mainly motivated by the fact that it is already implemented in the South African market for vanilla interest rate options. Such an approach then allowed for the joint modeling of forward rates, while at the same time producing vanilla option prices that are consistent with the observed market prices (as opposed to modeling each forward rate in isolation in the standard SABR model). This extension was based on the recent work by Rebonato [49] and Rebonato and White [52].

This chapter was, however, less detailed than the rest of the thesis. We only briefly highlighted some of the authors' obtained results as well as what these results imply. An in depth analysis of this model, as well as, other possible extensions require significantly more work and can be regarded as a research project on its own. Hence, this project did not attempt to provide a complete description of these types of models, or even provide proofs or implementations. Instead, this chapter was intended to rather serve as a brief introduction into this field of research, and will be pursued outside this thesis as an ongoing project.

Appendix A

Theorems and Definitions

This chapter provides some useful theorems and definitions, as given by Björk [4], that can be used to supplement the change-of-numeraire ideas and concepts presented in Chapter 3.

A.1 The Radon-Nikodym Theorem

Absence of arbitrage is closely connected to the existence of certain absolutely continuous measure transformations. The basic mathematical tool is the Radon-Nikodym Theorem (Björk [4]). This is presented below

Theorem A.1.1 (The Radon-Nikodym Theorem - Björk [4]) *Consider the measure space $(X, \mathcal{F}, \mu)$, where we assume that μ is finite, i.e. $\mu(X) < \infty$. Assume that there exists a measure ν on $(X, \mathcal{F})$ such that $\nu << \mu$ on $\mathcal{F}$. Then there exists a nonnegative function $f : X \to R$ such that*

$$f \text{ is } \mathcal{F} - \text{measureable},$$

$$\int_X f(x)\, d\mu(x) < \infty,$$

$$\nu(A) = \int_A f(x)\, d\mu(x), \text{ for all } A \in \mathcal{F}.$$

The function f is called the ***Radon-Nikodym derivative*** *of ν w.r.t. μ. It is uniquely determined μ-a.e. and we write*

$$f(x) = \frac{d\nu(x)}{d\mu(x)}$$

.

A.2 Equivalent Probability Measures

The following theorem presents a useful result known as the Abstract Bayes' Formula. This result explains how conditional expected values under a probability measure, say Q, is related to the condition expected values under another measure, say P.

Theorem A.2.1 (Bayes' Theorem - Björk [4]) *Assume that X is a random variable on $(\Omega, \mathcal{F}, P)$, and let Q be another probability measure on $(\Omega, \mathcal{F})$ with Radon-Nikodym derivative*

$$L = \frac{dQ}{dP} \text{ on } \mathcal{F}.$$

Assume that $X \in L^1(\Omega, \mathcal{F}, Q)$ and that $\mathcal{G}$ is a sigma-algebra with $\mathcal{G} \subseteq \mathcal{F}$. Then

$$E^Q[X|\mathcal{G}] = \frac{E^P[L \cdot X|\mathcal{G}]}{E^P[L|\mathcal{G}]}, \ P\text{-a.s.}$$

A.3 Likelihood Processes

Lastly, we will introduce the concept of a likelihood process. This is given in the theorem below.

Theorem A.3.1 (Likelihood Process - Björk [4]) *Consider a filtered probability space $(\Omega, \mathcal{F}, P, \underline{\mathcal{F}})$ on a compact interval $[0, T]$. Suppose that L_T is some nonnegative integrable random variable in $\mathcal{F}_T$. We can then define a new measure Q on $\mathcal{F}_T$ by setting*

$$dQ = L_T dP, \text{ on } \mathcal{F}_T,$$

and if

$$E^P[L_T] = 1,$$

the measure will also be a probability measure.

From its definition, L_T will be the Radon-Nikodym derivative of Q w.r.t. P on $\mathcal{F}_T$ so $Q << P$ on $\mathcal{F}_T$. Hence we will also have $Q << P$ on $\mathcal{F}_t$ for all $t \leq T$ and thus, by the Radon-Nikodym Theorem (A.1.1), there will exist a random process $L_t; 0 \leq t \leq T$ defined by

$$L_t = \frac{dQ}{dP}, \text{ on } \mathcal{F}_t.$$

The L process is defined as the likelihood process for the measure transformation from P to Q and is a $(P, \underline{\mathcal{F}})$ martingale.

A.4 The Martingale Approach to Arbitrage Theory

The martingale approach to financial derivatives is defined by Björk [4] as the most general approach for arbitrage pricing. Furthermore, this approach is also very efficient from a computational point of view.

Some of the arbitrage pricing concepts were already introduced in Section 3.2.1. This section will present theorems relating to market completeness and the impact of this on the price of a derivative.

Theorem A.4.1 (Market Completeness - Björk [4]) *A T-claim X can be replicated, alternatively it is reachable or hedgeable, if there exists a self-financing portfolio h such that*

$$V^h(T) = X, P - a.s.$$

In this case we say that h is a hedge against X. Alternatively, h is called a replicating or hedging portfolio. If every contingent claim is reachable we say that the market is complete.

Theorem A.4.2 (Second Fundamental Theorem - Björk [4]) *Assuming absence of arbitrage, the market is complete if and only if the martingale measure Q is unique.*

This then translates into the theorem presented below.

Theorem A.4.3 (Uniqueness of a Derivative Price - Björk [4]) *Different choices of Q will generically give rise to different price processes for a fixed claim X. However, if X is attainable then all choices of Q will produce the same price process, which then is given by*

$$\Pi(t; X) = V(t; h),$$

where h is the hedging portfolio. Different choices of hedging portfolios (if such exist) will produce the same price process.

A.5 Correlated Wiener Processes

We will consider how to define correlated Wiener processes. The arguments presented below were taken from the book by Björk [4]. In order to do this consider d independent standard (i.e. unit variance) Wiener processes $\overline{W}_1, \ldots, \overline{W}_d$. Furthermore, let a (deterministic and constant) matrix

$$C = \begin{bmatrix} c_{11} & c_{12} & \cdots & c_{1d} \\ c_{21} & c_{22} & \cdots & c_{2d} \\ \vdots & \vdots & \ddots & \vdots \\ c_{n1} & c_{n2} & \cdots & c_{nd} \end{bmatrix}$$

be given, and consider the $n-$dimensional process W, defined by

$$W = C\overline{W},$$

where

$$W = \begin{bmatrix} W_1 \\ \vdots \\ W_n \end{bmatrix}.$$

If we now assume that the rows of C have unit length, then it is evident that each of the elements of W are standard (i.e. unit variance) Wiener processes. Hence, we obtain the following

$$\begin{aligned} \rho_{ij}dt &= Cov[dW_i, dW_j] \\ &= E[dW_i \cdot dW_j] \\ &= E\left[\sum_{k=1}^{d} c_{ik}d\overline{W}_k \cdot \sum_{l=1}^{d} c_{jl}d\overline{W}_l\right] \end{aligned}$$

However, since $\overline{W}_1, \ldots, \overline{W}_N$ are assumed to be independent standard Wiener processes, we have that

$$\begin{aligned} \rho_{ij}dt &= \sum_{kl} c_{ik}c_{jl}E[d\overline{W}_k \cdot d\overline{W}_l] \\ &= C_i C_j' dt, \end{aligned}$$

i.e.

$$\rho = CC'.$$

A.6 Black's Model for European Options

Black's model for the pricing of European style options is given by Hull [32] below. This model is based on the model by Fischer Black [5] for valuing options on commodity futures. In this model, the underlying is assumed to be the forward price of an instrument as opposed to the spot price.

Theorem A.6.1 (Black's Model - Hull [32]) *Assume that the value of the underlying variable (to the forward contract) is given by V. The first case we will consider is the pricing of a European call option. In order to do this we need to define the following variables:*

T : *Time to maturity of the option*
F : *Forward price of* V *for a contract with maturity* T
F_0 : *Value of* F *at time zero*
K : *Strike of the option*
$P(t,T)$: *Price at time* t *of a zero-coupon bond paying one monetary unit at time* T
V_T : *Value of* V *at time* T
σ : *Volatility of* F

We have that the expected payoff of at time T *is given by*

$$E(V_T)N(d_1) - KN(d_2)$$

where $E(V_T)$ *is the expected value of* V_T *and*

$$\begin{aligned} d_1 &= \frac{ln[E(V_T)/K] + \sigma^2 T/2}{\sigma\sqrt{T}} \\ d_2 &= \frac{ln[E(V_T)/K] - \sigma^2 T/2}{\sigma\sqrt{T}} \\ &= d_1 - \sigma\sqrt{T}. \end{aligned}$$

Given $E(V_T) = F_0$, *we have that the value of the option is*

$$c = P(0,T)[F_0 N(d_1) - KN(d_2)]$$

where

$$\begin{aligned} d_1 &= \frac{ln[F_0/K] + \sigma^2 T/2}{\sigma\sqrt{T}} \\ d_2 &= \frac{ln[F_0/K] - \sigma^2 T/2}{\sigma\sqrt{T}} \\ &= d_1 - \sigma\sqrt{T}. \end{aligned}$$

The value of the corresponding put option is given by

$$p = P(0,T)[KN(-d_2) - F_0 N(-d_1)].$$

Appendix B

Derived Results

B.1 Forward Swap Rates

A forward swap rate is per definition the rate of the fixed leg of an interest rate swap that will ensure that the present value of the fixed leg will be equal to the present value of the floating leg of the swap. The derivation of this result, as presented below, follows the same arguments as given by Gatarek, Bachert and Maksymiuk [21].

Consider an interest rate swap that starts at T_s and ends at T_N. Then we have that the present value of the floating leg of the swap is given by

$$PV(\text{Floating Leg}) = \sum_{i=s+1}^{N} B(T_0, T_i) L_{T_{i-1}T_i}(T_0) \alpha_{T_{i-1}T_i},$$

and similarly the present value of the fixed leg of the swap is given by

$$PV(\text{Fixed Leg}) = \sum_{i=s+1}^{N} B(T_0, T_i) SR_{s,N}(T_0) \alpha_{T_{i-1}T_i}.$$

Now we can determine the swap rate through equating the present value of the fixed leg to the present value of the floating leg, i.e.

$$\sum_{i=s+1}^{N} B(T_0, T_i) L_{T_{i-1}T_i}(T_0) \alpha_{T_{i-1}T_i} = \sum_{i=s+1}^{N} B(T_0, T_i) SR_{s,T}(T_0) \alpha_{T_{i-1}T_i},$$

or

$$SR_{s,N}(T_0) = \frac{\sum_{i=s+1}^{N} B(T_0, T_i) L_{T_{i-1}T_i}(T_0) \alpha_{T_{i-1}T_i}}{\sum_{i=s+1}^{N} B(T_0, T_i) \alpha_{T_{i-1}T_i}}.$$

Using Equation (4.1.3) we can write above expression as

$$\begin{aligned} SR_{s,N}(T_0) &= \frac{\sum_{i=s+1}^{N}(B(T_0,T_{i-1})-B(T_0,T_i))}{\sum_{i=s+1}^{N}B(T_0,T_i)\alpha_{T_{i-1}T_i}} \\ &= \frac{B(T_0,T_s)-B(T_0,T_N)}{\sum_{i=s+1}^{N}B(T_0,T_i)\alpha_{T_{i-1}T_i}}. \end{aligned}$$

The forward swap rate $SR_{s,N}(T_0)$ will be used to determine strikes for ATM caps.

B.2 Recovering Black's Formula for Caplets in the LMM

This section will follow the work presented by Björk [4] and Götsch [22].

In the LMM we assume that the dynamics of $L_{T_iT_{i+1}}(t)$ under Q^{i+1} is given by

$$dL_{T_iT_{i+1}}(t) = \sigma_{T_iT_{i+1}}(t)L_{T_iT_{i+1}}(t)dW^{i+1}(t).$$

Firstly we will derive the distributional properties of $L_{T_iT_{i+1}}(t)$ as done in Götsch [22]. Using the Taylor expansion, we can obtain the dynamics of $\ln L_{T_iT_{i+1}}(t)$ as given below

$$\begin{aligned} d\ln L_{T_iT_{i+1}}(t) &= \frac{1}{L_{T_iT_{i+1}}(t)}dL_{T_iT_{i+1}}(t) - \frac{1}{2}\frac{1}{(L_{T_iT_{i+1}}(t))^2}(dL_{T_iT_{i+1}}(t))^2 \\ &= \sigma_{T_iT_{i+1}}(t)dW^{i+1}(t) - \frac{1}{2}\sigma^2_{T_iT_{i+1}}(t)dt \end{aligned}$$

Integrating both sides yields

$$L_{T_iT_{i+1}}(T) = L_{T_iT_{i+1}}(0)\exp\left\{-\frac{1}{2}\int_0^T \sigma^2_{T_iT_{i+1}}(t)dt + \int_0^T \sigma_{T_iT_{i+1}}(t)dW^{i+1}(t)\right\}.$$

The expression in the exponent is normally distributed, with the following properties

$$E\left[-\frac{1}{2}\int_0^T \sigma^2_{T_iT_{i+1}}(t)dt + \int_0^T \sigma_{T_iT_{i+1}}(t)dW^{i+1}(t)\right] = -\frac{1}{2}\int_0^T \sigma^2_{T_iT_{i+1}}(t)dt,$$

and

$$Var\left[-\frac{1}{2}\int_0^T \sigma^2_{T_iT_{i+1}}(t)dt + \int_0^T \sigma_{T_iT_{i+1}}(t)dW^{i+1}(t)\right] = \int_0^T \sigma^2_{T_iT_{i+1}}(t)dt.$$

Hence, we have that $L_{T_iT_{i+1}}(T)$ is log normally distributed. The next part of the derivation will follow arguments given in Björk [4]. Consider the payoff of a caplet as given below

$$\text{payoff} = \alpha_{T_iT_{i+1}}(L_{T_iT_{i+1}}(T_i) - X)^+$$

or

$$\text{payoff} = \alpha_{T_iT_{i+1}}(L_{T_iT_{i+1}}(T_i) - X).I\{L_{T_iT_{i+1}}(T_i) \geq X\}$$

where

$$I\{L_{T_iT_{i+1}}(T_i) \geq X\} = \begin{cases} 1 & \text{if } L_{T_iT_{i+1}}(T_i) \geq X, \\ 0 & \text{if } L_{T_iT_{i+1}}(T_i) < X. \end{cases}$$

We know that the price of above claim is given by its discounted expected value. In order to derive an arbitrage-free price we can use Theorem 3.2.4 and obtain the following under the T^{i+1} forward measure

$$\begin{aligned} &\text{Cpl}^{LMM} \\ &= B(0,T_{i+1})E^{i+1}[\alpha_{T_iT_{i+1}}(L_{T_iT_{i+1}}(T_i) - X).I\{L_{T_iT_{i+1}}(T_i) \geq X\}] \\ &= B(0,T_{i+1})\alpha_{T_iT_{i+1}}(E^{i+1}[L_{T_iT_{i+1}}(T_i).I\{L_{T_iT_{i+1}}(T_i) \geq X\}] \\ &- E^{i+1}[X.I\{L_{T_iT_{i+1}}(T_i) \geq X\}]) \end{aligned}$$

Firstly, consider the expectation

$$E^{i+1}[X.I\{L_{T_iT_{i+1}}(T_i) \geq X\}].$$

We can calculate this as given below

$$\begin{aligned} &E^{i+1}[X.I\{L_{T_iT_{i+1}}(T_i) \geq X\}] \\ =&XP^{i+1}[L_{T_iT_{i+1}}(T_i) \geq X] \\ =&XP^{i+1}\left[Z \leq \frac{\ln\left(\frac{L_{T_iT_{i+1}}(0)}{X}\right) - \frac{1}{2}\int_0^{T_i}\sigma^2_{T_iT_{i+1}}(t)dt}{\sqrt{\int_0^{T_i}\sigma^2_{T_iT_{i+1}}(t)dt}}\right], \end{aligned}$$

where Z is a standard normally distributed random variable. Let $N(x)$ indicate the cumulative probability distribution function for a standardized normal distribution. Then we can write above expectation as

$$E^{i+1}[X.I\{L_{T_iT_{i+1}}(T_i) \geq X] = XN(d_2),$$

where

$$d_2 = \frac{\ln\left(\frac{L_{T_iT_{i+1}}(0)}{X}\right) - \frac{1}{2}\int_0^{T_i}\sigma^2_{T_iT_{i+1}}(t)dt}{\sqrt{\int_0^{T_i}\sigma^2_{T_iT_{i+1}}(t)dt}}.$$

Now, let us consider the expression

$$B(0,T_{i+1})E^{i+1}[L_{T_iT_{i+1}}(T_i).I\{L_{T_iT_{i+1}}(T_i) \geq X\}].$$

In order to calculate the above expression, we will change the numeraire from $B(t,T_{i+1})$ to $B(t,T_i) - B(t,T_{i+1})$. Using Proposition 3.2.4, we have that

$$\begin{aligned} &B(0,T_{i+1})E^{i+1}[L_{T_iT_{i+1}}(T_i).I\{L_{T_iT_{i+1}}(T_i) \geq X\}] \\ =&\frac{1}{\alpha_{T_iT_{i+1}}}(B(0,T_i) - B(0,T_{i+1}))E^*[I\{L_{T_iT_{i+1}}(T_i) \geq X\}] \\ =&B(0,T_{i+1})L_{T_iT_{i+1}}(0)E^*[I\{L_{T_iT_{i+1}}(T_i) \geq X\}], \end{aligned}$$

since we know that

$$\alpha_{T_iT_{i+1}} L_{T_iT_{i+1}}(t) = \frac{B(t,T_i) - B(t,T_{i+1})}{B(t,T_{i+1})}.$$

Note that the expectation E^* relates to the martingale measure under which the process $1/L_{T_iT_{i+1}}(T_i)$ is a martingale. Using Taylor, we can obtain the dynamics of $1/L_{T_iT_{i+1}}(T_i)$ as

$$\begin{aligned} d\frac{1}{L_{T_iT_{i+1}}(T_i)} &= -\frac{1}{(L_{T_iT_{i+1}}(T_i))^2} dL + \frac{1}{(L_{T_iT_{i+1}}(T_i))^3}(dL)^2 \\ &= -\frac{1}{L_{T_iT_{i+1}}(T_i)} \sigma_{T_iT_{i+1}}(t) dW^*(t). \end{aligned}$$

Similarly to the start of the section, we can express $1/L_{T_iT_{i+1}}(T_i)$ as

$$\frac{1}{L_{T_iT_{i+1}}(T)} = \frac{1}{L_{T_iT_{i+1}}(0)} \exp\left\{ -\frac{1}{2}\int_0^T \sigma^2_{T_iT_{i+1}}(t)dt - \int_0^T \sigma_{T_iT_{i+1}}(t) dW^*(t) \right\}$$

Finally, we can write

$$\begin{aligned} & B(0,T_{i+1}) L_{T_iT_{i+1}}(0) E^*[I\{L_{T_iT_{i+1}}(T_i) \geq X\}] \\ =& B(0,T_{i+1}) L_{T_iT_{i+1}}(0) P^*[L_{T_iT_{i+1}}(T_i) \geq X] \\ =& B(0,T_{i+1}) L_{T_iT_{i+1}}(0) P^*\left[\frac{1}{L_{T_iT_{i+1}}(T_i)} \leq \frac{1}{X}\right] \\ =& B(0,T_{i+1}) L_{T_iT_{i+1}}(0) P^*\left[Z \leq \frac{\ln\left(\frac{L_{T_iT_{i+1}}(0)}{X}\right) + \frac{1}{2}\int_0^{T_i} \sigma^2_{T_iT_{i+1}}(t)dt}{\sqrt{\int_0^{T_i} \sigma^2_{T_iT_{i+1}}(t)dt}}\right] \\ =& B(0,T_{i+1}) L_{T_iT_{i+1}}(0) N(d_1), \end{aligned}$$

where

$$d_1 = \frac{\ln\left(\frac{L_{T_iT_{i+1}}(0)}{X}\right) + \frac{1}{2}\int_0^{T_i} \sigma^2_{T_iT_{i+1}}(t)dt}{\sqrt{\int_0^{T_i} \sigma^2_{T_iT_{i+1}}(t)dt}}.$$

Hence, we have that

$$\text{Cpl}^{LMM} = B(0,T_{i+1}) \alpha_{T_iT_{i+1}} [L_{T_iT_{i+1}}(0) N(d_1) - X N(d_2)],$$

which is very similar as that given by Black's formula (see Section A.6). The only difference is in the calculation of $d_{1,2}$. The term $d_{1,2}$ in Black's formula is given by

$$d_{1,2} = \frac{\ln\left(\frac{L_{T_iT_{i+1}}(0)}{X}\right) \pm \frac{1}{2} T_i \sigma^2_{T_iT_{i+1}.\text{caplet}}}{\sqrt{T_i \sigma^2_{T_iT_{i+1}.\text{caplet}}}},$$

while it is given by the LMM as

$$d_{1,2} = \frac{\ln\left(\frac{L_{T_iT_{i+1}}(0)}{X}\right) \pm \frac{1}{2}\int_0^{T_i} \sigma^2_{T_iT_{i+1}}(t)dt}{\sqrt{\int_0^{T_i} \sigma^2_{T_iT_{i+1}}(t)dt}}.$$

Comparing the last two expressions gives us a relationship between the Black and LMM caplet volatility:

$$T_i\sigma^2_{T_iT_{i+1}.\text{caplet}} = \int_0^{T_i} \sigma^2_{T_iT_{i+1}}(t)dt.$$

B.3 Recovering Black's Formula for Swaptions in the Swap-Rate-Based LMM

This section briefly discuss a different approach to deriving the volatility relationship between the Black and market model.

Firstly, instead of choosing a forward bond price as numeraire (see Section B.2), we will choose the associated annuity $A_{n,N}$ as the numeraire (it can be seen that this is a combination of traded assets). This will then imply that the swap rate will be a martingale under this measure (called the forward swap measure) and hence we can write that

$$dSR_{n,N}(t) = \sigma_{n,N}(t)SR_{n,N}(t)dW^{n,N}(t).$$

Applying Taylor expansions and integrating on both sides of the equation (as illustrated in B.2) one can obtain the following

$$SR_{n,N}(T) = SR_{n,N}(0)\exp\left\{-\frac{1}{2}\int_0^T \sigma^2_{n,N}(t)dt + \int_0^T \sigma_{n,N}(t)dW^{n,N}(t)\right\}.$$

The expression in the exponent is normally distributed, with the following properties

$$E\left[-\frac{1}{2}\int_0^T \sigma^2_{n,N}(t)dt + \int_0^T \sigma_{n,N}(t)dW^{n,N}(t)\right] = -\frac{1}{2}\int_0^T \sigma^2_{n,N}(t)dt,$$

and

$$Var\left[-\frac{1}{2}\int_0^T \sigma^2_{n,N}(t)dt + \int_0^T \sigma_{n,N}(t)dW^{n,N}(t)\right] = \int_0^T \sigma^2_{n,N}(t)dt.$$

Consider a swaption in which gives the holder the right to pay a fixed rate X, then the payoff consists of a series of cash flows equal to (see Hull [32])

$$\text{payoff} = \alpha_{T_iT_{i+1}}(SR_{n,N}(T_n) - X)^+.$$

The value of this payoff can then easily be calculated from first principles. The results are given below

$$\alpha_{T_iT_{i+1}} B(0,T_{i+1})[SR_{n,N}(0)N(d_1) - XN(d_2)],$$

where

$$d_{1,2} = \frac{\ln\left(\frac{SR_{n,N}(0)}{X}\right) \pm \frac{1}{2}\int_0^{T_n} \sigma_{n,N}^2(t)dt}{\sqrt{\int_0^{T_n} \sigma_{n,N}^2(t)dt}}.$$

If we once again compare with the Black equivalent

$$d_{1,2} = \frac{\ln\left(\frac{SR_{n,N}(0)}{X}\right) \pm \frac{1}{2}T_n V_{n,N}^2}{\sqrt{T_n V_{n,N}^2}},$$

then we can deduce that

$$T_n V_{n,N}^2 = \int_0^{T_n} \sigma_{n,N}^2(t)dt.$$

Appendix C

Matlab Code

This chapter will provide the Matlab code used in applications throughout this thesis. The code is presented in order to allow the reader to replicate some of the results and hence to allow a better understanding of the actual calculations needed in the implementation of the model.

C.1 Volatility Calibration

Volatility calibration was discussed in Chapter 9. It was shown that some of the calibration algorithms require minimization routines (and may even require numerical integration). Instead of creating the required routines, this thesis used some of the routines available in Matlab.

Similar to the rest of the thesis, we will present the code separately for the European and South African Markets. The actual code for each of these markets are presented in the sections below.

C.1.1 Calibrating to European Market Data

The market data used for this calibration is contained in the code below. The data was taken from the text by Gatarek, Bachert and Maksymiuk [21] and is presented in Chapter 7.

C.1.1.1 Separable Volatility Specification

The code used in this calibration routine consists of two user defined functions. The first function (or procedure in this specific case), minimizes an user defined function "PARTimeHomEUR" through using the Matlab defined function *lsqnonlin* (function for nonlinear least-squares problems). Furthermore, this first procedure was constructed such that this process starts the minimization process at a number of different starting points (specified according to user, results presented in this thesis used 50 different starting points). This gener-

ally allows for better results, especially if the objective function is complex of nature. This function is presented in the Matlab code below.

```
function x = LoopPARTimeHomEUR(n)

%increase number of function evaluations
options = optimset('MaxFunEvals',10000);

%choose initial point
x0 = [0.1;0.1;0.1;0.1];
%empty upper and lower bounds
lb=[];ub=[];

%perform first optimazation
[vect,fval] = lsqnonlin(@PARTimeHomEUR,x0,lb,ub,options);
fval %show intermediate results

for i=1:n
    i %included to show where in process

    %generate random starting points from
    %Uniform distrubution, allows for a
    %better aproximation of the global
    %minimum
    x0=unifrnd(-1,1,4,1);

    [vect2,fval2] = lsqnonlin(@PARTimeHomEUR,x0,lb,ub,options);

    fval2 %show intermediate results

    %at each step of the procedure we need to check if the new
    %starting point resulted in a lower function value
    if fval2 < fval
        vect = vect2;
        fval = fval2;
    end
end

vect %show optimal vector
x=fval;
end
```

The procedure presented above repeatedly references the function "PARTime-HomEUR". This function in turn represents the fitting of a time-homogeneous

function to a set of market given volatilities. The Matlab code for this function is given below.

```
function x = PARTimeHomEUR(x0)

%define input variables
v1 = x0(1,1);
v2 = x0(2,1);
v3 = x0(3,1);
v4 = x0(4,1);
YearFrac = [0;0.25;0.5028;0.7583;1.0139;1.2639;1.5167;1.7722;
            2.0278;2.2778;2.5306;2.7861;3.0417;3.2944;3.5472;
            3.8083;4.0611;4.3139;4.5667;4.8194;5.0722;5.3250;
            5.5778;5.8306;6.0861;6.3361;6.5889;6.8444;7.1000;
            7.3528;7.6056;7.8611;8.1167;8.3667;8.6194;8.8750;
            9.1361;9.3806;9.6333;9.8944;10.1472];
CaplVol = [0.1641;0.1641;0.1641;0.2015;0.2189;0.2365;0.2550;
           0.2212;0.2255;0.2298;0.2341;0.2097;0.2083;0.2077;
           0.2051;0.2007;0.1982;0.1959;0.1938;0.1925;0.1902;
           0.1879;0.1859;0.1844;0.1824;0.1804;0.1781;0.1766;
           0.1743;0.1724;0.1700;0.1677;0.1657;0.1637;0.1622;
           0.1623;0.1612;0.1599;0.1570];

%declare variables to be used in calculations
IntVol = zeros(39,1);
ResVol = zeros(39,1);
C = zeros(39,1);
B = zeros(39,1);
mtrx = zeros(39,39);

    for i = 1:39
        sum2 = 0;
        Ti = YearFrac(i+1,1);
        for j = 1:i
            Tj = YearFrac(j+1,1);
            Tprev = YearFrac(j,1);
            mtrx(i,j) =
            quad(@(t)RebTH(t,v1,v2,v3,v4,Ti),Tprev,Tj);
            sum2 = sum2 + mtrx(i,j);
        end
        IntVol(i,1) = sum2;
        B(i,1) =
        sqrt((YearFrac(i+1,1)*CaplVol(i,1)^2)/IntVol(i,1));
    end
```

```
sum = 0;

    for i = 1:39
        ResVol(i,1) = YearFrac(i+1,1)*CaplVol(i,1)^2
                    - IntVol(i,1);
        sum = sum + (YearFrac(i+1,1)*CaplVol(i,1)^2
            - IntVol(i,1))^2;
        C(i,1) = sqrt(IntVol(i,1)/YearFrac(i+1,1));
    end
    x = ResVol;
C; %can be used for vol graph
B; %factors needed for exact pricing of market caps

end
```

Note the definition of the vector B in the code presented above. This provides the scaling factors necessary to price back exactly to the given set of caplet prices. Furthermore, the vector C provides the model implied caplet volatilities which can be used to compare to the market given data. The code for the function "RebTH" is presented below (time-homogeneous function proposed by Rebonato [47]).

```
function y = RebTH(t,v1,v2,v3,v4,Ti)
y = (v1+(v2+v3*((Ti-t))).*exp(-v4*((Ti-t)))).^2;
end
```

A significant amount of emphasis is placed on the calibration of the model while ensuring a time homogeneous evolution of the term structure of volatilities. Following the calibration process, it is important to consider the evolution of the term structure as predicted by the model. In order to perform this analysis, we can run the code given below.

```
function x = PARTermStructEvolEUR()

%define input variables
YearFrac = [0;0.25;0.5028;0.7583;1.0139;1.2639;1.5167;1.7722;
            2.0278;2.2778;2.5306;2.7861;3.0417;3.2944;3.5472;
            3.8083;4.0611;4.3139;4.5667;4.8194;5.0722;5.3250;
            5.5778;5.8306;6.0861;6.3361;6.5889;6.8444;7.1000;
            7.3528;7.6056;7.8611;8.1167;8.3667;8.6194;8.8750;
            9.1361;9.3806;9.6333;9.8944;10.1472];

%set parameters of the time-homogeneous function equal to the
```

```
%values obtained from the minimization step
x0 = [0.112313592812041;-0.047580086207463;0.471041078023537;
      1.044461507040869];

v1 = x0(1,1);
v2 = x0(2,1);
v3 = x0(3,1);
v4 = x0(4,1);

%set the forward rate function equal to the constant values
%obtained from the minimization step
B = [1.328395061;0.989406727;0.844746596;0.949471864;
     0.983095912;1.036196499;1.106831117;0.960950532;
     0.986836244;1.017429591;1.051602673;0.957323067;
     0.967058399;0.980967328;0.98600271;0.981295579;
     0.98519002;0.989454161;0.994060022;1.002147283;
     1.00436107;1.005823979;1.008167147;1.012693546;
     1.013560992;1.013904699;1.012020248;1.0140724;
     1.010833759;1.009337779;1.004452614;0.999599303;
     0.995837872;0.991697402;0.99024625;0.998402896;
     0.998429587;0.997125657;0.985670182;1;1;1;1;1;1;
     1;1;1;1;1;1;1;1;1;1;1;1;1;1;1;1;1;1;1;1;1;1;1;1;
     1;1;1;1;1;1;1;1;1;1;1;1;1;1;1;1;1;1;1;1;1;1;1;1;1];

%declare variable to be used in calculations
volEvol=zeros(39,39);

for k=1:39
    for i = 1:39
        sum2 = 0;
        Ti = YearFrac(i+1,1);
        for j = 1:i
            Tj = YearFrac(j+1,1);
            Tprev = YearFrac(j,1);
            sum2 = sum2 +
            quad(@(t)RebTH(t,v1,v2,v3,v4,Ti),Tprev,Tj)
            *(B(i+k-1,1)^2);
        end
        volEvol(i,k) = sqrt(sum2/YearFrac(i+1,1));
    end
end
   x = volEvol;

end
```

C.1.1.2 Multi-Time Dependence Volatility Specification

This section will extend the code presented in the previous case through the inclusion of a time dependent component in the function "PARTimeHomEUR". The motivation for this extension was discussed in Section 9.2.2. Calibrating the model under this specification will require a two step approach and is briefly discussed below.

The first part of the calibration strategy under this methodology is still to fit a time-homogeneous function to the given market data using the code presented in Section C.1.1.1. This will result in an optimal set of parameters for the time-homogeneous function "RebTH".

The second part of the calibration will introduce a purely time dependent function while fixing the parameters of the function "RebTH" at the values obtained in the previous step. Given the specification of the time dependent function, we will use the numerical integration function (Matlab defined) *quadgk* as opposed to *quad*. This new function is more efficient for oscillatory integrands.

The code for the second part of the calibration is presented below (results presented in this thesis used 100 different starting points).

```
function x = LoopPARTimeHomEURStep2(n)

%increase number of function evaluations
options = optimset('MaxFunEvals',10000);

%choose initial point
x0 = [0.1;0.1;0.1;0.1;0.1;0.1];
%empty upper and lower bounds
lb=[];ub=[];
%perform first optimazation
[vect,fval] = lsqnonlin(@PARTimeHomEURStep2,x0,lb,ub,options);
fval %show intermediate results

for i=1:n
    i %included to show where in process

    %generate random starting points from
    %Uniform distribution
    x0=unifrnd(-1,1,6,1);

    [vect2,fval2] =
    lsqnonlin(@PARTimeHomEURStep2,x0,lb,ub,options);

    fval2 %show intermediate results
```

```
    %assignment statement
    if fval2 < fval
        vect = vect2;
        fval = fval2;
    end
end

vect %show optimal vector
x=fval;

end
```

This code is almost similar to the code presented in Section C.1.1.1. The only difference is the inclusion of two additional parameters. Next, let us consider the specification of the function "PARTimeHomEURStep2". This is presented in the code below.

```
function x = PARTimeHomEURStep2(e0)

%define input variables
e1 = e0(1,1);
e2 = e0(2,1);
e3 = e0(3,1);
e4 = e0(4,1);
e5 = e0(5,1);
e12 = e0(6,1);

YearFrac = [0;0.25;0.5028;0.7583;1.0139;1.2639;1.5167;1.7722;
            2.0278;2.2778;2.5306;2.7861;3.0417;3.2944;3.5472;
            3.8083;4.0611;4.3139;4.5667;4.8194;5.0722;5.3250;
            5.5778;5.8306;6.0861;6.3361;6.5889;6.8444;7.1000;
            7.3528;7.6056;7.8611;8.1167;8.3667;8.6194;8.8750;
            9.1361;9.3806;9.6333;9.8944;10.1472];
CaplVol = [0.1641;0.1641;0.1641;0.2015;0.2189;0.2365;0.2550;
           0.2212;0.2255;0.2298;0.2341;0.2097;0.2083;0.2077;
           0.2051;0.2007;0.1982;0.1959;0.1938;0.1925;0.1902;
           0.1879;0.1859;0.1844;0.1824;0.1804;0.1781;0.1766;
           0.1743;0.1724;0.1700;0.1677;0.1657;0.1637;0.1622;
           0.1623;0.1612;0.1599;0.1570];

%set parameters of the time-homogeneous function equal to the
%values obtained from the previous step
x0 = [0.112313592812041;-0.047580086207463;0.471041078023537;
```

```
     1.044461507040869];
v1 = x0(1,1);
v2 = x0(2,1);
v3 = x0(3,1);
v4 = x0(4,1);

%declare variables to be used in calculations
IntVol = zeros(39,1);
ResVol = zeros(39,1);
C = zeros(39,1);
B = zeros(39,1);
mtrx = zeros(39,39);

    for i = 1:39
        sum2 = 0;
        Ti = YearFrac(i+1,1);
        for j = 1:i
            Tj = YearFrac(j+1,1);
            Tprev = YearFrac(j,1);
            mtrx(i,j) = quadgk(@(t)RebTHTD(t,v1,v2,v3,v4,
            e1,e2,e3,e4,e5,e12,Ti),Tprev,Tj);
            sum2 = sum2 + mtrx(i,j);
        end
        IntVol(i,1) = sum2;
        B(i,1) =
        sqrt((YearFrac(i+1,1)*CaplVol(i,1)^2)/IntVol(i,1));
    end

sum = 0;

    for i = 1:39
        ResVol(i,1) = YearFrac(i+1,1)*CaplVol(i,1)^2
                    - IntVol(i,1);
        sum = sum + (YearFrac(i+1,1)*CaplVol(i,1)^2
            - IntVol(i,1))^2;
        C(i,1) = sqrt(IntVol(i,1)/YearFrac(i+1,1));
    end
    x = ResVol;
C; %can be used for vol graph
B; %factors needed for exact pricing of market caps

end
```

From the previous section we know that the vector B contains the scaling

factors necessary to price back exactly to the given set of caplet prices. Similarly, the vector C provides the model implied caplet volatilities which can be used to compare to the market given data. The only remaining part is the specification of the function "RebTHTD". This is presented below.

```
function y = RebTHTD(t,v1,v2,v3,v4,e1,e2,e3,e4,e5,e12,Ti)
y = ((v1+(v2+v3*((Ti-t))).*exp(-v4*((Ti-t)))).*((e1*
    sin(t*pi/10.1472+e2)+e2*sin(2*t*pi/10.1472+e3)+e3*
    sin(3*t*pi/10.1472+e4)+e4*sin(4*t*pi/10.1472+e5)).
    *exp(-e12*t))).^2;
end
```

It is worth making a short comment regarding the integrand defined in the code above. Instead of using a piecewise constant approach, the code above defines the integrand as a product of the time-homogeneous and time dependent parts. An alternative would be to define the time-homogeneous part outside the integral given this was determined in the first step. This approach is however less accurate and is not advised given the simplicity of the more accurate approach.

C.1.2 Calibrating to South African Market Data

The market data used for this calibration is contained in the code below. It was explained in detail in Chapter 8 how one can obtain a similar set from data sources such as Bloomberg.

C.1.2.1 Volatilities Depending on Time to Maturity

The actual calibration of the model under this specification was performed in Excel (due to the simplicity of the calculations) and hence we will not present the code for this calculation. The reader is referred to the detailed examples on the European market and the explanation in Section 9.1.1 for more information. This section will only provide the Matlab code that can be used to obtain the evolution of the term structure as we move through time (and consequently will contain the set of results as obtained in the calibration process).

```
function x = PARTermStructEvolSAMethod1()

%define input variables
YearFrac = [0;0.25;0.5;0.75;1;1.25;1.5;1.75;2;2.25;2.5;2.75;
            3;3.25;3.5; 3.75;4;4.25;4.5;4.75;5;5.25;5.5;5.75;
            6;6.25;6.5;6.75;7;7.25;7.5;7.75;8;8.25;8.5;8.75;
            9;9.25;9.5;9.75;10];
```

```
%the eta vector represent results of calibration
eta = [0.1251800000;0.1532304924;0.1803754778;0.1871761021;
       0.1713349996;0.1743498922;0.1754008774;0.2020176794;
       0.1230860516;0.1116119389;0.1033796353;0.1456600865;
       0.1067115833;0.0857576387;0.0673245282;0.1623817727;
       0.0754984185;0.0643623492;0.0477174685;0.1271469638;
       0.1072366752;0.1040128228;0.0985508929;0.1576069266;
       0.1009819830;0.0999304003;0.0931857425;0.1515116167;
       0.0965187676;0.0935643655;0.0913928914;0.1417441540;
       0.0891580170;0.0809256066;0.0913776855;0.1850756775;
       0.0880548857;0.0906366907;0.0715590840;0.1842219273];

%declare variables to be used in calculations
forwMatrx=zeros(40,40);
volEvol=zeros(40,40);

%create matrix containing volatilities of forward rates
for i = 1:40
    for j = 1:i
        forwMatrx(i, j) = eta(i-j+1,1);
    end
end

%calculate evolution of term structure
for k=1:40
    for i = k:40
        sum2 = 0;
        Ti = YearFrac(i-k+1+1,1);
        for j = k:40
            sum2 = sum2 + forwMatrx(i,j)^2*0.25;
        end
        volEvol(i-k+1,k) = sqrt(sum2/Ti);

    end
end
   x = volEvol;

end
```

C.1.2.2 Separable Volatility Specification

The code presented below is very similar to that presented in Section C.1.1.1. There are small differences with respect to the optimization routines (constrained vs. unconstrained used in the previous sections) and integration (use

an analytical formula as opposed to numerical integration). The core dynamics however remained relatively the same.

```
function [Fval,Fvect] = LoopPARTimeHomSA(n)

%increase number of function evaluations
options = optimset('MaxFunEvals',10000);

%choose initial point
x0 = [0.1;0.1;0.1;0.1];

%specify different constraints
A=[-1,-1,0,0;-1,0,0,0;0,0,0,-1];
b=[-0.08;-0.00001;-0.00001];
Aeq = [];beq = [];lb = []; ub = [];

%perform first optimization
[vect,fval] = fmincon(@PARTimeHomSA,x0,A,b,Aeq,beq,lb,ub,
              @nonLinConSA,options);
fval %show intermediate results

for i=1:n
    iter = i %included to show where in process
    bestEst = fval %included to show best value obtained
                   %thus far

    %generate random starting points from Uniform
    %distribution, allows for a better approximation
    %of the global minimum. Points generated adhere
    %to constraints defined above
    x0(1,1) = unifrnd(0,2,1,1);
    x0(4,1) = unifrnd(0,2,1,1);
    x0(3,1) = unifrnd(-1,1,1,1);

    x0(2,1) = unifrnd(-3,3,1,1);
    while (x0(1,1)+x0(2,1)) < 0
        x0(2,1) = unifrnd(-3,3,1,1);
    end
    [vect2,fval2] = fmincon(@PARTimeHomSA,x0,A,b,Aeq,beq,lb,
                    ub,@nonLinConSA,options);

    fval2 %show intermediate results

    %at each step of the procedure we need to check if the
```

```
    %new starting point resulted in a lower function value
    if fval2 < fval
        vect = vect2;
        fval = fval2;
    end
end

Fval=fval; %returns optimal value
Fvect = vect; %returns optimal vector
end
```

Nonlinear constraints are defined through the function "nonLinConSA". The problem at hand only require nonlinear inequality constraints (instead of restricting functions of the parameters, for example location of hump, to a specific value, i.e. equality constraints, the algorithm restricts it to a certain range). This is defined in the function below.

```
function [c,ceq] = nonLinConSA(x)

%define input variables
a=x(2,1);
b=x(3,1);
c=x(4,1);
d=x(1,1);

%define nonlinear inequality and equality constraints
c=abs(1-(b-c*a)/(c*b))-0.1;
ceq = [];

end
```

The definition of the function that needs to be minimized, i.e. "PARTimeHomSA" is given in the Matlab code below.

```
function x = PARTimeHomSA(x0)

%define input variables
v1 = x0(1,1);
v2 = x0(2,1);
v3 = x0(3,1);
v4 = x0(4,1);
YearFrac = [0;0.25;0.50;0.75;1.00;1.25;1.50;1.75;2.00;2.25;2.50;
            2.75;3.00;3.25;3.50;3.75;4.00;4.25;4.50;4.75;5.00;
            5.25;5.50;5.75;6.00;6.25;6.50;6.75;7.00;7.25;7.50;
```

```
            7.75;8.00;8.25;8.50;8.75;9.00;9.25;9.50;9.75;10.00];
CaplVol = [0.12518;0.13991;0.15458;0.16334;0.16497;0.16657;
           0.16786;0.17250;0.16773;0.16299;0.15850;0.15747;
           0.15416;0.15031;0.14625;0.14731;0.14408;0.14084;
           0.13752;0.13702;0.13575;0.13447;0.13311;0.13422;
           0.13305;0.13193;0.13070;0.13150;0.13045;0.12939;
           0.12834;0.12878;0.12776;0.12663;0.12576;0.12778;
           0.12687;0.12605;0.12495;0.12677];

%declare variables to be used in calculations
ResVol = zeros(40,1);
C = zeros(40,1);
B = zeros(40,1);
MktVaR = zeros(40,1);
ModelVaR = zeros(40,1);

    for i = 1:40
        Ti = YearFrac(i+1,1);
        sum2 = (THAnalInt(v2,v3,v4,v1,Ti,Ti)
             - THAnalInt(v2,v3,v4,v1,0,Ti));
        B(i,1) = sqrt((YearFrac(i+1,1)*CaplVol(i,1)^2)/sum2);
        ResVol(i,1) = YearFrac(i+1,1)*CaplVol(i,1)^2 - sum2;
        C(i,1) = sqrt(sum2/YearFrac(i+1,1));
        MktVaR(i,1) = YearFrac(i+1,1)*CaplVol(i,1)^2;
        ModelVaR(i,1) = sum2;
    end
C; %can be used for vol graph
B; %factors needed for exact pricing of market caps
MktVaR; %market variances
ModelVaR; %model variances

x=transpose(ResVol)*ResVol;

end
```

The function "THAnalInt" represents the analytical integration of the square of the instantaneous volatilities. This considerably reduced the required computational time and hence was preferred above the numerical integration technique of the previous section. The Matlab code for this function is presented below.

```
function y = THAnalInt(a,b,c,d,t,Ti)
y = (1/(4*c^3))*(4*a*c^2*d*(2*exp(c*(t-Ti)))+4*c^3*d^2*t
  - 2*4*b*c*d*exp(c*(t-Ti))*(c*(t-Ti)-1)+exp(c*(2*t-2*Ti))
```

```
  *(2*a^2*c^2+2*a*b*c*(1+c*(2*Ti-2*t))+b^2*(1+2*c^2*(t-Ti)^2
  +c*(2*Ti-2*t))));
end
```

As described throughout this thesis, it is important to consider the term structure evolution of volatilities following the calibration process. The Matlab code below provide the necessary calculations involved in this process.

```
function x = PARTermStructEvolSA()

%define input variables
YearFrac = [0;0.25;0.50;0.75;1.00;1.25;1.50;1.75;2.00;2.25;
            2.50;2.75;3.00;3.25;3.50;3.75;4.00;4.25;4.50;
            4.75;5.00;5.25;5.50;5.75;6.00;6.25;6.50;6.75;
            7.00;7.25;7.50;7.75;8.00;8.25;8.50;8.75;9.00;
            9.25;9.50;9.75;10.00];

%set parameters of the time-homogeneous function equal to the
%values obtained from the minimization step
x0=[0.105782518615748;-0.025782518615748;0.279813875241565;
    1.237840675388569];

v1 = x0(1,1);
v2 = x0(2,1);
v3 = x0(3,1);
v4 = x0(4,1);

%set the forward rate function equal to the constant values
%obtained from the minimization step
B = [1.103991272082396;1.031033788176418;1.033465682536949;
     1.036254830550857;1.019722331048633;1.019511728636313;
     1.027596142734424;1.062797384699251;1.044006225102150;
     1.027157730888388;1.012482991628495;1.020090257534752;
     1.012745317336438;1.001117275705254;0.987108252095278;
     1.007002990839056;0.996932604579362;0.985771672368137;
     0.973037137107645;0.979472887485776;0.979795526714303;
     0.979407274845969;0.977822748771328;0.993944059298312;
     0.992779869103672;0.991487194390559;0.988894615068184;
     1.001311105037045;0.999323134590358;0.996877471034461;
     0.994152553836903;1.002696183078788;0.999618645261241;
     0.995384702699757;0.992922600750649;1.013128336907268;
     1.009963032110269;1.007293753340009;1.002174131141280;
     1.020348694196970;1;1;1;1;1;1;1;1;1;1;1;1;1;1;1;1;1;
     1;1;1;1;1;1;1;1;1;1;1;1;1;1;1;1;1;1;1;1;1;1;1;1;1;1;
```

```
     1;1;1;1;1;1;1;1;1;1];

%declare variable to be used in calculations
volEvol=zeros(40,40);

for k=1:40
    for i = 1:40
        Ti = YearFrac(i+1,1);
        sum2 = (THNumInt(v2,v3,v4,v1,Ti,Ti)
             - THNumInt(v2,v3,v4,v1,0,Ti))*(B(i+k-1,1)^2);
        volEvol(i,k) = sqrt(sum2/YearFrac(i+1,1));
    end
end
   x = volEvol;

end
```

C.1.2.3 Multi-Time Dependence Volatility Specification

This section will present the code used for the third step of the calibration process when applied to the South African market. Most of the procedures are very similar to that given for the European market and hence the reader is referred to the discussions in Section C.1.1.2 for more details.

The code used specifying the minimization routines are given below (results presented used 2000 different starting points). Note that this step did not need to enforce any constraints and hence the code was changed back to make use of the unconstrained optimization routine.

```
function [Fval,Fvect] = LoopPARTimeHomSAStep2(n)

%increase number of function evaluations
options = optimset('MaxFunEvals',10000);

%choose initial point
x0 = [0.1;0.1;0.1;0.1;0.1;0.1];

%specify empty constraints
lb = []; ub = [];

%perform first optimization
[vect,fval] = lsqnonlin(@PARTimeHomSAStep2,x0,lb,ub,options);
fval %show intermediate results

for i=1:n
```

```
    iter = i %included to show where in process
    bestEst = fval %included to show best value optained thus
                   %far

    %generate random starting points from Uniform distribution,
    %allows for a better approximation of the global minimum.
    x0=unifrnd(-2,2,6,1);

    %perform optimization at new point
    [vect2,fval2] =
    lsqnonlin(@PARTimeHomSAStep2,x0,lb,ub,options);

    fval2 %show intermediate results

    %at each step of the procedure we need to check if the new
    %starting point resulted in a lower function value
    if fval2 < fval
        vect = vect2;
        fval = fval2;
    end
end

Fval=fval; %returns optimal value
Fvect = vect; %returns optimal vector
end
```

The function "PARTimeHomSAStep2" is defined below. Integration was switched back to numerical given the complexity of the integrand. This did however reduce the calculation speed considerably. Furthermore, note that the function "RebTHTD" was already defined in Section C.1.1.1 and hence not presented again.

```
 function x = PARTimeHomSAStep2(e0)

%define input variables
e1 = e0(1,1);
e2 = e0(2,1);
e3 = e0(3,1);
e4 = e0(4,1);
e5 = e0(5,1);
e6 = e0(6,1);

YearFrac = [0;0.25;0.50;0.75;1.00;1.25;1.50;1.75;2.00;2.25;2.50;
            2.75;3.00;3.25;3.50;3.75;4.00;4.25;4.50;4.75;5.00;
```

```
            5.25;5.50;5.75;6.00;6.25;6.50;6.75;7.00;7.25;7.50;
            7.75;8.00;8.25;8.50;8.75;9.00;9.25;9.50;9.75;10.00];
CaplVol = [0.12518;0.13991;0.15458;0.16334;0.16497;0.16657;
           0.16786;0.17250;0.16773;0.16299;0.15850;0.15747;
           0.15416;0.15031;0.14625;0.14731;0.14408;0.14084;
           0.13752;0.13702;0.13575;0.13447;0.13311;0.13422;
           0.13305;0.13193;0.13070;0.13150;0.13045;0.12939;
           0.12834;0.12878;0.12776;0.12663;0.12576;0.12778;
           0.12687;0.12605;0.12495;0.12677];

%set parameters of the time-homogeneous function equal to the
%values obtained from the previous step
x0 = [0.105782518615748;-0.025782518615748;0.279813875241565;
      1.237840675388569];

v1 = x0(1,1);
v2 = x0(2,1);
v3 = x0(3,1);
v4 = x0(4,1);

%declare variables to be used in calculations
ResVol = zeros(40,1);
C = zeros(40,1);
B = zeros(40,1);
MktVaR = zeros(40,1);
ModelVaR = zeros(40,1);

for i = 1:40
    Ti = YearFrac(i+1,1);
    sum2 =
    quadgk(@(t)RebTHTD(t,v1,v2,v3,v4,e1,e2,e3,e4,e5,e6,Ti),0,Ti);
    B(i,1) = sqrt((YearFrac(i+1,1)*CaplVol(i,1)^2)/sum2);
    ResVol(i,1) = YearFrac(i+1,1)*CaplVol(i,1)^2 - sum2;
    C(i,1) = sqrt(sum2/YearFrac(i+1,1));
    MktVaR(i,1) = YearFrac(i+1,1)*CaplVol(i,1)^2;
    ModelVaR(i,1) = sum2;
end
C; %can be used for vol graph
B; %factors needed for exact pricing of market caps
MktVaR; %market variances
ModelVaR; %model variances

x=ResVol;
end
```

Below is the code used for obtaining the evolution of the term structure of volatilities as we move through time. Note that no assumptions were made regarding forward rate specific components as we move through time, hence the resulting evolution will illustrate a shortening in the tail of the term structure.

```
function x = PARTermStructEvolSAStep2()

%define input variables
YearFrac = [0;0.25;0.50;0.75;1.00;1.25;1.50;1.75;2.00;2.25;
            2.50;2.75;3.00;3.25;3.50;3.75;4.00;4.25;4.50;
            4.75;5.00;5.25;5.50;5.75;6.00;6.25;6.50;6.75;
            7.00;7.25;7.50;7.75;8.00;8.25;8.50;8.75;9.00;
            9.25;9.50;9.75;10.00];

%set parameters of the time-homogeneous and time-dependent
%functions equal to the values obtained from the minimization
%steps
x0=[0.105782518615748;-0.025782518615748;0.279813875241565;
    1.237840675388569];

v1 = x0(1,1);
v2 = x0(2,1);
v3 = x0(3,1);
v4 = x0(4,1);

e0=[-4.922059515904149;-3.482772209499539;-1.493793256839924;
    0.366691267054780;-0.828297473387842;0.167607455829285];
e1 = e0(1,1);
e2 = e0(2,1);
e3 = e0(3,1);
e4 = e0(4,1);
e5 = e0(5,1);
e12 = e0(6,1);

%set the forward rate function equal to the constant values
%obtained from the minimization step
B=[1.073020559346012;0.997439292708948;0.997097970633483;
   0.998547732452972;0.982550709502084;0.983224898840092;
   0.992699065052335;1.029160485161995;1.014040784530846;
   1.001346240957347;0.991282228185541;1.003590014078435;
   1.001669754783236;0.995719240504868;0.987324476241737;
   1.012650204189403;1.007365161595972;1.000061646342033;
   0.990032855392082;0.998309712840622;0.999156905781757;
   0.998155509041908;0.995003773627218;1.009165217479395;
```

```
   1.005363119112331;1.001349902785679;0.996191997385803;
   1.006461794099936;1.002646497862292;0.998789847260976;
   0.994984408258803;1.002633180413091;0.998666484017373;
   0.993396076307753;0.989625935679350;1.008102268195251;
   1.003042088619024;0.998428208821044;0.991667086147701;
   1.008650999053897];

%declare variable to be used in calculations
volEvol=zeros(40,40);

for k=1:40
    Tprev = YearFrac(k,1);
    for i = 1:40-k+1
        sum2 = 0;
        Ti = YearFrac(i+1+k-1,1);
        sum2 = quadgk(@(t)RebTHTD(t,v1,v2,v3,v4,e1,e2,e3,
               e4,e5,e12,Ti),Tprev,Ti)*(B(i+k-1,1)^2);
        volEvol(i,k) = sqrt(sum2/YearFrac(i+1,1));
    end
end

   x = volEvol;

end
```

C.2 Joint Calibration

Joint calibration was discussed in Chapter 10. The calibration routines of some of these techniques will be presented in this section.

C.2.1 Calibrating to European Market Data

We only considered the different cascade calibration algorithms for the European market. The aim was to obtain results that matched the results of the authors of the techniques.

C.2.1.1 Cascade Calibration

The first code that we will present relates to the implementation of Algorithm 10.3.1. This allows for the calibration to the upper half of the swaption volatility matrix. The code is presented below.

```
function x= EURCCA(NbrRows)
```

```
%NbrRows indicates the number of rows in the swaption matrix
%that are of interest for the calibration

%define the input swaption matrix
V=[0.18,0.167,0.154,0.145,0.138,0.134,0.13,0.126,0.124,0.122;
0.181,0.162,0.145,0.135,0.127,0.123,0.12,0.117,0.115,0.113;
0.178,0.155,0.137,0.125,0.117,0.114,0.111,0.108,0.106,0.104;
0.167,0.143,0.126,0.115,0.108,0.105,0.103,0.1,0.098,0.096;
0.154,0.132,0.118,0.109,0.104,0.104,0.099,0.096,0.094,0.092;
0.147,0.1265,0.1125,0.1035,0.098,0.0975,0.094,0.0915,0.09,
0.0885;0.14,0.121,0.107,0.098,0.092,0.091,0.089,0.087,0.086,
0.085;0.1367,0.1173,0.1033,0.0947,0.089,0.088,0.086,0.0843,
0.0833,0.0823;0.1333,0.1137,0.0997,0.0913,0.086,0.085,0.083,
0.0817,0.0807,0.0797;0.13,0.11,0.096,0.088,0.083,0.082,0.08,
0.079,0.078,0.077];

%forward rates including first spot rate
FwdCrve = [0.0469;0.050114;0.055973;0.058387;0.060027;0.061315;
    0.062779;0.062747;0.062926;0.062286;0.063009;0.063554;
    0.064257;0.064784;0.065312;0.063976;0.062997;0.06184;
    0.060682;0.05936];
%forward rates excluding first spot rate
F = [0.050114;0.055973;0.058387;0.060027;0.061315;0.062779;
    0.062747;0.062926;0.062286;0.063009;0.063554;0.064257;
    0.064784;0.065312;0.063976;0.062997;0.06184;0.060682;
    0.05936];

%create set of discount factors - created from annual rates
%hence year fractions set to one - 1st disc factor associated
%with spot rate
for i = 1:20
    P(1,i) = (prod(1+FwdCrve(1:i),1))^-1;
end

%create different weights
for i = 1:10 %maturity
    for j = 1:10 %lenght
        for k = (i+1):(i+j)
            w(i,j,k-1)=P(1,k)/(P(1,i+1:i+j)*ones(i+j-i,1));
        end
        S(i,j) = (P(1,i)-P(1,i+j))/(P(1,i+1:i+j)
        *ones(i+j-i,1));
    end
end
```

```
%create input correlation matrix
theta = [0.0147;0.0643;0.1032;0.1502;0.1969;0.2239;0.2771;
    0.2950;0.3630;0.3810;0.4217;0.4836;0.5204;0.5418;
    0.5791;0.6496;0.6679;0.7126;0.7659];

n=2;
for i=1:19
    for k=1:n-1
        B(i,k)=cos(theta(i,k))*prod(sin(theta(i,1:k-1)),2);
    end
    B(i,n)=prod(sin(theta(i,1:n-1)),2);
end

rho=B*transpose(B);

%initialize forward rate volatilities
sigma=zeros(10,10);

for alpha = 0:NbrRows-1
    for beta = alpha+1:NbrRows

        s1=0;s2=0;s3=0;s4=0;
        for i = alpha + 1:beta-1
            for j = alpha + 1:beta-1
                for h = 0:alpha
                    s1 = s1+w(alpha+1,beta-alpha,i)
                    *w(alpha+1,beta-alpha,j)*F(i,1)*F(j,1)
                    *rho(i,j)*sigma(i,h+1)*sigma(j,h+1);
                end
            end
            for h = 0:alpha-1
                s2 = s2 + 2*(w(alpha+1,beta-alpha,beta)
                *w(alpha+1,beta-alpha,i)*F(beta,1)
                *F(i,1)*rho(beta,i)*sigma(beta,h+1)
                *sigma(i,h+1));
            end

            s4 = s4 + (w(alpha+1,beta-alpha,beta)
            *w(alpha+1,beta-alpha,i)*F(beta,1)*F(i,1)
            *rho(beta,i)*sigma(i,alpha+1));
        end

        for h = 0:alpha-1
```

```
            s3 = s3 + w(alpha+1,beta-alpha,beta)^2
            *F(beta,1)^2*sigma(beta,h+1)^2;
        end

        A=w(alpha+1,beta-alpha,beta)^2*F(beta,1)^2;
        B=2*s4;
        C=s1+s2+s3-(alpha+1)*S(alpha+1,beta-alpha)^2
        *V(alpha+1,beta-alpha)^2;

        sigma(beta,alpha+1)=(-B+sqrt(B^2-4*A*C))/(2*A);

    end
end


x=sigma;
end
```

Next, we will present the code relating to the implementation of Algorithm 10.3.2. This allows for the calibration to the entire swaption volatility matrix. The code is presented below.

```
function x= EURRCCA(NbrRows)

%NbrRows indicates the number of rows in the swaption matrix
%that are of interest for the calibration

%define the input swaption matrix
V=[0.18,0.167,0.154,0.145,0.138,0.134,0.13,0.126,0.124,0.122;
0.181,0.162,0.145,0.135,0.127,0.123,0.12,0.117,0.115,0.113;
0.178,0.155,0.137,0.125,0.117,0.114,0.111,0.108,0.106,0.104;
0.167,0.143,0.126,0.115,0.108,0.105,0.103,0.1,0.098,0.096;
0.154,0.132,0.118,0.109,0.104,0.104,0.099,0.096,0.094,0.092;
0.147,0.1265,0.1125,0.1035,0.098,0.0975,0.094,0.0915,0.09,
0.0885;0.14,0.121,0.107,0.098,0.092,0.091,0.089,0.087,0.086,
0.085;0.1367,0.1173,0.1033,0.0947,0.089,0.088,0.086,0.0843,
0.0833,0.0823;0.1333,0.1137,0.0997,0.0913,0.086,0.085,0.083,
0.0817,0.0807,0.0797;0.13,0.11,0.096,0.088,0.083,0.082,0.08,
0.079,0.078,0.077];

%forward rates including first spot rate
FwdCrve = [0.0469;0.050114;0.055973;0.058387;0.060027;0.061315;
    0.062779;0.062747;0.062926;0.062286;0.063009;0.063554;
```

```
    0.064257;0.064784;0.065312;0.063976;0.062997;0.06184;
    0.060682;0.05936];
%forward rates excluding first spot rate
F = [0.050114;0.055973;0.058387;0.060027;0.061315;0.062779;
    0.062747;0.062926;0.062286;0.063009;0.063554;0.064257;
    0.064784;0.065312;0.063976;0.062997;0.06184;0.060682;
    0.05936];

%create set of discount factors - created from annual rates
%hence year fractions set to one - 1st disc factor associated
%with spot rate
for i = 1:20
    P(1,i) = (prod(1+FwdCrve(1:i),1))^-1;
end

%create different weights
for i = 1:10 %maturity
    for j = 1:10 %lenght
        for k = (i+1):(i+j)
            w(i,j,k-1)=P(1,k)/(P(1,i+1:i+j)*ones(i+j-i,1));
        end
        S(i,j) = (P(1,i)-P(1,i+j))/(P(1,i+1:i+j)
        *ones(i+j-i,1));
    end
end

%create input correlation matrix
theta = [0.0147;0.0643;0.1032;0.1502;0.1969;0.2239;0.2771;
    0.2950;0.3630;0.3810;0.4217;0.4836;0.5204;0.5418;
    0.5791;0.6496;0.6679;0.7126;0.7659];

n=2;
for i=1:19
    for k=1:n-1
        B(i,k)=cos(theta(i,k))*prod(sin(theta(i,1:k-1)),2);
    end
    B(i,n)=prod(sin(theta(i,1:n-1)),2);
end

rho=B*transpose(B);

%initialize forward rate volatilities
sigma=zeros(19,10);
```

```
for alpha = 0:NbrRows-1
    for beta = alpha+1:NbrRows+alpha%ss%s

        if beta < NbrRows+alpha || alpha == 0

            %%%%%%%%%%%%%%%%%%%%%%%%%%%%%%%%%%%%%%%%%%%%
            %Start of normal CCA approach%%%%%%%%%%%%%%%
            %%%%%%%%%%%%%%%%%%%%%%%%%%%%%%%%%%%%%%%%%%%%
            s1=0;s2=0;s3=0;s4=0;
            for i = alpha + 1:beta-1
                for j = alpha + 1:beta-1
                    for h = 0:alpha
                        s1 = s1+w(alpha+1,beta-alpha,i)
                        *w(alpha+1,beta-alpha,j)*F(i,1)
                        *F(j,1)*rho(i,j)*sigma(i,h+1)
                        *sigma(j,h+1);
                    end
                end
                for h = 0:alpha-1
                    s2 = s2 +
                    2*(w(alpha+1,beta-alpha,beta)
                    *w(alpha+1,beta-alpha,i)*F(beta,1)
                    *F(i,1)*rho(beta,i)
                    *sigma(beta,h+1)*sigma(i,h+1));
                end

                s4 = s4 + (w(alpha+1,beta-alpha,beta)
                *w(alpha+1,beta-alpha,i)*F(beta,1)
                *F(i,1)*rho(beta,i)*sigma(i,alpha+1));
            end

            for h = 0:alpha-1

                s3 = s3 + w(alpha+1,beta-alpha,beta)^2
                *F(beta,1)^2*sigma(beta,h+1)^2;
            end

            A=w(alpha+1,beta-alpha,beta)^2*F(beta,1)^2;
            B=2*s4;
            C=s1+s2+s3-(alpha+1)
            *S(alpha+1,beta-alpha)^2
            *V(alpha+1,beta-alpha)^2;

            sigma(beta,alpha+1)=(-B+sqrt(B^2-4*A*C))
```

```
        /(2*A);
        %%%%%%%%%%%%%%%%%%%%%%%%%%%%%%%%%%%%%%%%%%%%%%%
        %End of normal CCA approach%%%%%%%%%%%%%%%%%%%%%
        %%%%%%%%%%%%%%%%%%%%%%%%%%%%%%%%%%%%%%%%%%%%%%%

    else if beta == NbrRows+alpha

        %%%%%%%%%%%%%%%%%%%%%%%%%%%%%%%%%%%%%%%%%%%%%%%
        %Second Part of Calculation%%%%%%%%%%%%%%%%%%%%%
        %%%%%%%%%%%%%%%%%%%%%%%%%%%%%%%%%%%%%%%%%%%%%%%
        s1=0;s2=0;s3=0;s4=0;
        for i = alpha + 1:beta-1
            for j = alpha + 1:beta-1
                for h = 0:alpha
                    s1 = s1+w(alpha+1,beta-alpha,i)
                    *w(alpha+1,beta-alpha,j)*F(i,1)
                    *F(j,1)*rho(i,j)*sigma(i,h+1)
                    *sigma(j,h+1);
                end
            end
            for h = 0:alpha-1
                s2 = s2 +
                2*(w(alpha+1,beta-alpha,beta)
                *w(alpha+1,beta-alpha,i)*F(beta,1)
                *F(i,1)*rho(beta,i)*sigma(i,h+1));
            end

            s4 = s4 + (w(alpha+1,beta-alpha,beta)
            *w(alpha+1,beta-alpha,i)*F(beta,1)
            *F(i,1)*rho(beta,i)*sigma(i,alpha+1));
        end

        for h = 0:alpha-1

            s3 = s3 +w(alpha+1,beta-alpha,beta)^2
            *F(beta,1)^2;
        end

        AA=w(alpha+1,beta-alpha,beta)^2
        *F(beta,1)^2+s3;
        BB=2*s4+s2;
        CC=s1-(alpha+1)*S(alpha+1,beta-alpha)^2
        *V(alpha+1,beta-alpha)^2;
```

```
            sigma(beta,alpha+1)=(-BB+sqrt(BB^2-4*AA*CC))
            /(2*AA);
            %%%%%%%%%%%%%%%%%%%%%%%%%%%%%%%%%%%%%%%%%%%
            %End of Second Part of Calculation%%%%%%%%%
            %%%%%%%%%%%%%%%%%%%%%%%%%%%%%%%%%%%%%%%%%%%

                for l = 1:alpha
                    sigma(beta,l)=sigma(beta,alpha+1);
                end

            end
        end

    end
end


x=sigma;
end
```

Both of the previous two algorithms required the filling of missing swaption data through using some exogenous interpolation technique. The last piece of code that will be presented in this section relates to the implementation of Algorithm 10.3.3. This enables the calibration to an incomplete set of swaptions data through the use of an endogenous interpolation technique. The code for this implementation is presented below.

```
function x= EURRCCAEI(NbrRows)

%NbrRows indicates the number of rows in the swaption matrix
%that are of interest for the calibration

%define the input swaption matrix
V=[0.18,0.167,0.154,0.145,0.138,0.134,0.13,0.126,0.124,0.122;
0.181,0.162,0.145,0.135,0.127,0.123,0.12,0.117,0.115,0.113;
0.178,0.155,0.137,0.125,0.117,0.114,0.111,0.108,0.106,0.104;
0.167,0.143,0.126,0.115,0.108,0.105,0.103,0.1,0.098,0.096;
0.154,0.132,0.118,0.109,0.104,0.104,0.099,0.096,0.094,0.092;
0.147,0.1265,0.1125,0.1035,0.098,0.0975,0.094,0.0915,0.09,
0.0885;0.14,0.121,0.107,0.098,0.092,0.091,0.089,0.087,0.086,
0.085;0.1367,0.1173,0.1033,0.0947,0.089,0.088,0.086,0.0843,
0.0833,0.0823;0.1333,0.1137,0.0997,0.0913,0.086,0.085,0.083,
0.0817,0.0807,0.0797;0.13,0.11,0.096,0.088,0.083,0.082,0.08,
0.079,0.078,0.077];
```

```
%define set of missing rows
K=ones(10,1);
K(6,1)=0;K(8,1)=0;K(9,1)=0;

%forward rates including first spot rate
FwdCrve = [0.0469;0.050114;0.055973;0.058387;0.060027;0.061315;
    0.062779;0.062747;0.062926;0.062286;0.063009;0.063554;
    0.064257;0.064784;0.065312;0.063976;0.062997;0.06184;
    0.060682;0.05936];
%forward rates excluding first spot rate
F = [0.050114;0.055973;0.058387;0.060027;0.061315;0.062779;
    0.062747;0.062926;0.062286;0.063009;0.063554;0.064257;
    0.064784;0.065312;0.063976;0.062997;0.06184;0.060682;
    0.05936];

%create set of discount factors - created from annual rates
%hence year fractions set to one - 1st disc factor associated
%with spot rate
for i = 1:20
    P(1,i) = (prod(1+FwdCrve(1:i),1))^-1;
end

%create different weights
for i = 1:10 %maturity
    for j = 1:10 %lenght
        for k = (i+1):(i+j)
            w(i,j,k-1)=P(1,k)/(P(1,i+1:i+j)*ones(i+j-i,1));
        end
        S(i,j) = (P(1,i)-P(1,i+j))/(P(1,i+1:i+j)
        *ones(i+j-i,1));
    end
end

%create input correlation matrix
theta = [0.0147;0.0643;0.1032;0.1502;0.1969;0.2239;0.2771;
    0.2950;0.3630;0.3810;0.4217;0.4836;0.5204;0.5418;
    0.5791;0.6496;0.6679;0.7126;0.7659];

n=2;
for i=1:19
    for k=1:n-1
        B(i,k)=cos(theta(i,k))*prod(sin(theta(i,1:k-1)),2);
    end
    B(i,n)=prod(sin(theta(i,1:n-1)),2);
```

```
end

rho=B*transpose(B);


%initialize forward rate volatilities
sigma=zeros(19,10);
sigmaj = zeros(19,1);

testtt=0;
alpha = 0;
while testtt == 0;
alpha;

    if K(alpha+1,1)==1
            for beta = alpha+1:NbrRows+alpha%ss%s
                if beta < NbrRows+alpha || alpha == 0
                    %%%%%%%%%%%%%%%%%%%%%%%%%%%%%%%%%%%%%%%%%%%%
                    %Start of normal CCA approach%%%%%%%%%%%%%%%
                    %%%%%%%%%%%%%%%%%%%%%%%%%%%%%%%%%%%%%%%%%%%%
                    s1=0;s2=0;s3=0;s4=0;
                    for i = alpha + 1:beta-1
                        for j = alpha + 1:beta-1
                            for h = 0:alpha
                                s1 = s1+w(alpha+1,beta-alpha,i)
                                *w(alpha+1,beta-alpha,j)*F(i,1)
                                *F(j,1)*rho(i,j)*sigma(i,h+1)
                                *sigma(j,h+1);
                            end
                        end
                        for h = 0:alpha-1
                            s2 = s2 +
                            2*(w(alpha+1,beta-alpha,beta)
                            *w(alpha+1,beta-alpha,i)*F(beta,1)
                            *F(i,1)*rho(beta,i)*sigma(beta,h+1)
                            *sigma(i,h+1));
                        end

                        s4 = s4 + (w(alpha+1,beta-alpha,beta)
                        *w(alpha+1,beta-alpha,i)*F(beta,1)
                        *F(i,1)*rho(beta,i)
                        *sigma(i,alpha+1));
                    end
                    for h = 0:alpha-1
```

```
                s3 = s3 +w(alpha+1,beta-alpha,beta)^2
                *F(beta,1)^2*sigma(beta,h+1)^2;
            end
            A=w(alpha+1,beta-alpha,beta)^2
            *F(beta,1)^2;
            B=2*s4;
            C=s1+s2+s3-(alpha+1)
            *S(alpha+1,beta-alpha)^2
            *V(alpha+1,beta-alpha)^2;
            sigma(beta,alpha+1)=(-B+sqrt(B^2-4*A*C))
            /(2*A);
            %%%%%%%%%%%%%%%%%%%%%%%%%%%%%%%%%%%%%%%%
            %End of normal CCA approach%%%%%%%%%%%%%%
            %%%%%%%%%%%%%%%%%%%%%%%%%%%%%%%%%%%%%%%%
        else if beta == NbrRows+alpha
            %%%%%%%%%%%%%%%%%%%%%%%%%%%%%%%%%%%%%%%%
            %Second Part of Calculation%%%%%%%%%%%%%%
            %%%%%%%%%%%%%%%%%%%%%%%%%%%%%%%%%%%%%%%%
            s1=0;s2=0;s3=0;s4=0;
            for i = alpha + 1:beta-1
                for j = alpha + 1:beta-1
                    for h = 0:alpha
                        s1 = s1+w(alpha+1,beta-alpha,i)
                        *w(alpha+1,beta-alpha,j)*F(i,1)
                        *F(j,1)*rho(i,j)*sigma(i,h+1)
                        *sigma(j,h+1);
                    end
                end
                for h = 0:alpha-1
                    s2 = s2 +
                    2*(w(alpha+1,beta-alpha,beta)
                    *w(alpha+1,beta-alpha,i)*F(beta,1)
                    *F(i,1)*rho(beta,i)*sigma(i,h+1));
                end

                s4 = s4 + (w(alpha+1,beta-alpha,beta)
                *w(alpha+1,beta-alpha,i)*F(beta,1)
                *F(i,1)*rho(beta,i)*sigma(i,alpha+1));
            end
            for h = 0:alpha-1

                s3 = s3 +w(alpha+1,beta-alpha,beta)^2
                *F(beta,1)^2;
```

```
                end
                AA=w(alpha+1,beta-alpha,beta)^2
                *F(beta,1)^2+s3;
                BB=2*s4+s2;
                CC=s1-(alpha+1)*S(alpha+1,beta-alpha)^2
                *V(alpha+1,beta-alpha)^2;
                sigma(beta,alpha+1)=(-BB+sqrt(BB^2-4*AA*CC))
                /(2*AA);
                %%%%%%%%%%%%%%%%%%%%%%%%%%%%%%%%%%%%%%%%%%
                %End of Second Part of Calculation%%%%%%%%
                %%%%%%%%%%%%%%%%%%%%%%%%%%%%%%%%%%%%%%%%%%
                for l = 1:alpha
                    sigma(beta,l)=sigma(beta,alpha+1);
                end

                end
            end

        end
    end

    if K(alpha+1,1)==0
        m=find(K(alpha+1:10),1,'first')+alpha-1;
        gmma=alpha;
        alpha=m;
        for beta = alpha+1:NbrRows+gmma-1%ss%s
            %%%%%%%%%%%%%%%%%%%%%%%%%%%%%%%%%%%%%%%%%%
            %Start CCA for missing entries%%%%%%%%%%%%%
            %%%%%%%%%%%%%%%%%%%%%%%%%%%%%%%%%%%%%%%%%%
            s1=0;s2=0;s3=0;s4=0;s11=0;s22=0;s33=0;
            for i = alpha + 1:beta-1
                for j = alpha + 1:beta-1
                    for h = 0:gmma-1
                        s1 = s1+w(alpha+1,beta-alpha,i)
                        *w(alpha+1,beta-alpha,j)*F(i,1)
                        *F(j,1)*rho(i,j)*sigma(i,h+1)
                        *sigma(j,h+1);
                    end
                    for h = gmma:alpha
                        s11 = s11+w(alpha+1,beta-alpha,i)
                        *w(alpha+1,beta-alpha,j)*F(i,1)
                        *F(j,1)*rho(i,j)*sigmaj(i)
                        *sigmaj(j,1);
                    end
```

```
            end
            for h = 0:gmma-1
                s2 = s2 +2*(w(alpha+1,beta-alpha,beta)
                *w(alpha+1,beta-alpha,i)*F(beta,1)
                *F(i,1)*rho(beta,i)*sigma(beta,h+1)
                *sigma(i,h+1));
            end
            for h = gmma:alpha-1
                s22 = s22 +
                2*(w(alpha+1,beta-alpha,beta)
                *w(alpha+1,beta-alpha,i)*F(beta,1)
                *F(i,1)*rho(beta,i)*1*sigmaj(i,1));
            end
            s4 = s4 + (w(alpha+1,beta-alpha,beta)
            *w(alpha+1,beta-alpha,i)*F(beta,1)
            *F(i,1)*rho(beta,i)*sigmaj(i,1));
        end
        for h = 0:gmma-1
            s3 = s3+w(alpha+1,beta-alpha,beta)^2
            *F(beta,1)^2*sigma(beta,h+1)^2;
        end
        for h = gmma:alpha-1
            s33 = s33+w(alpha+1,beta-alpha,beta)^2
            *F(beta,1)^2*1;
        end
        A=w(alpha+1,beta-alpha,beta)^2*F(beta,1)^2
        +s33;
        B=2*s4+s22;
        C=s1+s11+s2+s3-(alpha+1)
        *S(alpha+1,beta-alpha)^2
        *V(alpha+1,beta-alpha)^2;

        sigmaj(beta,1)=(-B+sqrt(B^2-4*A*C))
        /(2*A);
        %%%%%%%%%%%%%%%%%%%%%%%%%%%%%%%%%%%%%%%%
        %End CCA for missing entries%%%%%%%%%%%%%%%
        %%%%%%%%%%%%%%%%%%%%%%%%%%%%%%%%%%%%%%%%
        for j = gmma+1:alpha+1
            sigma(beta,j)=sigmaj(beta,1);
        end
    end
    for beta = NbrRows+gmma:NbrRows+alpha%ss%s
        %%%%%%%%%%%%%%%%%%%%%%%%%%%%%%%%%%%%%%%%
        %Second Part of Calculation%%%%%%%%%%%%%%%%
```

```
            %%%%%%%%%%%%%%%%%%%%%%%%%%%%%%%%%%%%%%%%%%%%
            s1=0;s2=0;s3=0;s4=0;
            for i = alpha + 1:beta-1
                for j = alpha + 1:beta-1
                    for h = 0:alpha
                        s1 = s1+w(alpha+1,beta-alpha,i)
                        *w(alpha+1,beta-alpha,j)*F(i,1)
                        *F(j,1)*rho(i,j)*sigma(i,h+1)
                        *sigma(j,h+1);
                    end
                end
                for h = 0:alpha-1
                    s2 = s2 +
                    2*(w(alpha+1,beta-alpha,beta)
                    *w(alpha+1,beta-alpha,i)*F(beta,1)
                    *F(i,1)*rho(beta,i)*sigma(i,h+1));
                end

                s4 = s4 + (w(alpha+1,beta-alpha,beta)
                *w(alpha+1,beta-alpha,i)*F(beta,1)
                *F(i,1)*rho(beta,i)*sigma(i,alpha+1));
            end
            for h = 0:alpha-1

                s3 = s3 + w(alpha+1,beta-alpha,beta)^2
                *F(beta,1)^2;
            end
            AA=w(alpha+1,beta-alpha,beta)^2*F(beta,1)^2
            +s3;
            BB=2*s4+s2;
            CC=s1-(alpha+1)*S(alpha+1,beta-alpha)^2
            *V(alpha+1,beta-alpha)^2;
            sigma(beta,alpha+1)=(-BB+sqrt(BB^2-4*AA*CC))
            /(2*AA);
            %%%%%%%%%%%%%%%%%%%%%%%%%%%%%%%%%%%%%%%%%%%%
            %End of Second Part of Calculation%%%%%%%%%%
            %%%%%%%%%%%%%%%%%%%%%%%%%%%%%%%%%%%%%%%%%%%%
             for l = 1:alpha
                sigma(beta,l)=sigma(beta,alpha+1);
             end
        end
    end

    alpha = alpha + 1;
```

```
        if alpha <= NbrRows-1
            testtt = 0;
        else
            testtt = 1;
        end

end

sigma(6,6)=sigma(5,5);sigma(8,8)=sigma(7,7);
sigma(9,8)=sigma(8,7);sigma(9,9)=sigma(8,8);

%calculate swaption volatilities given forward rate
%volatilities
Vmod=zeros(10,10);
for alpha = 0:NbrRows-1
    for beta=alpha+1:NbrRows+alpha
        sumMod=0;
        for i = alpha+1:beta
            for j = alpha+1:beta
                for h=0:alpha
                    sumMod = sumMod +
                    ((w(alpha+1,beta-alpha,i)
                    *w(alpha+1,beta-alpha,j)*F(i,1)*F(j,1)
                    *rho(i,j))/((alpha+1)
                    *S(alpha+1,beta-alpha)^2))
                    *(sigma(i,h+1)*sigma(j,h+1));
                end
            end
        end

        Vmod(alpha+1,beta-alpha)=sqrt(sumMod);
    end
end


x=sigma;%Vmod;
end
```

Notice that the code presented above can be adjusted in the last line to return the model implied swaption prices. This can be used as a measure of accuracy. Another important point to consider when implementing these algorithms, is the model implied evolution of the term structure of volatilities.

This can be obtained through running the following Matlab code.

```
function x = TermStructEvolEURRCCAEI()

%define input variables
YearFrac = [0;1;2;3;4;5;6;7;8;9;10;11;
            12;13;14;15;16;17;18;19;20];

%declare variables to be used in calculations
volEvol=zeros(10,10);

%create matrix containing volatilities of forward rates
forwMatrx= EURRCCAEI(10);

%calculate evolution of term structure
for k=1:10
    for i = k:10
        sum2 = 0;
        Ti = YearFrac(i-k+1+1,1);
        for j = k:10
            sum2 = sum2 + forwMatrx(i,j)^2*1;
        end
        volEvol(i,k) = sqrt(sum2/Ti);

    end
end
   x = volEvol;

end
```

C.2.2 Calibrating to South African Market Data

Given the number of historical correlations, we will not present the code used in the smoothing of the correlation surfaces. This can be provided on direct request. Consequently we will assume the parameters as given in order to keep the code as concise as possible. These parameters were obtained using a simple unconstrained minimization routine in Matlab.

C.2.2.1 Hull and White PCA Approach

The following code was used in obtaining the results presented in Section 10.5.2.

```
function x=HWFitResults(SimpleOrComplex)
%SimpleOrComplex indicates which parametric form to use. Set to 1
```

```
%for Rebonato's first parametric form and set to 0 for Rebonato's
%second parametric form

ResVect = zeros(33,3);
for i=1:33
    [x,y]=HWFitAndMeas(i,SimpleOrComplex);
    ResVect(i,1) = i;
    ResVect(i,2) = x;
    ResVect(i,3) = y;
end
x=ResVect;
end
```

The function HWFitAndMeas is defined by

```
function [x,y]=HWFitAndMeas(n,SimpleOrComplex)
%n represents the number of factors
%SimpleOrComplex indicates which parametric form to use. Set to 1
%for Rebonato's first parametric form and set to 0 for Rebonato's
%second parametric form

CorrRebFit = CorrFitRes(SimpleOrComplex);
[EigVec,EigVal]=eig(CorrRebFit);
DLTA=sqrt(diag(sum(EigVal(:,33-n+1:33),1),0));
C=EigVec(:,33-n+1:33)*DLTA;
temp1 = sqrt(diag(C*transpose(C)));
temp2 = zeros(33,n);
for j=1:n
    temp2(:,j)=temp1;
end

Cnew=C./temp2;
CorrHW=Cnew*transpose(Cnew);

diffHWRebFit=0;
for i = 1:33
    for j = 1:33
        diffHWRebFit=diffHWRebFit+
(CorrRebFit(i,j)-CorrHW(i,j))^2;
    end
end

x=diffHWRebFit; %SSE
y=sum(sum(EigVal(:,33-n+1:33),2),1)/33; %perc explained
```

```
end
```

The function CorrFitRes will be used throughout this section and is defined as

```
function x=CorrFitRes(SimpleOrComplex)
%Simple relates to Rebonato's 1st parametric form
%Complex relates to Rebonato's 2nd parametric form

%create set of expiries
tenr = [0.25:0.25:8.25];

if SimpleOrComplex==0
    x0 = [0.1297;10.4549;0.0580];
    pinf = x0(1,1);
    bta = x0(2,1);
    gmma = x0(3,1);
else if SimpleOrComplex==1
        x0=[0.2844;0.2194];
        pinf = x0(1,1);
        bta = x0(2,1);
    end
end

modelCorr = zeros(size(tenr,2),size(tenr,2));

for i = 1:size(tenr,2)
    for j = 1:size(tenr,2)
        if SimpleOrComplex==0
        modelCorr(i,j) = ((pinf + (1-pinf)*
exp(-bta*abs(tenr(1,i)^gmma-tenr(1,j)^gmma))));
        else if SimpleOrComplex==1
                modelCorr(i,j) = ((pinf + (1-pinf)*
exp(-bta*abs(tenr(1,i)-tenr(1,j)))));
            end
        end
    end
end



x=modelCorr;
```

C.2.2.2 Rebonato's Approach

The following code was used in obtaining the results presented in Section 10.5.3.

```
function xF=RebAngleFitResults()

global n

ResVect = zeros(32,2);

%number of factors to include in calculation
for l=2:33

    n=l;

    x0=normrnd(0,1,33,n-1);
    [x,fval] = fminunc(@RebAngleFitAndMeas,x0);

    for i=1:2
    x0=normrnd(0,1,33,n-1);
    [xL,fvalL] = fminunc(@RebAngleFitAndMeas,x0);
    if fvalL < fval
        fval = fvalL;
        x = xL;
    end
    end

    %xV = x ;
    yV = fval;

    ResVect(l-1,1) = l;
    ResVect(l-1,2) = yV;
end


xF=ResVect;
clear n

end
```

The function RebAngleFitAndMeas is defined by

```
function x=RebAngleFitAndMeas(parSet)
```

```
global n

%Simple relates to Rebonato's 1st parametric form
%Complex relates to Rebonato's 2nd parametric form
SimpleOrComplex = 1;

InputCorr = CorrFitRes(SimpleOrComplex);
B = zeros(33,n);

for i = 1:33
    for k=1:n-1
        B(i,k) = cos(parSet(i,k))*prod(sin(parSet(i,1:k-1)),2);
    end
        B(i,n) = prod(sin(parSet(i,1:n-1)),2);
end

modelCorr = B*transpose(B);

som = 0;
for i = 1:33
    for j = 1:33
        som = som + (InputCorr(i,j)-modelCorr(i,j))^2;
    end
end

x=som;

end
```

Bibliography

[1] L. Alfaro and F. Kanczuk. The subprime crisis hits emerging markets: Transmission and policy response in Brazil. Working Paper, www.econ.puc-rio.br, 2009.

[2] P. Balduzzi, G. Bertola, and S. Foresi. A model of target changes and the term structure of interest rates. *Journal of Monetary Economics*, 39:223–249, 1997.

[3] P. Balduzzi, S. R. Das, S. Foresi, and R. Sundaram. A simple approach to three-factor affine term structure models. *The Journal of Fixed Income*, 6:43–53, 1996.

[4] T. Björk. *Arbitrage Theory in Continuous Time*. Oxford University Press, 1998.

[5] F. Black. The pricing of commodity contracts. *Journal of Financial Economics*, 3:167–179, 1976.

[6] F. Black, E. Derman, and W. Toy. A one-factor model of interest rates and its application to treasury bond options. *Financial Analysts Journal*, 46:33–39, 1990.

[7] F. Black and P. Karasinski. Bond and option pricing when short rates are lognormal. *Financial Analysts Journal*, 47:52–59, 1991.

[8] A. Brace, D. Gatarek, and M. Musiela. The market model of interest rate dynamics. *Mathematical Finance*, 7:127–154, 1997.

[9] M.J. Brennan and E.S. Schwartz. A continuous time approach to the pricing of bonds. *Journal of Banking and Finance*, 3:133–156, 1979.

[10] D. Brigo and F. Mercurio. Calibrating LIBOR. *Risk*, pages 117–121, 2002.

[11] D. Brigo and F. Mercurio. *Interest Rate Models - Theory and Practice with Smile, Inflation and Credit*. Springer Finance, 2nd edition, 2007.

[12] D. Brigo and M. Morini. New developments on the analytical cascade swaption calibration of the LIBOR market model. Paper presented at the Fourth Italian Workshop on Mathematical Finance, 2002.

[13] D. Brigo and M. Morini. An empirically efficient analytical cascade calibration of the LIBOR model based only on directly quoted swaptions data. Working Paper, papers.ssrn.com, 2005.

[14] R. L. Burden and J. D. Faires. *Numerical Analysis*. Brooks/Cole, 2001.

[15] A.J.G Cairns. *Interest Rate Models*. Princeton University Press, 2004.

[16] A. Carverhill. When is the short rate markovian? *Mathematical Finance*, 4:305–312, 1994.

[17] J. Cox, J. Ingersoll, and S. Ross. A theory of the term structure of interest rates. *Econometrica*, 53:385–408, 1985.

[18] S. Dodds. Personal Communication with Rebonato, 1998.

[19] M.U. Dothan. On the term structure of interest rates. *Journal of Financial Economics*, 6:59–69, 1978.

[20] D. Duffie and R. Kan. A yield-factor model of interest rates. *Mathematical Finance*, 64:379–406, 1996.

[21] D. Gatarek, P. Bachert, and R. Maksymiuk. *The LIBOR Market Model in Practice*. John Wiley & Sons, Ltd, 2006.

[22] I. Götsch. *LIBOR Market Model*. VDM Verlag Dr. Müller, 2006.

[23] V. Gumbo. *A Theoretical and Empirical Analysis of the LIBOR Market Model and its Application in the South African SAFEX JIBAR Market*. PhD thesis, University of South Africa, 2007.

[24] W.B. Gwinner and A. Sanders. The sub prime crisis: Implications for emerging markets. Technical report, The World Bank, 2008.

[25] P.S. Hagan. Volatility conversion calculators. *Bloomberg*.

[26] P.S. Hagan, D. Kumar, A.S. Lesniewski, and D.E. Woodward. Managing smile risk. *Wilmott Magazine*, Autumn:84–108, 2002.

[27] P.S. Hagan and G. West. Interpolation methods for curve construction. *Applied Mathematical Finance*, 13:89–129, 2006.

[28] D. Heath, R.A. Jarrow, and A. Morton. Bond pricing and the term structure of interest rates: A new methodology for contingent claims valuation. *Econometrica*, 60:77–105, 1992.

[29] T. Ho and S. Lee. Term structure movements and pricing interest rate contingent claims. *Journal of Finance*, 41:1011–1029, 1986.

[30] J. Hull and A. White. Pricing interest rate derivative securities. *The Review of Financial Studies*, 3:573–592, 1990.

[31] J. Hull and A. White. Forward rate volatilities, swap rate volatilities, and the implementation of the LIBOR market model. Joseph L. Rotman School of Management, University of Toronto, 1999.

[32] J.C. Hull. *Options, Futures and Other Derivatives*. Prentice Hall, 6'th edition, 2006.

[33] P.J. Hunt and J.E. Kennedy. *Financial Derivatives in Theory and Practice*. John Wiley & Sons, Ltd, 2004.

[34] J. James and N. Webber. *Interest Rate Modeling*. John Wiley & Sons, LTD, 2000.

[35] F. Jamshidian. LIBOR and swap market models and measures. *Finance and Stochastics*, 1:293–330, 1997.

[36] R. Litterman and J. Scheinkman. Common factors affecting bond returns. *Journal of Fixed Income*, 1:54–61, 1991.

[37] F.A. Longstaff and E.S. Schwartz. Interest rate volatility and the term structure: A two-factor general equilibrium model. *Journal of Finance*, 47:1259–1282, 1992.

[38] R. Merton. The theory of rational option pricing. *Bell Journal of Economics and Management Sciences*, 4:141–183, 1973.

[39] K. Miltersen, K. Sandmann, and D. Sondermann. Closed form solutions for term structure derivatives with log-normal interest rates. *Journal of Finance*, 52:409–430, 1997.

[40] M. Morini. Calibrazione e strutture di covarianza del LIBOR market model. Master's thesis, University of Pavia, 2002.

[41] M. Morini. An analytical cascade calibration algorithm for the LIBOR model based only on directly quoted swaption volatilities. Working Paper, papers.ssrn.com, 2003.

[42] M. Musiela and M. Rutkowski. *Martingale Methods in Financial Modelling*. Springer-Verlag, 1997.

[43] Bank of Montreal. Interpreting Option Volatility, 1997.

[44] A. Pelsser. *Efficient Methods for Valuing Interest Rate Derivatives.* Springer Verlag, 2000.

[45] V. Piterbarg. Funding beyond discounting: collateral agreements and derivatives pricing. *Risk*, February:97–102, 2010.

[46] R.L. Rardin. *Optimization in Operations Research.* Prentice Hall, 1998.

[47] R. Rebonato. *Modern Pricing of Interest Rate Derivatives: The LIBOR Market Model and Beyond.* Princeton University Press, 2002.

[48] R. Rebonato. Interest-rate term-structure pricing models: a review. Working Paper, riccardorebonato.co.uk, 2003.

[49] R. Rebonato. A time-homogeneous, SABR-consistent extension of the LMM: Calibration and numerical results. Working Paper, riccardorebonato.co.uk, 2007.

[50] R. Rebonato and P. Jaeckel. The most general methodology to create a valid correlation matrix. *Journal of Risk*, 2:1–16, 2000.

[51] R. Rebonato, K. McKay, and R. White. *the SABR/LIBOR Market Model.* John Wiley & Sons Ltd, 2009.

[52] R. Rebonato and R. White. Linking caplets and swaptions prices in the LMM-SABR model. Working Paper, riccardorebonato.co.uk, 2007.

[53] www.reservebank.co.za Reserve Bank website.

[54] S.M. Schaefer and E.S. Schwartz. A two-factor model of the term structure: An approximate analytical solution. *Journal of Financial and Quantitative Analysis*, 19:413–424, 1984.

[55] J.A. Snyman. *Practical Mathematical Optimization: An Intorduction to Basic Optimization Theory and Classical and New Gradient-Based Algorithms.* Springer, 2005.

[56] O. Vasiček. An equilibrium characterization of the term structure. *Journal of Financial Economics*, 5:177–188, 1977.

[57] G. West. Calibration of the SABR model in illiquid markets. *Applied Mathematical Finance*, 12:371–385, 2005.

[58] C. Whitall. Dealing with funding. *Risk*, July:19–22, 2010.

[59] C. Whitall. The price is wrong. *Risk*, March:19–22, 2010.